Evaluating and exploiting the function of a *Leishmania major* type I nitroreductase in the development of novel leishmanicidal prodrugs

Thesis submitted to the University of London for
the degree of PhD

Andrew Alan Voak

Queen Mary University of London

Declaration by Candidate

I declare that the work presented in this thesis is my own and that the thesis presented is the one upon which I expect to be examined.

Signed (Candidate):..... Date.....

Full name:.....

Signed (Supervisor):..... Date.....

Full name:.....

Abstract

Leishmania are protozoan parasites responsible for the range of infections collectively known as leishmaniasis. Currently, drugs represent the only course of treatment. The nitroaromatic prodrugs are a class of agents that are used clinically used to treat trypanosomatid diseases; and in the parasites *Trypanosoma brucei* and *Trypanosoma cruzi* these compounds undergo reduction activation by enzymes homologous with bacterial type I nitroreductases (NTRs). From the *Leishmania major* genome database, we have identified a protein (LmNTR) that could catalyse this reaction. Based on co-factor, oxygen-insensitive activity and substrate range, we demonstrate that the LmNTR displays many characteristics of its bacterial counterparts. Gene deletion studies revealed that LmNTR is essential to the insect and mammalian stages of *L. major*. Null mutant parasites could not be generated while loss of a single *LmNTR* allele in the insect form conferred resistance to a range of nitroaromatic compounds without affecting their growth rate or ability to differentiate into infectious forms. Heterozygous lines could not establish an infection *in vitro* using a tissue culture model, or *in vivo*, in mice. As NTRs are absent from most eukaryotes, with trypanosomatids being a major exception, we exploit this difference to evaluate a library of nitroaromatic compounds against *L. major* parasites. Biochemical screens against the purified enzyme revealed that several compounds were effective substrates for LmNTR, generating higher activities than nifurtimox, the clinically used nitro-based agent that targets trypanosomes. Using phenotypic screens, we demonstrated that growth inhibition mirrored enzyme activity, with the most potent compounds generating IC_{50}'s <100 nM whilst having little effect on mammalian cells. *L. major* NTR was shown to play a key role in parasite killing as heterozygous lines displayed resistance to the compounds. In conclusion, we have shown that LmNTR is essential to the parasite and by exploiting its prodrug activating properties, identified several novel agents that provide new lead structures to treat leishmanial infections.

Acknowledgments

I would like to thank Dr Shane Wilkinson, without whom I would not have had the opportunity to begin this project, and without his overwhelming support I would not have been able to produce this thesis. I am also greatly indebted to the laboratory of Prof Debbie Smith, particularly Dr Helen Price and Ms Barbara Smith, for giving me the techniques and cell lines necessary to complete this work. I am also grateful to Dr Karin Seifert for the mouse work, and for the rest of the guys and girls at the LSHTM for some great discussions. Thanks too go out to Dr Belinda Hall, Dr Chris Bot, and (one day Drs) Emma Louise Meredith and Ricardo de Padua for all their support, both intellectual and alcoholic. I am very grateful to all the members, past and present, of both office 4.36, and the flat at 17 Banbury Road, for keeping me grounded in reality (for the most part) and never letting a day go by without giving me something to belly-laugh about. On that note, cheers to Wu Shu Kwan and IGN.com *et al.* as well, without the hobbies of kickboxing and general nerdery my soul would have calcified long ago.

Finally, my most heartfelt gratitude goes to my girlfriend Catherine and to my family, particularly my parents Alan and Irene. Without their unquestioning love and support this would have been impossible to start, let alone complete. This is for you.

Contents

1. Introduction

1.1 Trypanosomatid diseases

Organisms belonging to the class Kinetoplastida, order Trypanosomatida represent a group of obligate protozoal parasites (Stevens *et al.* 2001). They are characterised by having a long slender morphology and single flagellum that together give the cell a corkscrew-like motion (*trypano* = borer and *soma* = body), and by their intricate mitochondrial genome that forms a discrete region called the kinetoplast. Typically Trypanosomatida are monoxenous, primarily infecting insects, although some are heteroxenous, having complex life cycles involving more than one obligatory host. In humans, they are responsible for several major infections including human African trypanosomiasis (HAT) and Chagas disease (that are caused by the trypanosomes *Trypanosoma brucei* and *Trypanosoma cruzi* respectively), while more than 20 species of *Leishmania* result in a spectrum of pathologies termed leishmaniasis. Leishmaniasis ranges from a self-limiting form called cutaneous leishmaniasis (CL), a disfiguring version known as mucocutaneous leishmaniasis (MCL) to visceral leishmaniasis (VL), a fatal infection (Wiser 2010). Together the trypanosomal and leishmanial diseases are endemic throughout tropical and sub-tropical regions, with more than 500 million living in areas deemed at risk. Current estimates indicate that more than 20 million people are infected by the causative agents resulting in about 75,000-100,000 premature deaths each year (Stuart *et al.* 2008). With no immediate prospect of a vaccine, drugs represent the only effective course of treatment available against trypanosomal and leishmanial infections. However, current drug regimes are problematic as many are toxic, most are costly, and resistance is becoming more of an issue (Wilkinson *et al.* 2009). Against this backdrop, the development of new cost-effective treatments is a priority, but given that trypanosomatid diseases mainly affect developing countries, these infections are not deemed commercially attractive by

pharmaceutical companies. This has resulted in HAT, Chagas disease and leishmaniasis being largely neglected in terms of drug development (Balasegaram *et al.* 2008).

1.2 History of leishmaniasis

Documentary evidence suggests that leishmaniasis has been plaguing the human race for thousands of years. Pathologies reminiscent of CL are depicted on tablets from the 7th Century BC Assyria, some of which are believed to be derived from earlier texts, while 1st Century AD pre-Inca pottery from Peru and Ecuador appear to show skin lesions and facial deformities similar to MCL (Cox 2002). The first descriptions of CL lesions and sores were made by Muslim physicians during the 10th century, with the first account in English attributed to Alexander Russell in 1756. However, it took another 150 years for a link to be established between these disease pathologies and the pathogen. For CL, initial observations by Peter Borovsky in 1898 (cited in Cox 2002) identified the causative agent as a protozoan and revealed the relationship between the parasite and the host tissue, although James Homer Wright (Wright 1903) is usually credited with this observation; Borovsky's work was not widely circulated and hence not internationally recognized. Identification of the causative agent of VL is more clear cut, with William Leishman (Leishman 1903) and Charles Donovan (Donovan 1903) independently discovering the parasite as small round or oval bodies, later known as Leishman-Donovan bodies, in the spleens of patients. However, it was Ronald Ross who recognized that the Leishman-Donovan bodies were in fact a new type of protozoan parasite which he named *Leishmania donovani* (Ross 1903).

1.3 Geographical distribution and epidemiology of leishmaniasis

Leishmaniasis is a blood borne disease transmitted through the blood feeding habits of female sandflies belonging to the subfamily Phlebotominae. These infections are endemic in 88

tropical and sub-tropical countries across the World where an estimated 350 million people are at risk of infection (Figure 1.3.1). Many (72) of these nations are designated as "developing countries" and here leishmaniasis represents a major public health problem in regions least able to deal with the associated economic burden. Current estimates indicate that up to 12 million people are infected by *Leishmania*. The most common and least severe form of the disease is CL, causing up to 1½ million new cases per year with 90% of infections occurring in Afghanistan, Algeria, Brazil, Iran, Peru, Saudi Arabia and Syria. The main species responsible for this pathology are *L. major*, *L. tropica*, *L. aethiopica* and *L. infantum* in the Old World or the *L. mexicana* complex, *L. braziliensis* complex and *L. chagasi* in the New World (Herwaldt 1999). The most severe and life threatening form of leishmaniasis is VL, caused mainly by *L. donovani*, *L. infantum* and *L. chagasi*. Each year about 500,000 people are infected by these causative agents, predominantly in 5 regions namely Bangladesh, northeast India, Nepal, Sudan and Brazil, resulting in 50,000 deaths (Croft *et al.* 2003, Alvar *et al.* 2006, Piscopo *et al.* 2006). These figures make VL the second most serious protozoal disease in terms of morbidity after malaria. In many cases, patients may not realise they are infected and it is estimated that for every symptomatic case there are up to 20 asymptomatic infections, each acting as a reservoir for the parasite (Badaro *et al.* 1986, Badaro *et al.* 1986).

Recently, as a result of military activity, population migration, modern medical practices (blood transfusions, organ/bone marrow transplants), congenital transfer, intravenous drug usage and global warming, leishmaniasis has emerged as a problem in non-endemic areas (Cruz *et al.* 2002, Wright *et al.* 2008, González *et al.* 2010, Pavli *et al.* 2010). Worryingly, VL/Human Immunodeficiency Virus (HIV) co-infections have become a major issue in 35 countries. In this context, HIV infection exacerbates the risk of developing active VL in

asymptomatic carriers and this currently accounts for around 70% of all VL cases in Portugal, Spain, Italy and France (Desjeux *et al.* 2003).

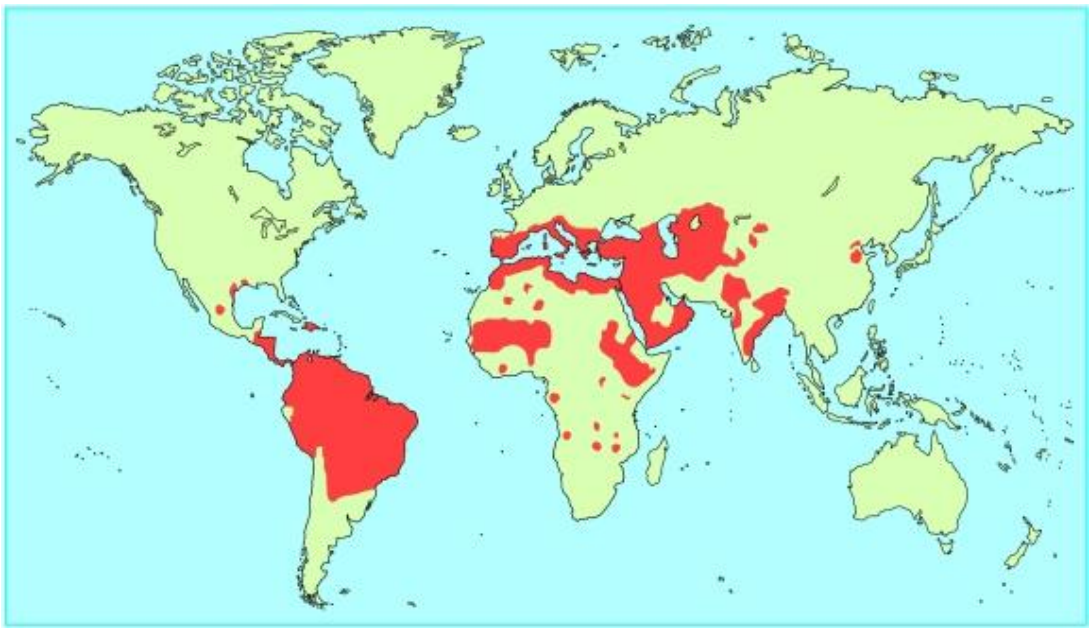

Figure 1.3.1: Geographical distribution of leishmaniasis
Regions highlighted in red indicate areas where leishmaniasis is endemic. Image taken from Davies *et al.* 2003.

1.4 *Leishmania* life cycle

The life cycle of *Leishmania* is complex, involving several morphologically distinct parasite forms in two diverse hosts (Figure 1.4.1). As with other trypanosomatid infections, leishmaniasis is spread by the haematophagous feeding habits of insect vectors. The agents responsible are pregnant, female sandflies with male flies taking no part in disease transmission. In the Old World, transmission occurs through flies belonging to the genus *Phlebotomus* while *Lutzomyia* is the main vector in the New World (Alvar *et al.* 1997). Transmission of *Leishmania* can be human to human, a mechanism that occurs predominantly in urban environments, or zoonotic, a route prevalent in rural area with animals such as dogs or cattle acting as important "reservoir hosts".

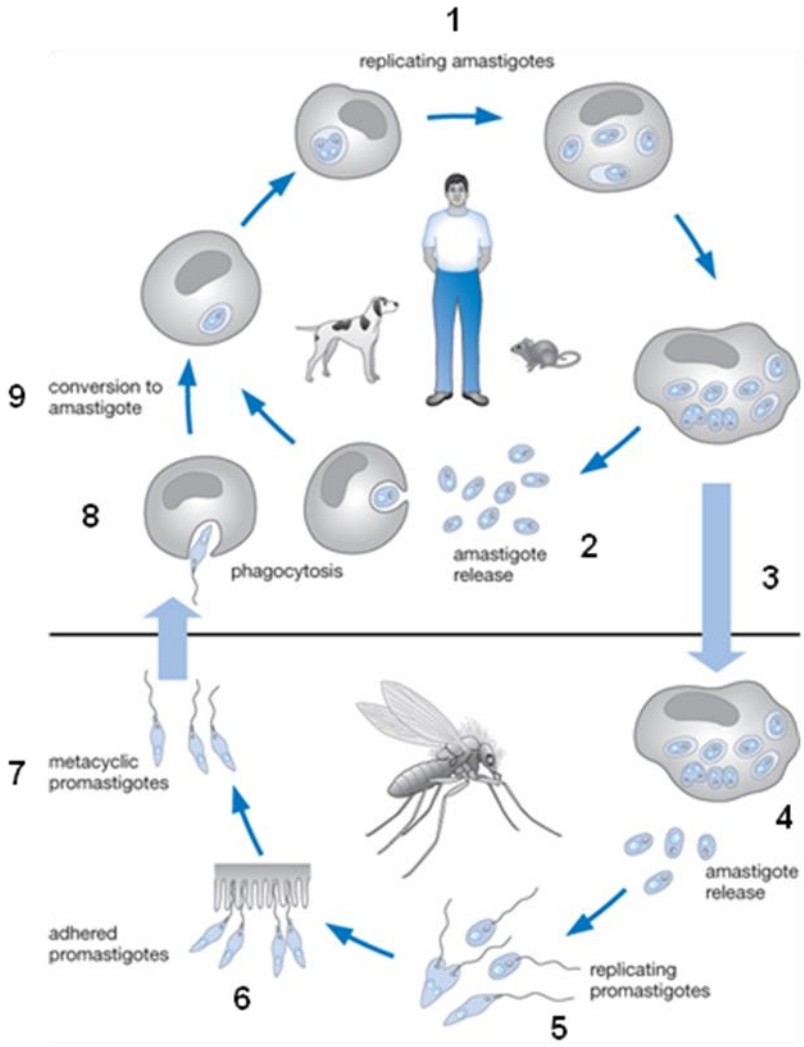

Figure 1.4.1: Life cycle of *Leishmania*
Leishmania amastigotes replicate by binary fission within the phagolysosome of mammalian macrophages (1). Eventually, these parasites rupture the mammalian cell and are released into the host's blood/lymph system where they are taken up by other macrophages by phagocytosis (2). Some infected immune cells are taken up by a female sandfly during her blood meal (3). In the insect's gut, the macrophage ruptures to release amastigotes (4) that differentiate into the promastigote life cycle stage (5). The promastigotes replicate by binary fission within the gut of the sandfly and adhere to the insect's gut epithelium (6). Some promastigotes differentiate into metacyclic promastigotes, detach from the gut epithelium and travel to the insect's cardia (7). During the fly's next blood meal the *Leishmania* metacyclic promastigote are transferred into the mammalian blood/lymph streams where they are engulfed by phagocytic macrophages (8). Within the mammalian cell the metacyclic cell differentiates into the amastigote form (9), and the cycle repeats. Image modified from Wiser (2010).

As a *Leishmania*-infected sandfly takes a blood meal, infective non-dividing metacyclic promastigote parasites present in the arthropod's cardia are regurgitated into the bloodstream

of the mammalian host. The nature of this reflux action is not fully understood although it appears to involve a dysfunctional stomodeal valve. This structure, which corresponds to an invagination between the insect's fore and mid gut, can be damaged by parasite expressed chitinases or blocked by a proteophosphoglycan gel-like substance known as the promastigote secretory gel (PSG) secreted by the protozoan (reviewed in Bates 2007). The outcome of either mechanism (damage or blockage) is that the stomodeal valve is not able to fully close and as a consequence, when an infected sandfly takes a blood meal, the ingested blood flows back along the insect's mouthparts, and back into the wound, washing metacyclic promastigote parasites into the mammalian host.

Once within the mammalian host, the parasite then invades macrophages or other phagocytic cells via opsonised phagocytosis (Mosser *et al.* 1992). Attachment of the pathogen to the host cell is mediated by the C3 component of the complement cascade which binds to the surface of the *Leishmania* cell. This is subsequently converted to an inactivated form, designated as iC3, by the zinc protease GP63 (Chaudhuri *et al.* 1988). The iC3 then functions as a ligand for complement receptors CR1 and CR3 on the mammalian immune cell with the interaction promoting uptake into the phagocytic cell. Generally, the first type of host cell to respond to leishmanial infection are the polymorphonuclear neutrophil granulocytes (PMN), possibly in response to chemotactic factors produced by the metacyclic promastigote (van Zandbergen *et al.* 2002). Once internalised, *Leishmania* has been reported to inhibit spontaneous death of the PMN cells, prolonging their life for 2-3 days as an apoptotic neutrophil (Aga *et al.* 2002). This allows the infected PMN cell to recruit and be ingested by macrophages. The macrophage then becomes the main host cell for the *Leishmania* parasite. This "Trojan horse" strategy (Laskay *et al.* 2003) allows the uptake of *Leishmania*, via apoptotic PMN cells (Fadok *et al.* 1998, Sun *et al.* 2001), without the activation of the macrophages antimicrobial

functions (Meagher *et al.* 1992). Additionally, the PSG secreted by the parasites has been shown to alter the L-arginine catabolism of the macrophages, resulting in the production of polyamines necessary for parasite proliferation within the mammalian cell (Rogers *et al.* 2009).

Once in the macrophage, the metacyclic promastigote is initially compartmentalised in the phagosome. Host cell lysosomes then fuse with this structure resulting in formation of the phagolysosome (also called the parasitophorous vacuole). The associated drop in pH that occurs during this process is believed to trigger differentiation of the metacyclic promastigote parasite into the intracellular amastigote form. This *Leishmania* stage loses its extended flagellum, becomes ovoid in shape and begins to divide by binary fission within the host cell. For reasons that have yet to be fully explained, possibly due to population density, the infected macrophage ruptures releasing amastigotes into the host's bloodstream. These infective parasites can then invade other macrophages thus propagating the infection in the mammalian host, a cycle that will keep going until the host resolves the infection, is cured via chemotherapy or the patient dies.

In some cases, *Leishmania*-infected macrophages can be transmitted back into the female sandfly when they take a blood meal. Once ingested, the infected macrophages burst releasing the amastigotes into the lumen of the insect's mid-gut. In this environment, the parasites differentiate into non-infectious promastigotes that have the typical trypanosomatid body shape: long slender morphology and single flagellum. This pathogen form attaches to the insect gut epithelium and begins to replicate by binary fission. Attachment to the insect gut wall is a key step in this part of the *Leishmania* life cycle as it prevents the promastigote from being excreted in the arthropod's faeces. This interaction is mediated by parasite

lipophosphoglycans (LPG) that form a glycocalyx coat that covers the entire parasite surface, including the flagellum. LPG contains a relatively short galactose-mannose-phosphate core with galactose side chains coupled to a glycophosphatidylinositol anchor that links the molecule to the cell membrane. The galactose side chains bind with lectins found on insect epithelial cells, such as the insect galectin PpGalec (Kamhawi *et al.* 2004), resulting in attachment of the parasite to the lining of the mid gut. Additionally, LPG serves to protect the parasite from digestive activities found in this hostile environment. Occasionally, possibly during a cell division event, non-dividing, infective metacyclic promastigotes are formed. Here, the LPGs nearly double in length, primarily through expansion of the galactose-mannose-phosphate core, and the galactose containing side chains become capped at their termini with arabinosyl residues resulting in disassociation of the LPG/lectin complex. The metacyclic is then released into the lumen of the insect's gut and migrates to the cardia ready to be transmitted back to another mammalian host.

1.5 Pathology, diagnosis and treatment

The term leishmaniasis covers a spectrum of disease pathologies caused by more than 20 different species of *Leishmania* (Alvar, Canavate *et al.* 1997, Desjeux 2004) ranging from the disfiguring cutaneous and mucocutaneous forms to the life threatening visceral type.

1.5.1 Cutaneous leishmaniasis

Cutaneous leishmaniasis, also known as Baghdad Boil, Oriental Sore, Jericho Buttons and White Leprosy, starts with a red lesion forming at the site of the sand fly bite. Dependent on the *Leishmania* species, the wound can develop directly into an ulcer with a raised border or may form a nodular structure that then progresses into the ulcerated state. The ulcer may remain open, producing a wound classified as a "wet" lesion, as typified by infections caused

by *L. major*, or crust over to form a "dry" lesion characteristic of *L. tropica* (Figure 1.5.1). Generally, the ulcers will self-heal often resulting in a permanent disfiguring scar, with the whole process taking between 2-6 months for *L. major* to 6-15 months for *L. tropica, L. panamensis* or *L. braziliensis* infections (Reithinger *et al.* 2007).

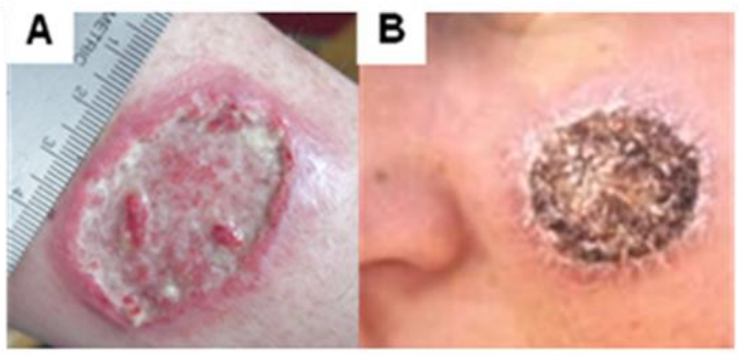

Figure 1.5.1: Skin lesion and scarring caused by cutaneous leishmaniasis
Wet (A) and dry (B) lesions indicative of cutaneous leishmaniasis present on the forearm and face, respectively, of the patients. Images provided by L. Harris (A) and Aytekin *et al.* 2006 (B).

Diagnosis of CL in endemic areas can be assessed by noting the clinical features (skin lesions) although definite detection of the parasite is required to categorically confirm infection. This can be accomplished rapidly and cheaply by the microscopic detection of cytoplasmic-stained (Leishman or Giemsa) amastigotes in macrophages from lesion scrapings or aspirates (Mehregan *et al.* 1999). However, harvesting samples is often painful to the patient and the identification of amastigotes as Leishman-Donovan bodies are often difficult to see without expert training. An alternative is the indirect serological techniques such as the leishmanin skin test (LST). This involves the intradermal injection of fixed promastigote cells or extracts and monitoring patients for a delayed-type hypersensitivity reaction (Weigle *et al.* 1991). Such approaches generally have higher sensitivities than the direct microscopic approaches, although false positive reactions are common.

Due to the self-healing nature of CL, treatment is usually reserved for patients where the lesion is particularly severe, where complicating secondary infections may arise or when there is a risk of developing MCL. In these cases, recommended treatments include intralesional or parenteral antimonials (sodium stibogluconate and meglumine antimoniate) or pentamidine (Blum *et al.* 2004).

1.5.2 Mucocutaneous leishmaniasis

Figure 1.5.2: Damage to the nasal pharynx region caused by mucocutaneous leishmaniasis
Image sourced from the "Illustrated lecture notes on Tropical Medicine" provided by the Institute of Tropical Medicine, Antwerp.

Mucocutaneous leishmaniasis, also known as espundia or American tegumentary leishmaniasis, is common in South America. It is most frequently associated with *L. braziliensis* but other species such as *L. panamensis*, *L. guyanensis*, *L. amazonensis*, *L. major*, *L. tropica*, and *L. infantum* are reported to mediate this most disfiguring form of the disease (Reithinger, Dujardin *et al.* 2007). MCL begins in the same way as CL, with a sore developing at the site of the insect bite and in 95-97% cases the disease does not progress any further. However, in the remaining situations, the parasites can metastasise via the lymph or blood to other sites including to mucocutaneous junctions (the nasal pharynx and the genitourinal area). Here, the mucosal tissues initially become inflamed followed by ulceration

that results in disfiguring lesions (Figure 1.5.2) (Marsden 1986) with the manifestation of MCL taking years to appear after the primary CL ulcer has healed. In many cases, the disease is complicated by secondary infections potentially leading to increased mortality. Diagnosis is carried out using similar approaches as to that described for CL *i.e.* clinical signs and symptoms, microscopical identification of amastigotes in specimens and LST; with treatment involving a 28 day course of pentavalent antimony or amphotericin B (Palumbo 2010). The prognosis depends on severity of the disease.

1.5.3 Visceral leishmaniasis

Figure 1.5.3: Pathology of visceral leishmaniasis
The markings outline the enlarged liver and spleen. Image sourced from the "Illustrated lecture notes on Tropical Medicine" provided by the Institute of Tropical Medicine, Antwerp.

Visceral leishmaniasis, also known as "kala azar", is the most severe leishmaniasis pathology, which if untreated can prove fatal. It is caused mainly by *L. donovani* and *L. infantum* which mediate the systemic spread of infection particularly to the spleen, liver, bone marrow and lymph nodes. The incubation period for VL can vary, ranging from 10 days to 34 months, although in most cases it takes 3-8 months for symptoms to appear (Stone *et al.* 1952, De Alencar 1958, Manson-Bahr *et al.* 1964). The most common clinical indicators

associated with VL include fever, cough, abdominal pain, diarrhoea, epistaxis (nosebleed), pancytopenia (shortage of all blood cells) leading to extreme anaemia, and cachexia (a state of general ill health typified by weight loss, loss of appetite and physical atrophy). Probably the most characteristic symptom of VL, however, is an enlarged abdomen resulting from a grossly enlarged spleen and liver (splenohepatomegaly) (Figure 1.5.3), eventually resulting in the complete loss of function in these organs (Guerin *et al.* 2002). As a systemic infection, death may result regardless of whether a patient is treated or not and often is as a result of secondary infection, although chances of survival are greatly increased with appropriate treatments (Gorski *et al.* 2010).

Diagnosis of VL usually involves the microscopical examination of spleen or bone marrow aspirates following cytoplasmic staining or by *in vitro* culturing of promastigote parasites from these clinical samples. Rapid seriological approaches such as the K39 dipstick and direct agglutination tests are available but due to cost are not generally used in many regions. Several drugs including pentavalent antimonials, liposomal amphotericin B, paromomycin and miltefosine are now available but the use of these is problematic (Sundar *et al.* 2005).

After recovery from VL caused by *L. donovani*, patients sometimes go on to develop post-kala-azar dermal leishmaniasis (PKDL). PKDL results in small measles-like lesions across the body which are usually self healing but can persist for years. PKDL patients are particularly common in areas of India where anthroponotic transmission is prevalent, with these individuals considered an important reservoir host for the VL-causing parasite (Ramesh *et al.* 2007).

1.6 Anti-leishmanial drug treatments

The frontline treatments used against leishmaniasis are pentavalent antimonials but their use is problematic: these therapies are generally toxic with clinical resistance on the rise, and often require medical supervision when administered (Sundar 2001, Guerin, Olliaro *et al.* 2002). Additionally, there is a wide variation in species sensitivity. Recent progress has been made in developing new leishmanicidal agents with several compounds such as amphotericin B, paromomycin and miltefosine coming to market. However, there are issues associated with these as some have teratogenic properties (thus limiting who can use these treatments), toxicity and cost (Berman 2005, Croft *et al.* 2012).

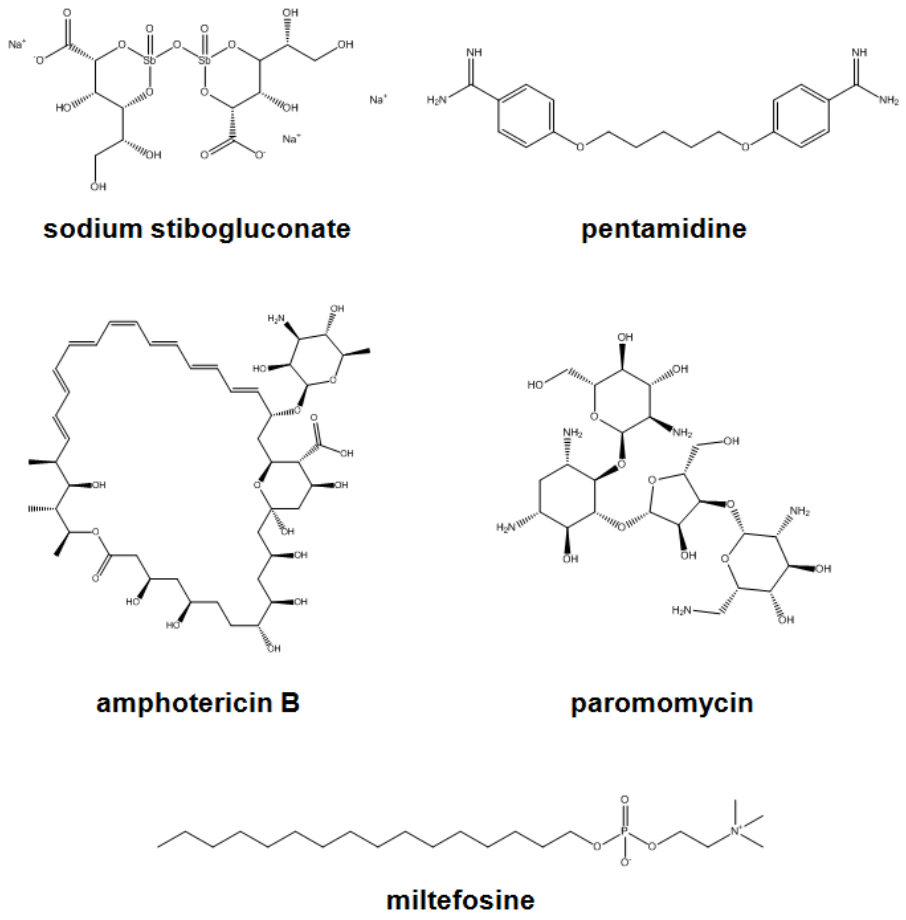

Figure 1.6.1: Structures of drugs used against leishmaniasis

1.6.1 Pentavalent antimonial drugs

Antimonial-containing compounds have been used as the frontline treatment of leishmaniasis for nearly 70 years following their introduction in 1945. Several variants are available including sodium stibogluconate (Pentostam®) or meglumine antimoniate (Glucantime®) with cheaper generic brands now in circulation (Moore *et al.* 2001). These are administered as a slow intravenous infusion (Pentostam®; manufactured by GlaxoSmithKline) or intramuscular injection (Glucantime®, manufactured by Aventis) at 20 mg kg^{-1} day^{-1} for 20-40 days depending on the *Leishmania* species and disease pathology (Guerin, Olliaro *et al.* 2002, Minodier *et al.* 2007). This class of treatments has a number of side effects, exacerbated by the long course treatment. These side effects include but are not limited to cardiotoxicity (in 7-10% of VL patients in Bihar state), hepatitis, pancreatitis, myalgias, fatigue, headache, nausea and can also result in treatment-related death (in 5-10% of VL patients in Bihar state) (Wiser 2010). Resistance to these drugs is steadily rising with this being a particular problem in certain states of India. For example, up to 60% of VL cases in Bihar are non-responsive to antimonial-based therapies (Croft *et al.* 2006).

The precise mode of action for Pentostam® and Glucantime® is unknown but both appear to function as prodrugs relying on conversion of the antimony atom from its inactive pentavalent state (SbV) into its cytotoxic trivalent (SbIII) form. Whether this activation step occurs in the mammalian host cell or the parasite is unclear. It has been shown that the *Leishmania* amastigotes express several enzymes such as thiol-dependent reductase and arsenite reductase that can catalyse this reaction (Denton *et al.* 2004, Zhou *et al.* 2004) although quite how the pentavalent antimonial compound is transported into the intracellular parasite is unknown. In contrast, uptake of the trivalent form by the parasite may involve an

aquaglycerporin (Gourbal *et al.* 2004), although how the SbV prodrug is activated within the host cell or at the amastigote surface remains unknown.

Based on laboratory selected drug-resistant parasites, it has been postulated that once activated, antimonials mediate their leishmanicidal activity by interfering with the pathogens thiol biology. Cells selected for antimonial resistance display elevated levels of trypanothione, a parasite specific conjugate consisting of two molecules of glutathione linked together by spermidine (Fairlamb *et al.* 1985). These cells possess an amplification of genes associated with trypanothione synthesis and/or elevated levels of a metal-thiol efflux pump (Dey *et al.* 1996, Grondin *et al.* 1997, Haimeur *et al.* 1999, Haimeur *et al.* 2000). Additionally, inhibition of the trypanothione synthesis pathway in resistant lines results in reversal of this phenotype (Haimeur, Brochu *et al.* 2000). Together this has led to the proposal that the antimonial drug interacts with trypanothione to form a metal-thiol conjugate. Elevation in the levels of trypanothione and/or the metal-thiol efflux pump results in this complex being rapidly and efficiently extruded from the intracellular milieu before it (either the SbV or SbIII form) can interact with protein thiol targets such as trypanothione reductase (Ouellette *et al.* 2004).

1.6.2 Pentamidine

Pentamidine is an aromatic diamidine first used to treat leishmaniasis in 1952. It is administrated through a series of intravenous or intraperitoneal injections at 4 mg kg^{-1} per dose, with 15-30 doses given over a course of 3-4 weeks (Guerin, Olliaro *et al.* 2002). However, the widespread use of pentamidine against leishmaniasis has been limited primarily due to the route of its administration and its off target effects: pentamidine can lead to serious side effects including tachycardia, hypotension, hyperglycemia and hypoglycaemia and less

severe toxicities that promote nausea, vomiting and diarrhoea (Helmick *et al.* 1985, Jha *et al.* 1991, Thakur *et al.* 1991, Berman 1997). As a result this diamidine is only recommended for use in locations where antimonial resistance is prevalent or where antimonials cannot be given to a patient (Nacher *et al.* 2001).

The precise mode of action of pentamidine is unclear. It is thought to be taken up via a carrier protein which has higher affinity for the drug in amastigotes than it does in promastigotes although the precise nature of this transporter has yet to be determined (Coelho *et al.* 2007). It has been suggested that once within the parasite, pentamidine enters the mitochondria via a permease where this organic cation binds to the negatively charged, AT rich sequences of the DNA network of kinetoplast (Cory *et al.* 1992, Basselin *et al.* 1998). This interaction promotes disintegration of the mitochondrial genome and consequently triggers cell death. Some strains of *Leishmania* particularly in India have developed resistance to this drug possibly due to a lack of accumulation of pentamidine in the mitochondrion of resistant cells (Basselin *et al.* 2002, Mukherjee *et al.* 2006).

1.6.3 Amphotericin B

This polyene agent, originally developed as an anti-fungal, has been shown to be highly effective in the treatment of antimonial-resistant VL (Thakur *et al.* 1996). In fact, it is the drug of choice in India due to the emergence of resistance to other classes of treatments. It is administered intravenously, at 7-10 mg kg^{-1} for up to 20 days. This dose is limited by amphotericin B's toxicity, with the observed side effects including uraemia (accumulation of nitrogen-based waste products in the blood), nephrotoxicity (kidney toxicity), anaemia and hypokalaemia (low blood potassium) (Davidson 1998, Bates *et al.* 2001, Harbarth *et al.* 2002). Additionally, it requires slow infusion over several hours, thus increasing costs due to

the requirement for hospitalisation (Eriksson *et al.* 2001). The mode of action of amphotericin B is proposed to involve binding to ergosterol present in the *Leishmania* cell membrane, with reduction in the relative levels of ergosterol in *L. donovani* mediating resistance to amphotericin B in the parasite (Mbongo *et al.* 1998). This promotes formation of aqueous and non-aqueous (ionic) pores that leads to osmotic instability and destruction of the ion balance of the cell subsequently followed by cell death (Cohen 2010).

Recently, different liposomal and micelle amphotericin B formulations such as AmBisome® have been developed resulting in treatments that have improved efficacy against *Leishmania* and significantly reduced toxicity (Bern *et al.* 2006). AmBisome® is intravenously injected at 10 mg kg^{-1} in 5-10 doses over 10 days. However, AmBisome® is very expensive, with a course of the drug costing up to US$ 2500 (each 50 mg ampoule costs US$ 18, Meheus *et al.* 2010), thus restricting their use in developing countries. Promisingly however, there are currently public-private partnerships in effect with the pharmaceutical company Gilead, in an effort to reduce the cost of AmBisome® to the developing world.

1.6.4 Miltefosine

Miltefosine is an orally administrated alkyl phosphocholine-based drug originally synthesized as an anti-cancer drug but shown to have good antiparasitic properties (Unger *et al.* 1989). It has excellent *in vivo* activity against *L. donovani*, with clinical trials revealing it to be highly effective against both CL and VL (Croft *et al.* 1987, Soto *et al.* 2006, Bhattacharya *et al.* 2007). Currently, miltefosine is registered for use in India (2002), Germany (2004) and Colombia (2005). Drug regimes take 28 days to complete at 100 mg kg^{-1} day^{-1}, and the observed side effects, typically nausea and diarrhoea, are generally mild and transient (Sundar *et al.* 2004). However, a significant drawback in the use of miltefosine is

teratogenicity issues, prohibiting its use in women of child-bearing age unless they are taking contraceptives (Berman 2005).

Precisely how miltefosine mediates its leishmanicidal activity is poorly understood, although suggestions accounting for its mode of action have been proposed. One hypothesis suggests that it may target alkyl-specific-acyl CoA acyltransferase, a key enzyme involved in ether lipid formation (Lux *et al.* 2000), with inhibition of this enzyme leading to plasma membrane instability. Alternatively, miltefosine may promote an apoptotic-like pathway that triggers parasite killing, but how this occurs has yet to be fully elucidated (Verma *et al.* 2004).

1.6.5 Paromomycin

Paromomycin is an aminoglycoside antibiotic derived from *Streptomyces rimosus* (Davidson *et al.* 2009). It is available in two formations as a 20% paromomycin topical ointment used in cases of CL (Stanimirovic *et al.* 1999), or as intramuscular injections to treat VL. In the case of VL, the standard dose is 15 mg kg^{-1} day^{-1} for 21 days, though an increased dose of 20 mg kg^{-1} day^{-1} for 21 days or increased duration of 15 mg kg^{-1} day^{-1} for 28 days can boost efficacy for some patients (Musa *et al.* 2010). Paromomycin is thought to mediate its leishmanicidal activity by inhibition of protein synthesis and it has been shown that it interacts with ribsomes, and can induce misreading of codons on mRNA transcripts on the leishmanial ribosome, preventing accurate translation and promoting the synthesis of mutant proteins (Maarouf *et al.* 1995, Fernandez *et al.* 2011). Accumulation of these mutant proteins might then compromise the survival of the parasite (Fernandez, Malchiodi *et al.* 2011). Although this course of treatment appears to be very promising, confusing and conflicting data in the literature show extreme variations in efficacy. For example, a recent meta-analysis of CL

treatment data (Kim *et al.* 2009) found percentage cure figures ranging from 4% (Moosavi *et al.* 2005) to 93% (Correia *et al.* 1996).

1.6.6 Imiquimod

A separate category of antileishmanials modulate the immune system in order to allow the patient to repel the infection, usually in conjunction with other drugs listed previously. The most commonly used of these is the imidazoquinoline imiquimod. This compound has exhibited antileishmanial properties through the induction of nitric oxide production in macrophages in experimental models (Buates *et al.* 1999). Furthermore, clinical studies have shown potential in using a topical imiquimod cream together with pentavalent antimonials (Arevalo *et al.* 2001, Miranda-Verástegui *et al.* 2005, Firooz *et al.* 2006), leading the World Health Organisation to include the use of imiquimod with pentavalent antimony as a second-line therapy in New World CL in its guidelines (WHO 1999).

1.7 *Leishmania* cell biology

Leishmania are microorganisms that share a number of key cellular features with other eukaryotes – they contain a nucleus, endoplasmic reticulum, Golgi apparatus *etc.* However, as with other members of the Kinetoplastida class of protozoa, they also harbour a number of unusual structures whose role/number can change during the course of the parasite's complex life cycle (Figure 1.7.1): for example, a lysosomal-like organelle named the megasome is present only in the amastigote form of certain species of *Leishmania* (Alexander *et al.* 1975). A few of these unusual features are discussed below (though this is not an exhaustive discussion).

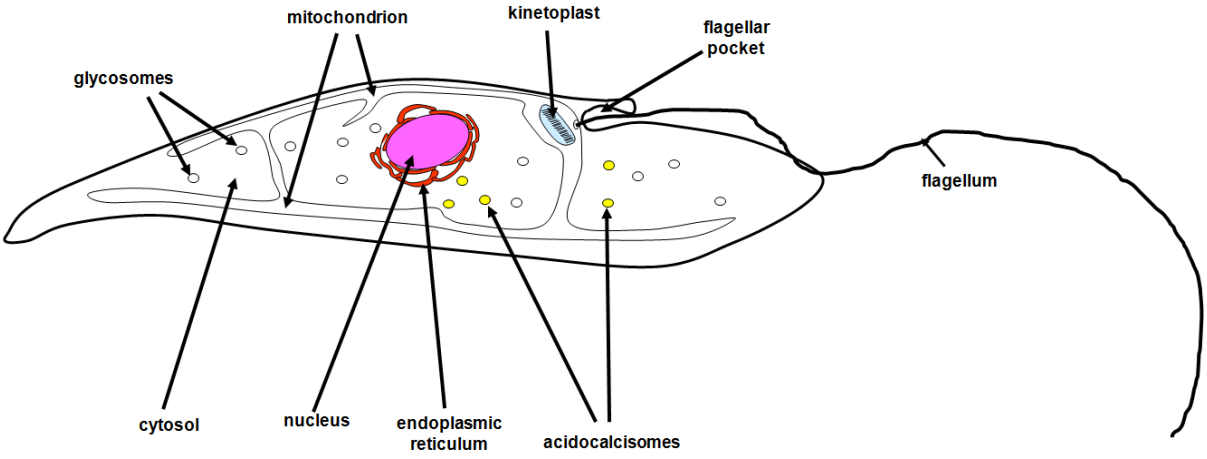

Figure 1.7.1: Schematic representation of a *Leishmania* promastigote cell
Important organelles are highlighted, including the glycosomes, flagellum and flagellar pocket, and the single mitochondrion with kinetoplast, supplied by Dr S. Wilkinson.

1.7.1 Glycosome

Glycosomes are small, spherical (~0.27 μm in diameter) organelles that contain an electron dense, proteinaceous matrix bounded by a single lipid bilayer. Evolutionarily, they are related to glyoxysomes of plants and peroxisomes of all other eukaryotes, with many of the enzymes and permeases typically found in these other microbodies also found in glycosomes (Borst 1989). As such, glycosomes fulfil many of the functions of peroxisomes including protection against oxidative stress, β-oxidation of fatty acids and ether lipid synthesis (Opperdoes *et al.* 1984, Wiemer *et al.* 1996, Heise *et al.* 1997, Wilkinson *et al.* 2002, Dufernez *et al.* 2006). Uniquely, they are the site where a number of important metabolic pathways including purine salvage, pyrimidine biosynthesis, gluconeogenesis and pentose phosphate pathway are compartmentalised (reviewed in Michels *et al.* 2006). Additionally, glycosomes also contain the first seven enzymes involved in glycolysis. Compartmentalisation of this pathway, coupled with the low permeability exhibited by the glycosomal membrane, allows for segregation of metabolites between this organelle and the cytosol, features that may account for the very high glycolytic fluxes displayed by Kinetoplastid parasites (Opperdoes *et al.*

1976, Fairlamb *et al.* 1980). However, it must be noted that most glycosomal studies have been conducted on *T. brucei*, particularly the bloodstream-form. As this parasite stage lacks mitochondrial cytochrome-dependent respiratory chains, it effectively behaves as an anaerobe relying on substrate level phosphorylation (*i.e.* glycolysis) for ATP production. Consequently, *T. brucei* bloodstream-form cells contain up to 240 glycosomes, which representing around 4-8 % of the cell's volume (Opperdoes, Baudhuin *et al.* 1984). For other trypanosomatids, as few as 10 glycosomes per cell have been recorded (*L. mexicana* amastigotes, Coombs *et al.* 1986) suggesting that these organelles potentially have subtle functions in different parasites.

1.7.2 Flagellum and flagellar pocket

Several life cycle stages of *Leishmania* possess a single whip-like appendage called the flagellum that emerges from the cell body via an invagination of the plasma membrane known as the flagellar pocket. The flagellum has a 9+2 microtubule axoneme, as found in other flagellated eukaryotes, supported by a paracrystalline structure called the paraflagellar rod unique to trypanosomatids (Ginger *et al.* 2008, Ralston *et al.* 2008). In addition to functioning as a locomotory organelle, the flagellum also has a series of other roles ranging from acting as a sensor that samples the surrounding environment, as an attachment site (replicating promastigotes readily adhering to insect gut epitheilial cells) and polarity marker (intracellular amastigote cells use their short stubby flagellum to orientate themselves in the macrophage phagolysosomes) (Warburg *et al.* 1989, Piper *et al.* 1995, Burchmore *et al.* 2003, Figarella *et al.* 2007, Bates 2008, Ginger, Portman *et al.* 2008, Gluenz *et al.* 2010).

The flagellar pocket is a separate and specialised compartment in its own right, having a distinct microtubular structure from the rest of the plasma membrane (Lacomble *et al.* 2009).

In *T. brucei*, the normal plasma membrane, known as the "pellicular plasma membrane", contains an underlying dense network of microtubules known as the subpellicular microtubules which are largely absent from the flagellar pocket (Lacomble, Vaughan *et al.* 2009). This arrangement facilitates vesicular trafficking into (endocytosis) and out of (exocytosis) the cell, with the structure playing key roles throughout the life cycle of the all trypanosomatid parasites ranging from immune evasion, mammalian cell invasion to nutrient/co-factor uptake (Overath *et al.* 1997, McConville *et al.* 2002, Kima 2007, Silverman *et al.* 2010).

1.7.3 Mitochondria and kinetoplast

All *Leishmania* contain a single, highly branched mitochondrion that has a dense matrix and sparse, thin, irregularly distributed cristae (de Souza *et al.* 2009). Like other mitochondria, they contain systems for oxidative energy production, as well as for the synthesis of iron-sulphur clusters and key metabolites (ter Kuile 1994, Kakkar *et al.* 2007, Saunders *et al.* 2010, Alfonzo *et al.* 2011, Serricchio *et al.* 2011). Mitochondria are also considered as a reservoir for components involved in apoptosis (programmed cell death) (Shaha 2006).

As with mitochondria from other eukaryotes, the *Leishmania* organelle contains its own genome. This genome is housed in a defined bar-like region called the kinetoplast which consists of a network of concatenated, circular DNA, called the kDNA. Based on size and copy number kDNA can be split into two types. One set of kDNAs, known as maxicircles, are between 20-40 kb in size with approximately 40-50 copies per mitochondrion. They contain several genes found in the mitochondrial genomes of other organisms such as rRNA genes, and genes encoding for metabolic enzymes that function in this organelle. In contrast, the second type of kDNA, known as minicircles, are between 0.5-1.5 kb in size and have a

high (5000-10,000) copy number per genome (Simpson 1973, Liu *et al.* 2005, de Souza, Attias *et al.* 2009). At a sequence level they are highly variable and encode for specialised RNA molecules called guide RNA (gRNA) (Stuart *et al.* 2005).

In many cases the genes present on the maxicircles are incomplete and classed as pseudogenes (also known as cryptogenes). In a process known as RNA editing, the "defective" genes undergo transcription to form a pre-mRNA (Perry *et al.* 1991, Benne 1993). Under the direction of specific gRNAs encoded by minicircle kDNAs, the pre-mRNA serves as a template for a protein complex called the "editosome" (Blum *et al.* 1990, Worthey *et al.* 2003). This acts to modify the transcript by the insertion or deletion of uridine residues to form a mature mRNA which is subsequently transcribed to produce a functional mitochondrial protein (Alfonzo *et al.* 1997).

1.8 Trypanosomatid genetics

1.8.1 Trypanosomatid genomics

In 2005, the *L. major*, *T. brucei* and *T. cruzi* genome sequences were published (Berriman *et al.* 2005, El-Sayed *et al.* 2005, Ivens *et al.* 2005). Comparison of their gene content and organisation revealed that these three genomes share a conserved core of around 6200 genes arranged in long, syntenic polycistronic clusters (El-Sayed *et al.* 2005) (Figure 1.8.1). Most differences between these genomes were found in genes that encode for species-specific life cycle adaptations and in their retroelement content (El-Sayed, Myler *et al.* 2005).

The genome of *L. major* (strain MHOM/IL/80/Friedlin) is diploid, with a haploid content of 32,816,678 bp and having on average a 59.7% GC content. These sequences are arranged across 36 chromosomes that vary in size from 0.3 to 2.5 Mb and consists of 911 RNA genes,

39 pseudogenes, and 8272 protein-coding genes (Wincker *et al.* 1996). Of these, 3083 protein-coding genes appear to fall within 662 putative families of related genes, with a mean gene density of 252 genes per Mb (Ivens, Peacock *et al.* 2005). Recently, the genomes of several other *Leishmania* species (*L. infantum*, *L. braziliensis*, *L. mexicana* and *L. tarentolae*) have been sequenced with these all displaying a high degree similarity in terms of gene sequence and order to each other (Peacock *et al.* 2007, Rogers *et al.* 2011, Raymond *et al.* 2012).

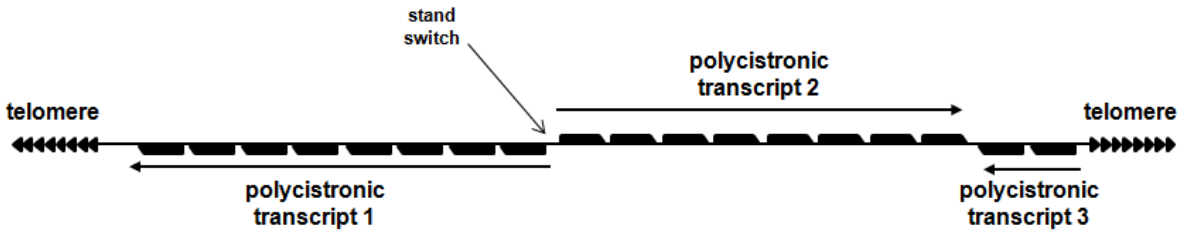

Figure 1.8.1: Schematic diagram of *Leishmania* chromosomal architecture
A standard *Leishmania* chromosome contains many long, unidirectional, polycistronic arrays of genes. At several points along the chromosome there are "strand switch" sites, both convergent and divergent, where the direction of the polycistronic array changes.

1.8.2 Trypanosomatid gene expression

Due to the heteroxenous nature of many kinetoplastid (*T. brucei*, *T. cruzi*, and *Leishmania spp*) parasites, large alterations in protein expression levels are required in order for these pathogens to survive the different environments they encounter during their complex life-cycles. Unlike most eukaryotes, the regulation of gene expression by these parasites generally does not rely upon transcription through the activation/repression of gene specific promoter regions. Instead, the arrangement of genes in the trypanosomatid genomes appears to facilitate the transcription of long, continuous, unidirectional, polycistronic arrays, with regulation of gene expression mainly occurring at a posttranscriptional level (Clayton *et al.* 2007). The genes within these arrays generally have unrelated functions and therefore do not conform to the operon arrangement as observed in prokaryotes (Clayton 2002). The gene arrays are separated by short AT-rich "strand switch regions", or SSRs, which have a

distinctive secondary structure and are postulated to be the site where transcription is initiated, possibly driven by epigenetic factors (Tosato *et al.* 2001, Puechberty *et al.* 2007; Siegel *et al.* 2009, Thomas *et al.* 2009). Through a process of *trans*-splicing and polyadenylation, the polycistronic mRNA transcripts are processed into functional, single gene mRNA transcripts ready for translation (Clayton and Shapira 2007 and Figure 1.8.2). The fine tuned expression necessary for the different parasite life cycle stages, as exemplified by genomic and proteomic studies (Cohen-Freue *et al.* 2007, Pescher *et al.* 2011), can be regulated via a number of different mechanisms ranging from the processing of the matured mRNA, its subsequent export from the nucleus, the stability of the mature mRNA, regulation of translation, and then finally regulation of the protein itself, through post-translational modification, for example (Clayton and Shapira 2007, Kramer 2012).

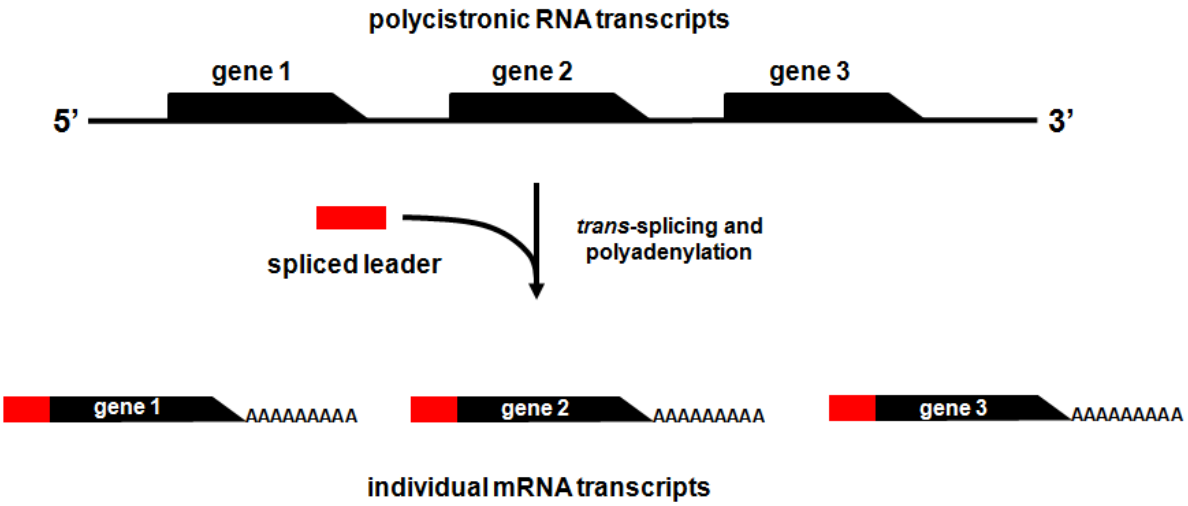

Figure 1.8.2: Schematic diagram showing the posttranscriptional processing of polycistronic RNA into functional mRNA in *Leishmania*.

1.8.3 Genetic manipulation of *Leishmania*

Currently, a substantial "toolbox" of reverse genetic techniques is available to investigate the biology of *Leishmania* genes within the parasite itself (Roberts 2011). These methodologies rely on using electroporation-based approaches to introduce genetic material into the target organism, with recent "nucleofection" developments in trypanosomes greatly increasing

efficiencies (Alsford *et al.* 2011, Coustou *et al.* 2012). DNA constructs, designed to facilitate gene deletion, over expression and protein localisation, can either integrate into the nuclear genome by homologous recombination or be maintained as episomes – for example, pTEX (Kelly *et al.* 1992). To generate stable cell lines, recombinant parasites are selected by exerting an appropriate drug pressure such that only cells engineered to express an appropriate drug resistance cassette survive. Several selectable marker systems are now in use with *Leishmania* and include G418/neomycin phosphotransferase, blasticidin/blasticidin-S deaminase, puromycin/puromycin N-acetyl-transferase and hygromycin/hygromycin phosphotransferase (Cruz *et al.* 1990, Cruz *et al.* 1991, Freedman *et al.* 1993, Goyard *et al.* 2000). To drive expression of such markers, or other genes of interest, correct mRNA processing must occur within the parasite. This is achieved by incorporating *trans*-splicing and polyadenylation DNA sequences either side of the marker gene. Such sequences are generally derived from homologous (the *Leishmania* species under study) or heterologous (from other *Leishmania* or *Trypanosoma* species) housekeeping genes such as α-/β-tubulin or glyceraldehyde 3-phosphate dehydrogenase (GAPDH).

Using transfection techniques, there are many ways in which the expression level of a target gene can be modulated. Exogenous copies of such a gene can be cloned into either integrative or episomal expression vectors that when introduced into the parasite result in expression of the target DNA sequence (Wilkinson *et al.* 2008). This basic approach can be modified such that tagged versions of the protein can be expressed with the recombinant lines facilitating sub-cellular location or protein purification. Several peptide tags are available for a selection of different applications including purification/affinity tags such as the poly(His) tag, fluorescent tags such as the green and red fluorescent proteins (GFP and RFP), and epitope tags such as 9E10 (c-myc) and the HA-tag (Fritze *et al.* 2000, Liu *et al.* 2001, Chen *et al.*

2005). Alternatively, a gene of interest can be deleted from the parasite genome through targeted, homologous gene replacement (Wilkinson, Taylor *et al.* 2008). Due to the diploid nature of the *Leishmania* parasites, any single copy gene would have to go through two separate rounds of gene replacement to completely remove the gene from the genome (Cruz and Beverley 1990, Cruz, Coburn *et al.* 1991). However, attempting this on essential genes often results in selection of aberrant cells that have undergone chromosomal amplification or aneuploidy (such as trisomy), due to the unusual plasticity of the *Leishmania* genome (Bastien *et al.* 1992; Cruz *et al.* 1993). Against this backdrop, null mutant lines can be constructed in cells expressing an ectopic copy (integrated elsewhere in the genome or as an episome) of the target gene. The loss of the ectopic copy expression in such a null background can then be followed in the absence of selective pressures. This can be achieved by directly monitoring the rate of loss of an episome for example by Southern hybridisation. Alternatively, expression of the ectopic gene could be under the control of a regulator, with tetracycline generally used as an inducer, or under the control of the untranslated DNA sequences that normally flank a developmentally regulated gene. The former situation has been used extensively with *T. brucei* and, although described for some species, is not widely used for *Leishmania* (Clayton 1999). For the latter mechanism, the 3'UTR's of several genes such as amastin and A2 have been used to "suppress" expression of a target gene in one life cycle stage with expression enhanced in other parasite forms (Charest *et al.* 1994, Rochette *et al.* 2005).

In other organisms RNA interference (RNAi) has been extensively used to reduce the expression level of a target protein. RNAi is a cellular process in which the introduction of a specific sequence of double-stranded RNA results in the removal of the corresponding, specific mRNA from the cell. This naturally results in the rapid "knock down" in the

production of the target protein that the mRNA encoded. Again, this approach is extensively used in *T. brucei* research (Kolev *et al.* 2011). Whether it can be used to investigate gene function in *Leishmania* appears to be species dependent as most *Leishmania* species lack the biological machinery required to drive the RNAi process whereas others, notably *L. braziliensis* and others subgenus *Viannia* parasites, appear to express activities that facilitate this pathway (Lye *et al.* 2010).

1.8.4 Genetically modified reporter parasites used in *Leishmania* screening

The classical drug screening methods when determining the potency of a compound against *Leishmania* generally involves the direct quantification of parasite loads using light microscopy. To facilitate this, cells are usually stained with a dye such as Giemsa or Leishman, particularly when evaluating pathogen loads within a host cell. However, these systems are laborious, time consuming and not readily amenable to high throughput analysis. Consequently, several genetically modified *Leishmania* cell lines have been developed that express a given reporter protein whose activity can be readily assayed and measured as a function of parasite load. One of the first reporter expression systems developed for use in *Leishmania* was based on β-galactosidase, encoded *lacZ* gene from *E. coli*, and initially used as a validation assay for parasite transfection protocols (LeBowitz *et al.* 1991). However, it was not until 2003 when this was applied to drug screening (Okuno *et al.* 2003). Here, *L. amazonensis* promastigotes were stably transfected with a *lacZ*-containing episomal construct with expression of the reporter maintained in the mammalian life cycle stages. Tagged cells were readily visualised by fluorescence and light microscopy in the presence of the chromogenic substrate 5-bromo-4-chloro-3-indolyl-β-D-galactopyranoside. However, this system is not without disadvantages as it is not particularly sensitive, the episomal copy number (and hence reporter expression levels) varies from cell to cell, while some

mammalian cell types (including macrophages) express endogenous levels of β-galactosidase. In an effort to improve this system, the expression of other enzymatic reporters including β-lactamase has been adapted for use with *Leishmania*, but these too suffer from sensitivity problems as compared to other systems (Buckner *et al.* 2005).

Modifying *Leishmania* cell lines with GFP is now commonplace (Kamau *et al.* 2001, Singh *et al.* 2004, Singh *et al.* 2009, Bolhassani *et al.* 2011, Pulido *et al.* 2012), as this method is cheap, safe, simple, and allows for easy kinetic monitoring. However, there are issues of sensitivity associated with GFP too. Particularly in its native form, GFP (and other fluorescent proteins) does not give the sensitivity of reporter gene systems based on an enzymatic reaction. In fact, miniaturisation of an assay into a 96-well microtitre plate proved problematic due to this relatively low fluorescent signal, restricting the application of fluorescent proteins to high throughput drug screening regimens. Consequently in 2003 a multimeric form of GFP was developed that proved sensitive enough for analysis on 96-well plates (Chan *et al.* 2003). Another problem is that most GFP reporter systems use episomes, and these are not stably maintained within *Leishmania*. This resulted in cell lines that required regular addition of the relevant selection antibiotic to keep stable and quantifiable levels of fluorescence. This particular issue has been overcome recently, with a stably integrated GFP-encoding gene into both New and Old World *Leishmania* species allowing for longer studies without the need for the addition of selection antibiotics (Singh, Gupta *et al.* 2009, Bolhassani, Taheri *et al.* 2011).

The third reporter gene system used in *Leishmania* relies upon the parasite expressing the luciferase gene whose activity can be monitored via light detection. Several luciferase-based episomal and integrative DNA constructs have been transfected into many different species

of *Leishmania* with stable cell lines readily obtained (Roy *et al.* 2000, Lang *et al.* 2005). Using luciferin as substrate, activity of the reporter can be monitored by detection of the resultant luminescence signal using a luminometer. This method is sensitive, rapid, reproducible and compatible with high throughput screening with all parasite stages amenable to analysis. However, disadvantages with this procedure include the requirements for expensive lysis and luciferin-containing assay buffers. Recent developments in imaging technologies coupled with novel luciferase variants now permit the imaging of parasite populations in a live animal model in real time (Thalhofer *et al.* 2010, Michel *et al.* 2011). Using such a resource, it will be of great interest to follow a course of an infection *in vivo* in the presence of drug treatment.

1.9 Nitroaromatic compounds

1.9.1 An overview of the nitroaromatics

Nitroaromatic compounds encompass a wide range of compounds characterised by at least one nitro-group attached to an aromatic ring (Figure 1.9.1) (Grunberg *et al.* 1973). While some occur naturally, such as the broad spectrum antibiotics chloramphenicol and azomycin, most are synthetic, created through the production of plastics, dyes, solvents, pesticides, food additives, explosives and pharmaceuticals (Spain 1995, Peres *et al.* 2000, Rieger *et al.* 2002, Roldan *et al.* 2008). A large number of nitroaromatic compounds have medicinal use, particularly as antibiotics. These include nitrofurans and nitroimidazoles, two classes of broad spectrum antimicrobials that can be used to treat urinary and gastrointestinal tract infections. However, the use of many nitroaromatics have been discontinued in Europe and USA due to reports of mutagenicity (Takahashi *et al.* 2000, Padda *et al.* 2003, Hiraku *et al.* 2004; reviewed in McCalla 1983), but elsewhere, these drugs are commonly prescribed. These concerns lead to a degree of paranoia and scepticism across the entire range of

nitroaromatics, even in cases where a compound's toxicology had not been investigated. As stated by the Nobel laureate pharmacologist Sir James Black "the most fruitful basis for the discovery of a new drug is to start with an old drug" (Raju 2000). Based on this philosophy, there has been a renaissance in looking at the medicinal value of nitroaromatics, stimulated by the rise in antimicrobial drug resistance to existing chemotherapies and as a means to developing new anti-tumour drugs. This has shown that several nitro-based compounds are not as toxic as initially thought (Trunz *et al.* 2011, Tweats *et al.* 2012) while retrospective analysis of clinical trial data coupled with a costing evaluation have resulted in proposals for the reinstatement of nitrofurantoin as a treatment for targeting uncomplicated urinary tract infections in developed countries (Kashanian *et al.* 2008, Arya *et al.* 2009, McKinnell *et al.* 2011). Against this backdrop, several other nitroaromatic compounds are currently undergoing evaluation for treatments of infectious organisms including PA-824 against *Mycobacterium tuberculosis* (which has now entered phase II clinical trials, Stover *et al.* 2000, Diacon *et al.* 2012, Diacon *et al.* 2012), and fexinidazole against *Trypanosoma brucei* and *Leishmania donovani* (Kaiser *et al.* 2011, Wyllie *et al.* 2012) while others such as SN23862, CB1954 and nifurtimox are emerging as anti-cancer therapies (Denny 2003, Chen *et al.* 2009, Saulnier Sholler *et al.* 2006, Saulnier Sholler *et al.* 2009). Additionally, the nitrothiazole nitazoxanide is currently the first-line treatment choice for *Cryptosporidium* and *Giardia* protozoal infections (Abboud *et al.* 2001, Rossignol *et al.* 2001, Anderson *et al.* 2007).

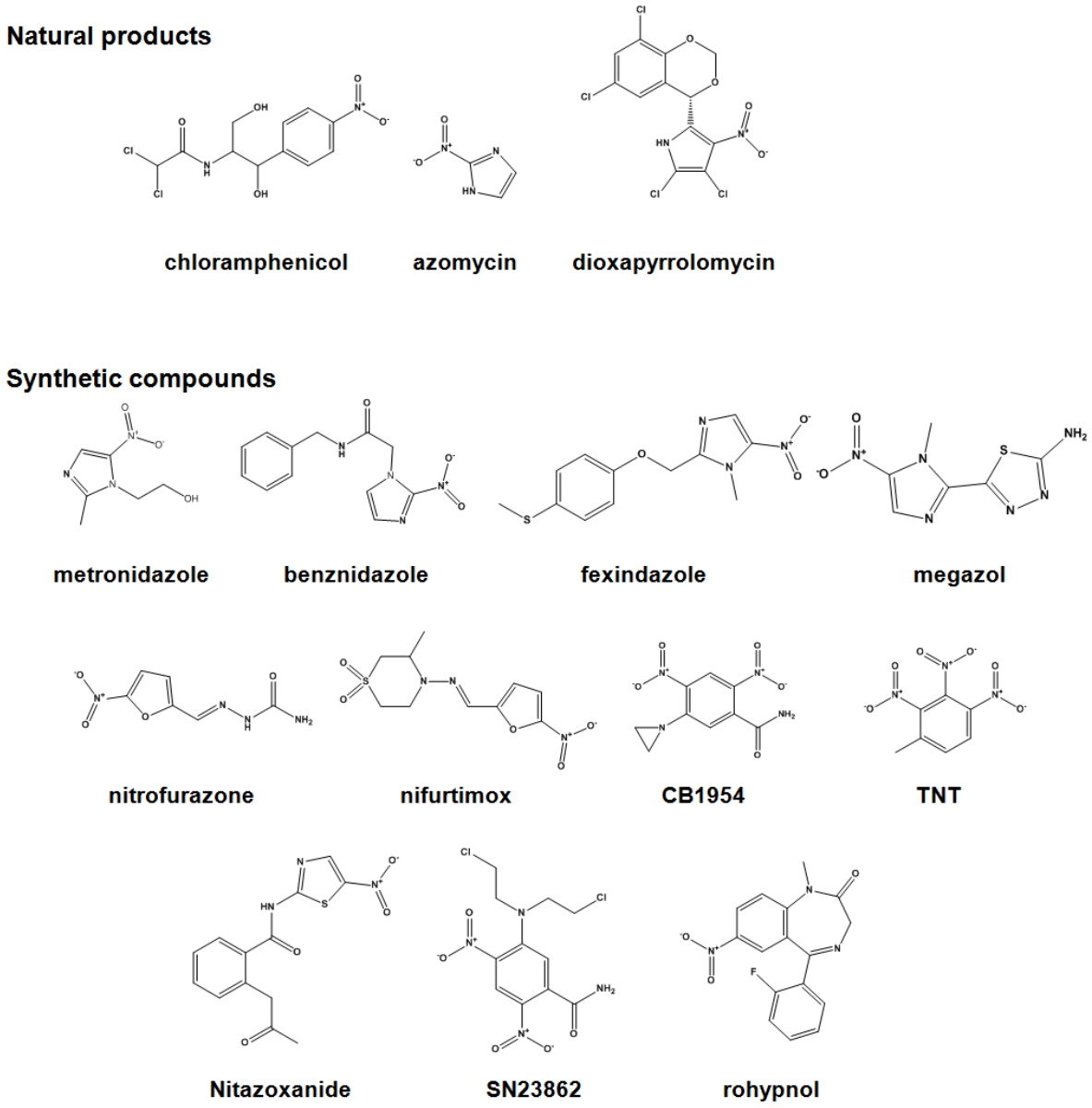

Figure 1.9.1: Structures of common nitro-compounds.

1.9.2 Nitroaromatic compounds as anti-trypanosomatid agents

The antimicrobial value of nitroaromatic compounds were first reported during the 1940's when nitrofuran-based agents were shown to exhibit cytotoxic activities against a range of bacteria (Dodd *et al.* 1944). This stimulated a series of screening programmes against other microorganisms in an effort to find new cures against these infectious agents. One group of microbes to come under such scrutiny were protozoan parasites. In the case of trypansomatids such as *T. brucei*, such efforts identified nitrofurazone as a lead compound (Packchanian

1955, Evens *et al.* 1957). Unfortunately, though nitrofurazone was deemed to be effective in humans against the parasites, it not only failed to completely remove parasitaemia (undesirable due to the possibility of relapse, particularly in immune-compromised patients), but also caused several cases of neuropathological toxicity (polyneuritis) that ultimately resulted in the discontinuation of these clinical trials (Cancado *et al.* 1964). However, these studies highlighted that other nitroaromatics could be used to combat trypanosome infections, with nifurtimox and benznidazole proving the most interesting against Chagas disease (Grunberg *et al.* 1967, Bock *et al.* 1969).

Nifurtimox ((*RS*)-3-methyl-*N*-[(1*E*)-(5-nitro-2-furyl)methylene]thiomorpholin-4-amine 1,1-dioxide) is a 5-nitrofuran compound marketed under the name Lampit™ (Bayer AG). Since its introduction in 1964, it has represented the front-line treatment for acute Chagas disease across South America. This orally administered therapy is given at a dosage of 8-10 mg kg^{-1} day^{-1} in 3 tablets for up to 120 days. It is readily absorbed from the gastrointestinal tract and metabolised in the liver, resulting in a half-life of around 3 hours (Wilkinson and Kelly 2009). However, gastrointestinal toxicity and central nervous system side effects coupled with concerns about its mutagenic/carcinogenic activity, limited efficacy and variation in strain susceptibility have all contributed to the discontinuation of use of this drug in Brazil, Argentina, Chile and Uruguay, while in the United States nifurtimox is only available following consultation with the CDC (Center for Disease Control) (Hidron *et al.* 2012). Despite this, interest in nifurtimox, in conjunction with the ornithine analogue eflornithine (a program known as nifurtimox-eflornithine combinational therapy, or NECT) has been renewed over the last decade in the treatment of human African trypanosomasis. Recent trials have shown that this combination represents an effective, safe, low cost alternative to other existing treatments and has resulted in NECT being added to the World Health Organisation (WHO) Essential Medicines List for the treatment of late-stage West African sleeping

sickness (Priotto *et al.* 2006, Checchi *et al.* 2007). Intriguingly, nifurtimox is also been trialled as therapy targeting certain cancers following the serendipitous finding that it is effective against paediatric neuroblastoma (Saulnier Sholler, Kalkunte *et al.* 2006, Saulnier Sholler, Brard *et al.* 2009; Koto *et al.* 2011, Saulnier Sholler *et al.* 2011).

Benznidazole (*N*-benzyl-2-(2-nitro-1*H*-imidazol-1-yl)acetamide), a 2-nitroimidazole marketed under the name Radanil™/Rochagan™ (Hoffman-La Roche), is the current front-line drug used against early stage Chagas disease. This is administered at 5-10 mg kg^{-1} day^{-1} in 2 oral doses over a 30-60 day period. As with nifurtimox, benznidazole is readily absorbed from the gastrointestinal tract and undergoes first pass metabolism in the liver. This, in conjunction with its excretion in urine and faeces, results in benznidazole having a half-life of around 12 hours in humans. There is some evidence to suggest that benznidazole is also effective against the chronic stage of *T. cruzi* infection, though these observations tend to be anecdotal, with few rigorous trials and meta-analyses (Reyes *et al.* 2005). To evaluate the value of benznidazole against this disease stage, a large international program of clinical trials is currently underway, called the BENEFIT (BENznidazole Evaluation for Interrupting Trypanosomiasis) project (Marin-Neto *et al.* 2009). Although benznidazole is considered safer than nifurtimox, it is reportedly mutagenic and can still cause a range of side effects including agranulocytosis, seizures, dermatitis and polyneuropathy (Castro *et al.* 1988, Viotti *et al.* 2009).

Following the discovery that nifurtimox and benznidazole are viable treatments for kinetoplastid disease, several other anti-trypanocidal screening programs using nitroaromatics have been undertaken. Interestingly, these can be broadly divided into two differing approaches. For nitroimidazoles, large scale screens have tended to be empirical in nature, with different types of compound classes and sub-classes being systematically tested directly

against the parasite (De Carneri 1969, Ross *et al.* 1972, Ross *et al.* 1973, Ross *et al.* 1973, Ross *et al.* 1975, Ross *et al.* 1975, Winkelmann *et al.* 1977, Winkelmann *et al.* 1978, Winkelmann *et al.* 1978, Winkelmann *et al.* 1978). In contrast, many other nitroaromatics such as nitrofurans, nitrothiophenes and nitrobenzyl-based agents have been tested in smaller scale screens using derivatives designed to interact with parasite-specific metabolic pathways, such as trypanothione homeostasis (Cerecetto *et al.* 1998, Cerecetto *et al.* 2000, Aguirre *et al.* 2004, Aguirre *et al.* 2006), sterol biosynthesis (Gerpe *et al.* 2008, Gerpe *et al.* 2009) and purine uptake (Stewart *et al.* 2004, Baliani *et al.* 2005, Baliani *et al.* 2009). Such screens produced a number of promising lead structures, including fexinidazole and megazol, both of which are effective against *T. cruzi* and *T. brucei in vivo* (Filardi *et al.* 1982, Raether *et al.* 1983, Bouteille *et al.* 1995). Whereas fexinidazole originally did not progress further than animal studies, a significant research effort was made to ascertain the trypanocidal mechanism of megazol. These studies demonstrated that megazol enters the parasite by passive diffusion, and then undergoes activation by nitroreduction with both 1- and 2-electron reduction pathways reported (Viode *et al.* 1999, Barrett *et al.* 2000, Wilkinson, Taylor *et al.* 2008). Unfortunately, further work showed that megazol causes considerable DNA damage to host cells and as a consequent trials with this compound were suspended (Poli *et al.* 2002, Enanga *et al.* 2003, Nesslany *et al.* 2004). However, since then progress has been made in testing megazol analogues and derivatives in the hope to find similar trypanocidal effects, but with lowered mutagenicity (Chauviere *et al.* 2003, Carvalho *et al.* 2004, Carvalho *et al.* 2007, Carvalho *et al.* 2008, Salomao *et al.* 2010). In *Leishmania*, trials have been performed using nitrofurans (nifurtimox, nitrofurazone and furazolidone for example) but these drugs lacked efficacy in animal models or lacked sufficient selectivity toward the parasite (Haberkorn 1979, Berman *et al.* 1983, Neal *et al.* 1988). However, recent screens using novel nitrofuran derivatives and other nitroaromatic and nitroheterocyclic compounds including

nitroimidazoles and nitrotriazoles have shown some promise (Alipour *et al.* 2011, Papadopoulou *et al.* 2011, Tahghighi *et al.* 2011, Tahghighi *et al.* 2012, Wyllie, Patterson *et al.* 2012).

Recently, the Drugs for Neglected Diseases initiative (DNDi, www.dndi.org) sponsored a study which has resulted in the re-evaluation of fexinidazole as a potential treatment for human African trypanosomiasis. The DNDi have signed an agreement with the pharmaceutical company Sanofi-Aventis for the development, manufacture and distribution of this nitroimidazole, and clinical trials are in progress. Torreele *et al.* (2010) have shown that although fexinidazole appears to be mutagenic in the bacterial Ames test, no genotoxicity was measured in *in vitro*, *in vivo* and *ex vivo* experiments using mammalian cells (Torreele *et al.* 2010).

1.10 Activation of nitroaromatic compounds

Antimicrobial nitroaromatic compounds generally function as "prodrugs" and must be activated before mediating their cytotoxic effects. This occurs by reduction of the conserved nitro group attached to the aromatic ring leading to formation of a nitro anion radical or hydroxylamine derivative, reactions catalysed by oxidoreductase enzymes known as nitroreductases (NTR) (Figure 1.10.1). As nitroaromatic compounds are rare in nature, nitroreductase activity is generally mediated by enzymes that have alternative functions *in vivo*. For example, cytochrome P450 reductase readily mediates the 1-electron reduction of many nitro-based compounds including metronidazole, but their biological function involves the transfer of reducing equivalents from NADPH to cytochrome P450 (Orna *et al.* 1989).

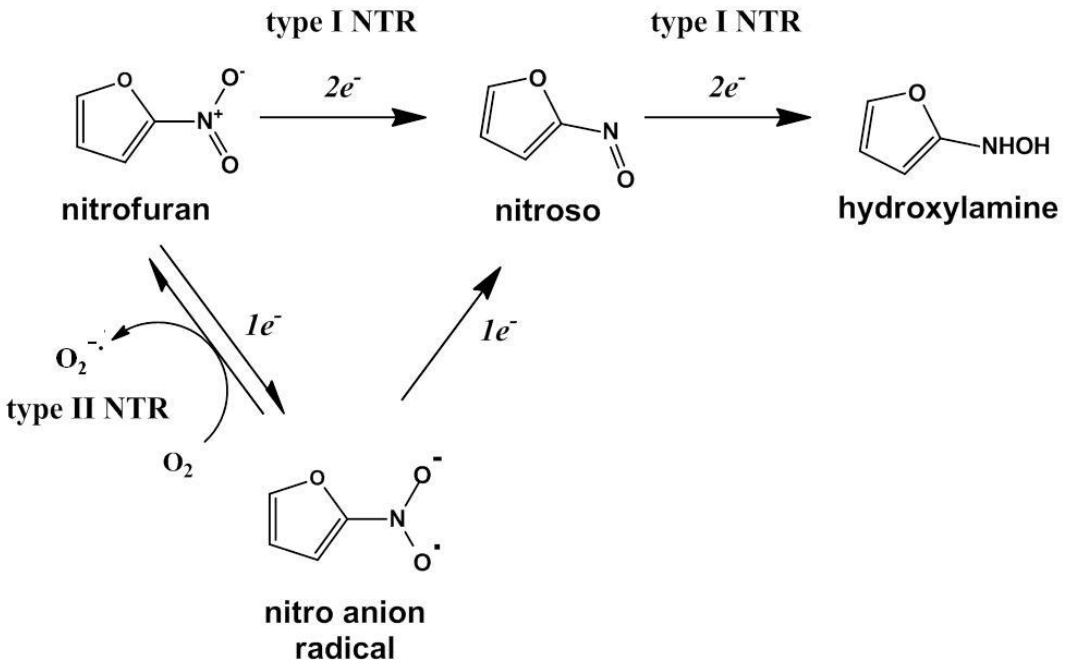

Figure 1.10.1: Reduction pathway of a nitroaromatic by the nitroreductases
Shown as an example here, the nitroheterocycle 5-nitrofuran is reduced through a 1e- reduction by a type II NTR (downward reaction) to form a nitro anion radical. In anaerobic conditions this can be further reduced to the 5-nitrosofuran derivative of the nitroaromatic. However, in the presence of oxygen the nitro anion radical species is converted back into the original nitro-based substrate, liberating the superoxide anion in a "futile cycle". Consequently type II NTRs are known as "oxygen sensitive". If the compound is reduced by a type I NTR (top reaction), the compound goes through a single step $2e^-$ reduction to the 5-nitrosofuran derivative. Type I NTRs are thus deemed "oxygen insensitive". The 5-nitrosofuran derivative can be further metabolised by another type I NTR-mediated $2e^-$ reduction to the 5-hydroxylaminofuran derivate.

Based on oxygen sensitivity, flavin cofactor and the nitro reduction product, NTRs can be broadly divided into two classes, type I or type II NTRs (Figure 1.10.1). Type I NTRs, originally identified as factors that, once lost or expression is reduced, mediates resistance in prokaryotes to nitrofuran-based drugs (McCalla *et al.* 1978, Whiteway *et al.* 1998 and others), are "oxygen insensitive", FMN-containing enzymes found predominantly in bacteria and absent from most eukaryotes, with several protozoan parasites, including trypanosomes, being major exceptions (Nixon *et al.* 2002, Muller *et al.* 2007, Wilkinson, Taylor *et al.* 2008, Pal *et al.* 2009). They mediate a series of 2-electron reduction events that convert the

conserved nitro group to a hydroxylamine derivative via an unstable nitroso intermediate (Peterson *et al.* 1979). This conversion has a major effect on the electron distribution on the aromatic ring as nitro groups are electron withdrawing while hydroxylamine substituents are electron donating. Dependent on the ring structure, this electronic rearrangement promotes distinct fates to the newly formed reduction product. For example, the hydroxylaminofuran derivative generated from nitrofurans can be processed to either form a nitrenium ion that then promotes DNA adduct formation through esterification with guanine (McCalla *et al.* 1971, Streeter *et al.* 1988, Corbett *et al.* 1995); generate DNA crosslinking adducts (McCalla, Reuvers *et al.* 1971, Denny 2003); or promote cleavage of the aromatic ring to yield toxic nitriles (Gavin *et al.* 1966, Peterson, Mason *et al.* 1979, Hall *et al.* 2011). In contrast, the 2-hydroxylaminoimidazole derivative generated from 2-nitroimidazoles can rearrange to a 5-hydroxyl-2-iminoimidazole derivatives *via* a nitrenium ion form in neutral conditions. Through the addition of water this 5-hydroxyl-2-iminoimidazole becomes a 2-amino-4,5-dihydroxylimidazole intermediate, which can degrade to release glyoxal, a metabolite that readily forms adducts with a range of biological molecules, such as amino acid side chains and guanosine (Whitmore *et al.* 1986, Whitmore *et al.* 1986, Thornalley 2008, Hall *et al.* 2012).

In contrast, type II NTRs are ubiquitous, with examples being found across all life forms – for example human NADPH:cytochrome P450 reductase (Orna and Mason 1989) and the bacterial nitroaryl reductases (Angermaier *et al.* 1983). They use FAD or FMN as a cofactor, and mediate a 1-electron reduction of the conserved nitro group leading to the formation of an unstable nitro anion radical (Figure 1.10.1). In the presence of oxygen, type II NTR activity is said to be “oxygen sensitive”, the radical can undergo futile cycling to produce superoxide anions ($O_2^{\cdot-}$) and regenerate the parental compound. This activation process

predominates in mammalian cells (Peterson, Mason *et al.* 1979, Moreno *et al.* 1982). Under hypoxic conditions, a nitroso form can be produced by either the interaction of two nitro anion radicals (which also regenerates the parent compound) or by a further 1-electron reduction of the nitro anion radical (Moreno, Docampo *et al.* 1982) (Figure 1.10.1). The nitroso form can then promote cellular damage directly or undergo reduction to the hydroxylamine derivative which then precipitates the pathways described above for type I NTRs (Kedderis *et al.* 1989, Leitsch *et al.* 2007). It is proposed that this anaerobic activation pathway underlies the basis of selective toxicity for antimicrobial nitroimidazoles such as metronidazole and prodrug activation in hypoxic tumours.

Not all nitroreductases fall into these two groups, with several enzymes displaying features characteristic of both type I/II NTRs. For example, the mammalian thioredoxin reductase is a FAD-containing (type II characteristic) selenoprotein that can reduce nitroaromatic substrates by both 1- (type II characteristic) and 2- (type I characteristic) electron reductions; while the mammalian NAD(P)H:quinone reductase (NQO1; also known as DT-diaphorase) and xanthine oxidase are both FAD-containing (type II characteristic) enzymes that mediate the 2- (type I characteristic) electron reduction of their target substrate (Knox *et al.* 1993; Croft and Coombs 2003; Cenas *et al.* 2006). Therefore, not all enzymes follow the above, relatively simple classification system.

1.11 Activation of nitroaromatic compounds by trypanosomatids

Before the report that trypanosomatids expressed type I NTRs, it had been assumed that the antiparasitic activity exhibited by the nitroaromatic compounds nifurtimox and benznidazole was primarily due to the action of type II NTRs, and thus involved induction of oxidative stress. This was supported by observations that trypanosomal extracts when treated with

nifurtimox generated superoxide anions and nitro anion radicals, although such findings were never noted for benznidazole (Docampo *et al.* 1979, Docampo *et al.* 1981, Viode, Bettache *et al.* 1999). Subsequent studies revealed that the 1-electron reduction of nifurtimox *in vitro* could be performed by a range of flavoproteins including trypanothione reductase, adrenodoxin reductase, lipoamide dehydrogenase and cytochrome P450 reductase (Blumenstiel *et al.* 1999, Viode, Bettache *et al.* 1999). This mode of action proved initially attractive given that trypanosomes were believed to have a limited enzymatic capacity to metabolise reactive oxygen species (Boveris *et al.* 1980, Fairlamb *et al.* 1992). However, it is now clear that these proposals were incorrect as trypanosomatids do express a range of superoxide and peroxide metabolising pathways, with these being distinct from those possessed by other eukaryotic organisms (Flohe *et al.* 1999, Wilkinson *et al.* 2002, Wilkinson *et al.* 2003, Irigoin *et al.* 2008). To date the only functional evidence for the involvement of the superoxide anion in nifurtimox toxicity is indirect, coming from studies on the superoxide dismutase B1 (SODB1) isoform where *T. brucei TbSODB1* null mutants and *T. cruzi TcSODB1* over expressers have been shown to be more susceptible to the nitrofuran than wild type cells (Temperton *et al.* 1998, Prathalingham *et al.* 2007). Genetic analysis of *T. brucei* or *T. cruzi* engineered to express altered levels of oxygen-sensitive NTRs activators, for example cytochrome P450 reductase or trypanothione reductase, or other components of the trypanosomal oxidative defence system, generate parasites that display the same susceptibility to nifurtimox as control cells (Kelly *et al.* 1993, Wilkinson *et al.* 2000, Wilkinson, Meyer *et al.* 2002, Wilkinson, Obado *et al.* 2002, Wilkinson *et al.* 2006, Hall, Bot *et al.* 2011, Hall and Wilkinson 2012). Therefore, as both trypanosomal and mammalian cells can undergo futile cycling leading to superoxide anion production, then induction of oxidative stress via activation by type II NTRs does not explain nifurtimox's selectivity towards *T. brucei* or *T. cruzi*.

Based on flavin co-factor, oxygen-insensitive activity, substrate range and inhibition profiles it has now been shown that trypanosomes express a type I NTR that displays many of the characteristics of its bacterial counterparts (Wilkinson, Taylor *et al.* 2008). This mitochondrially targeted enzyme non-covalently binds FMN as cofactor , utilizes NADH as reductant and catalyzes the reduction of a wide range of nitroaromatic and quinone-based substrates via a ping-pong mechanism – an activity readily inhibited by dicoumarol (Wilkinson, Taylor *et al.* 2008, Bot *et al.* 2010, Hall *et al.* 2010, Hall, Bot *et al.* 2011, Hall and Wilkinson 2012, Mejia *et al.* 2012; Hall, Meredith and Wilkinson, unpublished). Using *in vitro* drug selection, gene manipulation, biochemical analysis and functional genomics approaches, it is now clear that this enzyme plays a key role in the nifurtimox and benznidazole activation within trypanosomes resulting in cleavage of the heterocyclic rings to produce an unsaturated open chain nitrile or glyoxal, respectively. (Wilkinson, Taylor *et al.* 2008, Baker *et al.* 2011, Hall, Bot *et al.* 2011, Alsford *et al.* 2012, Hall and Wilkinson 2012, Mejia, Hall *et al.* 2012). Also, the type I NTR has been implicated in the antiparasitic activity of fexinidazole against *T. brucei* and *L. donovani* (Sokolova *et al.* 2010;Wyllie, Patterson *et al.* 2012) and exploited to evaluate whether other nitroaromatic compounds have potential as trypanocidal agents (Bot, Hall *et al.* 2010, Hall, Wu *et al.* 2010; Hu *et al.* 2011, Papadopoulou, Trunz *et al.* 2011, Papadopoulou *et al.* 2012). From such screens, certain aziridinyl nitrobenzamide (ANB), nitrobenzyl phosphoramide mustard (NBPM) and nitrotriazole derivatives show considerable promise against bloodstream-form *T. brucei* and *T. cruzi* amastigotes, the parasite stages present in the mammalian host, with many having superior selectivity against the pathogen as compared to nifurtimox.

Although the biological function of the type I NTR has yet to be elucidated, its activity is essential to infective form trypanosomes: *TbNTR* cannot be deleted from the genome of

bloodstream-form *T. brucei* unless the cells express an ectopic copy of the gene, while *T. cruzi* epimastigotes *TcNTR*$^{-/-}$ null mutant lines are unable to infect mammalian cells (Wilkinson, Taylor *et al.* 2008). Based on mitochondrial location and substrate preference it appears that the trypanosomal type I NTR may actually function as a NADH:ubiquinone oxidoreductase (Wilkinson, Taylor *et al.* 2008; Hall, Meredith and Wilkinson, unpublished). This hypothesis is supported by data obtained from deep sequence analysis of *T. brucei* populations selected for nifurtimox resistance using a whole genome loss of function screen which revealed that several "hits" were involved in ubiquinone-9 biosynthesis (Alsford, Eckert *et al.* 2012; Hall, Meredith and Wilkinson, unpublished). If this is the case then the trypanosomal type I NTR may be involved in helping to maintain the mitochondrial NAD^+/NADH balance with reducing equivalents transferred onto ubiquinone.

In addition to the above nitroreductase, trypanosomes and *Leishmania* also express an enzyme that shows both typeI/II characteristics. The prostaglandin F2α synthase (PGFS, also known as "old yellow enzyme") from *T. cruzi* has been shown to mediate the 2-electron reduction of selected quinone and nitroaromatic substrates *in vivo* though only under anaerobic conditions (Claes *et al.* 2009). Intriguingly, this study reported that the enzyme was able to metabolise nifurtimox but not benznidazole and appears to contradict a finding which indicates that a laboratory selected benznidazole resistant *T. cruzi* cell line showed a 6-fold reduction in TcPGFS expression (Piscopo and Mallia 2006). Interestingly, the same study also reported that wild type *T. cruzi* strains which exhibited "natural" resistant to nifurtimox and/or benznidazole do not show this alteration (Piscopo and Mallia 2006). One possibility to account for these discrepancies could be a mix up of nifurtimox and benznidazole during the biochemical characterisation of TcPGFS. Alternatively the laboratory generated benznidazole resistant lines may have undergone significant genotypic alterations in comparison to the

initial parental line. This is evidenced as several other proteins/genes including cytosolic/mitochondrial tryparedoxin peroxidases, iron superoxide dismutase A, tyrosine aminotransferase and ascorbate peroxidase (and others) all show altered expression levels in this line (Nogueira *et al.* 2006, Andrade *et al.* 2008, Murta *et al.* 2008, Rego *et al.* 2008, Campos *et al.* 2009, Nogueira *et al.* 2012). This has led to confusion as to which event(s) actually cause benznidazole resistance and what has arisen as a consequence of the selection event. The propensity of *T. cruzi* to undergo large karyotypic changes has been well documented especially in relation to drug selection (Nozaki *et al.* 1996, Wilkinson, Taylor *et al.* 2008, Mejia, Hall *et al.* 2012). Therefore, the involvement of PGFS in mediating nitroheterocyclic drug resistance has not been adequately demonstrated.

2. Research Aim

Nitroheterocyclic prodrugs such as nifurtimox and benznidazole are used to treat a number of parasitic infections. In a significant breakthrough, it has been shown that trypanosomes, pathogens related to *Leishmania*, activate these drugs using a bacterial-like, type-I nitroreductase. We now have the opportunity to extend these finding to investigate whether the nitroreductase activity can be exploited in the treatment of leishmaniasis.

Our specific aims are to:

1. Determine the biochemical properties of the type I nitroreductase expressed by *Leishmania major* (LmNTR).
2. Investigate the importance of LmNTR during the parasite's life cycle.
3. Develop a reporter system for use in intracellular form *Leishmania*
4. Conduct biochemical and phenotypic drug screens using an array of nitroaromatic compounds against the *Leishmania* promastigote and amastigotes.

3. Materials and Methods

3.1 General stocks

3.1.1 Organisms

The organisms used in this study are listed in Table 3.1.1

organism	source
Leishmania major MHOM/IL/80/Friedlin	Prof D. Smith, University of York
Human acute monocytic leukaemia line THP-1	Dr K. Seifert, LSHTM
Escherichia coli XL-1Blue	Laboratory stock
Escherichia coli BL21+	Laboratory stock

Table 3.1.1: Organisms used in this study

3.1.2 Oligonucleotide primers

All primers used in this study as listed in Appendix A. These were sourced from Sigma-Genosys.

3.1.3 Nitroaromatic compounds

The structures of the nitroheterocyclic and nitrobenzyl compounds used in this study are listed in Appendix B. These were provided by Prof Longqin Hu (Rutger's, The State University of New Jersey, USA), Dr Nuala Helsby (University of Auckland, New Zealand), Dr Nubia Boechat (Far Manguinhos, Brazil), Dr Priscille Brodin (Institute Pasteur Korea, Republic of Korea), Dr Maria Papadopoulou (NorthShore University Health System, USA) and Dr Adrian Dobbs (Queen Mary University of London, UK).

3.2 Cell culturing

3.2.1 Maintenance of parasite lines

The promastigote form of *L. major* MHOM/IL/80/Friedlin was cultured at 27°C in M199 medium (Invitrogen) supplemented with 20 % (v/v) tetracycline-free foetal bovine serum (Autogen Bioclear), 4 mM sodium bicarbonate, 40 mM HEPES pH7.4, 0.1 mM adenine, 0.005 % (w/v) haemin, 25000 U L^{-1} penicillin and 25 mg L^{-1} streptomycin (all Sigma-Aldrich). Once prepared with the appropriate supplements the medium was filter sterilised. In some experiments the growth medium was solidified with 1.0 % (w/v) Agar No.1 (Oxoid). Transformed parasites were grown in or on the above medium containing 20 (solid) or 40 (liquid) mg L^{-1} G418, 10 mg L^{-1} blasticidin or 20 mg L^{-1} puromycin (all drugs from PAA Laboratories Ltd) as appropriate.

The metacyclic promastigote-form of *L. major* MHOM/IL/80/Friedlin was harvested from stationary phase promastigote-form cultures (7-10 days old) using an agglutination technique (da Silva *et al.* 1987), Briefly, cultures were incubated at room temperature for 15 minutes in the presence of 50 mg L^{-1} peanut lectin (Sigma-Aldrich). Promastigote parasites were pelleted (100 g for 5 minutes) and the metacyclic-containing supernatant removed.

The amastigote-form of *L. major* MHOM/IL/80/Friedlin was cultured as follows: *L. major* metacyclic promastigotes, harvested as described above, were transferred to a differentiated culture of THP-1 cells (Section 3.3.2) and allowed to infect the mammalian cells overnight at 37°C under a 5 % (v/v) CO_2 atmosphere: generally a ratio of 20 parasite cells per mammalian cell. The following day, free parasites were removed by extensively washing the monolayer (with fresh mammalian growth medium) and then placed in fresh mammalian growth

medium. Amastigote parasites were then grown at 37°C under a 5 % (v/v) CO_2 atmosphere for between 4-6 days.

3.2.2 Maintenance of mammalian lines

The THP-1 cell line was grown at 37°C under a 5 % CO_2 atmosphere in RPMI-1640 medium (PAA Laboratories Ltd.) supplemented with 2 mM pyruvate, 2 mM sodium glutamate, 25000 U L^{-1} penicillin and 2.5 mg L^{-1} streptomycin, 20 mM HEPES (pH 8.0) (all Sigma-Aldrich) and 10% (v/v) tetracycline-free-fetal calf serum (Autogen Bioclear).

3.2.3 Maintenance of bacterial strains

E. coli strains were grown in NZCYM medium (10 g L^{-1} enzymatic casein digest, 1 g L^{-1} Casamino acids, 5 g L^{-1} yeast extract, 5 g L^{-1} NaCl, 0.98 g L^{-1} $MgSO_4$) (Sigma-Aldrich) supplemented with 100 mg L^{-1} ampicillin (Sigma-Aldrich) where appropriate. In some experiments, the growth medium was solidified with 1.5 % (w/v) Agar no.1 (Oxoid).

3.2.4 Cell storage

For long term storage, bacterial strains and *Leishmania* lines were deposited as frozen stocks in liquid nitrogen (parasite lines) or at -80^{o}C (prokaryotic strains) in growth medium containing 20% (v/v) glycerol (Sigma-Aldrich). Bacterial strains were frozen directly at -80^{o}C in 1.2 mL cryogenic vials (Nunc). *Leishmania* lines, in 1.2 mL cryogenic vials (Nunc), were frozen slowly (1-2 days) to -80^{o}C using a Cryo 1°C Freezing Container (Nalgene) containing isopropanol (VWR International), then transferred to liquid nitrogen for long-term storage.

Mammalian (THP-1) cells were frozen in fresh growth medium containing 20% (v/v) glycerol (Sigma-Aldrich) at a density of 1 x 10^5 cells mL^{-1}. Frozen stocks were generated as described for *Leishmania* lines using the Cryo 1°C Freezing Container (Nalgene).

Eukaryotic cell lines were revived by quickly thawing the contents of the frozen vial. Thawed cells were pelleted by centrifugation for 5 minutes (parasites at 1640 g, mammalian cells at 100 g) and washed in 10 mL of the appropriate medium. Cells were then re-suspended in fresh medium as per normal culturing.

3.3 Anti-proliferation assays

3.3.1 *L. major* promastigotes

All growth inhibition assays were carried out in 96-well plates. *L. major* promastigotes in the logarithmic phase of growth were seeded at 5 x 10^5 cells mL^{-1} in 200 μL growth medium containing different concentrations of drug. After incubation at 25°C for 6 days, resazurin (Sigma-Aldrich) was added to each well to a final concentration of 12.5 mg L^{-1} (or 2.5 μg per well). The plates were then incubated at 27°C and the degree of fluorescence noted at 24 hrs using a Gemini Fluorescent Plate reader (Molecular Devices) at λ_{EX} = 530 nm and λ_{EM} = 585 nm with a filter cut-off set at 550 nm. The colour/fluorescence change resulting from the reduction of resazurin is proportional to the number of live cells. Control growth assays were also performed in the absence of compound (no drug control, 100 % parasite growth) and the absence of cells/compound (background, 0 % parasite growth). These were then used when determining the growth concentration of compounds that inhibited parasite growth by 50 % (IC_{50}).

3.3.2 *L. major* amastigotes

All growth inhibition assays were carried out in 96-well plates. THP-1 cells were seeded at 2.5 x 10^4 cells mL^{-1} in 200 μL mammalian cell growth medium and incubated at 37°C in a 5 % (v/v) CO_2 atmosphere for 3 days in the presence of 20 ng mL^{-1} phorbol 12-myristate 13-acetate (PMA) (Sigma-Aldrich): PMA promotes differentiation to macrophage cells (Tsuchiya *et al.* 1980, Fleit *et al.* 1991). Freshly purified *L. major* metacyclic cells resuspended in mammalian growth medium (5 x 10^5 cells mL^{-1}) were added to twice-washed macrophage monolayers resulting in a parasite:macrophage cell ratio of ~20:1. Following overnight infection at 37°C in a 5 % (v/v) CO_2 atmosphere, the cultures were washed twice in mammalian growth medium to remove non-internalized parasites, before addition of 200 μL fresh mammalian growth medium containing the compound to be tested. Drug-treated infections were incubated for a further 3 days at 37°C under a 5% (v/v) CO_2 atmosphere. The growth medium was removed and the cells washed twice in fresh medium to remove any extracellular parasites. The cells were then lysed in 100 μL lysis buffer (Promega) and 10 μL aliquots transferred to a white 96-well plate. Alternatively, for early screening 50 μL aliquots of triplicate lysates were pooled into a separate well, and then 10 μL of the pooled lysate analysed. Luciferase activity was measured by adding 50 μL enzyme substrate reagent (Promega) to the lysed extract and light emission measured on a TopCount luminescence and β-plate counter (Perkin Elmer). Control growth assays were also performed in the absence of compound (no drug control, 100 % parasite growth) and the absence of cells/compound (background, 0 % parasite growth). These were then used when determining the IC_{50} value for each compound.

3.3.3 Mammalian cells

All growth inhibition assays were carried out in 96-well plates. THP-1 cells were seeded at 2.5 x 10^4 cells mL^{-1} in 200 μL mammalian cell growth medium and incubated at 37^oC in a 5 % (v/v) CO_2 atmosphere for 3 days in the presence of 20 ng mL^{-1} PMA. The THP-1 cells were then washed twice in fresh growth medium and incubated for a further 24 hrs. Following overnight incubation at 37°C in a 5 % (v/v) CO2 atmosphere, the cultures were washed twice in mammalian growth medium to replicate the amastigote proliferation assay, before addition of 200 μL fresh mammalian growth medium containing the compound to be tested. Drug-treated infections were incubated for a further 3 days at 37°C under a 5% (v/v) CO_2 atmosphere. The growth medium was removed and the cells washed twice in fresh medium before the addition of resazurin (Sigma-Aldrich) in mammalian growth medium to a final concentration of 12.5 mg L^{-1} (or 2.5 μg per well). The plates were then incubated at 37°C under a 5% (v/v) CO_2 atmosphere and the degree of fluorescence noted after 24 hrs using a Gemini Fluorescent Plate reader (Molecular Devices) at λ_{EX} = 530 nm and λ_{EM} = 585 nm with a filter cut-off set at 550 nm. The colour/fluorescence change resulting from the reduction of resazaurin is proportional to the number of live cells. Control growth assays were also performed in the absence of compound (no drug control, 100 % parasite growth) and the absence of cells/compound (background, 0 % parasite growth). These were then used when determining the concentration of compounds that inhibited parasite growth by 50 % (IC_{50}).

3.4 DNA extraction techniques

3.4.1 Plasmid DNA extraction

Small scale plasmid DNA preparations (5-20 μg) were extracted from *Escherichia coli* using the *AccuPrep*® Nano-Plus Plasmid Mini Extraction Kit (Bioneer), according to the

manufacturer's instructions. Briefly, 5 mL NZCYM containing 100 mg ampicillin L^{-1} was inoculated with the desired *E. coli* strain and incubated overnight at 37^{o}C with vigorous aeration. The cells were pelleted (3000 g for 5 minutes), resuspended then lysed in an alkali buffer containing RNase A (Bioneer). The pH of the lysate was then adjusted by addition of neutralization buffer and the resultant chromosomal DNA/cell debris removed by centrifugation (16000 g for 10 minutes). The cleared lysate was passed through a nucleic acid-binding spin column such that DNA molecules bind to the silica membrane within the column. Salts and precipitates were then removed by a series of centrifugation and ethanol-based wash steps, before eluting the DNA off the column into 50-100 µL low salt buffer (Bioneer) (10 mM Tris-HCl, 1 mM EDTA). Plasmid samples were then stored at -20°C.

For larger scale plasmids, DNA preparations (50-100µg DNA) were extracted from *Escherichia coli* using the Qiagen QIAfilter® Midiprep kit, according to the manufacturer's instructions. Briefly, 100 mL NZCYM containing 100 mg ampicillin L^{-1} was inoculated with the desired *E. coli* strain and incubated overnight at 37^{o}C with vigorous aeration. The cells were pelleted (3000 g for 10 minutes) and the initial lysis stages performed as described for the small scale plasmid DNA extraction protocol. The lysate was then passed through a QIAfilter cartridge and the clear extract transferred into a nucleic acid-binding HiSpeedMidi-Tip. The HiSpeedMidi-Tip contains a resin designed to operate by gravity flow such that it retains the plasmid DNA. The DNA was extensively washed in a high salt, isopropanol-based buffer maintained at a neutral pH, then eluted off the HiSpeedMidi-Tip using an alkali high salt, isopropanol-based buffer. The DNA was then concentrated and desalted by a series of isopropanol and ethanol precipitation steps before elution of the plasmid into 250-750 µL low salt buffer (Qiagen) (10 mM Tris-HCl, 1 mM EDTA). Plasmid samples were then stored at -20°C.

3.4.2 Parasite genomic DNA extraction

L. major genomic DNA was harvested using a SDS-based lysis/phenol:chloroform protocol adapted from Kelly *et al.* (1993). *L. major* cells from 10-50 mL promastigote-form cultures were pelleted (1000 g for 10 minutes), washed in PBS (137 mM NaCl, 2.7 mM KCl, 10 mM Na_2HPO_4, 1.76 mM KH_2PO_4, pH 7.6) (Sigma-Aldrich) and then resuspended in TEN buffer (50 mM Tris-Cl pH 8.0, 50 mM EDTA, 50 mM NaCl) (all Sigma-Aldrich) containing 100μg mL^{-1} proteinase K (Sigma-Aldrich). Sodium dodecyl sulphate (SDS) (Sigma-Aldrich) was then added to a final concentration of 1 % (w/v), and the mixture incubated at 37°C overnight or at 54°C for 2 hrs. The lysis solution was then gently mixed with an equal volume of phenol (Sigma-Aldrich). The aqueous/organic phases were partitioned by centrifugation (3555 g for 10 minutes) and the aqueous phase collected. An equal volume of phenol:chloroform (1:1) (Sigma-Aldrich) was then added to the aqueous phase, mixed and partitioned as described above and the aqueous phase retained. If required, the phenol/chloroform step was repeated. The DNA containing aqueous phase was finally transferred to a fresh tube. A few drops (~20-30 μL) of 1 M $MgCl_2$ (VWR International) were then added and the chromosomal DNA precipitated using an equal volume of isopropanol (VWR International). The resultant fibrous material was collected, transferred to a fresh 1.5 mL centrifuge tube, washed with 70 % (v/v) ethanol and left to air dry for ~5 minutes. Finally, the genomic DNA was dissolved in EB elution buffer (Qiagen) with a concentration of 30 μg mL^{-1} heat-treated (100°C for 10 minutes) RNase A (Sigma-Aldrich).

3.5 DNA manipulation techniques

3.5.1 DNA purification

DNA fragments (100 base pairs - 10 kilo base pairs) were purified from liquid or from agarose gel slices using the *AccuPrep*® PCR Purification or the *AccuPrep*® Gel Purification

Kits (both Bioneer), in accordance to manufacturer's instructions. For DNA samples in liquid, a high salt buffer was applied to a DNA binding column (containing chaotropic salts). Under these conditions, the DNA binds to the silica membrane within the column. Salts and precipitates were then removed by a series of centrifugations and ethanol-based wash steps, before eluting DNA off the column into 30-50 μL low salt buffer (Bioneer) (10 mM Tris-HCl, 1 mM EDTA). Samples were then stored at -20°C.

To purify a DNA fragment from an agarose gel slice the mass, hence volume, of that slice was determined. This was then solubilised in three volumes of Gel Binding Buffer (Bioneer) at 50°C until the agarose had completely dissolved. One volume of isopropanol was added to the solution and the mixture applied to a DNA binding column. The sample was then treated as described above when purifying DNA fragments in solution.

Additionally, to prepare for *L. major* transfection DNA was further purified from the eluents described above using ethanol precipitation. Samples were treated with sodium acetate (pH 5.2) (Sigma-Aldrich) to a final concentration of 0.3M. After mixing, DNA was precipitated by adding 2 volumes of cold 100 % ethanol, followed by incubating at -20^{o}C for 20 minutes. DNA was pelleted in a microcentrifuge at 20000 g for 10 minutes and washed in 70 % ethanol. The DNA was spun down again, the majority of supernatant removed, and the pellet air dried. The pellet was then dissolved in 5 μL (per transfection) of sterile distilled water.

3.5.2 DNA amplification

DNA fragments were amplified using polymerases and the associated buffers from New England Biolabs (NEB). Each 50μL reaction contained ThermoPol Reaction Buffer (20mM Tris-Cl pH8.8, 10mM $(NH_4)_2SO_4$, 10mM KCl, 2mM $MgSO_4$, 0.1% Triton X-100), 200μM

dNTPs, 0.1ng μL^{-1} template DNA, forward and reverse primers at (typically) 0.5 μM, and 20U mL^{-1} *Taq* or VENT *Pfu* polymerase (depending on application). Additional $MgSO_4$ (NEB) was supplemented as necessary.

Using a TC-412 thermal cycler (Techne), a standard DNA amplification programme consisted of one cycle at 96°C for 1 minute (initial melting stage), then 30 cycles of the following: 96°C for 30 seconds (denaturing stage), 55°C for 30 seconds (annealing stage), 72°C for 60 seconds (extension stage). Based on the properties of the oligonucleotide primers, the annealing temperature and extension times were varied as necessary.

3.5.3 DNA restriction digestion

The restriction enzymes used (all from New England Biolabs), along with their relevant restriction buffers, are listed in Table 3.5.1. A typical restriction digestion was set up as follows. In a total volume of 50 μL, the DNA (5 μL) sample was mixed with 10X restriction buffer (5 μL), appropriate for particular enzyme under study, and sterile distilled water (39 μl). When necessary, bovine serum albumin was supplemented into the reaction to a final concentration of 100 mg L^{-1} and the volume of sterile distilled water adjusted accordingly. Restriction enzyme (1 μL: 10-20 units) was added and the tube contents consolidated by centrifugation. The tube was then placed at an appropriate incubation temperature, generally 37^oC, for 1-3 hours. The reaction was halted by addition of a $1/10^{th}$ volume (5 μL) of loading dye (10 mM Tris-HCl pH 7.6, 0.03% bromophenol blue, 0.03% xylene cyanol FF, 60% glycerol, 60 mM EDTA) (Fermentas) to the mixture.

restriction enzyme	restriction site	NEB buffer
*Apa*I	GGGCC^C	4
*Asc*I	GG^CGCGCC	4
*Bam*HI	G^GATCC	3
*Hin*dIII	A^AGCTT	2
*Kpn*I	GGTAC^C	1
*Sac*I	GAGCT^C	1
*Sac*II	CCGC^GG	4
*Sal*I	G^TCGAC	3
*Sbf*I	CCTGCA^GG	4
*Sca*I	AGT^ACT	3
*Xba*I	T^CTAGA	4
*Xho*I	C^TCGAG	4

Table 3.5.1: Restriction enzymes, their restriction sites and corresponding NEB buffer used in this study
The "^" symbol denotes the DNA cleavage site on the single strand shown.

3.5.4 DNA ligation

A typical DNA ligation reaction was set up as follows. In a total volume of 20 μL, varying amounts of vector and insert DNA were mixed with 2 μL 10X T4 DNA ligation buffer (500 mM Tris-HCl pH 7.5, 100 mM $MgCl_2$, 10 mM ATP and 100 mM dithiothreitol) (New England Biolabs) and the volume adjusted to 19 μL with sterile distilled water. T4 DNA ligase (1 μL: 400 units) (New England Biolabs) was then added to the mixture and the reaction consolidated by centrifugation. The reaction was then incubated at room temperature for 2-4 hours, or in certain cases the reaction was placed at 4ºC overnight. The amount of vector and insert DNA used in ligation reactions was judged by visualisation on an ethidium bromide-stained agarose gel and a molar ratio of 5:1 (insert:vector) for "sticky-end" ligations and 10:1 for "blunt-end" ligations was applied.

3.5.5 Bacterial DNA transformation

Competent bacteria were prepared the day of transformation. An overnight culture of *E. coli* was diluted 1:50 into NZCYM medium and grown for around 2 hours at 37ºC (optical density at 600 nm was judged between ~0.6-1.0). The cells (1 mL culture) were pelleted at 3555 g for 5 minutes, re-suspended in 1 mL ice-cold 0.1 M $CaCl_2$ (Sigma-Aldrich) and then incubated on ice for 10 minutes. Cells were harvested and the pellet re-suspended in 0.1 mL ice-cold 0.1 M $CaCl_2$. The DNA to be transformed was then added to the competent cells: 15-30 μL of a ligation or 1 μL of pure plasmid DNA. The bacteria/DNA mix was incubated on ice for 30 minutes, then heat shocked at 42ºC for 90 seconds before being placed back on ice for 2 minutes. Transformation mixes were then transferred on to NZCYM agar plates containing appropriate antibiotic selection. Agar plates were then incubated overnight at 37ºC to allow colonial growth.

3.5.6 Parasite DNA transfection

Early to mid-log phase *L. major* (2×10^7 per transfection) were pelleted at 1000 g for 10 minutes, washed in PBS, then resuspended in 1 mL PBS and transferred to a 1.5 mL microcentrifuge tube. Cells were then spun down at 2000 g for 5 minutes in a microcentrifuge and all supernatant removed. The pellet was then resuspended in 100 μL Human T-cell Nucleofector® solution (Lonza), 5 μg of purified DNA (Section 3.5.1) added, and the mixture transferred to an Amaxa® cuvette (Lonza), before electroporation in the Amaxa® nucleofection machine (Lonza) using the program U-033. The DNA/*L. major* mixture was then transferred to prewarmed M199, and incubated for 24 hrs at 27°C.

The following day, plates were prepared containing M199 with 1% agar, 1.2 μg mL^{-1} biopterin (Sigma-Aldrich) and the necessary selection drug (Section 3.2.1), and equilibrated

at 27^{o}C for 2 hrs. Transfected parasites were then pelleted at 1000 g for 10 minutes, resuspended in 100 μL M199, and spread evenly across the M199-agar plates. The plates were sealed with Parafilm® (VWR international) and incubated for 1-4 weeks at 27^{o}C until colonies appear. Colonies were transferred to liquid M199 and cultured as described in Section 3.2.1 for analysis.

3.5.7 DNA sequencing

For Custom DNA Service sequencing (Eurofins MWG Operon), 0.75-2 μg of template DNA and 150 pmol in 15 μL of appropriate oligonucleotide primer were used for sequencing by the facility.

3.5.8 Gel electrophoresis: DNA

Conventional agarose gel electrophoresis was used to fractionate DNA molecules in the size range of 200 bp to 10 kbp. The agarose concentration, voltage and run times were altered to optimise separation in the desired range. A standard agarose gel was made by dissolving an appropriate amount of Molecular Grade Agarose (Bioline) in 1x TAE buffer (40 mM Tris base, 40 mM acetic acid, 1 mM EDTA) (Sigma-Aldrich) containing ethidium bromide (0.1 mg L^{-1}) (Sigma-Aldrich). Generally, an agarose concentration of 0.6-1.0% (w/v) was used. Following casting, the solidified gel was placed in electrophoresis buffer (1x TAE containing ethidium bromide), samples loaded into the wells, including a GeneRuler™ 1 kb DNA ladder marker (Fermentas), and a constant voltage applied across the gel. Generally, a run time of 1-2 hours was employed when using a constant voltage of between 3-5 V cm^{-1}. Migration of the sample through the agarose matrix was followed by monitoring the bromophenol blue/xylene cyanol dye fronts. When the DNA had migrated the desired distance, the gel was analysed on a UV transilluminator and documented (Syngene).

3.5.9 DNA blotting

Agarose gels were depurinated for 15 minutes in 0.25 M HCl (VWR International), washed in distilled water, and then soaked in denaturation buffer (0.5 M NaOH, 1.5 M NaCl) (both Sigma-Aldrich) for 30 minutes. The gel was washed in distilled water, and soaked in neutralisation buffer (0.5 M Tris-HCl, 1.5 M NaCl, pH 7.2) for 60 minutes. Nucleic acids were transferred to a 0.22 μm MAGNA, nylon membrane (GE Water & Process Technologies) by capillary action (Southern 1975) using a 20X SSC solution (3 M NaCl, 0.3 M Sodium Citrate, pH 7.0) (Sigma-Aldrich) drawn by layers of paper towels for 16-24 hours. The gel was placed on a 3MM filter paper 'wick' (GE Healthcare) wetted with 20X SSC, with the wick base submerged in a bath of 20X SSC. The nylon membrane was cut to the gel size and placed on top of the gel, then three sheets of 3MM filter paper again cut to the gel size**,** were placed on top. A pile of paper towels were placed on top of this construct and weighted down to compress the "sandwich". The gel was lined with clingfilm to prevent short-circuit of the capillary action. Following transfer, the nucleic acid was cross-linked to the membrane using a UV cross-linker (Stratagene), using an auto-algorithm, with the DNA side of the membrane facing the UV bulbs. Membranes were stored at 4^{o}C in aluminium foil.

3.5.10 DNA probes

Non-radioactive DNA probes were generated using the PCR DIG Probe Synthesis kit (Roche), in accordance to manufacturer's instructions. Briefly, in a 50 μL reaction, 5 μL 10X Expand High Fidelity reaction buffer, containing 1.5 mM $MgCl_2$, was combined with the forward and reverse primer (both between 0.1-1 μM), template DNA (approximately 10-100 pg if using a plasmid) and 5 μL Probe Synthesis Mix containing 2 mM dATP, dCTP and dGTP plus 1.3 mM dTTP/0.7 mM DIG-labelled dUTP. The volume of the reaction was adjusted to 49.25 μL with sterile distilled water to which 0.75 μL (2.6 units) of DNA

polymerase was added. Using a TC-412 thermal cycler (Techne), a DNA amplification programme was used consisting of one cycle at 96°C for 2 minute (initial melting stage), 30 cycles of the following: 96°C for 30 seconds (denaturing stage), 60°C for 30 seconds (annealing stage), 72°C for 60 seconds (extension stage). A single final elongation step at 72°C for 7 minutes was then carried out. Based on the properties of the oligonucleotide primers, the annealing temperature and extension times were varied as necessary. The resultant DIG-containing DNA fragment was analysed and purified following gel electrophoresis.

3.5.11 DNA hybridisation

Nylon membranes containing immobilised, single stranded DNA were pre-hybridised with 5X SSC buffer containing 0.5 % (w/v) SDS**,** 1X Denhardts solution (200 mg L^{-1} Ficoll® 400, 200 mg L^{-1} polyvinylpyrrolidone, 200 mg L^{-1} Bovine Serum Albumin) (all Sigma-Aldrich) and 0.2 mg ml^{-1} denatured, sheared salmon sperm DNA (Sigma-Aldrich) at 65°C for 6 hours. The DNA probe was denatured (95°C for 5 minutes), added immediately to the pre-hybridisation solution and incubated at 65°C overnight. The following morning, a series of stringency washes were performed firstly using 2X SSC/0.2% (w/v) SDS solution at 68^{o}C for 15 minutes and then in 0.2X SSC/0.2% (w/v) SDS at 68^{o}C for 15 minutes. Hybridisation was detected using the DIG Luminescent Detection Kit (Roche) as per the manufacturer's instructions. Briefly, the membrane was treated with an alkaline phosphatase-conjugated α-DIG antibody, before washing. The membrane was then covered in a solution containing the dioxetane CSPD®, which is then (after incubation at 37^{o}C for 10 minutes) metabolised by the alkaline phosphatase in a luminescent reaction. This luminescence is then detected and recorded using Amersham Hyperfilm ECL (GE Life Sciences).

3.6 Plasmid constructs

3.6.1 Construction of vectors that facilitate heterologous expression of LmNTR in *E. coli*

The LmNTR catalytic domain (residues 87-323) was amplified from the *L. major* Friedlin genome with the oligonucleotide primers LmNTR-1 (forward) and LmNTR-2 (reverse), generating a 717 bp fragment. The fragment was purified then digested with restriction enzyme combination *Bam*HI+*Hind*III and cloned into the corresponding sites of the expression vector pTrcHis-C (Invitrogen), resulting in pTrcHis-C-ΔLmNTR.

3.6.2 Construction of vectors that facilitate *LmNTR* gene deletion

DNA fragments containing the flanks from *LmNTR* were amplified from *L. major* Friedlin genomic DNA using the oligonucleotide primer combinations LmNTR-9/LmNTR-10 for the 5' flank, and LmNTR-11/LmNTR-13 for the 3' flank. This generated 731 and 1,076 bp fragments respectively that were digested with *Sac*I+*Xba*I and *Apa*I+*Kpn*I respectively. The fragments were gel purified and sequentially cloned on each side of a puromycin resistance cassette (PAC) from p5'TbNTRKO-PAC (Dr S. Wilkinson) to form pLmNTRKO-PAC.

The vector pTbNTRKO-BSR (Dr S. Wilkinson) was digested with *Xba*I+*Apa*I releasing a DNA fragment containing the blasticidin-S deaminase gene plus *T. brucei* tubulin 5' and 3' UTRs (required for efficient expression of the drug resistance genes). This fragment was purified and cloned into the *Xba*I+*Apa*I sites of pLmNTRKO-PAC such that the puromycin N-acetyl-transferase-containing resistance cassette was replaced by the *bsr*-containing sequence, to form pLmNTRKO-BSR.

3.6.3 Construction of *L. major* episomal vectors that introduce ectopic copies of *LmNTR*

The gene encoding LmNTR was amplified from *L. major* genomic DNA using VENT *Pfu* and the primers LmNTR-4/LmNTR-2. The 972 bp fragment generated was purified, digested with *Bam*HI+*Hind*III then ligated into the corresponding sites of the trypanosomatid expression vector pTEX (Kelly, Ward *et al.* 1992) to form pTEX-LmNTR.

3.6.4 Construction of constitutive *L. major* integrative luciferase expression vector

A sequence corresponding to the *L. major* 5' spacer/promoter ribosomal RNA was amplified from *L. major* Friedlin genomic DNA using the primer pairs LmrRNA-1/LmrRNA-2 resulting in a 300 bp fragment. This was purified, digested with the *Sac*I+*Bam*HI enzyme combination and ligated into the corresponding sites of *Trypanosoma cruzi* reporter vector pRiboTEX-Luc (Bot, Hall *et al.* 2010) to form pLm5'RiboTEX-Luc. A sequence corresponding to the *L. major* 3' spacer ribosomal RNA region was amplified from *L. major* Friedlin genomic DNA using the primer pairs LmrRNA-3/LmrRNA-4 resulting in a 850 bp fragment. This DNA was purified, digested with *Kpn*I and cloned into the single *Kpn*I site of pLm5'RiboTEX-Luc. Restriction mapping of the resultant plasmid with *Sbf*I+*Asc*I determined the orientation of the insert. Plasmids with the correct arrangement were called pLmRIX-Luc-0.

A derivative of pLmRIX-Luc-0 was generated containing a polypyrimidine tract and splice leader addition site sequence upstream the *T. cruzi MPX* gene was inserted upstream of the luciferase reporter. Using the plasmid pTAG404 (Dr S. Wilkinson) as template, amplification reactions using primers LmrRNA-5/LmrRNA-6 were carried out, resulting in the generation of a 300 bp fragment. This DNA was purified, digested with *Bgl*II+*Bam*HI and cloned into the unique *Bam*HI site of pLmRIX-Luc. Restriction mapping of the resultant plasmids with

*Sac*I+*Hin*dIII determined the orientation of the insert. The final construct was subsequently called pLmRIX-Luc

3.6.5 Construction of constitutive *L. major* integrative LmNTR expression vector

The gene encoding LmNTR was amplified from *L. major* genomic DNA using VENT *Pfu* and the primers LmNTR-4/LmNTR-18. The resultant 972 bp DNA fragment was digested with *Bam*HI+*Xho*I and cloned into the *Bam*HI+*Sal*I sites of pLmRIX-Luc, replacing the luciferase gene. The construct was named pLmRIX-LmNTR.

3.7 Protein analysis

3.7.1 Heterologous expression of recombinant LmNTR

An overnight culture (50 mL) of *E. coli* BL21(+) cells harbouring the plasmid pTrc-HisC-ΔLmNTR was diluted into 2 L NZCYM broth containing 100 mg mL^{-1} ampicillin and grown for 4 hours at 37°C. The culture was transferred to 16^{o}C an incubated with aeration for 30 minutes before addition of isopropyl-β-d-thiogalactopyranoside to a final concentration of 1 mM. The culture was then incubated overnight at 16^{o}C. The cells were harvested by centrifugation (5000 g for 20 minutes) and the pellet stored at -20^{o}C.

3.7.2 Purification of recombinant LmNTR

The *E. coli* pellet containing cells induced to express recombinant ΔLmNTR, stored at -20^{o}C, was thawed then resuspended in 80 mL Lysis Buffer (50 mM NaH_2PO_4, pH 7.8; 500 mM NaCl; 8 protease inhibitor mix tablets (Roche)). This mixture was then supplemented with DNAse, RNAse, lysozyme, and 1 % (w/v) CHAPS (all Sigma-Aldrich) and incubated on ice for 30 minutes in order to lyse the cells. The extract was sonicated and cell debris removed by centrifugation (27000 g for 30 minutes at 4°C). The clarified supernatant was then applied to

a 2 mL pre-packed nickle-nitrilotriacetic acid (Ni-NTA) (Qiagen) column and the column copiously washed in 40 mL Wash Buffer 1 (50 mM NaH_2PO_4 pH7.8, 500 mM NaCl, 50 mM imidazole) then in 40 mL Wash Buffer 2 (50 mM NaH_2PO_4 pH7.8, 500 mM NaCl, 100 mM imidazole). Recombinant protein was eluted off the column using 10-20 x 0.5 mL aliquots of Elution Buffer (50 mM NaH_2PO_4 pH7.8, 500 mM NaCl, 500 mM imidazole, 1% (w/v) CHAPS). After elution, yellow fractions were collected and glycerol was added to a final volume of 20 % (v/v). This solution was then redistributed into 0.5 mL aliquots and frozen for future use at -80^{o}C.

3.7.3 Gel electrophoresis: protein

Pre-cast gels (Biorad) were used for protein electrophoresis with a Mini-Protean III system (Biorad). Protein samples (10-20 μL) were mixed with 5X Sample Buffer (10 % SDS (w/v); 10 % β-mercaptoethanol (v/v); 20 % glycerol (v/v); 0.2 M Tris, pH 6.8; 0.05 % bromophenol blue (w/v)) (all Sigma-Aldrich) and denatured at 96^{o}C for 5 minutes. The samples were separated on 12% polyacrylamide gels with 1X SDS-PAGE running buffer (25 mM Tris-HCl, 200 mM glycine, 0.1 % (w/v) SDS) using a constant voltage 150 V for 60-90 minutes. Gels were stained for 2 hours in Coomassie Blue solution (0.2% (w/v) Coomassie brilliant blue, 7.5% (v/v) acetic acid, and 50% (v/v) ethanol) followed by de-staining in boiling distilled water. Samples were run alongside a PageRuler Prestained Protein ladder (Fermentas) as a marker.

3.7.4 Flavin cofactor determination

The flavin co-factor bound to trypanosomal NTRs was established by determining the fluorescence spectrum in acidic and neutral buffers (Faeder *et al.* 1973). Purified protein was desalted through a Zeba spin column (Thermo Scientific) and boiled for 5 min. In a total

volume of 100 μL, clarified supernatants (90 μL) containing 0.5 mg LmNTR were mixed with 10 μl 50 mM NaH_2PO_4 pH7.6 or 1 M HCl (final pH = 2.2). The fluorescence profile for each treatment was then determined using a Gemini Fluorescent Plate Reader (Molecular Devices (UK) Ltd, Wokingham, UK) with an λ_{EX} of 450 nm and a λ_{EM} of 480-600 nm. The resultant patterns were compared with profiles obtained using FMN and FAD standards.

3.7.5 Nitroreductase assay

ΔLmNTR activity was followed by monitoring the change in absorbance at 340 nm corresponding to NADH consumption using a Lambda 25 spectrophotometer (Perkin Elmer) (Wilkinson, Taylor *et al.* 2008). A standard reaction (1 mL) containing 50 mM Tris-Cl pH7.5, 100 μM NADH and 100 μM electron acceptor was incubated at room temperature for 5 min from which the background reaction rate was determined. The assay initiated by addition of the LmNTR (35 μg) and the rate of NADH consumption recorded. The enzyme activity was then calculated using an ε value of 6,220 M^{-1} cm^{-1}, giving values of enzyme activity in nmol NADH oxidised min^{-1} mg $\Delta LmNTR^{-1}$. The absorbance spectrum (320-600nm) for each electron acceptor was determined previously and shown not to interfere with the analysis: at the concentrations used, no significant signal was detected at 340 nm for any of the compounds tested.

4. Developing a luciferase reporter cell line to screen compounds against amastigote *L.major*

Several drug screening regimens are now in place for use with *Leishmania*, each with their own advantages and disadvantages (Sereno *et al.* 2007). The classical method involves visualising Giemsa stained intracellular *Leishmania* within tissue culture derived mammalian macrophages using light microscopy (Berman *et al.* 1980). This system although reproducible is laborious, subjective, and incompatible with a high throughput screening regimen, requiring a practised eye. To speed up drug discovery against these medically important organisms, recombinant *Leishmania* parasites expressing an array of reporter markers have been developed (see Section 1.8.4) (Sereno, Cordeiro da Silva *et al.* 2007). After reviewing the advantages and disadvantages of each of these systems, it was decided that the most suitable option for the development of an assay to be used in a multi-well plate format would involve the construction of luciferase expressing *L. major* cells, specifically one where the reporter gene had been integrated into the genome of the parasite. To this end, we obtained the published construct pGM-αNEOαLUC that targets the ribosomal DNA loci of both *L. major* and *L. donovani* (Roy, Dumas *et al.* 2000). However, following several failed attempts at transforming this DNA vector into *E. coli*, it was decided that we should develop our own luciferase expression construct. This would then be used to produce a *L. major* reporter cell line that could then be employed to rapidly screen various compounds against the intracellular, amastigote life cycle stage.

4.1 Construction of a luciferase-expressing reporter cell line of *L. major*

The first stage in the production of the luciferase-expressing *L. major* cell line is to create the DNA constructs needed to transfect into promastigote form parasites. Using the *T. cruzi* episomal expression pRiboTEX-Luc as a starting plasmid (Bot, Hall *et al.* 2010), a two step

cloning strategy was devised involving the introduction of DNA sequences from the *L. major* ribosomal DNA (rDNA) promoter/spacer region either side of a luciferase/neomycin phosphotransferase-containing cassette (Figure 4.1.1).

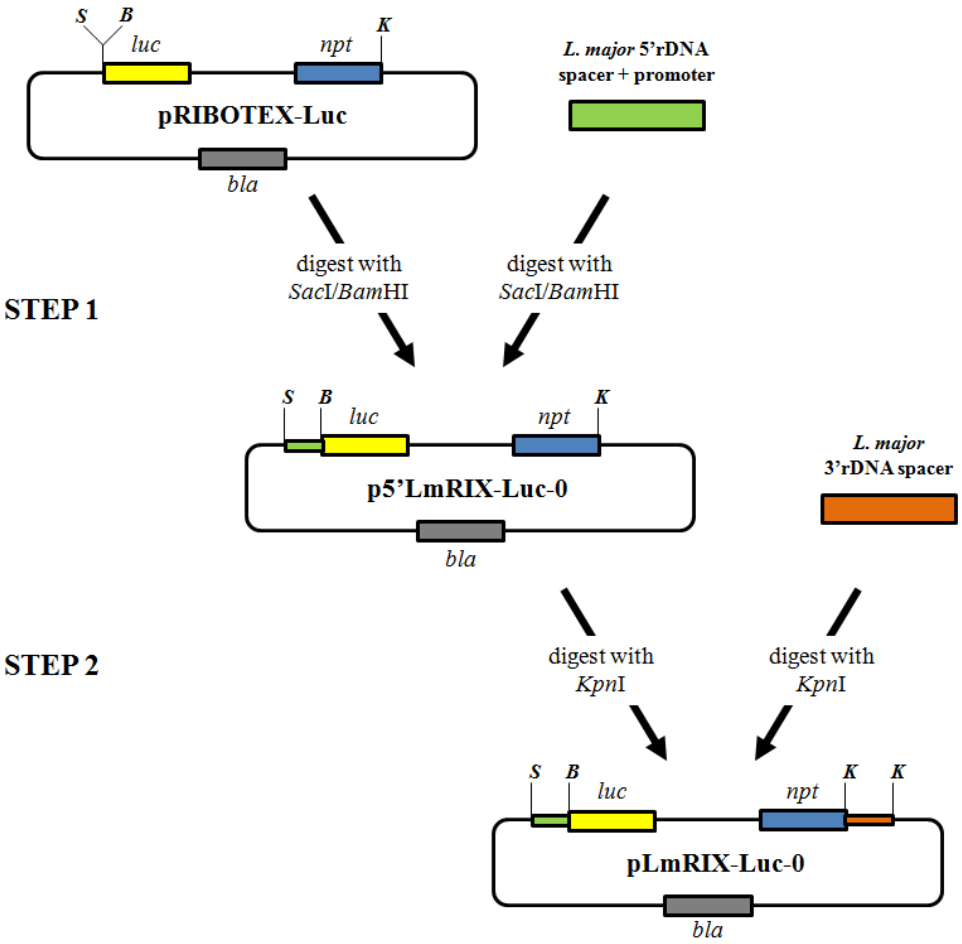

Figure 4.1.1: Schematic representation outlining the two-step construction of pLmRIX-Luc-0
In the first step, the 5' ribosomal DNA (rDNA) spacer/promoter region from *L. major* Friedlin was amplified from genomic DNA using VENT *Pfu* and the primers LmrRNA-1/LmrRNA-2. The resultant DNA fragment (green box) was digested with *Sac*I+*Bam*HI and cloned into the corresponding sites of pRiboTEX-Luc (supplied by Dr C Bot) to form p5'LmRIX-Luc-0. In step 2, the 3' rDNA spacer from *L. major* Friedlin was amplified from genomic DNA using VENT *Pfu* and the primers LmrRNA-3/LmrRNA-4. The resulting fragment (orange box) was digested with *Kpn*I, and ligated into the corresponding site of p5'LmRIX-Luc-0 generating pLmRIX-Luc-0. The DNA sequences encoding for the ß-lactamase (*bla*; grey), luciferase (*luc*; yellow) and neomycin phosphotransferase (*npt*; blue) genes are highlighted. The *Sac*I (*S*), *Bam*HI (*B*) and *Kpn*I (*K*) restriction sites are also noted.

In the first cloning step, the 5' flank consisting of a 300 bp region centred on the rDNA array transcription initiation site (*i.e.* the ribosomal promoter), as identified by Martinez-Calvillo *et*

al. (2001), was amplified from *L. major* Friedlin genomic DNA using the primer combination LmrRNA-1/LmrRNA-2. The resultant DNA fragment was digested with *Sac*I+*Bam*HI and cloned into the corresponding sites of pRiboTEX-Luc (Bot, Hall *et al.* 2010), replacing the *T. cruzi* rRNA promoter sequence, to form p5'LmRIX-Luc-0. In the second cloning step, the 3' flank, consisting of a ~850 bp DNA sequence derived from the 3' end of the rDNA spacer, was amplified from *L. major* Friedlin genomic DNA using the primers LmrRNA-3/LmrRNA-4. This fragment was digested with *Kpn*I and ligated into the corresponding site of p5'LmRIX-Luc-0. The orientation of the 3' flank was then determined by restriction digestion using *Sbf*I+*Asc*I which generated diagnostic 5.0 and 3.0 kbp fragments when the insert had been cloned as desired. The resultant ~8.0 kbp plasmid, called pLmRIX-Luc-0 (Figure 4.1.2), was verified by restriction mapping and sequencing analysis.

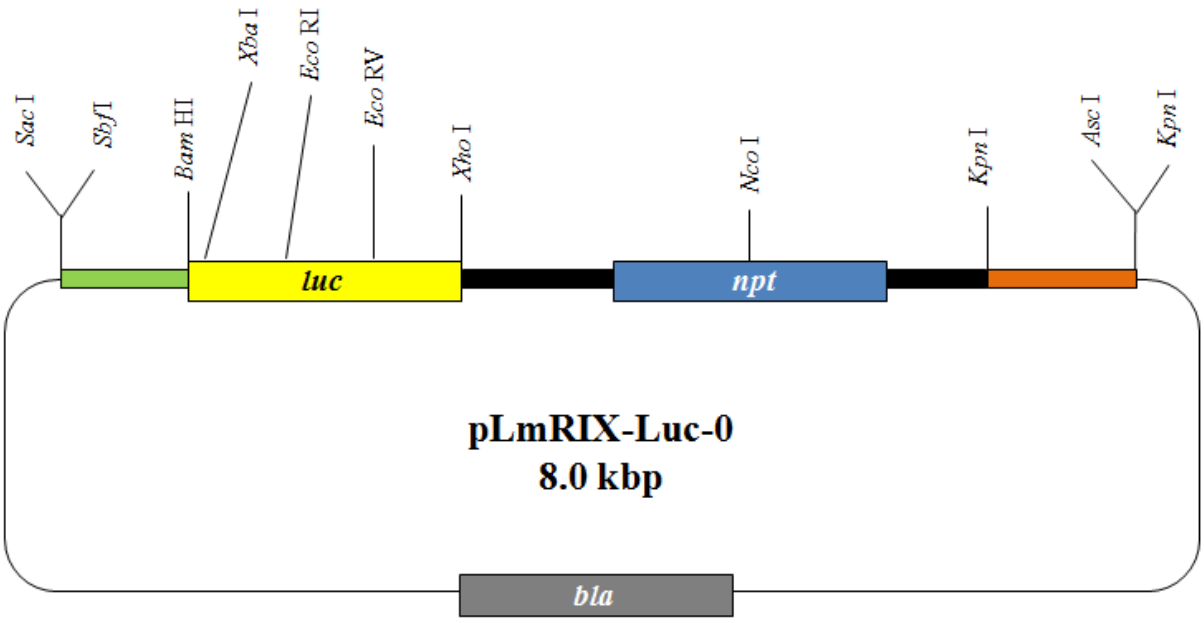

Figure 4.1.2: Restriction map of plasmid pLmRIX-Luc-0
The *L. major* 5' rDNA spacer/promoter (green) and 3' rDNA spacer (orange) as described in Figure 4.1.1 are noted. The DNA sequences encoding for the β-lactamase (*bla*; grey), luciferase (*luc*; yellow) and neomycin phosphotransferase (*npt*; blue) genes are highlighted. The black boxes flanking the *ntp* gene correspond to the intergenic and 3' untranslated region from *T. cruzi* GAPDH. These facilitate expression of the *npt* gene and, in the case of the intergenic sequence, provide a polyadenylation sequences used in the processing of the *luc* mRNA.

Before electroporation into *L. major* promastigotes, pLmRIX-Luc-0 was digested with the restriction enzymes *Sbf*I+*Asc*I, releasing a ~5.0 kbp DNA fragment containing the *Leishmania* rDNA/luciferase/neomycin phosphotransferase-containing sequences from the ~3.0 kbp vector backbone. The larger fragment was gel purified and then introduced into the parasite by electroporation. Recombinant *L. major* cells were then selected on agar plates containing G418. After 3-4 weeks, colonies visible on the media surface were transferred into M199 medium containing G418 and cultured as described in Section 3.2.1. After two rounds of sub-culturing, equal aliquots of wild type *L. major* Friedlin and three independent LmRIX-Luc-0 containing parasite clones in the stationary phase of growth were lysed and the luciferase activity determined (Figure 4.1.3).

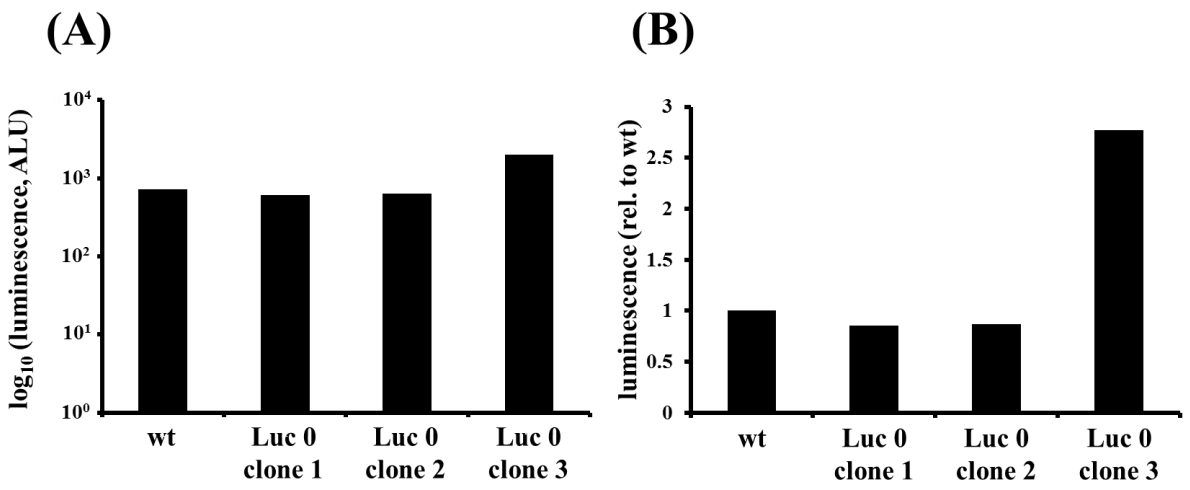

Figure 4.1.3: Luciferase expression by *L. major* promastigotes transfected with pLmRIX-Luc-0
The luciferase activity, as measured in arbitrary light units (ALU), of extracts derived from recombinant *L. major* promastigote clones transfected with pLmRIX-Luc-0 (Luc 0 clones 1, 2 and 3) was determined and compared to that of the parental line (*L. major* Friedlin; wt). For all assays, cells in stationary phase of growth (~$5x10^7$ cells mL^{-1}) were lysed, and extracts from 1 x 10^6 parasites analysed. The data are presented as (A) background corrected luminescence, and (B) luminescence relative to wild type. All readings were from one off experiments. The luminescence activities of all three recombinant parasite extracts was equivalent to that observed for wild type promastigotes.

Comparison of the luminescence signal of recombinant parasite extracts with that displayed by the parental control revealed that all lystates had equivalent luciferase activities. This

strongly suggests that expression of the reporter was not occurring at a significant level. Analysis of the rDNA sequences present in pLmRIX-Luc-0 established that certain post-transcriptional regulatory elements required for the correct expression of the luciferase within the trypanosomatids were missing from this construct. To rectify this oversight, a 270 bp sequence containing the polypyrimidine tract and spliced leader addition site located upstream of the *T. cruzi* mitochondrial tryparedoxin peroxidase gene was amplified from the plasmid pTAG404 (supplied by Dr Shane Wilkinson) using the primers LmrRNA-5/LmrRNA-6. The resultant DNA fragment was digested with *Bgl*II+*Bam*HI then cloned into a unique *Bam*HI site present in pLmRIX-Luc-0 and located between the 5' rDNA flank and the luciferase gene to form the ~8.3 kbp plasmid pLmRIX-Luc (Figures 4.1.4 and 4.1.5). Orientation of the insert was determined using a *Sac*I+*Hin*dIII diagnostic digest. This plasmid was verified by restriction mapping and DNA sequencing.

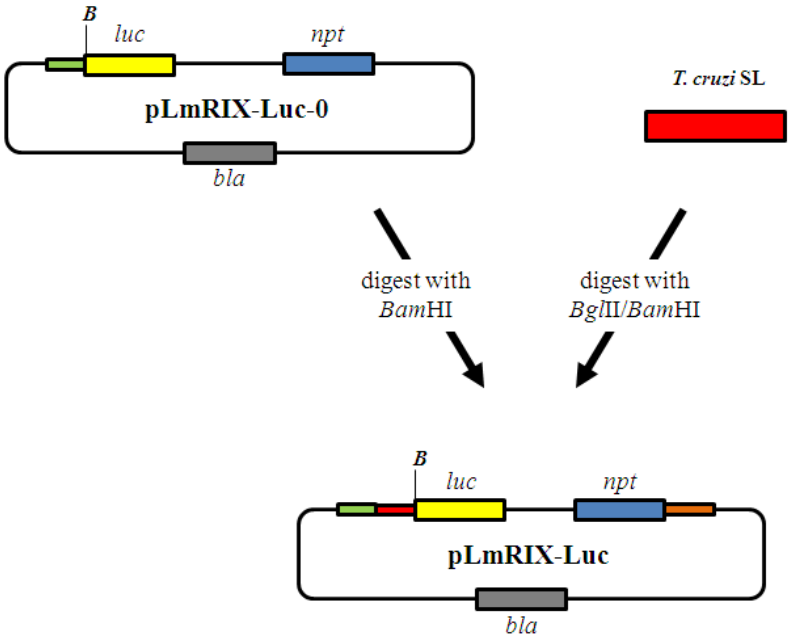

Figure 4.1.4: Schematic representation outlining the construction of the luciferase expression vector pLmRIX-Luc
The polypyrimidine tract/splice leader addition site located upstream of the *T. cruzi* mitochondrial tryparedoxin peroxidase gene (red box) was amplified from the plasmid pTAG404 using VENT *Pfu* and the primers LmrRNA-5/LmrRNA-6. The resultant DNA fragment was doubly digested with *Bgl*II+*Bam*HI and cloned into the *Bam*HI site (*B*) of pLmRIX-Luc-0. DNA sequences encoding for the ampicillin (*bla*; grey) and neomycin (*npt*; blue) resistance cassettes, the luciferase reporter (*luc*; yellow), the *L. major* 5' rDNA spacer/promoter (green) and the 3' *L. major* rDNA spacer (orange) are all highlighted.

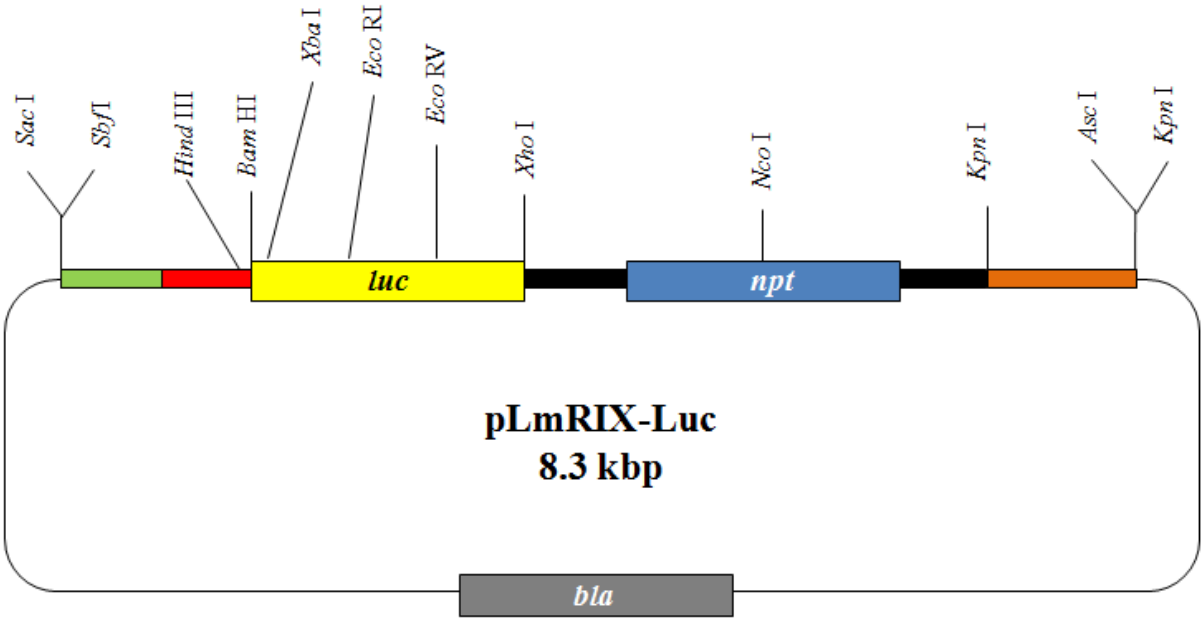

Figure 4.1.5: Restriction map of the luciferase expression vector pLmRIX-Luc
The polypyrimidine tract and splice leader addition site located upstream of the *T. cruzi* mitochondrial tryparedoxin peroxidase gene (red) is highlighted. The DNA sequences encoding for the β-lactamase (*bla*; grey), luciferase (*luc*; yellow) and neomycin phosphotransferase (*npt*; blue) genes plus the *L. major* 5' rDNA spacer + promoter (green) and 3' rDNA spacer (orange) are also noted.

As with pLmRIX-Luc-0, the plasmid pLmRIX-Luc was digested with *Sbf*I+*Asc*I, releasing a ~5.3 kbp DNA fragment containing the expression cassette from the ~3.0 kbp vector backbone. The larger fragment was gel purified, electroporated into *L. major* promastigotes and G418 selection performed as described in Section 3.2.1. After several rounds of culturing the luciferase activity from 1 x 10^6 clonal recombinant parasites and wild type cells was determined (Figure 4.1.6). In this case, comparison of the luminescence signal of extracts derived from *L. major* containing the luciferase expression construct were between 200 to 1000-fold greater than that observed from wild type lysates. This clone-to-clone variation is believed to be dependent upon which rRNA array the construct integrated into, with certain rRNA arrays expressed at higher levels than others (Alsford *et al.* 2005, Alsford *et al.* 2008).

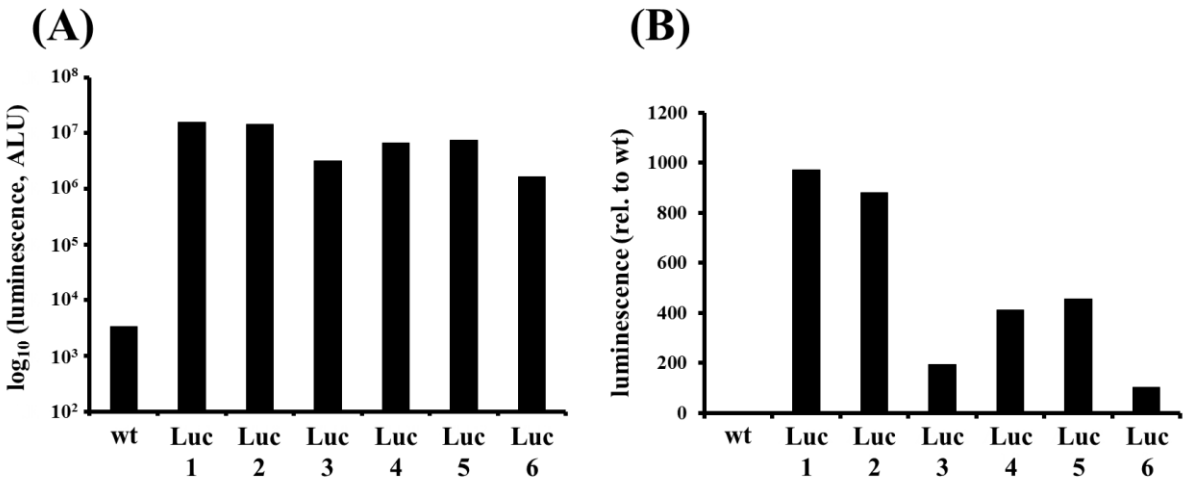

Figure 4.1.6: Luciferase expression by *L. major* promastigotes transfected with construct LmRIX-Luc
The luciferase activity, as measured in arbitrary light units (ALU), of extracts derived from six recombinant *L. major* promastigote (Luc 1-6) clones transfected with pLmRIX-Luc was determined and compared to that of the parental line (*L. major* Friedlin; wt). For all assays, cells in stationary phase of growth (~$5x10^7$ cells mL^{-1}) were lysed, and extracts from 1 x 10^6 parasites analysed. The luminescence activity was between 200 to 1000-fold higher in the six recombinant parasite extracts than wild type levels.

4.2 Characterising luciferase-expressing *L. major* promastigotes

As noted above, luciferase expression by the *L. major* clones varies (Figure 4.1.6). As one of the main uses for this reporter system is to develop a high throughput drug screening procedure, the culture exhibiting the highest reporter activity, namely LmRIX-Luc clone 1, was selected for further analysis – this particular clone had a relative luciferase level approximately three orders of magnitude greater than non-transformed parental cells. This clone was examined to determine how it relates to wild type cells in terms of its growth profiles, its ability to differentiate from one life cycle form to another, and also whether these recombinant parasites were infectious. Initially, assays were performed to monitor whether integration of the DNA into the *L. major* genome or subsequent expression of the reporter gene affected parasite growth (Figure 4.2.1). In these experiments, *L. major* LmRIX-Luc clone 1 and wild-type Friedlin cells were grown in parallel. Starting at density at 1 x 10^5 parasites mL^{-1} the culture was followed over the next 10 days and the growth curves of the

cell lines established. Over this time frame, the non-infectious promastigote recombinant parasites exhibited a similar growth profile to that displayed by the wild type culture with both cell lines having an approximate doubling time of around 18 hours. This indicates that integration of LmRIX-Luc into the *L. major* genome, and the resulting luciferase expression, has no effect on promastigote growth rates. This demonstrates that pLmRIX can be used as a general purpose integrative plasmid containing any required gene, without the plasmid components affecting parasite growth.

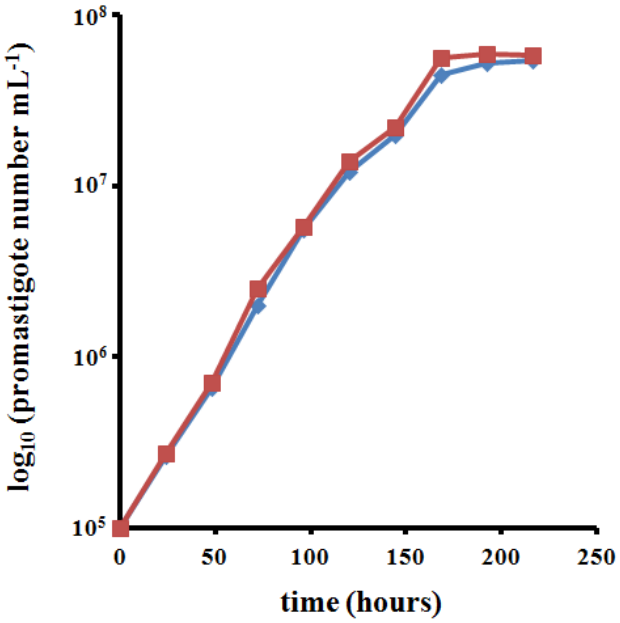

Figure 4.2.1: Growth of *L. major* luciferase-expressing promastigotes
The growth of luciferase-expressing (red) and wild type (blue) *L. major* promastigotes was monitored until cultures were in the stationary phase of growth. At day 0, both lines were seeded at $1x10^5$ cells mL^{-1}, and parasite loads (expressed as promastigote number mL^{-1}) determined every day over a 9 day period. The parasite lines used were *L. major* Friedlin (wild type) and *L. major* Friedlin LmRIX-Luc clone 1 (recombinant). Over the period examined, all *L. major* promastigote lines grew at equivalent rates. This experiment was repeated on two further occasions and the same profile was observed.

Next, we evaluated whether there was a correlation between cell number and luciferase activity using two approaches, both giving similar results (Figure 4.2.2). In the first method, carried out while investigating the growth of recombinant parasites, equal volumes of culture were collected over the first 9 days and assayed for luminescence. This clearly demonstrates that as the cell density increases so does the reporter signal. In the second procedure, the

luciferase activity was determined using fixed numbers of parasites (625 to 160,000). Again, a clear linear correlation between luminescence and cell number (over the range used here) was observed.

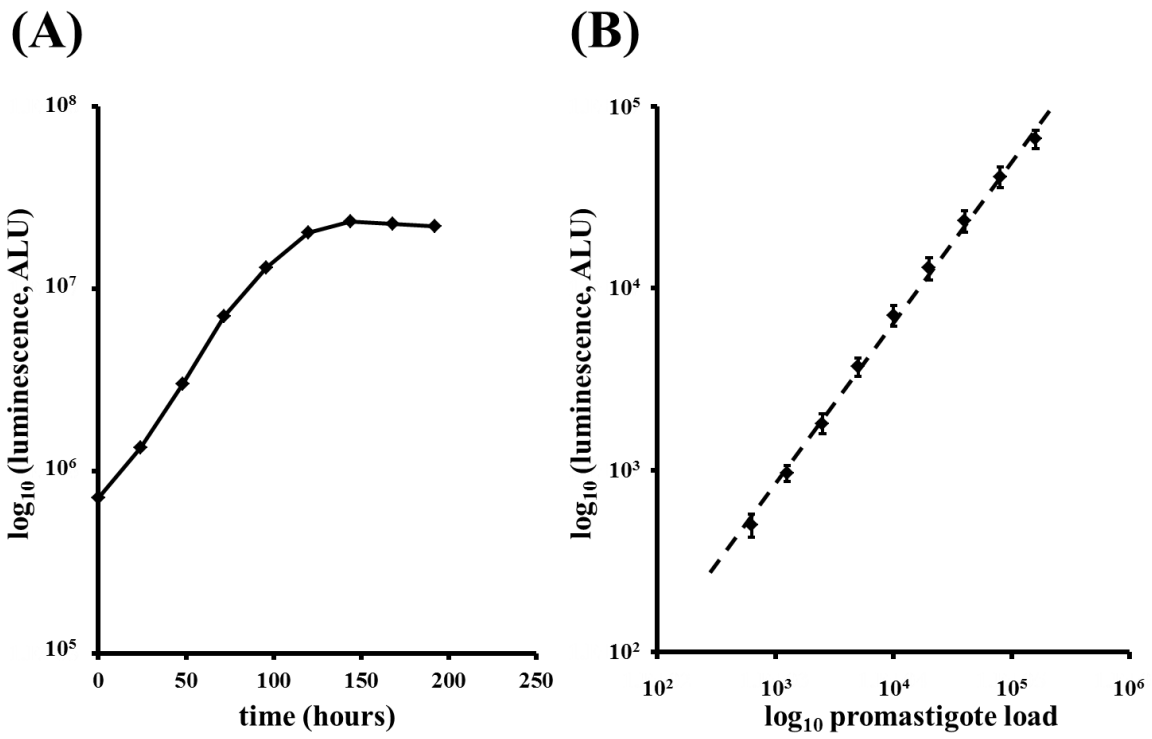

Figure 4.2.2: Correlation between luciferase activity and *L. major* promastigote load
(A) The growth of luciferase-expressing *L. major* (clone 1) was monitored over a 9 day period. At day 0, promastigote cells were seeded at $1x10^5$ cells mL^{-1} and every 20-24 hours, an aliquot (1 mL) was pelleted and the cells resuspended in 200 μL lysis buffer. A 20 μL aliquot of the lysate was then assayed for luciferase activity, as measured in arbitrary light units (ALU). The profile obtained directly reflects the growth pattern observed in Figure 4.2.1. (B) The luciferase activity, as measured in arbitrary light units (ALU), from 625 to 160,000 luciferase expressing *L. major* promastigotes was determined. Three independent readings were taken for each parasite load and the values are means ± standard deviation. Graphs A and B show a linear correlation between parasite load and luciferase activity.

After showing that luciferase expression has no apparent adverse affects on promastigote growth, experiments were conducted to evaluate whether the transgenic parasites could be used in drug screening in a 96-well plate format. Recombinant parasites were grown in the presence of different concentration of nifurtimox for a period of 3 days at 27^oC. After lysis 20

μL aliquots from each well were taken and the luciferase activity determined: all drug concentrations were assayed in triplicate. The luminescence signal obtained from drug treated extracts was then compared to no drug (100% growth) and no parasite (0% growth) controls and a dose response curve generated (Figure 4.2.3). From these plots, the concentration of nifurtimox that inhibited parasite growth by 50% (IC_{50}) was calculated to be 7.5 ± 0.42 μM and is in line with the IC_{50} value (6.3 ± 0.1 μM) determined using the fluorescent vital dye resazurin (Meredith and Wilkinson, unpublished).

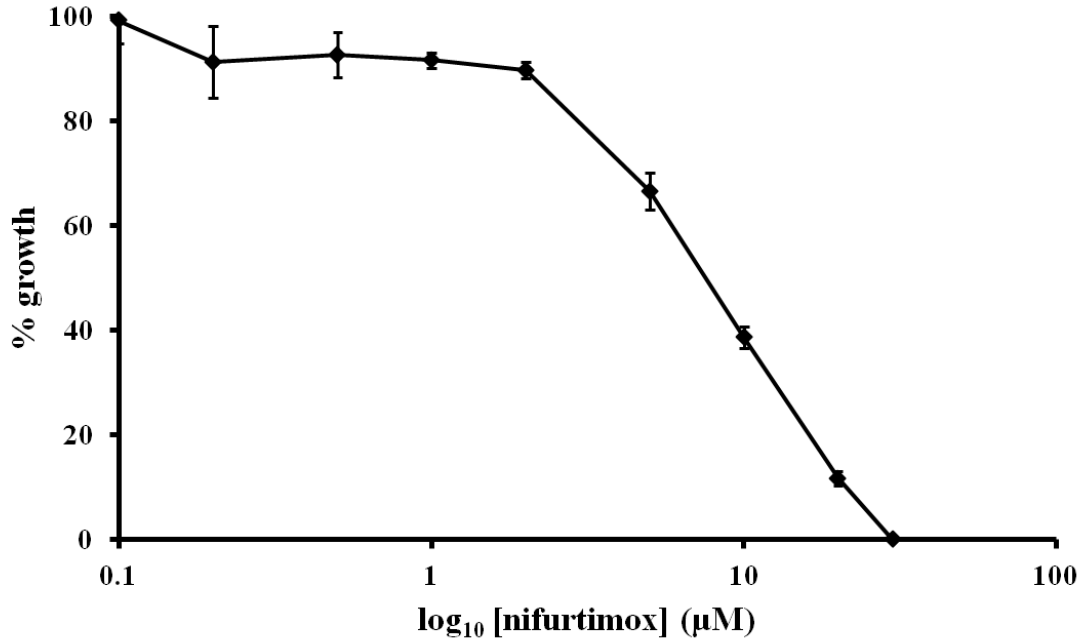

Figure 4.2.3: Susceptibility of luciferase-expressing *L. major* promastigotes to nifurtimox
Luciferase-expressing *L. major* promastigotes were seeded at 1 x 10^6 cells mL^{-1} into a 96-well microtitre plate with varying concentrations of nifurtimox. The cultures were then incubated for 3 days at 27°C before the addition of 50 μL lysis buffer. A 20 μL aliquot of the lysate was then assayed for luciferase activity. A dose response curve was presented as a percentage of the signal given by parasites incubated in the absence of nifurtimox. From this curve, the drug concentration that inhibited parasite growth by 50% (IC_{50}) was established. The data are the means from 3 experiments ± standard deviations.

After establishing that growth of *L. major* promastigote growth is not affected by luciferase expression, the ability of the LmRIX-Luc clone 1 to form infectious metacyclic promastigotes was studied. While determining the growth profile of non-infectious

promastigotes, parasite samples were collected and, using a well-characterised agglutination technique (da Silva and Sacks 1987), metacyclic parasites were quantified following purification (Figure 4.2.4). This shows that as the non-infectious promastigote culture reaches the stationary phase of growth (density of above 1 x 10^7 cells mL^{-1}) they start to differentiate into metacyclic parasites such that by day 8 there are approximately 2.5 x 10^5 metacyclics present per mL of culture representing between 0.4 to 0.5% of the total number of cells. This is similar to results reported elsewhere in the literature (da Silva and Sacks 1987) and shows that integration of LmRIX-Luc into the *L. major* genome, and the resulting luciferase expression, has no effect on the ability of these parasites to differentiate from the non-infectious to the infectious form.

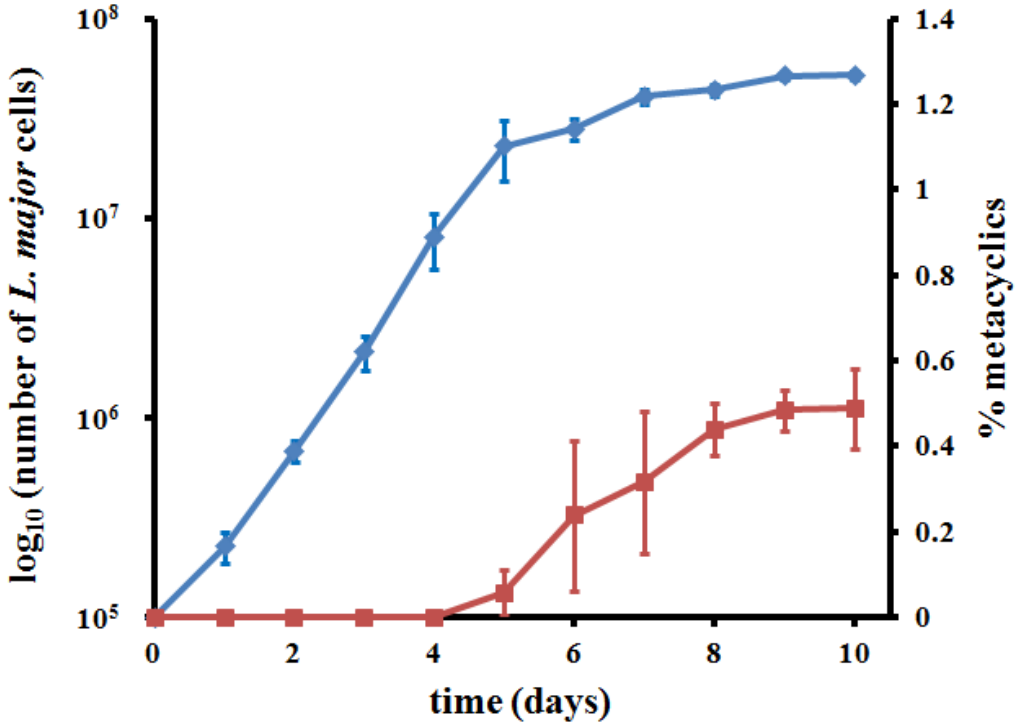

Figure 4.2.4: Growth curve and metacyclic production in LmRIX-Luc *L. major* (clone 1) The growth of luciferase-expressing *L. major* cells (blue diamonds, left axis) was monitored until cultures were in the stationary phase of growth as Figure 4.2.1. At day 5, 1 mL aliquots were taken from the cultures and metacyclics purified. The metacyclics were then counted and presented as a percentage of the overall number of *L. major* cells (red squares, right axis). This shows that LmRIX-Luc *L. major* are able to produce metacyclic cells, and these begin to develop from non-infective promastigotes when the culture reaches a density of around 1 x 10^7 cells mL^{-1}. The data are the means from triplicate repeats ± standard deviations.

4.3 Characterising luciferase-expressing *L. major* amastigotes

After demonstrating that luciferase expression does not affect the growth and differentiation of promastigote-form parasites, we then examined whether the reporter affected the intracellular mammalian stage. Using a human macrophage cell line (differentiated THP-1 cells) and purified metacyclic, luciferase-expressing *L. major*, infection and subsequent amastigote growth experiments were carried out to determine the optimal ratio of parasite to mammalian cells needed to obtain reproducible luminescence (Figure 4.3.1).

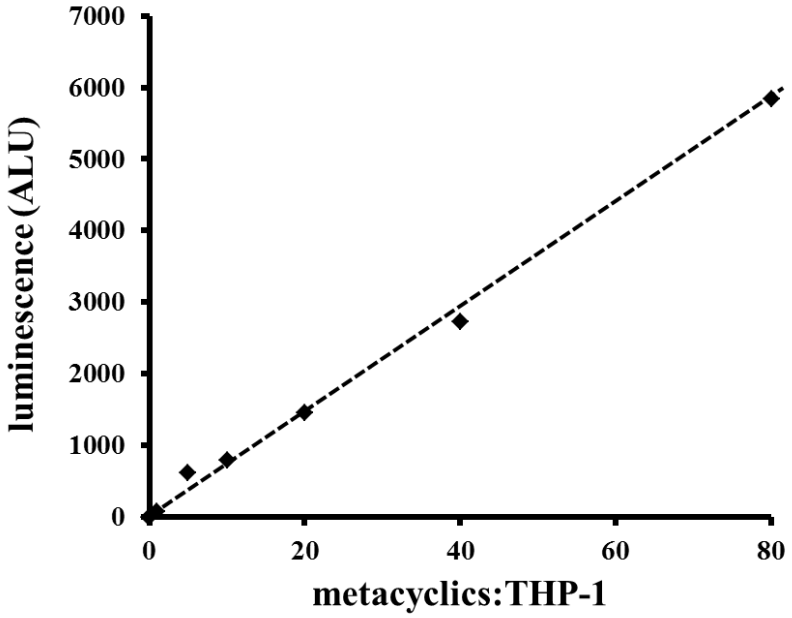

Figure 4.3.1: Correlation between luciferase activity and *L. major* metacyclic load
Differentiated THP-1 cells seeded at 2.5 x 10^4 cells mL^{-1} in a 96-well microtitre plate were infected overnight with varying numbers of purified luciferase-expressing *L. major* metacyclic parasites. The ratio of parasite to mammalian cell ranged from 0:1 to 80:1. Non-internalised parasites were then removed by extensive washing in culture medium and the amastigote parasites grown for 3 days at 37°C in a 5% CO_2 atmosphere. The growth medium was removed, the cells lysed (in 100 μL lysis buffer) and the luciferase activity, as measured in arbitrary light units (ALU), for each extract (20 μL) was determined. A linear correlation between the number of infectious metacyclic cells used in the initial infection and luciferase activity was observed throughout the range used.

A linear correlation was observed such that when few metacyclic parasites were used to infect the THP-1 line (<20:1) a low luminescence signal (and hence pathogen load) was observed in cultures 3 days post-infection. In contrast, when a high pathogen to mammalian

cell ratio was used (>20:1) a readily detectible luciferase activity was observed. However, the numbers of purified metacyclic-form parasites needed to conduct further infection assays at parasite:mammalian cells ratios >20:1 (*i.e.* 40:1 and 80:1) was prohibitive. For example, the number of metacyclic cells required to conduct an 80:1 infection ratio within a single 96-well plate experiment would need 100 to 150 mL promastigote cells in the stationary phase. Based on luciferase activity and promastigote culture volumes we decided that a ratio of 20 infectious *L. major* cells per macrophage was optimal for our needs.

We next conducted a time course experiment to determine how the reporter activity of luciferase expressing *L. major* amastigotes varies with time post-infection. Using a 20:1 parasite:mammalian cell ratio we carried out an infection and then at 24 hour intervals evaluated the luminescence signal, with all time points performed in triplicate (Figure 4.3.2). For the first 24 to 48 hours post-infection no significant difference was observed in luciferase activity in any of the replicate cultures. In the following 24-48 hours (*i.e.* 72 to 96 hours post-infection) the reporter signal increased approximately 3-fold, indicating that amastigote replication was occurring. For the 72 hour post-infection time point, little difference in the luciferase activity was observed between the three triplicates whereas at the latter time point a pronounced difference was detected. When repeated and data taken at time points beyond 96 hours, the luciferase activity fell back to levels equivalent to background (non-infected mammalian cells), similar to that observed for *L. donovani* (Roy, Dumas *et al.* 2000). Why there is this apparent drop in reporter activity is unclear. Based on our observations, all further studies involving infection of differentiated THP-1 cells and subsequent intracellular parasite growth were carried out for no longer than 72 hours post-infection.

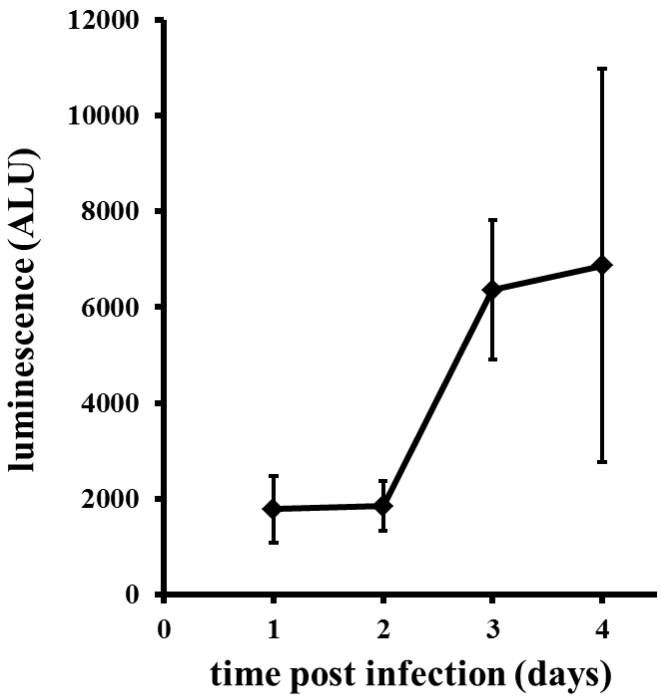

Figure 4.3.2: Growth of in intracellular luciferase-expressing *L. major* amastigotes
Differentiated THP-1 cells seeded at 2.5 x 10^4 cells mL^{-1} in a 24-well microtitre plate were infected overnight with 5 x 10^5 metacyclic cells mL^{-1}. After infection, non-internalised parasites were then removed by extensive washing in culture medium and then on each day (up to the 4^{th} day post-infection), a subset of wells were lysed (in 100 μL lysis buffer) and the luciferase activity, as measured in arbitrary light units (ALU), determined for each extract (20 μL).Following background correction, the luminescence signal was plotted against time. The data are the means from triplicate repeats ± standard deviations.

After showing that the luciferase-expressing *L. major* line is infective to culture derived macrophages, we next determined whether it could infect a live animal model. Here, purified luciferase-expressing metacyclic promastigotes were inoculated into the footpad of BALB/c mice (three mice per cell line) and the ability of the pathogen to cause lesion pathology compared with wild type Friedlin controls assayed in parallel (Figure 4.3.3). By analysis of the size of the footpad wound it was clear that luciferase-expressing *L. major* cells retained their infectivity. However, the time taken for the pathology to appear was approximately twice that as compared to the wild type *L. major*: on average a lesion took 31 days to be detected in mice infected with wild type parasites while this was about 57 days for the recombinant line. This may suggest that in an animal system, luciferase expression by the

microbe may slightly reduce infectivity or could slow amastigote cell division. Alternatively, this difference could reflect an error in the initial metacyclic cell count such that fewer recombinant parasites were inoculated into the host organism, or inherent variation in this *in vivo* model. This issue can be addressed by increasing the sample size. Equally, differences in the time that each cell line has been in *in vitro* culture could also give rise to the observed profile. Interestingly, both cell lines generated a similar wound diameter (5 to 7 mm) before euthanisation. This would suggest that once an infection has become established the recombinant line behaves in the same way as wild type parasites, perhaps indicating that the problem identified above reflects an experimental error rather than a biological property.

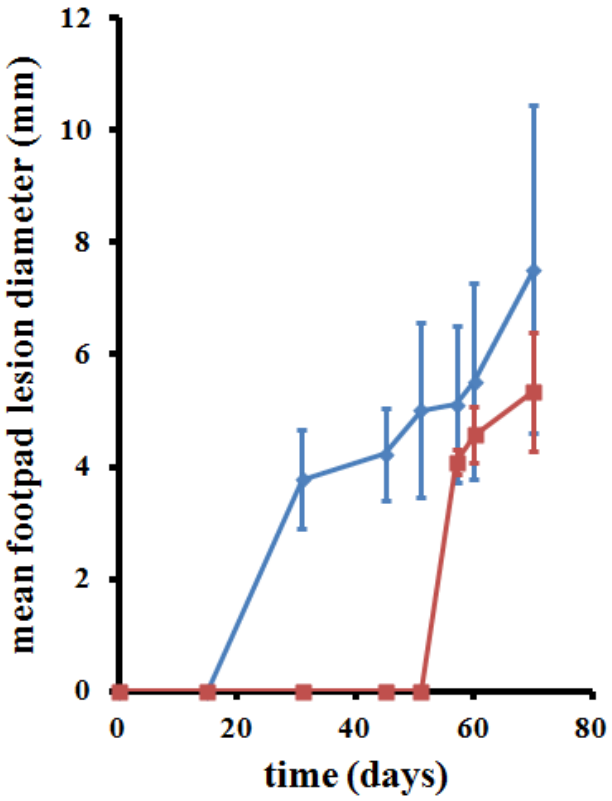

Figure 4.3.3 Luciferase-expressing *L. major* are infectious in a mouse model
Purified luciferase-expressing (red) and wild type (blue) metacyclic parasites (2 x 10^6) were inoculated into the footpad of BALB/c mice. Periodically, the size of the lesion was measured. All infections were done in triplicate and the data is expressed as the mean lesion size (in mm) ± standard deviation. Although a lag in lesion size was initially observed, by day 60 onwards no significant difference was noted in the wound size generated by wild type and luciferase-expressing *L. major*. All *in vivo* work was performed at the London School of Hygiene and Tropical Medicine by Dr Karin Seifert.

4.4 Validating the luciferase-based drug screening assay for use with *L. major* amastigotes

Following the demonstration that luciferase-expressing *L. major* are infectious in both *in vitro* and *in vivo* models, we next evaluated whether this recombinant line could be used in 96-well plate drug assay. Using the parameters determined above, we infected differentiated THP-1 cells with recombinant parasites (20 parasites per mammalian cell) and then cultured the intracellular amastigote cells in the presence of different concentrations of nifurtimox (Figure 4.4.1). After 72 hours growth post-infection, the medium was removed, the cells lysed and the luciferase activity for each culture determined: all growth assays at each drug concentration were conducted in triplicate (Section 3.3.2).

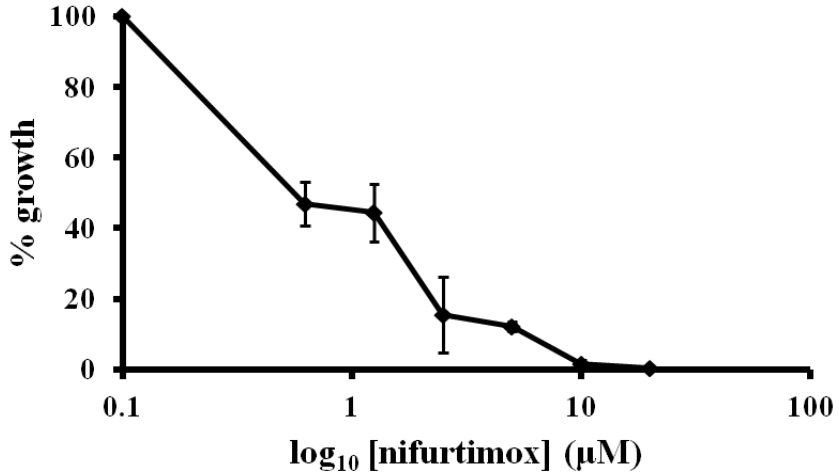

Figure 4.4.1: Susceptibility of luciferase-expressing *L. major* amastigotes to nifurtimox
In a 96-well plate format, differentiated THP-1 cells seeded at 2.5 x 10^4 cells mL^{-1} were infected overnight with 5 x 10^5 cells mL^{-1} purified luciferase-expressing *L. major* metacyclic parasites (giving a ratio of 20 parasites per mammalian cell). Non-internalised parasites were removed by extensive washing in culture medium and the amastigote parasites grown for 3 days at 37^{o}C in a 5% CO_2 atmosphere in the presence of different concentrations of nifurtimox. Cells were then lysed (in 50 μL lysis buffer) and the luciferase activity, as measured in arbitrary light units, for each extract (10 μL) determined. Data, expressed as a dose response curve, is shown as a percentage of the luminescence signal generated by parasites grown in the absence of nifurtimox. For the curve, the concentration of nifurtimox that inhibited parasite growth by 50% was established. The data are the means from 3 experiments ± standard deviations.

In these experiments, the controls consisted of mammalian cells infected with *L. major* grown in the absence of drug (100% parasite growth); and uninfected mammalian cells that gave a

background luciferase activity (0% parasite growth). The signals generated by drug-treated extracts were then compared against the infected/non-infected controls and a dose response curve generated (Figure 4.4.1). Additionally, comparing the luminescence values and deviations of the positive and negative controls, gives a Z factor score of 0.790, labelling this assay as "excellent" (Zhang *et al.* 1999). From these plots, the IC_{50} value for nifurtimox was calculated to be 0.58 ± 0.06 μM (Table 4.4.1). This is significantly lower than the promastigote IC_{50} noted above. Interestingly, mammalian intracellular stage *T. cruzi* is also more susceptible to nifurtimox than their insect stage counterparts (Bot, Hall *et al.* 2010).Why this is the case is unclear given that the bloodstream and procyclic forms of *T. brucei* have similar IC_{50} values, though this could reflect a contrast between intracellular and extracellular parasites (Table 4.4.1, Enanga, Ariyanayagam *et al.* 2003). When the susceptibility of differentiated THP-1 cells to nifurtimox was determined, the IC_{50} value was calculated to be >100 μM (Table 4.4.1). This indicates that this nitrofuran has a selective toxicity (The ratio of IC_{50} against mammalian cells/IC_{50} against the parasite) of >170. Therefore based on our data nifurtimox shows selective killing of the *L. major* amastigotes within an intracellular milieu and that the observed leishmanicidal activity is not due to death of the mammalian cell.

L. major		***T. cruzi***		***T. brucei***		**THP-1**
promast	**amast**	**epimast**	**amast**	**PCF**	**BSF**	
7.5 ± 0.42	0.58 ± 0.06	2.78 ± 0.20	0.24 ± 0.04	4.89 ± 0.12	5.58 ± 0.86	>100

Table 4.4.1: Susceptibility of *L. major, T. cruzi, T. brucei* and THP-1 cells to nifurtimox
All data are average IC_{50} values ± standard deviations given in μM. The growth inhibition data for *T. cruzi* epimastigotes (epimast) and amastigotes (amast) taken from Wilkinson, Taylor *et al.* 2008 and Bot, Hall *et al.* 2010, respectively, *T. brucei* procyclic (PCF) and bloodstream (BSF) forms from Enanga, Ariyanayagam *et al.* 2003. The *L. major* promastigote (promast) and amastigote (amast) were generated using the luciferase-expressing line reported here. The cytotoxicity of nifurtimox to differentiated THP-1 cells was also examined.

4.5 Chapter summary

The development of a luciferase reporter system in *L. major* has demonstrated that:

1. The construct pLmRIX-Luc contains all the mRNA processing elements (including splice leader and polypyrimidine tract addition sites) required to express the luciferase within *L. major* promastigote and amastigote cells.
2. Expression of luciferase at levels ~1000 times that of wild type appears not to impair the ability of the parasites to grow or produce infective metacyclic cells.
3. Luciferase activity shows a linear relationship to cell number, with luminescent signals detectable down to 625 promastigote cells.
4. Using this recombinant line, promastigote and amastigote drug screening protocols have been developed and validated using nifurtimox. Reliable dose-dependent growth response curves were generated from which accurate IC_{50} values with low variation were determined.
5. A pilot study has shown that the LmRIX-Luc parasites are able to infect and proliferate in a mouse model causing lesion pathology. This opens up the possibility for using these cells in *in vivo* imaging.

5. Evaluating the role of a *L. major* type I nitroreductase

5.1 Identification of a *L. major* type I nitroreductase

Type 1 nitroreductases are a group of enzymes that mediate the reduction of a wide range of nitroaromatic and quinone-based substrates. They were originally believed to be restricted to prokaryotes and absent from eukaryotes. However, recent studies have shown that this is not the case with several eukaryotic microorganisms, including *Giardia*, *Entamoeba*, trypanosomes and yeast containing type I NTRs (Nixon, Wang *et al.* 2002, Muller, Wastling *et al.* 2007, Wilkinson, Taylor *et al.* 2008, Pal, Banerjee *et al.* 2009, Bang *et al.* 2012). Furthermore, this enzyme has been implicated in the activation of a series of nitroaromatic prodrugs in trypanosomes (Hu *et al.* 2003, Wilkinson, Taylor *et al.* 2008, Bot, Hall *et al.* 2010, Hall, Wu *et al.* 2010, Baker, Alsford *et al.* 2011, Hall, Bot *et al.* 2011, Hall and Wilkinson 2012, Mejia, Hall *et al.* 2012). Consequently this oxidoreductase was investigated in *L. major*. BLASTP searches using the *T. cruzi* and *T. brucei* NTR (TcNTR and TbNTR; Gene ID Tc00.1047053510611.60 and Tb427.07.7230 respectively) amino acid sequences, coupled with text searches using the string "nitroreductase" on the *L. major* GeneDB (http://www.genedb.org/genedb/leish) webpage, identified a NTR homologue within this leishmanial parasite. Similar searches of the TryTriDB website has identified sequences encoding orthologous oxidoreductive enzymes found in a range of other *Leishmania* species (http://tritrypdb.org/tritrypdb/). The single copy, putative *L. major* NTR gene designated *LmNTR* (Gene ID LmjF05.0660) consists of a 972 bp open reading frame localised to chromosome 5 in the genome of the parasite (Figure 5.1.1 A). Comparison of the *Leishmania* and *Trypanosoma NTR* genomic loci reveals a high degree of synteny with the adjacent genes being conserved through millions of years of evolution. *LmNTR* encodes for a 323 amino acid protein with a predicted size of 34.7 kDa and an isoelectric point of 8.84. The full length protein is ~90% identical to NTRs from *L. mexicana* (Gene ID LmxM.05.0660) and *L.*

infantum (Gene ID LinJ.05.0660), ~75% identical to the enzyme from *L. braziliensis* (Gene ID LbrM.05.0650) and has ~50% identity to TcNTR and TbNTR. When compared to the bacterial counterparts such as *E. coli* nfsB and *Bacillus cereus* NAD(P)H nitroreductase (GenBank Accession numbers NP_415110 and NP_832770, respectively) the highest levels of sequence identity is around 20%

(A)

```
atgcttcgccgcagcccccgcttgctattggttgcagcaggggcccgccctgccgcctcc
 M  L  R  R  S  P  R  L  L  L  V  A  A  G  A  R  P  A  A  S
acccctcgagccagcgaggccgccggcacctgtggcaacgaggagcgccacagcaacacc
 T  P  R  A  S  E  A  A  G  T  C  G  N  E  E  R  H  S  N  T
agcagtggccatggtggttttctagccacactgcgccatctcgtggcgtggaaccgcacg
 S  S  G  H  G  G  F  L  A  T  L  R  H  L  V  A  W  N  R  T
aacgcggcggccgccgcatcgtcgtcatccgtgtcgtgcgcagaaaccccagcatgcgtc
 N  A  A  A  A  A  S  S  S  S  V  S  C  A  E  T  P  A  C  V
agcagcagcgcagcactcgacgccgtcgaggccgtcgtgcgcgaccggtggacgtgccgg
 S  S  S  A  A  L  D  A  V  E  A  V  V  R  D  R  W  T  C  R
cagttcgacacggcgaagccgatagacctcgacactctcaagcgcgtcttggcggcgacg
 Q  F  D  T  A  K  P  I  D  L  D  T  L  K  R  V  L  A  A  T
acccgcgccccgactggtttcaaccttcaggggtggcacgcggtcgtcgtcaccaatgag
 T  R  A  P  T  G  F  N  L  Q  G  W  H  A  V  V  V  T  N  E
gcggtgcgggagcagctcttcaaggcagcgctcggccagccgcaggtgctgcaggcgccg
 A  V  R  E  Q  L  F  K  A  A  L  G  Q  P  Q  V  L  Q  A  P
gcaactgtcgtcttcgttggggacacagagccggagcggaacgcgccgcaggcgcttgag
 A  T  V  V  F  V  G  D  T  E  P  E  R  N  A  P  Q  A  L  E
atgggtctcgagacgggctactacagccccctctacggtgccacctacctccgcaacatc
 M  G  L  E  T  G  Y  Y  S  P  L  Y  G  A  T  Y  L  R  N  I
tactacctcatgcacggcggtcctatgcagtcgatggccgccgtaaagtcggtcgtgagt
 Y  Y  L  M  H  G  G  P  M  Q  S  M  A  A  V  K  S  V  V  S
gcgtggtacagccgggcggctggcacgccgctcatctccgtcccggtgagccgcaccggc
 A  W  Y  S  R  A  A  G  T  P  L  I  S  V  P  V  S  R  T  G
tacgcgtggaagcagacgatgattccggcgacgacgttcgtgaatctctgcaccgccgcc
 Y  A  W  K  Q  T  M  I  P  A  T  T  F  V  N  L  C  T  A  A
ggctgggagacttgcatgatggagggcatcgacgaagatgccgtgaagcgcgcgttggga
 G  W  E  T  C  M  M  E  G  I  D  E  D  A  V  K  R  A  L  G
gtgccggcggaacgatacactgtgccggtcatcatcagcgtcggctacgcgaccgccacg
 V  P  A  E  R  Y  T  V  P  V  I  I  S  V  G  Y  A  T  A  T
gaggccgagaaacgtcaggtgtgcagctcgcgcttcgcgacgccacacaccgtgcggtgg
 E  A  E  K  R  Q  V  C  S  S  R  F  A  T  P  H  T  V  R  W
aacaagttctag
 N  K  F  -
```

(B)

Figure 5.1.1: Domain structure of LmNTR
(A) The nucleic and deduced amino acid sequence of LmNTR is shown. (B) The LmNTR protein sequences can be divided into two distinct domains. The region highlighted in grey represents a putative amino terminal leader sequence absent from the bacterial sequences. The region highlighted in green corresponds to the catalytic domain and represents the sequence cloned into the pTrcHis-C expression vector

Analysis of the LmNTR revealed that the protein sequence can be divided into two distinct domains (Figure 5.1.1 B). By comparison to the bacterial sequences (Figure 5.1.2), residues 1-85 appear to represent an amino terminal extension. This is borne out using the SignalP (http://www.cbs.dtu.dk/services/SignalP) (Petersen *et al.* 2011) algorithm which indicates that this region possess a cleavage site between amino acids 20 and 21. Further analysis using PSORT II (http://psort.hgc.jp/form2.html) suggests that this protein may be mitochondrial (~40% probability) with the iPSORT (http://ipsort.hgc.jp/) algorithm indicating that the first nine amino acids (MLRRSPRLL), characterized by the presence of hydrophobic and basic amino acids and a lack of acidic residues, make up a mitochondrial targeting peptide. As TbNTR is located in the mitochondrion of bloodstream-form *T. brucei*, it is tempting to speculate that this region performs the same targeting role for LmNTR.

Residues 93-296 of LmNTR correspond to a nitroreductase catalytic domain (Pfam PF00881). Comparison of the region from bacterial, trypanosomal and leishmanial type I NTRs demonstrate that it is highly variable, possessing several key conserved residues involved in FMN co-factor binding (Figure 5.1.2) (Parkinson *et al.* 2000, Wilkinson, Taylor *et al.* 2008, Mejia, Hall *et al.* 2012). Based on charge and hydrophobicity, other sites do share some similarity with these postulated to be involved with substrate binding, particularly in relation to the electron donor, NAD(P)H (Parkinson, Skelly *et al.* 2000). Below we describe the characterisation of the nitroreductase domain following heterologous expression in *E. coli* and purification of the recombinant protein.

Figure 5.1.2: ClustalW2 analysis of type 1 nitroreductases across a selection of trypanosomatid and bacterial species

Amino acid sequence alignment of the type 1 nitroreductases from the trypanosomes *T. cruzi* CL Brenner (both genes due to the hybrid nature of the genome of this strain, TcCLB.510611.60 and TcCLB.506791.70) and *T. brucei* (Tb927.7.7230); *Leishmania* species *L. major* (LmjF.05.0660) *L. infantum* (LinJ.05.0660), *L. mexicana* (LmxM.05.0660) and *L. brazilienesis* (LbrM.05.0650); and the bacteria *Escherichia coli* (NP_415110), *Shigella dysenteriae* (EIQ63968), *Salmonella enterica* (ZP_03221487) and *Bacillus cereus* (NP_832770). Amino acids that may interact with the flavin co-factor (bold and red) and consist of the putative targeting signal (yellow box, using the iPSORT algorithm) are all highlighted. Residues that are common to all eleven sequences are shown with an asterix.

5.2 Heterologous expression and purification of recombinant LmNTR

To investigate the function of LmNTR, a region (residues 87-323, Figure 5.1.1) containing the catalytic domain was amplified from *L. major* Friedlin genomic DNA using the primers LmNTR-1/LmNTR-2. The resultant 717 bp fragment (designated *ΔLmNTR*) was digested with *Bam*HI+*Hin*dIII and cloned into the corresponding sites of the expression vector pTrcHis-C (schematic representation shown in Figure 5.2.1). This generated the plasmid pTrcHisC-ΔLmNTR (Figure 5.2.2).

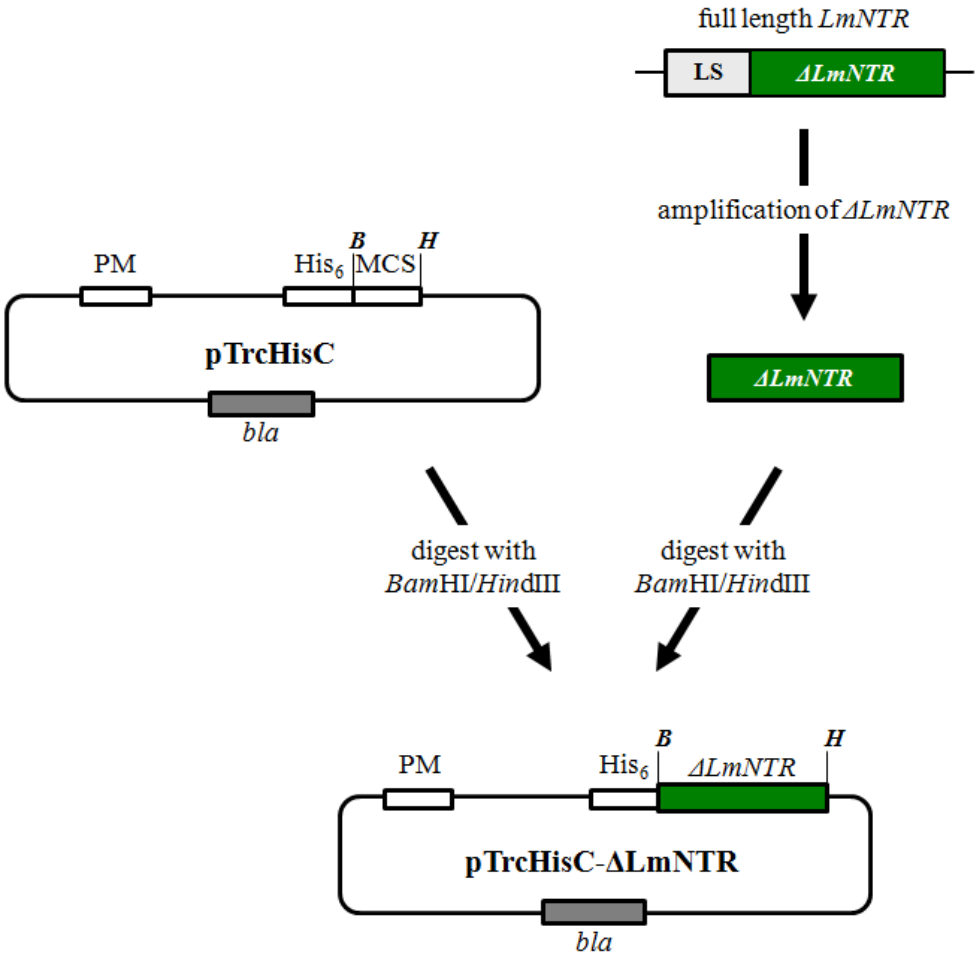

Figure 5.2.1: Schematic representation outlining the construction of the *E. coli* expression vector pTrcHisC-ΔLmNTR
A DNA fragment containing the LmNTR catalytic domain (*ΔLmNTR*; dark green) was amplified from *L. major* genomic DNA using VENT *Pfu* and the primers LmNTR-1/LmNTR-2. This fragment was digested with *Bam*HI+*Hin*dIII and cloned into the corresponding sites of pTrcHisC (Invitrogen) to form pTrcHisC-ΔLmNTR. DNA sequences encoding for β-lactamase (*bla*; grey), the *LmNTR* leader sequence (LS; light grey) and the expression vector's promoter machinery (PM), multiple cloning site (MCS) and polyhistidine tag (His_6) are all highlighted. The *Bam*HI (*B*) and *Hin*dIII (*H*) restriction sites are also noted.

In the pTrcHis system, recombinant LmNTR is tagged at its amino terminal with a histidine-rich motif (His_6) and the Xpress™ epitope (Invitrogen), sequences that facilitate purification and detection of the protein following expression in a suitable *E. coli* strain. Sequencing confirmed that the *L. major* gene had be cloned in-frame with these ancillary regions.

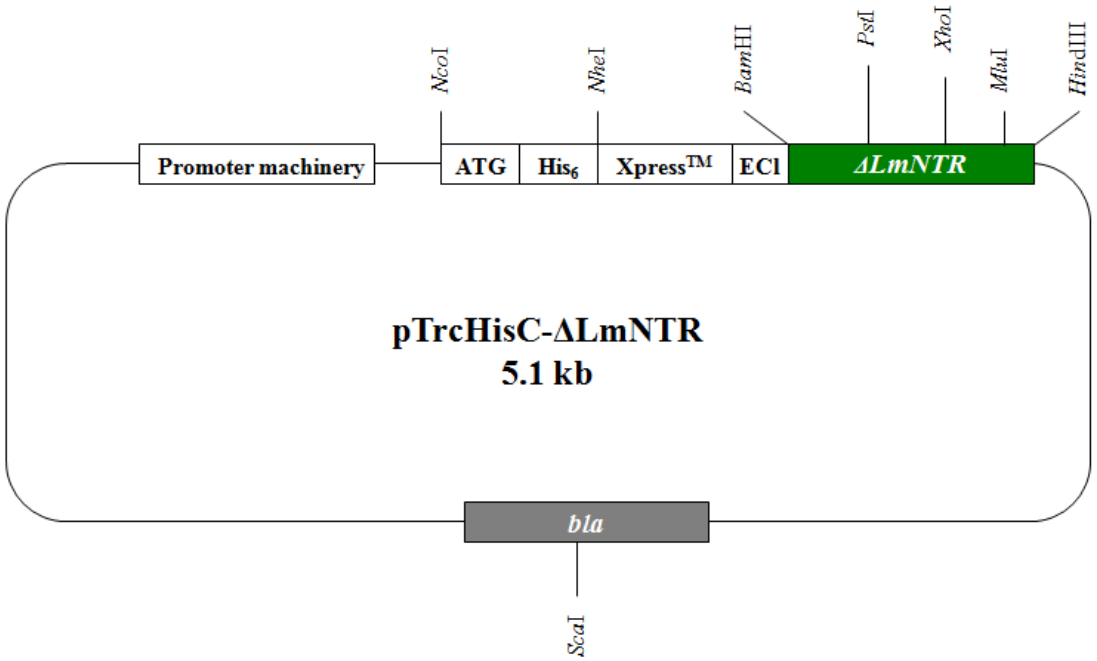

Figure 5.2.2: Restriction map of the *E. coli* expression vector pTrcHisC-ΔLmNTR
The gene encoding LmNTR, minus the gene leader sequence (*ΔLmNTR*), is highlighted in dark green. The DNA sequences encoding for β-lactamase (*bla*; grey), the ATG start codon, polyhistidine tag (His_6), Xpress™ epitope and an enterokinase cleavage site (ECl) are also noted.

The plasmid pTrcHisC-*ΔLmNTR* was then transformed into *E. coli* BL21(+), a strain used for expressing proteins from this system. Based on conditions used to purify trypanosomal type I NTRs (Hall *et al.*, 2010) a pilot expression study was carried out. This involved diluting an overnight *E. coli* [pTrcHisC-*ΔLmNTR*] culture 1:50 fold and growing the bacteria at 37°C for 4 hours. The culture was transferred to 16°C and incubated with aeration for 30 minutes. IPTG was then added to a final concentration of 1 mM and the cells incubated overnight at 16°C. Extracts were generated and a ~30 kDa band was detected by Western-blot analysis using a monoclonal antibody that recognises the Xpress™ epitope in the soluble fraction of

lysates (results not shown). Use of other bacterial growth medium other than NZCYM (*e.g.* Luria-Bertani broth) failed to generate sufficient levels of soluble protein. Once these conditions had been established the culture volume was scaled up to 2 L and the expression experiments repeated. The resultant clarified extract (generated as described in Section 3.7.1) was then applied to an Ni-NTA column and recombinant LmNTR readily purified by one round of affinity chromatography, with all elutions being yellow in colour (Figure 5.2.3). This expression and purification protocol routinely generated 10-50 mg recombinant LmNTR per litre of bacterial culture. Elution of this column was carried out using a 50 mM $NaHPO_4$ pH7.8/500 mM NaCl buffer containing 500 mM imidazole and 1% (w/v) CHAPS. If the detergent was omitted from the elution buffer then most of the His_6-tagged protein remained bound to the column. This suggests that the recombinant LmNTR may not solely be binding to nickel present in the resin via the poly-histidine tag and could be binding to the matrix support.

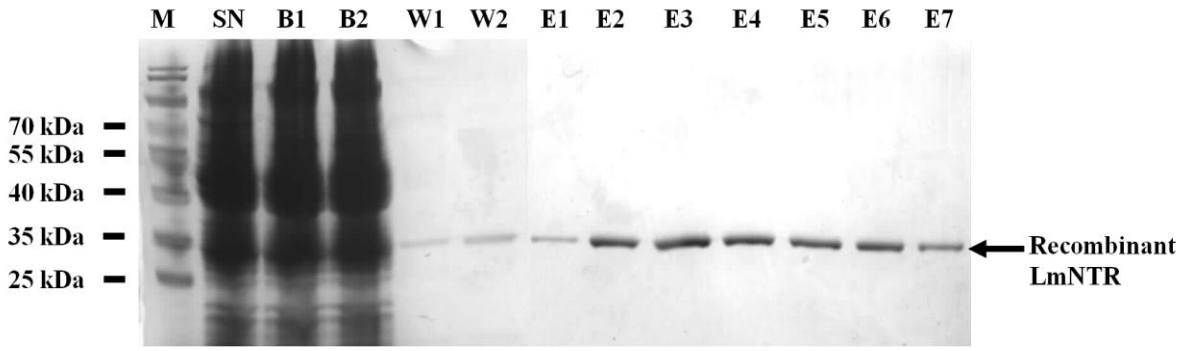

Figure 5.2.3: Purification of recombinant LmNTR
Fractions collected at various stages of His_6-tagged ΔLmNTR purification were fractionated on a 12% polyacrylamide gel and visualised by Coomassie-staining. The clarified supernatant of an *E. coli* (pTrcHic-ΔLmNTR) cell lysate (SN) was loaded onto a Ni-NTA column and the flow through collected (B1), and then reapplied (B2). The column was washed extensively with 50 mM (W1) and 100 mM (W2) imidazole-containing solutions (see Section 3.7.1). His_6-tagged ΔLmNTR was eluted off the column using a solution containing 500 mM imidazole; 1% CHAPS (E1-E7). A band of approximately 30 kDa was observed in all wash and elution fractions and corresponds to recombinant LmNTR. The Prestained Protein Marker (M) is indicated.

5.3 Unravelling the biochemical properties of LmNTR

A characteristic feature of all type I NTRs relates to their ability to bind FMN as co-factor (Roldan, Perez-Reinado *et al.* 2008). During purification it was noticeable that all elution fractions containing recombinant LmNTR were yellow suggesting that this parasite enzyme was a flavoprotein. To confirm that this was the case and also identify the nature of the flavin a fluorescence-based assay was employed (Faeder and Siegel 1973) (Figure 5.3.1).

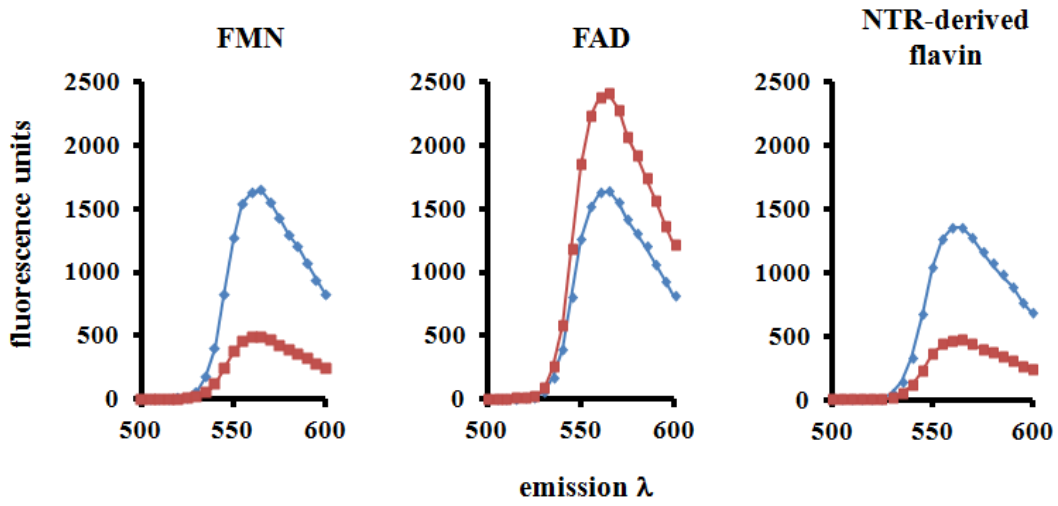

Figure 5.3.1: Evaluating the co-factor in recombinant ΔLmNTR
Fluorescence spectra of FMN, FAD (both 50 μM) and supernatant from boiled purified, recombinant LmNTR (0.5 mg) at pH 7.6 (blue line) and pH 2.2 (red line) was determined using an excitation λ at 450 nm and emission λ between 480-600 nm. All the fluorescence analyses were carried out in triplicate and the profiles are derived from the mean values.

Purified recombinant protein was passed through a desalting spin column and the flow through collected. The protein (0.5 mg) was boiled and sample clarified. The fluorescence profile of the yellow supernatant was then evaluated under neutral and acidic pHs using an excitation wavelength of 450 nm and excitation spectrum of 480 to 600 nm. FAD and FMN were treated in parallel and acted as reference standards. Under these conditions, the NTR-derived sample and FMN exhibited maximal fluorescence in a pH 7.5 buffer having a peak emission around 560 nm. Under acidic conditions (pH 2.2) this signal was quenched. For FAD, the fluorescence observed under neutral pH conditions is enhanced in acidic buffers.

Based on the fluorescence characteristics and release of the flavin from the protein backbone following boiling, the data strongly suggest that LmNTR non-covalently bind FMN as co-factor, in agreement with observations made with the two trypanosomal enzymes (Hall & Wilkinson, unpublished).

Type I NTRs can metabolise a wide range of nitroaromatic and quinone-based substrates using NADPH and/or NADH as electron donor. In the presence of an appropriate electron acceptor, reactions involving the oxidation of these two reductants can be readily followed in a spectrophotometer by following the change in absorbance at 340 nm (Figure 5.3.2 A). Using NADH as electron donor and benznidazole as electron acceptor, we evaluated whether this reaction was pH dependant (Figure 5.3.2 B). Several Trizma® base buffers ranging in pH from 7 to 9 were tested. From these results, high activity levels were observed between pHs 7 to 8, with maximal activity recorded at pH 7.5. At pH 8.5 and 9, enzyme activity was approximately 1/3rd that at pH 7.5. Importantly, these reactions take place under normoxic conditions and indicate that LmNTR activity towards benznidazole is oxygen-insensitive.

Using benznidazole as a substrate and in pH 7.5 buffer, we next examined which of the reduced nicotinamide adenine dinucleotides LmNTR had preference for: both TcNTR and TbNTR favour NADH as electron donor with TcNTR not interacting with NADPH at all (Wilkinson, Taylor *et al.* 2008; Hall & Wilkinson, unpublished). Under these aerobic conditions LmNTR could readily metabolise this nitroimidazole using NADH, with only minimal oxidation occurring when using NADPH (Figure 5.3.2 C). In the presence of 100μM NADH and 100μM benznidazole, the rate of change in absorbance at 340 nm can be readily followed as a steady deflection. The gradient of the resultant slope can be determined from which the enzyme activity calculated in nmol NADH consumed mg^{-1} ΔLmNTR min^{-1}. In the

case of Figure 5.3.2 C for example, this reveals a difference in enzyme activity of 110 nmol NADH consumed mg^{-1} ΔLmNTR min^{-1} in blue, against 50 nmol NADPH consumed mg^{-1} ΔLmNTR min^{-1} in red.

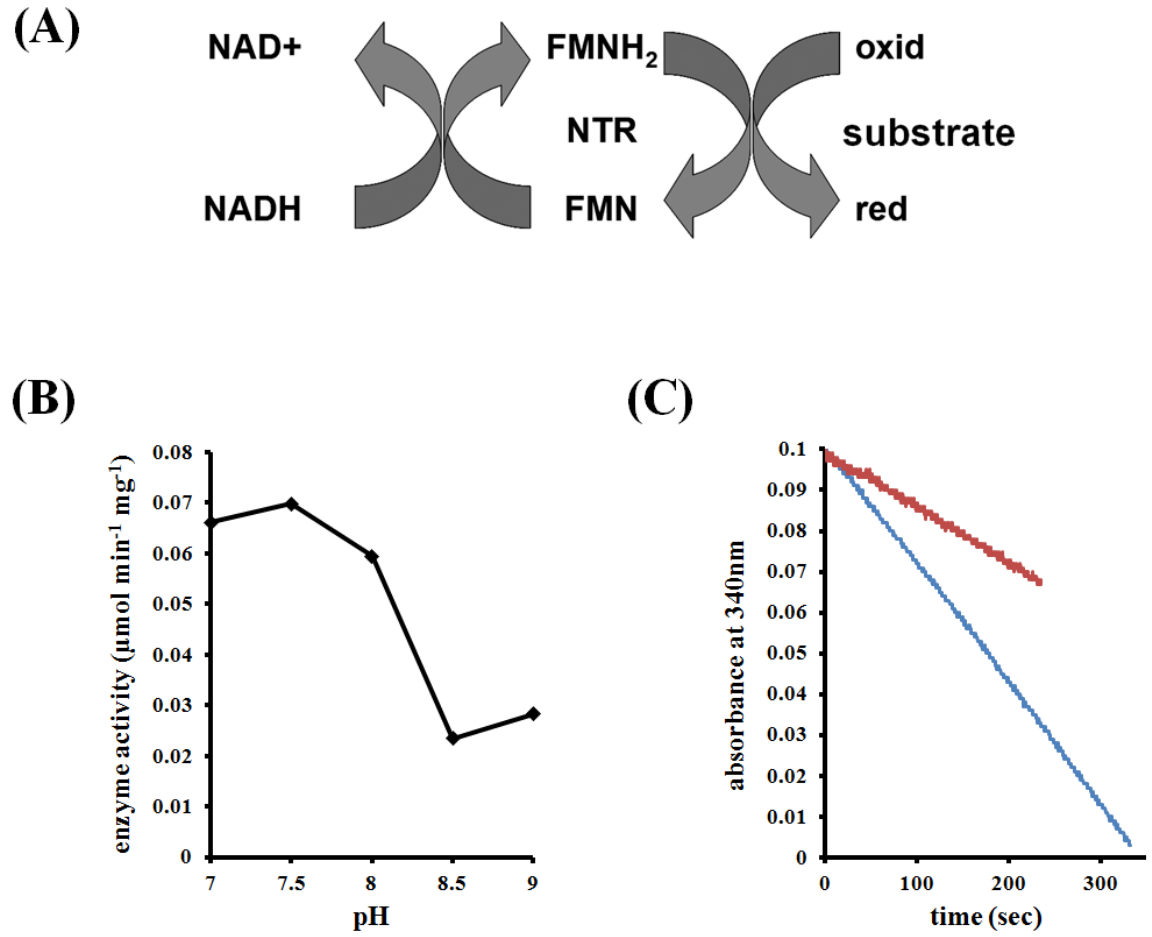

Figure 5.3.2: Formation of a NADH consumption assay using recombinant ΔLmNTR to screen nitroaromatic compounds as possible substrates.
(A) Schematic representation for the reduction of quinone and nitroaromatic based substrates by NTRs using NADH as electron donor; 'red' represents the reduced and 'oxid' the oxidized form of the substrate (figure modified from Wilkinson, Taylor *et al.* 2008). (B) The metabolism of benznidazole (100 µM) by LmNTR (35 µg) was monitored in buffers with different pH values (pH 7.0-9.0), using NADH (100 µM) as electron donor. LmNTR activity was expressed as µmol NADH oxidised min^{-1} mg $LmNTR^{-1}$. (C) NTR activity was monitored by following the oxidation of NADH (100 µM, blue line) or NADPH (100 µM, red line) in the presence of LmNTR (35 µg) and benznidazole (100 µM). The curve shows the rate of change in absorbance at 340 nm which corresponds to the oxidation of NAD(P)H to $NAD(P)^+$, and highlights the increased enzyme activity when using NADH as electron donor.

To further investigate the type of kinetics that LmNTR displays toward NADH, assays were carried out using various concentrations of reductant against a fixed concentration of benznidazole (Figure 5.3.3 A). For this substrate, double reciprocal plots were linear at all concentrations of electron acceptor with the slopes remaining roughly parallel, a pattern characteristic of a ping-pong mechanism. Likewise, reciprocal assays using a fixed concentration of NADH and varying amounts of benznidazole generated a similar pattern of parallel slopes (Figure 5.3.3 B). The slope profiles observed only occurred over a limited concentration range, with noncompetitive substrate inhibition detected when the NADH or benznidazole level was above 200 μM (Figure 5.3.3 C and D respectively).

After establishing the enzyme assay and determining that LmNTR displays typical oxidoreductase ping-pong type kinetics (at least towards benznidazole), we next evaluated the substrate range displayed by the parasite enzyme. A series of nitroaromatic and quinone-based compounds were assayed to determine whether these could drive LmNTR activity. Such assays were carried out using a fixed concentration of electron donor (NADH), a fixed amount of enzyme and varying concentrations of the electron acceptor. In many cases (benznidazole, metronidazole, LH32, LH33, LH37, duroquinone and coenzyme Q1) the oxidation of NADH was followed although for others (nifurtimox, nitrofurazone and nitrofurantoin) the direct reduction of substrate was monitored (such electron acceptors usually had a prohibitively high absorbance at 340 nm). Analysis of the resulting slopes (see Figure 5.3.2 A as example), the enzyme activities were determined and double reciprocal (Lineweaver-Burk) plots generated. From this graphs, kinetic data (apparent K_M, apparent V_{MAX} and k_{CAT}/K_M) was calculated (Table 5.3.1).

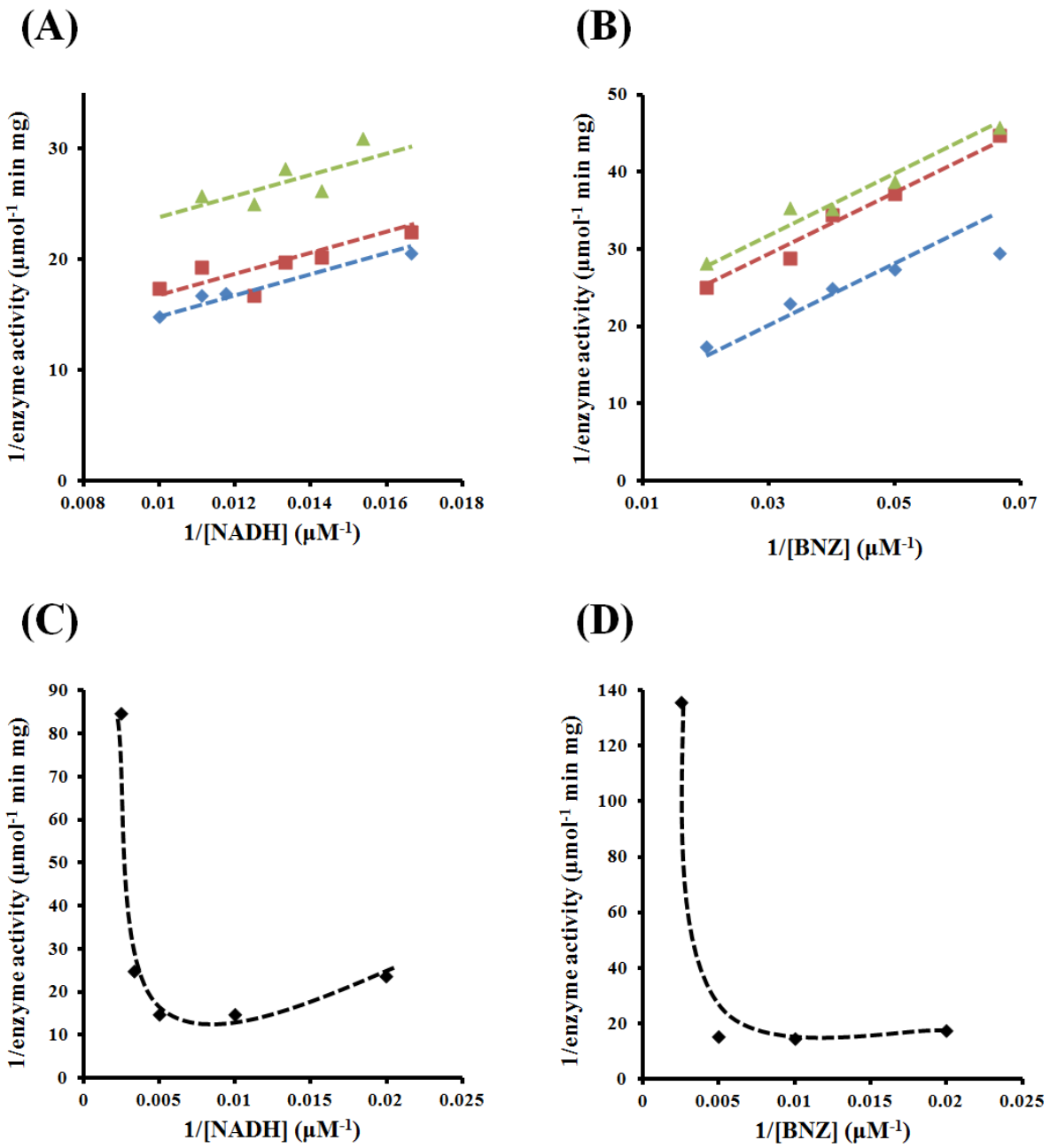

Figure 5.3.3: Ping pong kinetics of recombinant ΔLmNTR
Lineweaver-Burk reciprocal plots showing parallel best fit lines indicative of ping-pong kinetics. (A) Enzyme activity in nmol NADH consumed min^{-1} mg $\Delta LmNTR^{-1}$ while varying NADH concentration at three set benznidazole concentrations: 100µM (blue diamonds), 75µM (red squares) and 50µM (green triangles). (B) Enzyme activity in nmol NADH consumed min^{-1} mg $\Delta LmNTR^{-1}$ while varying benznidazole concentration at three set NADH concentrations: 100µM (blue diamonds), 80µM (red squares) and 75µM (green triangles). (C) Noncompetitive substrate inhibition caused by high levels of NADH causing the enzyme activity to rapidly drop. (D) Noncompetitive substrate inhibition caused by high levels of benznidazole causing the enzyme activity to rapidly drop.

The analysis of these assays (Table 5.3.1) shows that LmNTR has a wide substrate range. Additionally, by observing the k_{CAT}/K_M (a measure of enzyme efficiency) it appears that LmNTR has a substrate preference for quinone compounds (particularly coenzyme Q1), which possibly hints towards the biological function of this enzyme within the parasite.

compound class	compound name	apparent K_M (μM)	apparent V_{MAX} (nmol min^{-1} mg^{-1})	k_{CAT}/K_M (M^{-1} s^{-1})
nitroimidazole	benznidazole	22.0	78.7	2.5×10^3
	metronidazole	2.4	17.9	5.2×10^3
nitrofuran	nifurtimox	9.7	50.9	3.7×10^3
	nitrofurazone	4.7	68.3	1.0×10^4
	nitrofurantoin	3.9	56.7	1.0×10^4
nitrobenzyl compounds	CB1954	13.1	85.9	4.6×10^3
	LH32	28.8	100.7	2.5×10^3
	LH33	8.2	114.2	9.8×10^3
	LH37	7.1	71.7	7.1×10^3
quinones	duroquinone	9.8	140.6	1.0×10^4
	coenzyme Q1	5.1	145.2	2.0×10^4

Table 5.3.1: Activity of recombinant LmNTR towards a range of nitroaromatic and quinone-based substrates
The apparent V_{MAX} and K_M values of LmNTR (35 μg) toward various nitroaromatic and quinone-based substrates (0-100 μM) were determined in the presence of NADH (100 μM). For benznidazole, metronidazole, LH32, LH33, LH37, duroquinone and coenzyme Q1, activity was followed by monitoring the rate of NADH oxidation (ΔAbs_{340nm}) and the kinetic values calculated using a ε = 6,220 M^{-1} cm^{-1}. For nitrofurans, assays were carried out by following the direct reduction of the nitroheterocycle. Kinetic values were calculated using ε = 18,000, 12,000 or 15,000 M^{-1} cm^{-1} for nifurtimox (ΔAbs_{435nm}), nitrofurazone or nitrofurantoin (both ΔAbs_{400nm}), respectively from which the amount of reductant consumed per reaction was determined, assuming that 4 molecules of NADH are oxidized per molecule of nitrofuran reduced (Hall, Bot *et al.* 2011). For CB1954, activity was monitored by detecting production of the hydroxylamine (ΔAbs_{425nm}). Kinetic values were determined using a ε = 1,200 M^{-1} cm^{-1} from which the amount of NADH oxidized per reaction was determined, assuming that 4 molecules of reductant are turned over per molecule of CB1954 reduced (Race *et al.* 2007, Bot, Hall *et al.* 2010). The apparent V_{MAX} values are expressed as nmol NADH oxidized min^{-1} mg^{-1} and apparent K_M value in μM. The specificity constant (k_{cat}/K_M), expressed in M^{-1} s^{-1}, was determined and assumed one catalytic site per 30 kDa monomer.

5.4 Functional analysis of LmNTR within *L. major*

The application of reverse genetics has been routinely used for several decades to study gene function in a variety of different organisms. In the case of *Leishmania*, this approach has been facilitated by development of reliable DNA transfection protocols, a series of genetic tools that permit the functional analysis of a gene/protein of interest within the parasite itself and free access to a well organised genome sequence database. Below, the efforts made to alter the level of LmNTR in *L. major* by introducing ectopic copies of the gene on episomal or integration expression vectors, or by deleting one or both *LmNTR* alleles from the nuclear genome are described.

5.4.1 Expression of elevated levels of LmNTR

A series of attempts to construct cell lines expressing elevated levels of LmNTR (and tagged derivatives) through the introduction of ectopic copies of *LmNTR* into the parasite were carried out. Initial efforts involved amplifying the complete *LmNTR* open reading frame (plus the STOP codon) from *L. major* Friedlin genomic DNA using the primers LmNTR-4/LmNTR-2. The resultant ~970 bp DNA fragment was digested with *Bam*HI+*Hin*dIII and cloned into the corresponding sites pTEX-TcGPXI (Wilkinson, Meyer *et al.* 2002) such that the *TcGPXI* gene was replaced by *LmNTR* to form pTEX-LmNTR (Figure 5.4.1). This episomal construct was confirmed through restriction digest mapping (restriction map shown in Figure 5.4.2) and DNA sequencing.

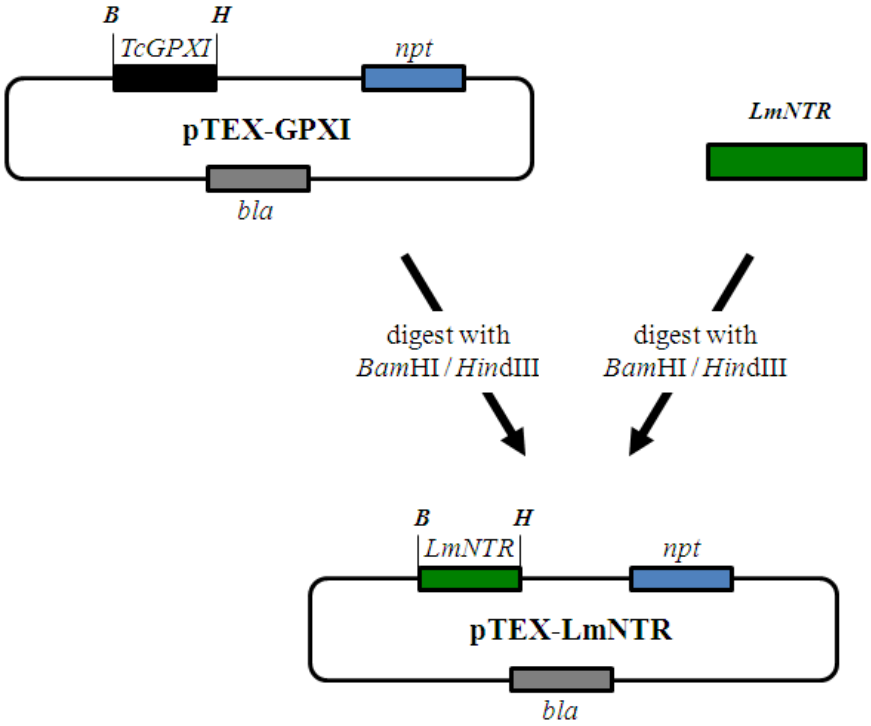

Figure 5.4.1: Schematic representation outlining the construction of the episomal *Leishmania* expression vector pTEX-LmNTR

The gene encoding LmNTR (*LmNTR*; dark green) was amplified from *L. major* genomic DNA using VENT *Pfu* and the primers LmNTR-4/LmNTR-2. The resultant DNA fragment was digested with *Bam*HI+*Hin*dIII and cloned into the corresponding sites of pTEX-TcGPXI (Wilkinson, Meyer *et al.* 2002), replacing the TcGPXI gene, to form pTEX-LmNTR. The DNA sequences encoding for ampicillin (*bla*; grey) and neomycin (*npt*; blue) resistance, and TcGPXI (black) are all highlighted. The *Bam*HI (*B*) and *Hin*dIII (*H*) restriction sites are also noted.

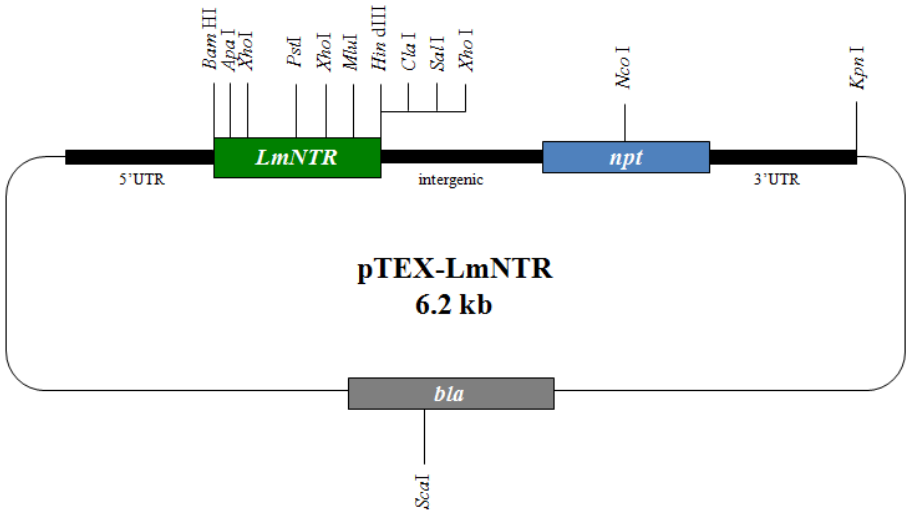

Figure 5.4.2: Restriction map of the episomal *Leishmania* expression vector pTEX-LmNTR

The DNA sequences encoding for LmNTR (*LmNTR*; dark green), β-lactamase (*bla*; grey), and neomycin phosphotransferase (*npt*; blue) are highlighted. The black boxes flanking *LmNTR* and *npt* genes correspond to the 5' UTR, intergenic and 3' UTR regions from *T. cruzi* GAPDH and facilitate gene expression.

This plasmid was then used in multiple (11) transfections of *L. major* Friedlin promastigotes on numerous (7) occasions. In all cases no stable G418-resistant parasite colonies were observed after 4 weeks of selection. However, positive controls (transfecting the heterozygote cell lines with an episomal GFP expression plasmid, pTEX-GFP, in parallel) did result in G418-resistant promastigotes. A derivative of pTEX-LmNTR was generated designed to facilitate expression of a c-myc (9E10) epitope-tagged version of the oxidoreductase (pTEX-LmNTR-9E10). As with the untagged protein, repeated electroporation of this episomal vector into *L. major* promastigotes failed to generate recombinant parasites.

To determine whether elevated LmNTR expression could be facilitated using an integrative system, the full length gene (plus STOP codon) was amplified from *L. major* Friedlin genomic DNA using the primers LmNTR-4/LmNTR-18. The resultant ~970 bp DNA fragment was digested with *Bam*HI+*Sal*I and cloned into the *Bam*HI+*Xho*I sites of pLmRIX-Luc such that the luciferase gene was replaced by *LmNTR* to form pLmRIX-LmNTR (Figure 5.4.3).

Following restriction mapping and DNA sequencing to confirm the nature of this construct (Figure 5.4.4), the plasmid was digested with *Sbf*I+*Asc*I to liberate an *LmNTR*-containing fragment of ~4.6 kbp, which was then purified and transfected into *L. major* promastigotes using the Amaxa® Nucleofector® system. As for the pTEX-based constructs, multiple (5) transfections carried out on 3 separate occasions using pLmRIX-LmNTR failed to generate G418-resistant cells. However, positive controls (transfecting the heterozygote cell lines with the pLmRIX-Luc construct, in parallel) did result in G418-resistant promastigotes. Electroporation of a c-myc (9E10) tagged version of *LmNTR* using this integration system also did not generate transformants.

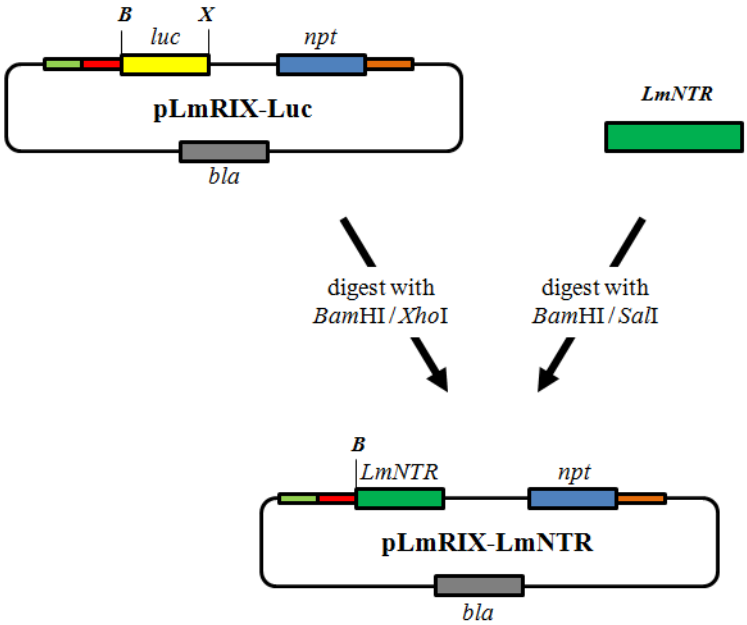

Figure 5.4.3: Schematic representation outlining the construction of the integrative *Leishmania* expression vector pLmRIX-LmNTR

The gene encoding LmNTR (*LmNTR*; dark green) was amplified from *L. major* genomic DNA using VENT *Pfu* and the primers LmNTR-4/LmNTR-18. The resultant DNA fragment was digested with *Bam*HI+*Xho*I and cloned into the *Bam*HI+*Sal*I sites of pLmRIX-Luc, replacing the luciferase gene. The DNA sequences encoding for ampicillin (*bla*; grey) and neomycin phosphotransferase (*npt*; blue) resistance, luciferase (*luc*; yellow), the *L. major* 5' rDNA spacer/promoter (green), 3' *L. major* rDNA spacer (orange), and the *T. cruzi* mitochondrial tryparedoxin peroxidase polypyrimidine tract/splice leader addition site (red) are all highlighted. The *Bam*HI (*B*), and *Xho*I (*X*) restriction sites are also noted.

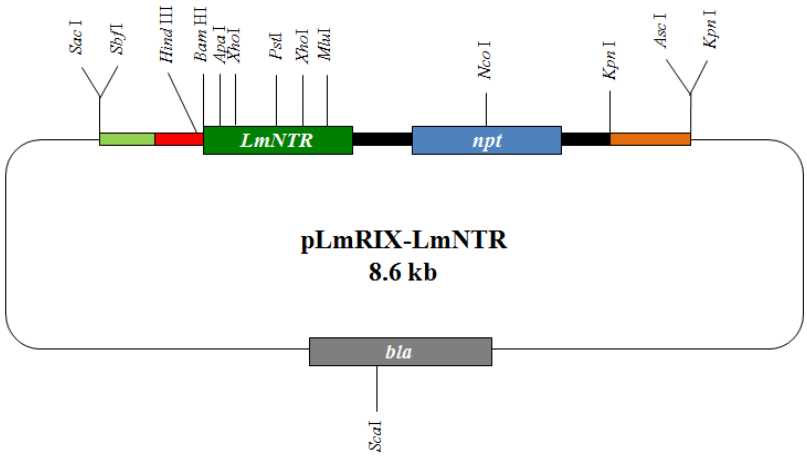

Figure 5.4.4: Restriction map of the integrative *Leishmania* expression vector pLmRIX-LmNTR

The DNA sequences encoding for β-lactamase (*bla*; grey), LmNTR (*LmNTR*; dark green) and neomycin phosphotransferase (*npt*; blue) are all highlighted. The *T. cruzi* mitochondrial tryparedoxin peroxidase polypyrimidine tract/splice leader addition site (red), *L. major* 5' rDNA spacer/promoter (light green) and *L. major* 3' rDNA spacer (orange) are also noted. Additionally, the black boxes flanking *npt* correspond to the intergenic and 3' UTR from *T. cruzi* GAPDH and facilitate expression of *LmNTR* and neomycin phosphotransferase genes.

From our data it appears that introducing an ectopic copy of *LmNTR* (and thus possibly increasing the expression of LmNTR) into *L. major* promastigotes is deleterious to these cells. A similar property has been observed using *T. cruzi* epimastigotes where over expression of TcNTR (wild type and tagged versions) could also not be carried out (Wilkinson, unpublished results).

5.4.2 *LmNTR* gene deletion studies

An alternative way to alter the copy number of *LmNTR* (and thus, theoretically, the levels of LmNTR) is to remove one or both genes from the wild type *L. major* genome to create heterozygous or null mutant lines. The phenotypic effect of such an event can then be elucidated. To achieve this, two gene deletion constructs were designed to replace each allelic copy of *LmNTR* by homologous recombination with antibiotic resistance cassettes. To construct the first vector, based around the gene encoding for puromycin N-acetyl-transferase (*pac*), a two step cloning strategy was used (Figure 5.4.7). Initially, primers (LmNTR-9/LmNTR-10) to the DNA sequence immediately upstream of *LmNTR* were designed to facilitate amplification of a ~700 bp fragment (designated 5' LmNTR UTR) using *L. major* Friedlin genomic DNA as template. The resultant fragment was digested with *Sac*I+*Xba*I and cloned into the corresponding sites of the *pac*-containing vector p5'TbNTRKO-PAC (supplied by Dr S Wilkinson). In this cloning event, the 5' TbNTR UTR sequence was replaced with the 5' LmNTR UTR fragment to form p5'LmNTRKO-PAC. In the second cloning step, primers (LmNTR-11/LmNTR-13) to the DNA sequence immediately downstream of *LmNTR* were designed to facilitate amplification of a ~1 kbp fragment (designated 3' LmNTR UTR) using *L. major* Friedlin genomic DNA as template. This fragment was digested with *Apa*I+*Kpn*I and cloned into the corresponding sites of p5'LmNTRKO-PAC to generate pLmNTRKO-PAC (Figure 5.4.8). At each stage the

constructs (p5'LmNTRKO-PAC and pLmNTRKO-PAC) were confirmed by restriction mapping and DNA sequencing.

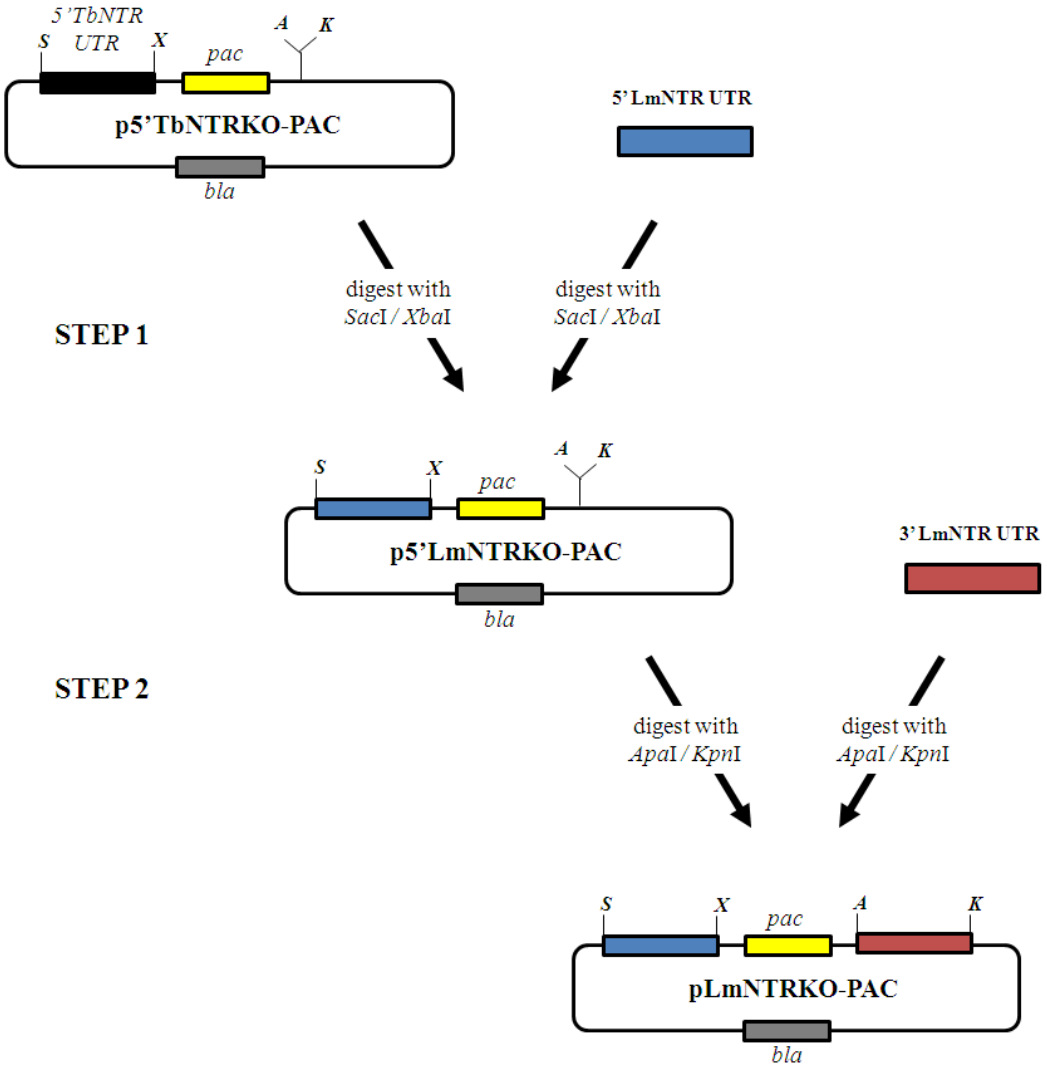

Figure 5.4.7: Schematic representation outlining the two-step construction of pLmNTRKO-PAC

In the first step, the 5' UTR of *LmNTR* (blue) was amplified from *L. major* Friedlin genomic DNA using VENT *Pfu* and the primers LmNTR-9/LmNTR-10. The resultant DNA fragment was digested with *Sac*I+*Xba*I and cloned into the corresponding sites of p5'TbNTRKO-PAC (supplied by Dr S Wilkinson), replacing the 5' UTR from *TbNTR* (black), to form p5'LmNTRKO-PAC. In step 2, the 3' UTR of *LmNTR* (red) was amplified from *L. major* Friedlin genomic DNA using VENT *Pfu* and the primers LmNTR-11/LmNTR-13. The resulting fragment was digested with *Apa*I+*Kpn*I, and ligated into the corresponding site of p5'LmNTRKO-PAC generating pLmNTRKO-PAC. The DNA sequences encoding for β-lactamase (*bla*; grey) and puromycin N-acetyl-transferase (*pac*; yellow) are highlighted. The *Sac*I (*S*), *Xba*I (*X*), *Apa*I (*A*) and *Kpn*I (*K*) restriction sites are also noted.

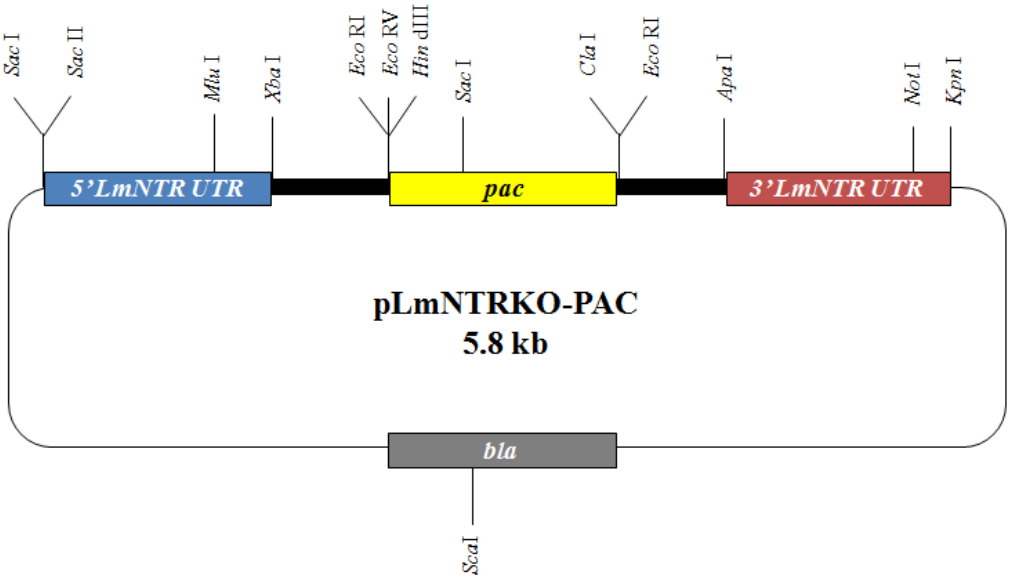

Figure 5.4.8: Restriction map of the LmNTR gene deletion vector pLmNTRKO-PAC
The DNA sequences encoding for puromycin N-acetyl-transferase (*pac*; yellow) and β-lactamase (*bla*; grey) are highlighted while the 5' (blue) and 3' (red) UTRs from *LmNTR* are also noted. The black boxes flanking the *pac* gene correspond to the UTRs from *T. brucei* tubulin repeats and these facilitate expression of this resistance marker in the parasite.

Once the pLmNTRKO-PAC construct had been made, a second gene deletion vector based around the gene encoding for blasticidin-S deaminase (*bsr*) was constructed (Figure 5.4.9). A *bsr*-containing resistance cassette was excised from the vector pTbNTRKO-BSR (supplied by Dr S Wilkinson) following digestion with *Xba*I+*Apa*I. The resultant fragment (~970 bp) was then cloned the corresponding sites of pLmNTRKO-PAC such that the *pac*-containing resistance cassette was replaced with the *bsr* counterpart. This generated the plasmid pLmNTRKO-BSR (Figure 5.4.10). This construct was confirmed by restriction mapping and DNA sequencing.

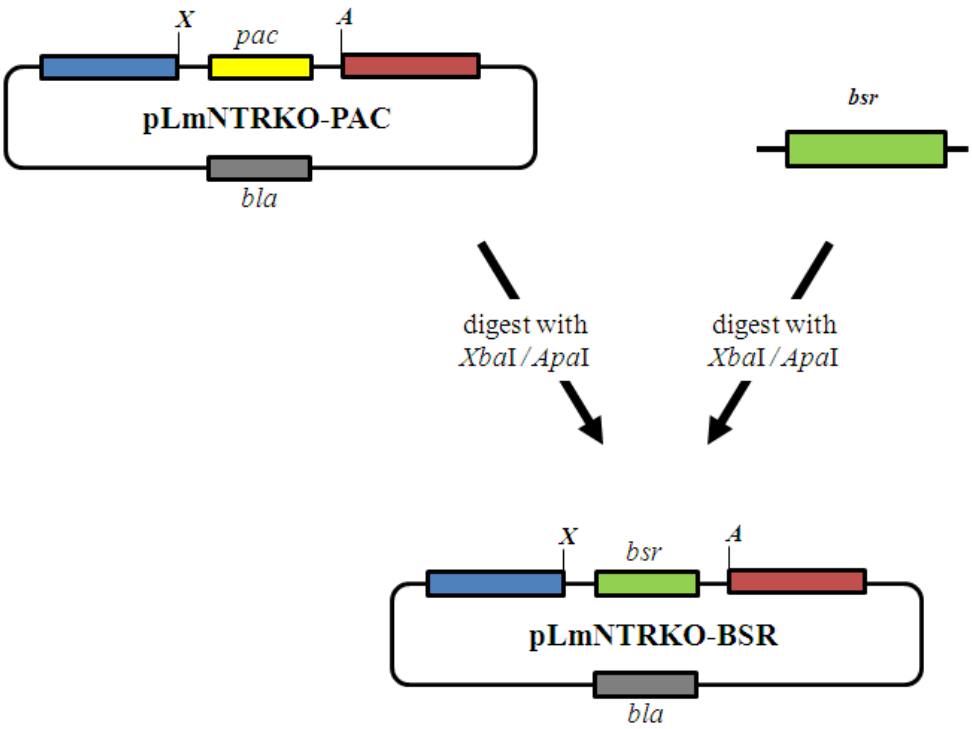

Figure 5.4.9: Schematic representation outlining the construction of pLmNTRKO-BSR
The vector pTbNTRKO-BSR (Wilkinson, Taylor *et al.* 2008) was digested with *Xba*I+*Apa*I releasing a DNA fragment containing the blasticidin-S deaminase (*bsr*; light green) gene plus *T. brucei* tubulin 5' and 3' UTRs (black bars). This fragment was purified and cloned into the *Xba*I+*Apa*I sites of pLmNTRKO-PAC such that the puromycin N-acetyl-transferase-containing resistance cassette (*pac*; yellow + *T. brucei* tubulin 5' / 3' UTRs designated as flanking black bars) was replaced by the *bsr*-containing sequence, to form pLmNTRKO-BSR. The DNA sequence encoding for ampicillin resistance (*bla*; grey) as well as the 5' (blue) and 3' (red) UTR from *LmNTR*, are also highlighted. *X* and *A* correspond to *Xba*I and *Apa*I restriction sites, respectively.

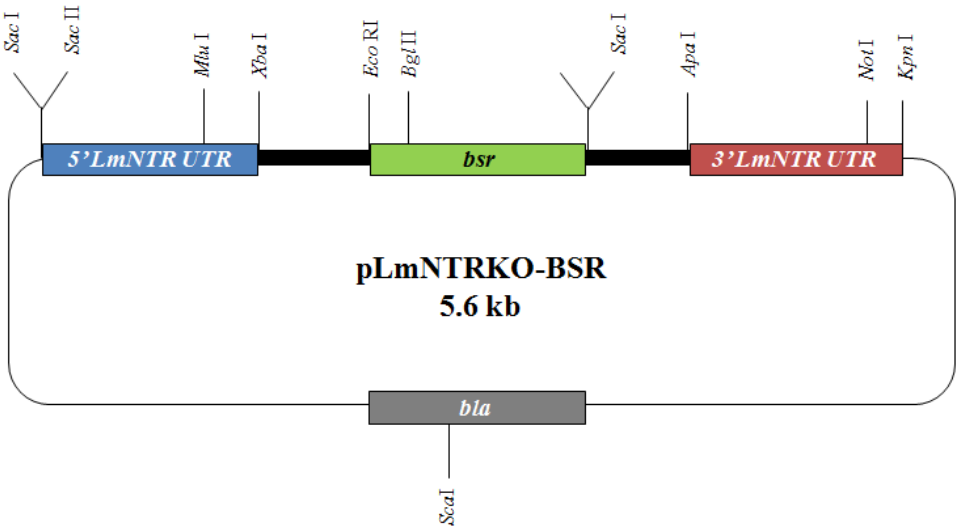

Figure 5.4.10: Restriction map of the LmNTR gene deletion vector pLmNTRKO-BSR
The DNA sequences encoding for blasticidin-S deaminase (*bsr*, light green) and the β-lactamase (*bla;* grey) are highlighted while the 5' (blue) and 3' (red) UTRs from *LmNTR* are also noted. The black boxes flanking the *bsr* gene correspond to the *T. brucei* tubulin 5'/3' UTRs and facilitate expression of this resistance marker in the parasite.

Prior to their introduction into *L. major* promastigotes, both deletion constructs were processed to release the gene targeting fragment from the plasmid backbone. For the *pac*-containing vector, restriction digestion using *Sac*I+*Kpn*I resulted in two bands: one of ~3.0 kbp, corresponding to the *LmNTR* targeting fragment, and the second at ~2.8 kbp which corresponds to the vector backbone. The ~3.0 kbp band was gel purified. For the *bsr*-containing vector, the plasmid was digested with *Sca*I and the single ~5.6 kbp fragment purified: this particular enzyme cleaves the plasmid within the sequence encoding for β-lactamase (*bla*) present in the vector backbone. This purified ~5.6 kbp fragment was then subject to a second round of restriction digestion using *Sac*II+*Kpn*I. This produced three bands, two of which correspond to the unwanted plasmid backbone. The third ~2.8 kbp fragment that corresponds to the *bsr*-containing *LmNTR* targeting fragment was gel purified.

Both the *pac* and *bsr*-containing *LmNTR* targeting fragments (~3.0 and ~2.8 kbp, respectively) were introduced into *L. major* promastigotes using the Amaxa® Nucleofector® system. Recombinant *L. major* cells were then selected on agar plates containing the appropriate antibiotic. After 3-4 weeks, colonies visible on the media surface were transferred into M199 medium containing either puromycin or blasticidin as applicable and cultured as described in Section 3.2.1. After two rounds of sub-culturing, genomic DNA from several putative *pac* and *bsr*-containing heterozygote clones (designated as $LmNTR^{+/-}$ PAC or $LmNTR^{+/-}$ BSR) was extracted and digested with the restriction enzyme *Apa*I. Following size fractionation, the agarose gel was transferred onto nylon membrane and used in Southern hybridisation, using the 5' LmNTR UTR as probe. This particular restriction enzyme (*Apa*I) was chosen for such an analysis following *in silico* restriction mapping using DNA sequences around the *LmNTR* loci, downloaded from the *L. major* genome database. Based on this, we predicted that an *Apa*I band of ~1.7 kbp was detected in digested *L. major* Friedlin genomic

DNA when using the 5' LmNTR UTR as probe (Figure 5.4.11 A) with one of the *Apa*I restriction sites in the 5' region of *LmNTR* itself, and the other being upstream within the intergenic region. Integration of the *pac* or *bsr*-containing constructs at the *LmNTR* loci results in the complete deletion of the oxidoreductase gene and loss of the associated *Apa*I restriction site. However, both constructs do introduce an alternative *Apa*I site as part of their resistance cassette (Figures 5.4.8 and 5.4.10). As such, Southern hybridization of *Apa*I-digested *LmNTR*$^{+/-}$ PAC or *LmNTR*$^{+/-}$ BSR genomic DNAs using the 5' LmNTR UTR probe is predicted to detect diagnostic bands at ~2.9 or ~2.7 kbp, respectively (Figure 5.4.11 A). When the actual hybridisations were performed, the above expected bands sizes were detected indicating that LmNTR heterozygote clones had been produced (Figure 5.4.11 B). It is interesting to note that the stoichiometry of the bands shown by the *LmNTR*$^{+/-}$ PAC clone indicates trisomy, with an extra copy of wild type LmNTR (Figure 5.4.11 B, lane 2).

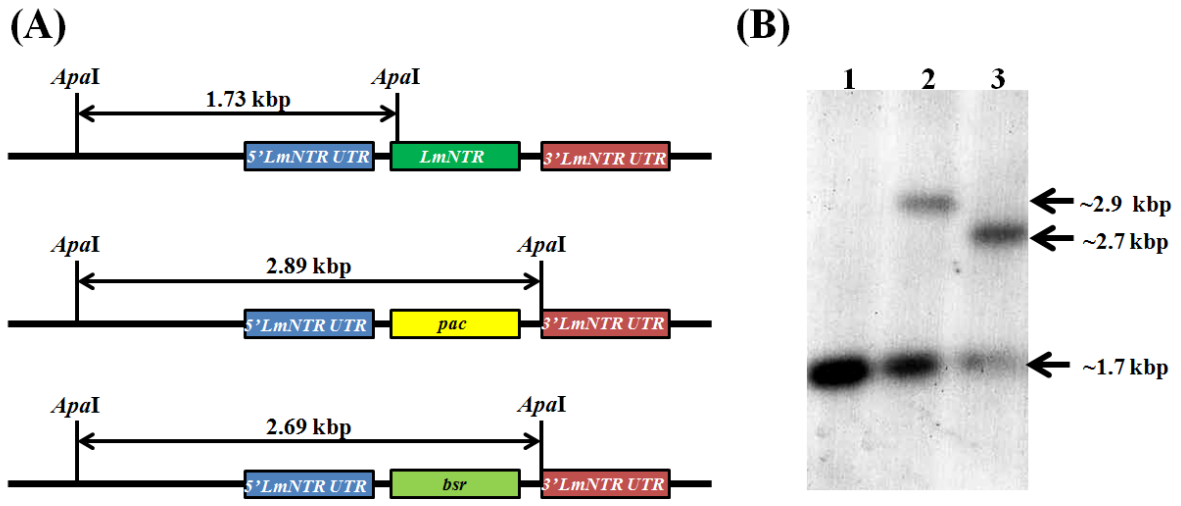

Figure 5.4.11: Disruption of NTR in *L. major*
(A) Schematic representation outlining the *LmNTR* allele (dark green) and the effects of gene disruption with vectors based around the puromycin N-acetyl-transferase (*pac*; yellow) or blasticidin-S (*bsr*; light green) resistance cassettes. The 5' (blue) and 3' (red) UTRs of *LmNTR* are highlighted. The restriction sites for the enzyme *Apa*I and the expected fragment sizes (in kbp) following *Apa*I digestion of *L. major* genomic DNA are shown. (B) Autoradiographs of *Apa*I digested genomic DNA from wild type *L. major* Friedlin (lane 1) and *LmNTR*$^{+/-}$ PAC and BLA heterozygous clones (lanes 2 and 3, respectively). Southern blots were hybridised with labelled 5' *LmNTR* UTR probe. Sizes given are in kbp.

We next attempted to generate *L. major LmNTR* null mutant lines. Despite multiple (16) electroporations performed on 7 separate occasions, no double drug resistant parasites were obtained. However, positive controls (transfecting the heterozygote cell lines with an episomal GFP expression plasmid, pTEX-GFP, in parallel) resulted in double drug resistant promastigotes. In these experiments, the *pac*-containing *LmNTR* targeting vector was transfected into the *LmNTR*$^{+/-}$ BSR line and *vice versa*, all to no avail. This inability to generate *LmNTR* null mutants strongly suggests that the function of this enzyme is essential for the growth of *L. major* promastigotes. Unfortunately, rescue experiments were deemed unfeasible based on our previous finding that expression of ectopic copies of *LmNTR* promastigotes is deleterious in this parasite life cycle stage.

To help evaluate the phenotypic properties displayed by heterozygote line, the *L. major LmNTR*$^{+/-}$ BSR cells were electroporated with the ~5.3 kbp *Sbf*I/*Asc*I DNA fragment that contains the integrative luciferase expression system (LmRIX-Luc). Selection on agar plates yielded a number of drug (G418) resistant clones. The luciferase activity in extracts derived from these lines was shown to be comparable with that generated from the lysates described previously in Section 4.2 (data not shown).

5.4.3 Characterisation of the *L. major LmNTR*$^{+/-}$ heterozygote parasites

To assess the effect of a single *LmNTR* gene replacement we established the growth properties of promastigote-form parasites with respected to wild type cells. Starting at a density of 1 x 10^5 parasites mL^{-1} the growth of a *LmNTR*$^{+/-}$ BSR clone (clone 2) was followed over the next 10 days and growth curves of the cultures established (Figure 5.4.12). This was performed in triplicate. Over this time frame, the promastigote recombinant parasites exhibited a similar growth profile to that displayed by the wild type culture with both cell

lines having an approximate doubling time of around 18 hours. Similar experiments were performed using a *LmNTR*$^{+/-}$ PAC clone and no growth defect was recorded using this line either (data not shown). This indicates that loss of a single *LmNTR* allele has no effect on the promastigote growth rate.

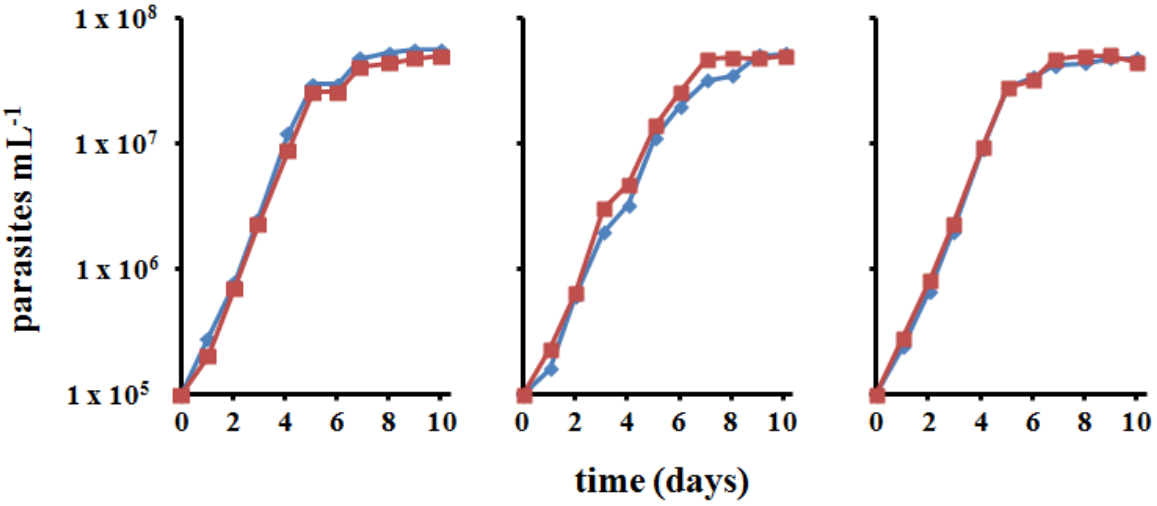

Figure 5.4.12: Growth of *LmNTR*$^{+/-}$ heterozygote promastigotes parasites
The growth of *L. major LmNTR*$^{+/-}$ (BSR) heterozygote clone (red squares) and wild type *L. major* Friedlin (blue diamonds) promastigote parasites was monitored until cultures were in the stationary phase of growth. At day 0, both lines were seeded at 1x10^5 cells mL^{-1}, and parasite loads ($\log_{10}$ number of parasites mL^{-1}) determined every day over a 10 day period. Three independently derived growth curves for each cell line are shown.

Previous work using *T. cruzi* and *T. brucei* lines with reduced NTR expression has shown that these cells display resistance to nitroheterocyclic compounds (Wilkinson, Taylor *et al.* 2008). To determine whether this is the case for *L. major* promastigotes, the susceptibility of the *LmNTR*$^{+/-}$ heterozygote lines to nifurtimox was determined and compared to controls performed in parallel (Figure 5.4.13). From the resultant dose response curves, the IC_{50} values of wild type parasites was calculated to be 4.07 ± 0.21 μM while that recorded for the recombinant line was almost 3-fold higher at 11.49 ± 0.59 μM.

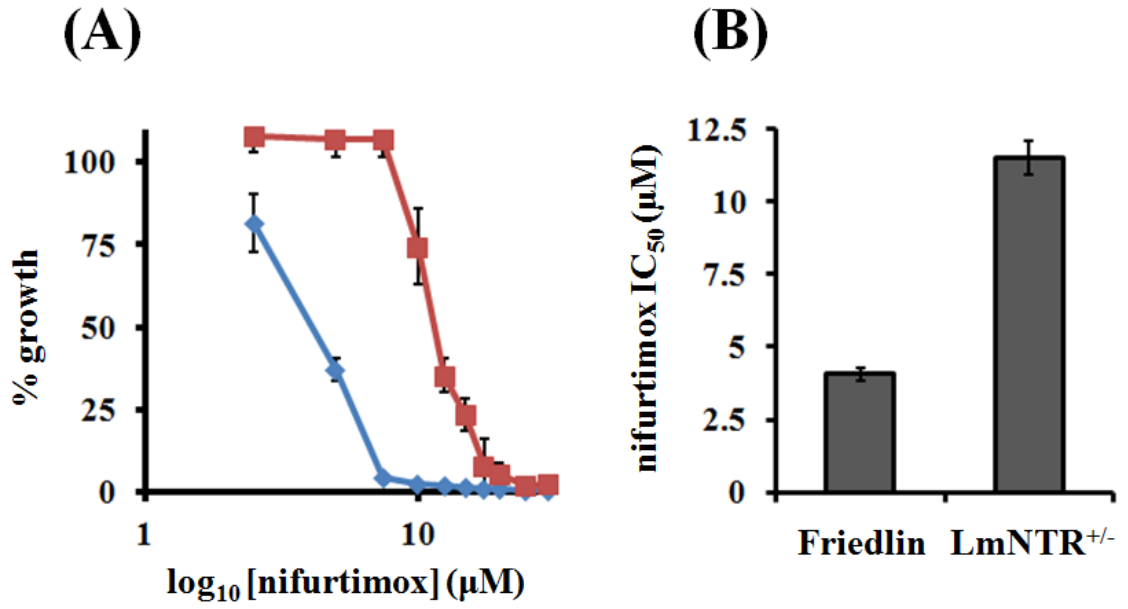

Figure 5.4.13: Susceptibility of *L. major* Friedlin wild type and *LmNTR* heterozygous parasites to nifurtimox
(A) Dose response curves of *L. major* cells expressing lower levels of LmNTR (*LmNTR*$^{+/-}$ heterozygote; red) to nifurtimox was compared to *L. major* Friedlin wild type (in blue) parasites. The data points are averages derived from experiments performed in quadruplicate. (B) From the dose response curves, the IC_{50} values of *L. major* Friedlin and *LmNTR* heterozygote cells were determined. The data points are averages ± standard deviation derived from experiments performed in quadruplicate.

While determining the above growth profiles, parasite samples were collected from day 5 onward and, using a well-characterised agglutination technique (da Silva and Sacks 1987), metacyclic parasites were purified then quantified (Figure 5.4.14). Assessment of the numbers of metacyclics as a percentage of the total cell populations indicated that the *LmNTR*$^{+/-}$ heterozygote promastigotes differentiate into the infectious-form cells at levels equivalent to wild type parasites when they reach the stationary phase of growth (density of above 1 x 10^7 cells mL^{-1}). Therefore, loss of a single *LmNTR* allele has no effect on the differentiation of promastigote parasites in to metacyclic-form cells.

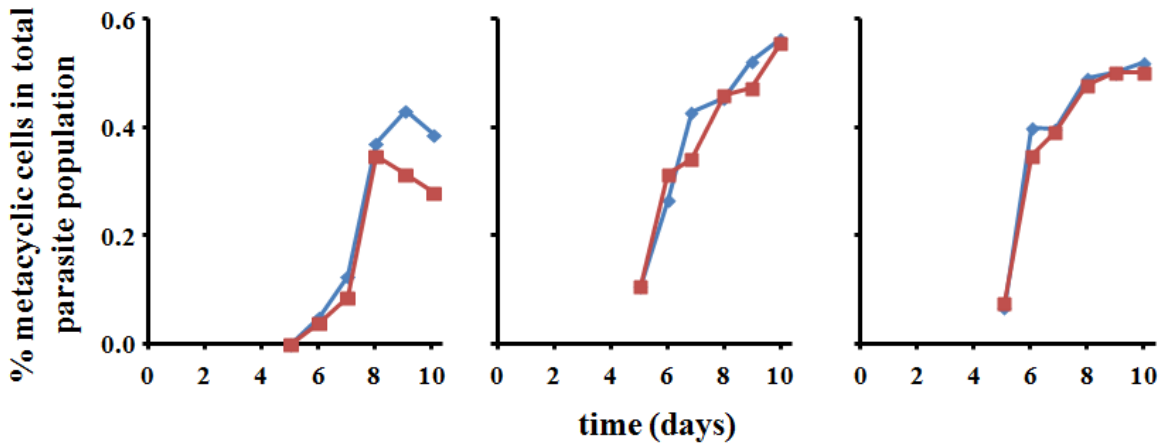

Figure 5.4.14: Metacyclic production in *LmNTR*$^{+/-}$ (BSR) *L. major*
The growth of *L. major LmNTR*$^{+/-}$ (BSR) heterozygote clone 2 (red squares) and wild type *L. major* Friedlin (blue diamonds) promastigotes was monitored until cultures were in the stationary phase of growth (see Figure 5.4.12). At day 5 (and every day until day 10), an aliquot (1 mL) of each culture was taken and metacyclic parasites purified following agglutination of promastigotes using peanut lectin (see Section 3.2.1). The number of metacyclic parasites was then determined. For each cell line, metacyclic loads from three independent cultures were evaluated. The data is expressed as a % metacyclics load in the total *L. major* population.

Next, we assessed the ability of *LmNTR* heterozygote cells to infect mammalian cells using an *in vitro* tissue culture protocol or animals. For the former experiments we made use of the luciferase expressing *LmNTR*$^{+/-}$ BSR line (see Section 5.4.2): these cells were shown to exhibit a promastigote growth and metacyclogenesis at levels equivalent to wild type/non-luciferase expressing *LmNTR* heterozygotes (data not shown). A series of mammalian differentiated THP-1 cultures were infected with purified luciferase-expressing *L. major* Friedlin or *LmNTR*$^{+/-}$ BSR metacyclic parasites under the conditions previously noted (Section 4.3). At time intervals, extracts were generated from cultures and the luciferase activity determined over a 4 day post-infection period (Figure 5.4.15). After correcting for background luminescence (lysed, uninfected macrophages), the reporter signal generated from *LmNTR*$^{+/+}$ homozygote amastigotes increased appearing to plateau by day 4 post-infection. In contrast, *LmNTR*$^{+/-}$ heterozygote cultures exhibited luminescence values equivalent to background, giving a highly statistically significant difference between the two

cell lines by day 3 (Student's t-test, $p < 0.01$). Based on these data it appears that disruption of one *LmNTR* allele results in haploid insufficiency such that *L. major* amastigotes are unable to grow.

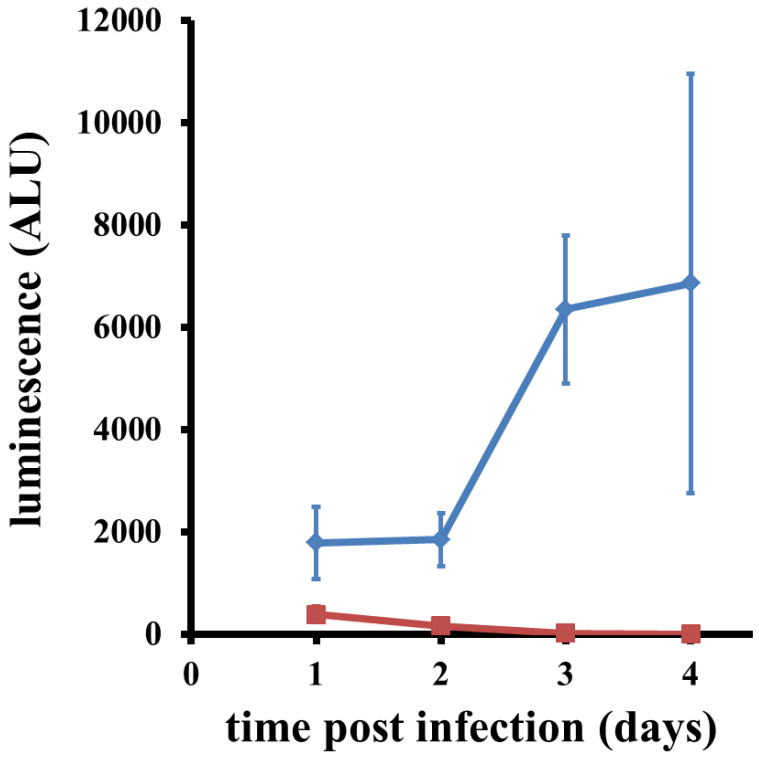

Figure 5.4.15: Growth of *LmNTR*$^{+/-}$ heterozygote amastigote parasites in tissue cultured mammalian cells
In a 24-well plate, differentiated THP-1 cells (2.5 x 10^4 cells per well) were infected overnight with purified metacyclic *L. major* (5 x 10^5 cells per well, giving a ratio of 20 parasites per mammalian cell). The following day, non-internalised parasites were removed by extensive washing before growing the cells at 37^{o}C in a 5% CO_2 atmosphere in fresh medium. On days 1, 2, 3 and 4 post-infection, cells were lysed (in 100 µL lysis buffer) and the luciferase activity, as measured in arbitrary light units (ALU), for 20 µL of each extract was determined. The background corrected luciferase activity, used as a measure of amastigote load, was plotted against time. The cell lines used were a luciferase-expressing *L. major LmNTR*$^{+/-}$ (BSR) heterozygote clone (red squares) and luciferase-expressing *L. major* Friedlin (blue diamonds), with three independent cultures per cell line evaluated at each time point. The data are means from the replicate counts ± standard deviations.

To determine whether the *in vitro* amastigote proliferation defect translates to problems with *in vivo* infectivity, BALB/c mice were infected with wild type or *LmNTR*$^{+/-}$ heterozygote *L. major* metacyclic cells, through injection into their footpad. Over a period of 80 days, the

mice were studied and measurements taken of any footpad lesion that developed. Over an 80 day period, the presence and size of any footpad lesions was monitored. For mice infected with wild type parasites, a wound was detected by day 31 that gradually increased in size to give lesions that ranged in size from 5.5 to 9.5 mm diameter. By day 75 these mice were euthanized. Interestingly, the three mice infected with *LmNTR*$^{+/-}$ heterozygote cells presented no signs of lesion by day 80 (Figure 5.4.16). This strongly indicates that the function of LmNTR is important in establishing and expansion of a *L. major* infection.

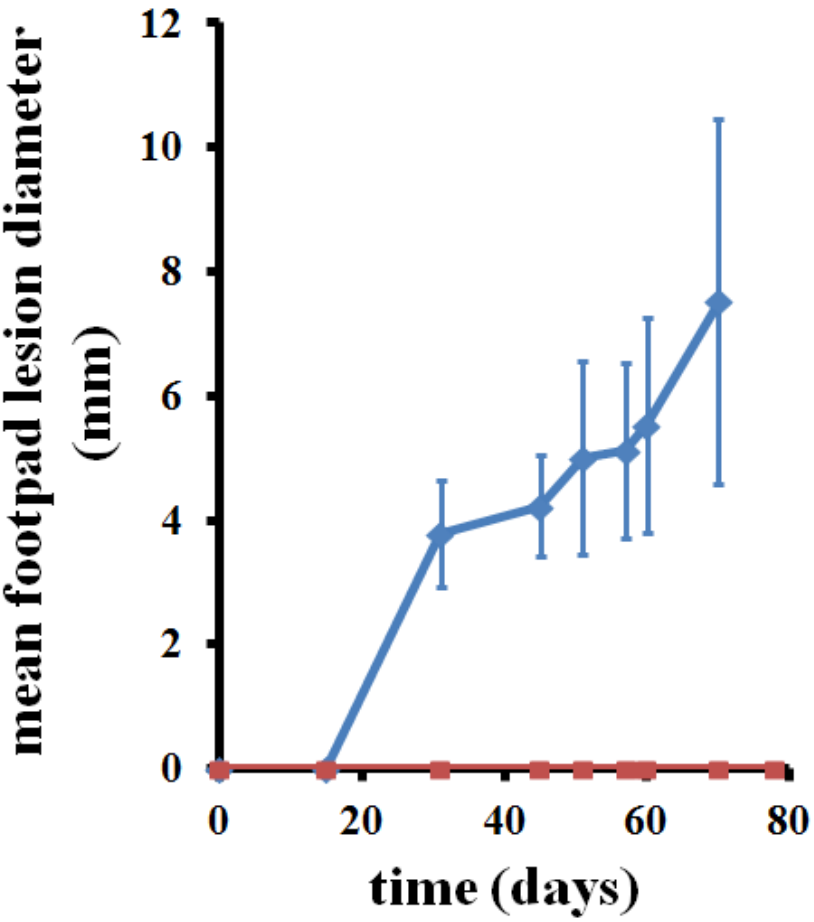

Figure 5.4.16 *LmNTR*$^{+/-}$ heterozygote *L. major* are not infectious to mice
Purified *LmNTR*$^{+/-}$ (BSR) heterozygote clone (red squares) and wild type *L. major* Friedlin (blue diamonds) metacyclic parasites (2 x 10^6) were inoculated into the footpad of BALB/c mice. Periodically, the size of the lesion was measured. For each cell line, three mice were infected and the data is expressed as the mean lesion size (in mm) ± standard deviation. All *in vivo* work was performed at the London School of Hygiene and Tropical Medicine by Dr Karin Seifert.

5.5 Chapter summary

Characterisation of LmNTR has shown that:

1. The *L. major* genome contains a single gene encoding for a type 1 nitroreductase, designated as LmNTR.
2. The catalytic domain of LmNTR can be heterologously expressed in *E. coli* and readily purified as a His_6-tagged recombinant protein.
3. The purified recombinant protein non-covalently binds FMN as a cofactor.
4. The purified recombinant protein mediates the metabolism of a wide range of nitroaromatic and quinone-based compounds, preferentially using NADH as source of reductant.
5. Metabolism of nitroaromatic and quinone-based substrates occurs in the presence of oxygen via a ping-pong kinetic mechanism.
6. Expression of elevated levels of LmNTR in *L. major* promastigotes appears to be deleterious to cell growth.
7. In promastigote-form parasites, a single *LmNTR* allele can be readily deleted from the *L. major* genome indicating that reduction in levels of this enzyme does not affect promastigote growth or metacyclogenesis.
8. In promastigote-form parasites, both allelic copies of *LmNTR* cannot be deleted from the *L. major* genome, indicating that complete absence of this enzyme is lethal to promastigotes.
9. $LmNTR^{+/-}$ heterozygotes are unable to replicate in the intracellular amastigote-form parasites in tissue culture or animal model systems indicating haploid insufficiency.
10. The above data demonstrate that LmNTR levels play a crucial role in the parasite growth of the two replicative stages tested here.

6. Evaluating nitroaromatic compounds as leishmanicidal prodrugs

Current treatments used against the various forms of leishmaniasis are problematic (Croft and Olliaro 2012). Several cause unwanted toxic side effects, resistance in a clinical context has been reported for others while most require medical supervision for administration. Additionally, many of the drugs that have recently come onto the market are expensive and their use is restricted. Against this backdrop, there is an urgent requirement for new, safe and cost effective therapies that can ideally be given as an oral dose. One group of compounds that meets many of these prerequisites are the nitroaromatics. Although concerns about the toxicity and mutagenic activity of some chemicals in this class have been raised, a number of the most commonly prescribed antibiotics belong to this grouping, for example metronidazole, tinidazole, furazolidone, nitrofurazone *etc.* Here, we report the biochemical and leishmanicidal screens of a range of novel nitroaromatic compounds aimed at evaluating their potential as antiparasitic agents, and examine the role played by LmNTR in these activities. A total of 52 structures across 4 distinct compound classes were analysed consisting of 22 nitrobenzyl phosphoramide mustards (NBPMs), 13 aziridinyl nitrobenzamides (ANBs), 8 nitrofurans and 9 nitrobenzamides. Below, the biochemical/cytotoxicity screens performed for each of these classes are described.

6.1 Biochemical and toxicity screening of nitrobenzyl phosphoramide mustards

Phosphoramide mustards such as cyclophosphamide and ifosfamide have been used as anticancer agents since the late 1950s (Arnold *et al.* 1958, Colvin 1999, Carli *et al.* 2003). These structures have recently been combined with a nitrobenzyl substituent group to generate a series of nitroreductase activated prodrugs . In mammalian cell lines engineered to express the *E. coli* type I nitroreductase, such compounds exhibit significant levels of cytotoxicity while certain variants display trypanocidal properties (Hu, Yu *et al.* 2003, Hall,

Wu *et al.* 2010, Hu, Wu *et al.* 2011). Using compounds supplied by Prof Lonqin Hu (Rutgers, the State University of New Jersey), we evaluated their potential against *L. major* then tested investigated their toxicity toward mammalian cells.

Initially, biochemical screens were conducted using purified recombinant LmNTR and a range of NBPMs to determine whether these compounds functioned as substrate for the parasite enzyme, and to elucidate any structure-activity relationships. In the presence of 35 μg LmNTR, assays were performed using fixed concentrations of nitroaromatic (100 μM) and reductant (NADH; 100 μM) and the rate of oxidation of NADH followed by monitoring the change in absorbance at 340 nm (Section 3.7.5) with each compound analysed in triplicate. From the resulting slopes, the enzyme activity was calculated and expressed as nmol NADH oxidised min^{-1} mg $\Delta LmNTR^{-1}$ as a bar chart (Figure 6.1.1).

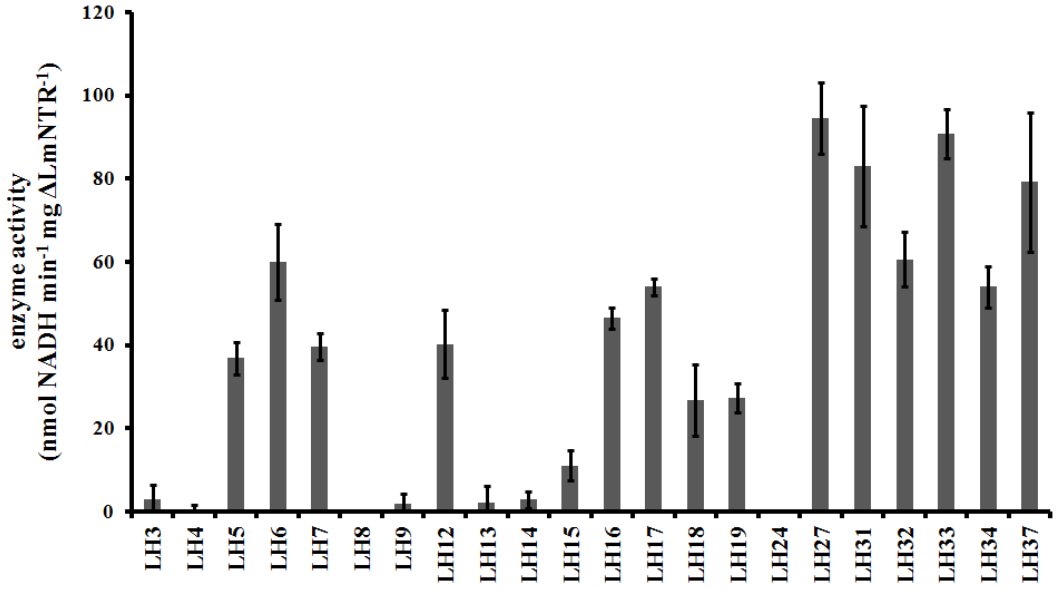

Figure 6.1.1: Evaluating nitrobenzyl phosphoramide mustards as LmNTR substrates
A series of NBPMs were assayed to determine whether they could drive LmNTR activity. Enzyme assays were performed using a 50 mM Tris-Cl pH 7.5 buffer, 100 μM NADH and 100 μM electron acceptor. The assay mixture was incubated at room temperature for 5 min from which the background reaction rate was determined. The assay was then initiated by addition of recombinant LmNTR (35 μg), and the rate of NADH consumption was recorded by following the change in absorbance at 340 nm. From the resultant graphs, the enzyme activity was then calculated using an ε value of 6,220 M^{-1} cm^{-1}, giving values of enzyme activity in nmol NADH min^{-1} mg $\Delta LmNTR^{-1}$. The values shown are the means of data from three experiments ± standard deviations.

Of the 22 compounds analysed, 8 structures (designated as cyclic NBPMs) consisted of a nitrobenzyl group attached either directly or through a carbamate linker to a cyclophosphamide grouping with 14 structures (designated as acyclic NBPMs) containing the phosphoramide mustard as part of a linear arrangement linked to the a nitrobenzyl group containing various substituents (Appendix B). Based on this preliminary biochemical screen, the compounds could be divided into those that were not LmNTR substrates (activity <20 nmol NADH oxidised min^{-1} mg $\Delta LmNTR^{-1}$), those that stimulated a moderate activity (between 20-60 nmol NADH oxidised min^{-1} mg $\Delta LmNTR^{-1}$) and those that were readily metabolised by the parasite enzyme (>60 nmol NADH oxidised min^{-1} mg $\Delta LmNTR^{-1}$). Using this as a crude measure, 3 cyclic NBPMs (LH5, 6 and 12) were evaluated as moderate substrates while 5 showed little or no LmNTR activity. In contrast, most (11) of the cyclical structures were metabolised by LmNTR with 4 (LH27, 31, 33 and 37) showing high levels of activity. Of those substrates driving the higher activities, 3 contain halogen groups attached to the nitrobenzyl ring.

We next evaluated the growth inhibitory properties of the NBPMs towards *L. major* promastigotes and amastigotes using resazurin or luciferase as reporter, respectively (Section 3.3). An initial screen with all 22 compounds was conducted using a fixed concentration of 30 μM against the promastigote and 10 μM against the amastigote, due to the apparent difference in susceptibilities between these two life cycle forms mentioned in Section 4.4. For the compounds that exhibited leishmanicidal properties in the initial assays, secondary screens were performed using a range of drug concentrations: 0, 0.3, 1, 3, 10 and 30 μM against *L .major* promastigotes and 0, 0.1, 0.3, 1, 3 and 10 μM against *L .major* amastigotes. From the resultant growth inhibition data, dose response curves for each agent were plotted (Figure 6.1.2) and the IC_{50} values determined (Table 6.1.1).

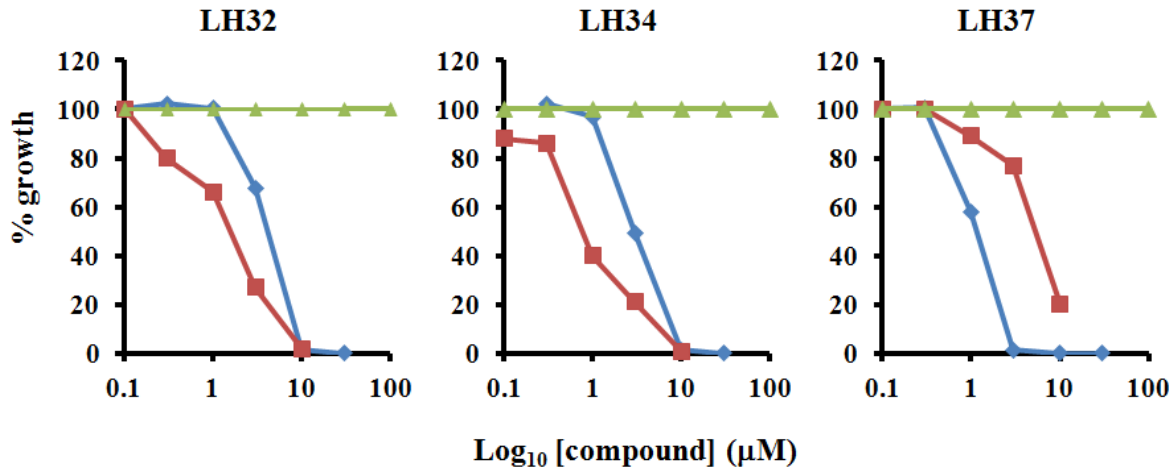

Figure 6.1.2: Dose response curves of *L. major* and THP-1 cells to nitrobenzyl phosphoramide mustards
Various concentrations of leishmanicidal NBPMs were tested against *L. major* and THP-1 cells. The growth inhibitory effect of each treatment was evaluated and dose response curves constructed for promastigotes (blue line), amastigotes (red line) and THP-1 cells (green line). In all cases the drug treatments were performed in triplicate and the plots shown represent the average growth inhibition obtained at each concentration. The curves for compounds LH32, LH34 and LH37 are shown.

compounds	*L. major* IC_{50} (μM)		differentiated THP-1 IC_{50} (μM)	selective toxicity
	promastigotes	amastigotes		
LH3-9 LH12-15; LH17-18; LH24	>30	>10	nd	nd
LH16	15.6 ± 1.13	2.75 ± 0.40	>100	>36
LH19	>30	4.72 ± 0.55	>100	>21
LH27	16.23 ± 0.29	4.65 ± 0.15	>100	>22
LH31	9.05 ± 0.56	7.00 ± 0.40	>100	>14
LH32	4.72 ± 0.23	1.09 ± 0.21	>100	>92
LH33	5.88 ± 0.28	0.21 ± 0.07	>100	>476
LH34	3.10 ± 0.28	0.77 ± 0.12	>100	>143
LH37	1.29 ± 0.08	2.17 ± 0.27	>100	>46

Table 6.1.1: Susceptibility of *L. major* and THP-1 cells to nitrobenzyl phosphoramide mustards
For all data, the IC_{50} values are averages ± standard deviation (where appropriate) derived from experiments performed in triplicate. The selective toxicity compares a compound's IC_{50} value against the mammalian line with that recorded against *L. major* amastigotes. nd is not determined.

We then determined the growth inhibitory properties displayed by all the leishmanicidal NBPMs towards differentiated THP-1 cells using resazurin as reporter (Figure 6.1.2; Table 6.1.1). Under these conditions none of the compounds showed significant *in vitro* toxicity. Comparison of the mammalian toxicity IC_{50} value with that determined against the *L. major* amastigote for a given compound gives a crude measure of its selectivity (Table 6.1.1). For 3 compounds (LH32, 33 and 34), selective toxicity values of around 100 or greater were observed.

To demonstrate that NTR plays a role in NBPM prodrug activation within the parasite itself, the susceptibility of *L. major LmNTR*$^{+/-}$ heterozygote promastigotes to LH33 and LH34 was investigated (Figure 6.1.3). For both compounds, cells with reduced levels of the nitroreductase were more resistant to the agent than wild type controls. For LH33, wild type *L. major* had an IC_{50} value of 4.73 ± 0.29 μM while *L. major LmNTR*$^{+/-}$ heterozygote cells had an IC_{50} value of 7.66 ± 0.23 μM; and for LH34, wild type *L. major* had an IC_{50} value of 3.70 ± 0.40 μM while *L. major LmNTR*$^{+/-}$ heterozygote cells had an IC_{50} value of 12.14 ± 0.84 μM (Figure 6.1.4).

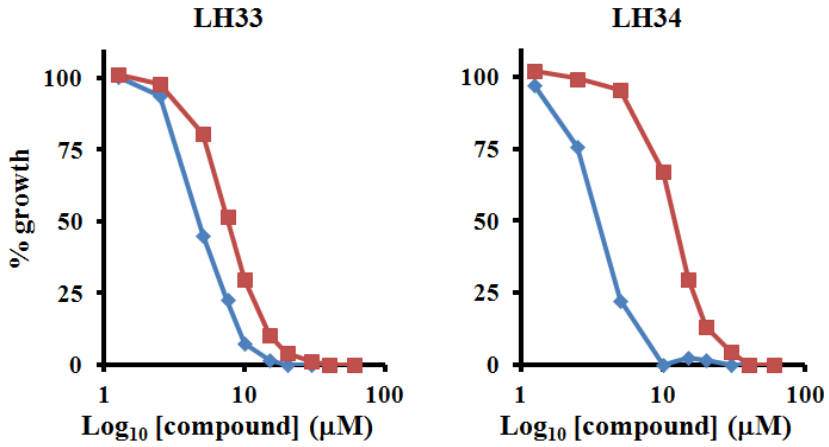

Figure 6.1.3: Dose response curves of *L. major* Friedlin wild type and *LmNTR* heterozygous parasites to LH33 and LH34
Dose response curves of *L. major* cells having lower levels of LmNTR (*LmNTR* heterozygote; red) to LH33 and LH34 was compared to *L. major* Friedlin wild type (in blue) parasites. The data points are averages derived from experiments performed in quadruplicate.

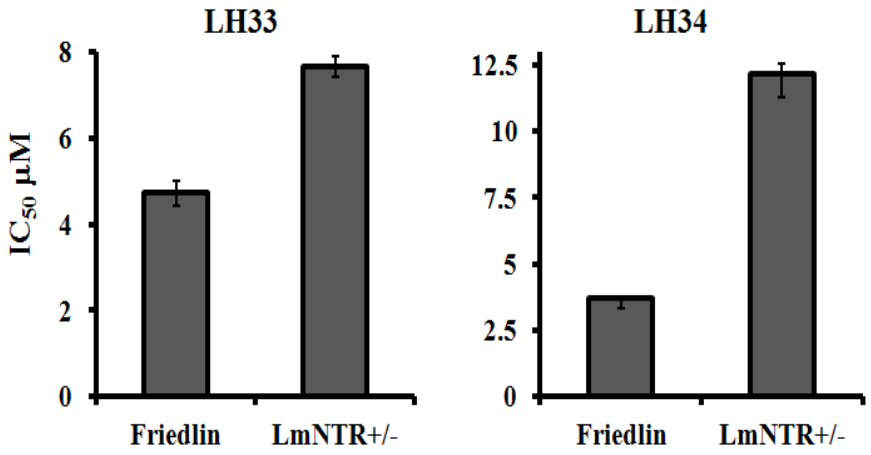

Figure 6.1.4: IC_{50} values of *L. major* Friedlin wild type and *LmNTR*$^{+/-}$ heterozygous parasites to LH33 and LH34
From the dose response curves shown in Figure 6.1.3, the IC_{50} values of *L. major* Friedlin and *LmNTR* heterozygote cells was determined. The data points are averages ± standard deviation derived from experiments performed in quadruplicate.

Based on our findings, NBPMs that contain the phosphoramide mustard as part of an acyclic structure and have halogen substituents on the nitrobenzyl ring are the most readily metabolised by the LmNTR enzyme and represent the most potent agents against both *L. major* promastigotes and amastigotes. Some (LH32, 33 and 33) have IC_{50} values of 1 µM or less against the intracellular stage without inducing mammalian cell toxicity.

6.2 Biochemical and toxicity screening of aziridinyl nitrobenzamides

The ANB class of nitroaromatic compounds are derived from the lead CB1954 (also called tretazicar). This structure was initially developed as an anticancer agent and is undergoing clinical evaluation in two distinct regimes, involving either a bacterial type I NTR-based gene therapy approach or in partnership with caricotamide in the Prolarix™ combinatorial treatment (Chung-Faye *et al.* 2001, Patel *et al.* 2009). CB1954 and several derivatives are trypanocidal, an activity that is dependent on type I NTR expression by the parasites (Bot, Hall *et al.* 2010). As with the NBPMs, we evaluated whether 13 ANBs, supplied by Dr Nuala Helsby (University of Auckland) and Developmental Therapeutics Program/National Cancer

Institute, were substrates for the LmNTR enzyme before assessing their toxicity towards *L. major* and mammalian cells.

As described previously, biochemical tests using fixed amounts of electron donor (NADH; 100 μM) and acceptor (ANB; 100 μM) were performed in the presence of purified recombinant ΔLmNTR (35 μg). However, examination of the absorbance spectrum of CB1954 and its derivatives revealed that during reduction they exhibit considerable changes in absorbance at 340 nm themselves. This precluded following NADH oxidation as a means of monitoring enzyme activity. Consequently, these compounds were assayed at 425 nm, the peak absorbance of the hydroxylamine derivative of this class of compounds (Race, Lovering *et al.* 2007, Bot, Hall *et al.* 2010) (Figure 6.2.1).

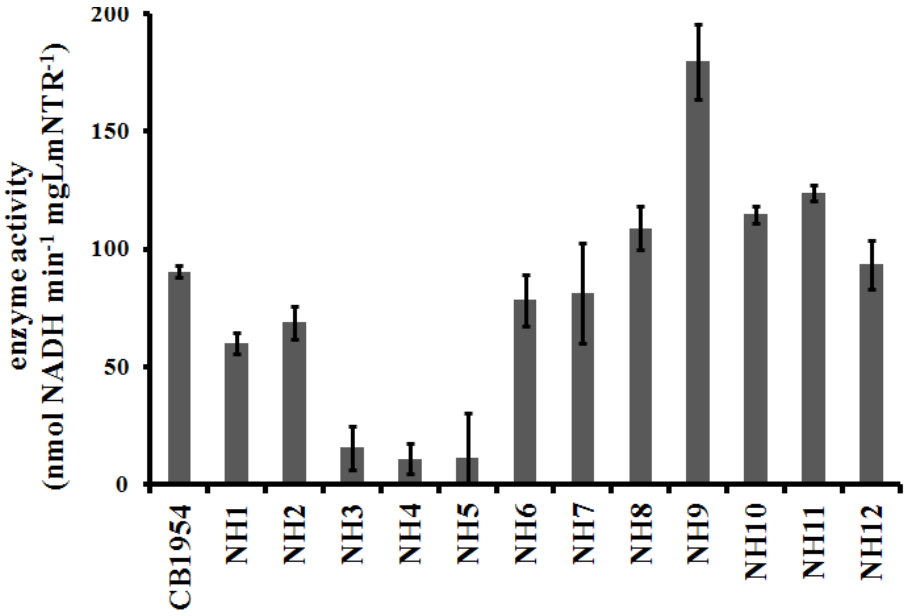

Figure 6.2.1: Biochemical screens of aziridinyl nitrobenzamides
Recombinant LmNTR activity assays across a series of ANBs. Enzyme assays were performed using a 50 mM Tris-Cl pH 7.5 buffer, 100 μM NADH and 100 μM electron acceptor. The assay mixture was incubated at room temperature for 5 min from which the background reaction rate was determined. The assay was then initiated by addition of recombinant LmNTR (35 μg). The rate of ANB consumption was recorded by determining the rate of increase in absorption at 425 nm that corresponds to the production of the hydroxylamine derivative from the parent compound. The enzyme activity was then calculated using an ε value of 1,220 M^{-1} cm^{-1} and assuming that 4 molecules of NADH are oxidised per molecule of ANB reduced (Race, Lovering *et al.* 2007, Bot, Hall *et al.* 2010), expressed in nmol NADH mg $\Delta LmNTR^{-1}$ min^{-1}.

This class of compounds, like the NBPMs, show a range of ΔLmNTR activities, with 9 compounds, including CB1954, displaying enzyme activities greater than 50 nmol NADH min^{-1} mg $\Delta LmNTR^{-1}$. It is interesting to note that NH3-5 exhibit low enzyme activities. These compounds represent a sub-class of ANBs that contain only one nitro substituent at the 2-position on the benzyl ring with in respect to the aziridinyl moiety: all other compounds contain two nitro groups on the benzyl ring at both the 2 and 4-positions.

The growth inhibitory properties of the ANBs towards *L. major* promastigotes and amastigotes were then determined (Section 3.3). As with the NBPMs, an initial screen was conducted against both life cycle stages using the fixed concentrations of nitroaromatic (10 μM against both parasite forms). The structures NH3-5 and NH7-8 had no effect on either parasite form with NH9 and NH12 having no activity against promastigote cells. Secondary screens were then conducted for the leishmanicidal compounds identified from the initial test using a variety of different drug ranges. The resultant growth inhibition data was then used to generate dose response curves for each agent tested (Figure 6.2.2) from which the IC_{50} values were determined (Table 6.2.1).

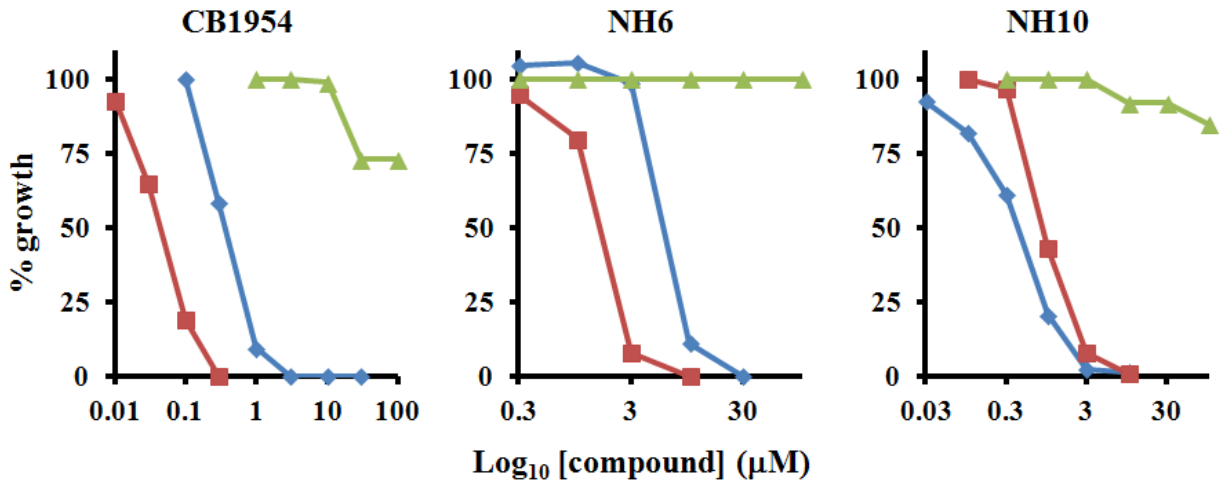

Figure 6.2.2: Dose response curves of *L. major* and THP-1 cells to aziridinyl nitrobenzamides
Various concentrations of leishmanicidal ANBs were tested against *L. major* and THP-1 cells. The growth inhibitory effect of each treatment was evaluated and dose response curves constructed for promastigotes (blue line), amastigotes (red line) and THP-1 cells (green line). In all cases the drug treatments were performed in triplicate and the plots shown represent the average growth inhibition obtained for each concentration. The curves for compounds CB1954, NH6 and NH10 are shown.

compounds	*L. major* IC_{50} (μM)		differentiated THP-1 IC_{50} (μM)	selective toxicity
	promastigotes	amastigotes		
NH3-5; NH7-8	>10	>10	nd	nd
CB1954	0.42 ± 0.01	0.05 ± 0.02	>100	>2000
NH1	7.32 ± 0.63	11.15 ± 2.01	>100	>9
NH2	1.48 ± 0.18	2.95 ± 1.14	>100	>34
NH6	6.85 ± 0.18	2.10 ± 0.22	>100	>48
NH9	>10	0.67 ± 0.05	>100	>149
NH10	0.49 ± 0.04	0.56 ± 0.05	>100	>178
NH11	0.91 ± 0.07	0.06 ± 0.01	>100	>1667
NH12	>10	1.32 ± 0.02	>100	>76

Table 6.2.1: Susceptibility of *L. major* and THP-1 cells to aziridinyl nitrobenzamides
For all data, the IC_{50} values are averages ± standard deviation (where appropriate) derived from experiments performed in triplicate. The selective toxicity compares the IC_{50} value against the mammalian line with that recorded against *L. major* amastigotes for a given compound. nd is not determined.

The cytotoxicity screens against differentiated THP-1 cells revealed that none of the tested compounds displayed significant inhibitory activity towards this mammalian line (Figure 6.2.2; Table 6.2.1). Comparisons of the IC_{50} data indicated that several compounds (CB1954, NH9, NH10 and NH11) all show significant selectivity against *L. major* amastigotes with two recording selective toxicity values in excess of 1500-fold. As such these compounds warrant further attention with regards to drug development targeting cutaneous leishmaniasis and possibly against other forms of this disease.

6.3 Susceptibility screening of other nitroaromatic compounds

In addition to the aziridinyl containing nitrobenzamides, several non-aziridinyl based antimycobacterial nitrobenzamide structures, developed by Dr Priscille Brodin (Institute Pasteur, Korea) (Christophe *et al.* 2009), were evaluated as potential leishmanicidal agents. Initial biochemical screens using purified ΔLmNTR and a range of these compounds were performed, aimed at determining whether any of these structures functioned as substrate for the parasite enzyme. All assays were conducted using fixed concentrations of nitroaromatic (100 μM) and reductant (NADH; 100 μM) and the rate of oxidation of NADH followed by monitoring the change in absorbance at 340 nm (Section 3.7.5). Purified recombinant LmNTR (35 μg) was then added to the reaction and the NADH oxidation monitored. From the resulting slopes, the enzyme activity was calculated and expressed as nmol NADH oxidised min^{-1} mg $\Delta LmNTR^{-1}$ as a bar chart (Figure 6.3.1). Most nitrobenzamide compounds tested generated a reasonable level of NADH oxidation indicating that these compounds are effectively metabolised by LmNTR. The only substrate that failed to generate an enzymatic response was IPK2 with two further chemicals (IPK6 and IPK9) omitted from these assays due to solubility problems.

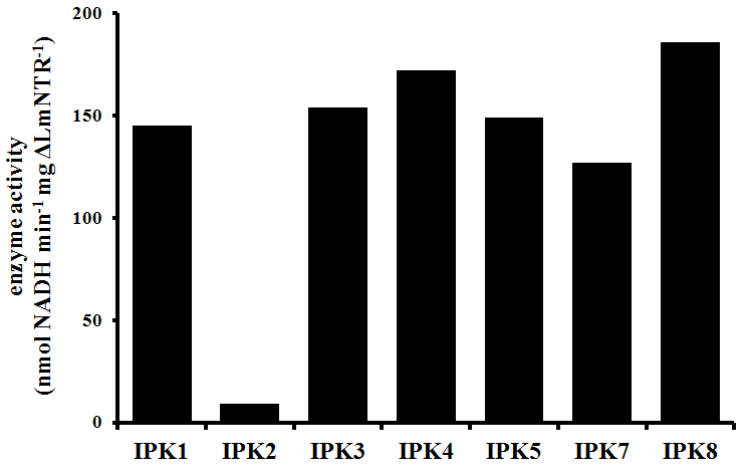

Figure 6.3.1: Evaluating nitrobenzamides as substrates for LmNTR
The enzymatic activity of LmNTR towards IPK compounds was investigated. Using an assay buffer containing 50 mM Tris-Cl pH 7.5 buffer, 100 μM NADH and 100 μM electron acceptor the background rate of NADH oxidation was followed for 5 min at room temperature by monitoring the change in absorbance at 340 nm: no compound exhibited significant absorbance properties at this wavelength. The assay was then initiated by addition of recombinant LmNTR (35 μg), and the rate of NADH oxidation monitored. From the resultant graphs, the enzyme activity was then calculated using an ε value of 6,220 M^{-1} cm^{-1}, giving values of enzyme activity in nmol NADH min^{-1} mg $\Delta LmNTR^{-1}$. The values shown are from single assays conducted by Ms Carissa Chu, an undergraduate student. IPK6 and IPK9 were not analysed due to precipitation of substrates during the assay.

Next, the leishmanicidal activities of all 9 nitrobenzamides were evaluated against promastigote and amastigote form parasites (Section 3.3). As with the other nitroaromatics, preliminary screens were conducted using the fixed concentrations of nitroaromatic (30 μM against the promastigote and 10 μM against the amastigote). This demonstrated that all structures had antimicrobial activity against intracellular parasites with only two (IPK1 and 8) effective against the insect stage. Secondary screens on the leishmanicidal compounds were then performed using a variety of different drug concentrations and from the resultant growth inhibition data, dose response curves were generated (Figure 6.3.2) from which the IC_{50} values were determined (Table 6.3.1).

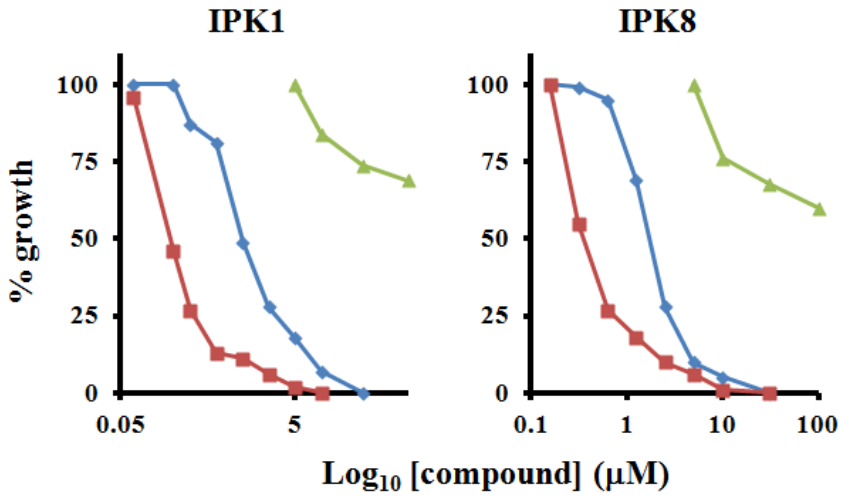

Figure 6.3.2: Dose response curves of *L. major* and THP-1 cells to nitrobenzamides Various concentrations of leishmanicidal nitrobenzamide were tested against *L. major* and THP-1 cells. The growth inhibitory effect of each treatment was evaluated and dose response curves constructed for promastigotes (blue line), amastigotes (red line) and THP-1 cells (green line). In all cases the drug treatments were performed in triplicate and the plots shown represent the average growth inhibition obtained at each concentration. The curves for compounds IPK1 and IPK8 are shown.

To evaluate cytotoxicity, growth inhibition studies at concentrations up to 100 μM were then carried out on differentiated THP-1 cells. As for the anti-parasitic experiments, dose response curves were generated (see Figure 6.3.2 as an example) from which the IC_{50} values for particular compounds were determined (Table 6.3.1). For most compounds, toxicity was observed at the highest concentration (100 μM) but even at this drug level all cultures displayed more than 50% growth. Comparisons of mammalian and amastigote IC_{50} data indicated that all showed significant selectivity toward intracellular *L. major*, with one (IPK6) recording a selective toxicity value in excess of 1500-fold and several others (IPK3 and IPK7) around 500.

compounds	*L. major* IC_{50} (μM)		differentiated THP-1 IC_{50} (μM)	selective toxicity
	promastigotes	amastigotes		
IPK1	1.34 ± 0.40	0.20	>100	>500
IPK2	>10	0.86	>100	>116
IPK3	>10	0.20	>100	>500
IPK4	>10	1.00	>100	>100
IPK5	>10	1.05	>100	>95
IPK6	>10	0.06	>100	>1667
IPK7	>10	0.21	>100	>476
IPK8	1.79 ± 0.21	0.35	>100	>286
IPK9	>10	0.61	>100	>164

Table 6.3.1: Susceptibility of *L. major* and THP-1 cells to nitrobenzamides
For promastigote and THP-1 data, the IC_{50} values are averages ± standard deviation (where appropriate) derived from experiments performed in triplicate. For the amastigote data, the IC_{50} values are derived from three independent lysates that were pooled prior to luminescence detection and appear without standard deviations. The selective toxicity compares a compound's IC_{50} value against the mammalian line with that recorded against *L. major* amastigotes. nd is not determined.

To conclusively demonstrate that the leishmanial type I NTR plays a key role in nitrobenzamide activation in the parasite itself, the susceptibility of *L. major LmNTR*$^{+/-}$ heterozygote promastigotes was investigated. For IPK1 (Figure 6.3.3 A), one of the two compounds effective against this particular life cycle stage, cells with reduced levels of the nitroreductase were approximately 2-fold more resistant to the compound than controls: wild type *L. major* had an IC_{50} value of 2.85 ± 0.31 μM to IPK1 while *L. major LmNTR* heterozygote cells had an IC_{50} value of 5.30 ± 0.83 μM (Figure 6.3.3 B).

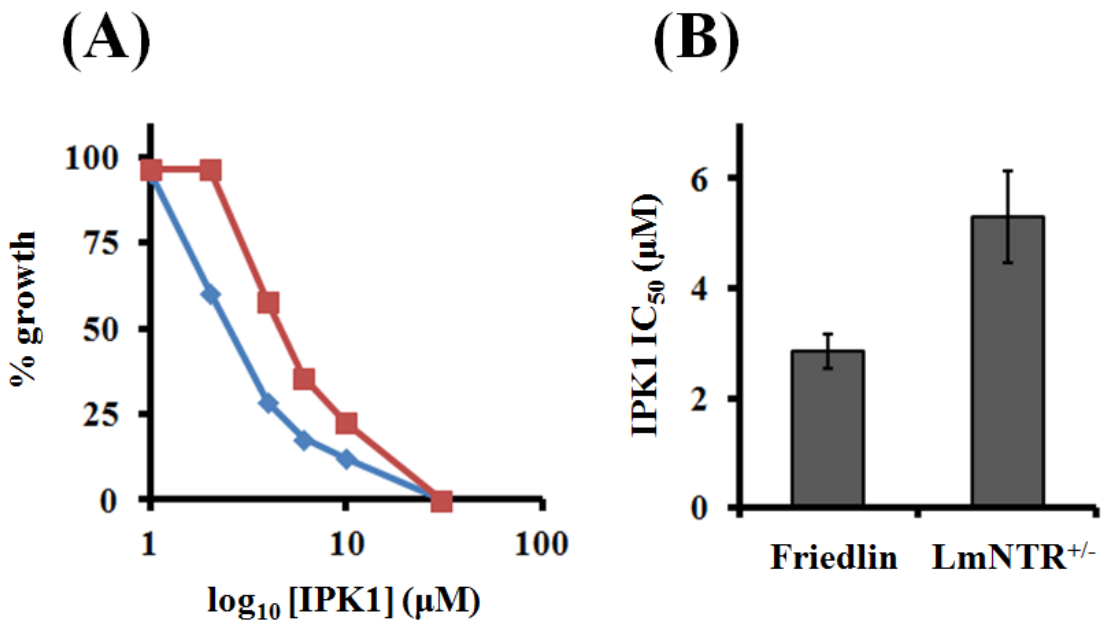

Figure 6.3.3: Susceptibility of *L. major* Friedlin wild type and *LmNTR*$^{+/-}$ heterozygous parasites to IPK1
(A) Dose response curves of *L. major* cells expressing lower levels of LmNTR (*LmNTR* heterozygote; red) to IPK1 was compared to *L. major* Friedlin wild type (in blue) parasites. The data points are averages derived from experiments performed in quadruplicate. (B) From the dose response curves, the IC_{50} values of *L. major* Friedlin and *LmNTR*$^{+/-}$ heterozygote cells were determined. The data points are averages ± standard deviation derived from experiments performed in quadruplicate.

The final class of nitroaromatic tested were a series of nitrofurans synthesized by Dr Adrian Dobbs (Queen Mary University of London). Due to time constraints, only toxicity screens were conducted targeting the *L. major* replicative forms and THP-1 cells. In growth inhibition assays, all compounds displayed potency against promastigote and amastigote parasites with several displaying significant cytotoxicity toward the mammalian cell line (Figure 6.3.4; Table 6.3.2). Despite this, some structures showed selectivity against the intracellular parasite, generating reasonable selective toxicity ratios – for example MNG5a and MNG10a are 153- and 234-fold more effective against the parasite than the mammalian cell respectively.

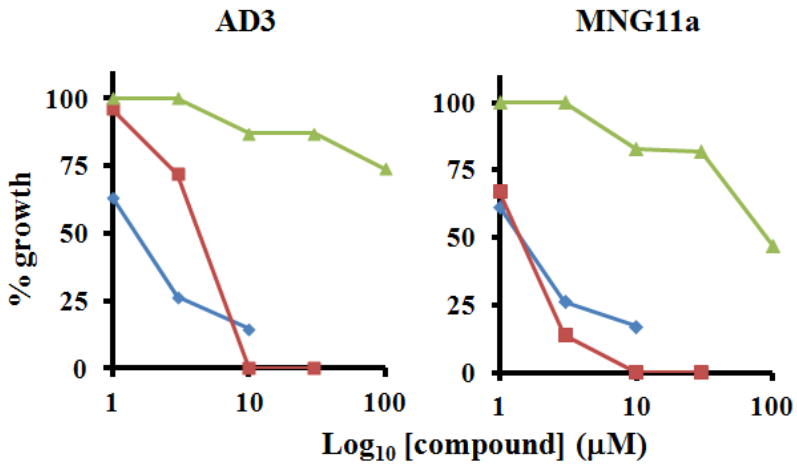

Figure 6.3.4: Dose response curves of *L. major* and THP-1 cells to nitrofurans
Various concentrations of leishmanicidal nitrofuran were tested against *L. major* and THP-1 cells. The growth inhibitory effect of each treatment was evaluated and dose response curves constructed for promastigotes (blue line), amastigotes (red line) and THP-1 cells (green line). In all cases the drug treatments were performed in triplicate and the plots shown represent the average growth inhibition obtained at each concentration. The curves for compounds AD3 and MNG11a are shown.

compounds	*L. major* IC_{50} (µM)		differentiated THP-1 IC_{50} (µM)	selective toxicity
	promastigotes	amastigotes		
nifurtimox	6.28 ± 0.04	2.15 ± 0.01	>100	>47
AD1	4.60 ± 2.55	9.75	nd	nd
AD2	0.43 ± 0.02	1.50	15.90 ± 0.50	11
AD3	1.23 ± 0.21	5.15	>100	>19
MNG5a	2.13 ± 0.12	0.65	99.50 ± 8.38	153
MNG7a	3.35 ± 0.4	1.80	>100	>56
MNG10a	0.22 ± 0.01	0.35	81.88 ± 13.09	234
MNG11a	1.08 ± 0.15	1.45	93.82 ± 2.01	65

Table 6.3.2: Susceptibility of *L. major* and THP-1 cells to nitrofuran-based compounds
For promastigote and THP-1 data, the IC_{50} values are averages ± standard deviation (where appropriate) derived from experiments performed in triplicate. For the amastigote data, the IC_{50} values are derived from three independent lysates that were pooled prior to luminescence detection and appear without standard deviations. The selective toxicity compares the IC_{50} value against the mammalian line with that recorded against *L. major* amastigotes for a given compound. nd is not determined.

The above screens against *L. major* amastigotes using 52 nitroaromatic compounds identified 15 compounds that show selective growth inhibition (selectivity toxicity ratios of >100). Some of these structures are shown in Figure 6.3.5. This represents a hit rate of just below 30% and clearly demonstrates how understanding the basic biology behind prodrug activation can aided in identifying new lead compounds that warrant further evaluation to treat leishmaniasis.

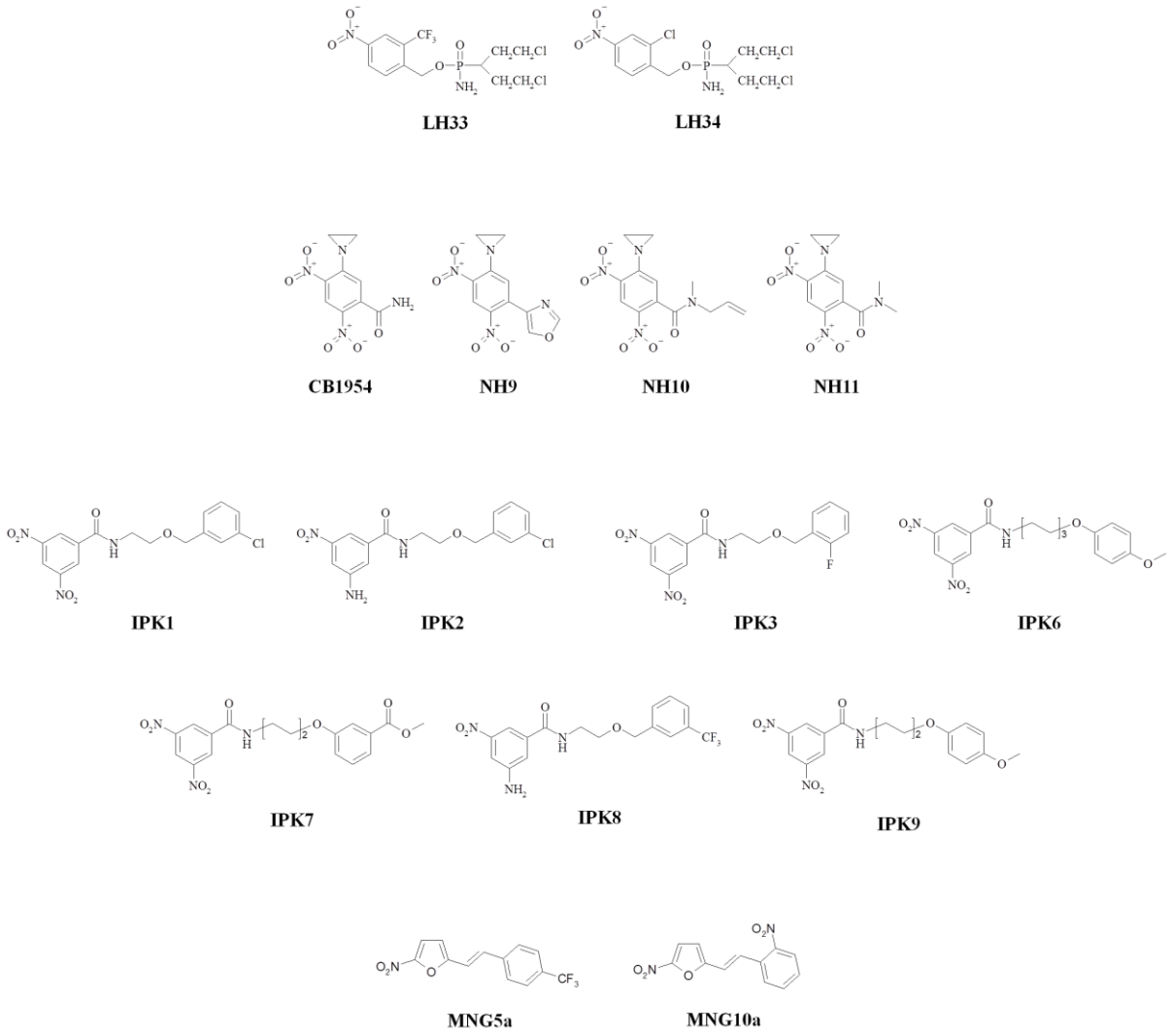

Figure 6.3.5: Structures of the several effective compounds identified in the *L. major* amastigote screens

6.4 Chapter summary

By assaying several classes of nitroaromatic compound as potential ΔLmNTR substrates, as well as inhibitors of *L. major* growth in both life cycle stages, we have demonstrated that:

1. Halogenated acyclic NBPMs show significant activity using recombinant, purified ΔLmNTR.
2. Halogenated acyclic NBPMs also show strong antiparasitic properties and high selectivity against mammalian cells. LH33 and LH34 show IC_{50} values against amastigote *L. major* in the nano molar range.
3. ANB compounds lacking a second nitro group on the 4-position of the aromatic ring in respect to the aziridinyl moiety (sub-class Ib) exhibited little to no ΔLmNTR activity, unlike the other ANBs which drive significant NADH turnover.
4. ANB compounds that exhibit activity in the biochemical screen show strong antiparasitic behaviour (with the exception of NH7) and high selectivity. Most promising are CB1954 and NH11, which exhibit IC_{50} values against amastigote *L. major* of 0.05 ± 0.02 μM and 0.06 ± 0.01 μM respectively.
5. The nitrobenzamides tested show great promise as potential future leishmaniasis therapies, as all 9 compounds show IC_{50} values against amastigote *L. major* of around or below 1 μM, with all exhibiting high selectivity.
6. The nitrofuran compounds tested show reasonable parasite killing properties, however 4 of the 9 compounds tested unfortunately show cytotoxicity against mammalian cells, with IC_{50} values against differentiated THP-1s lower than 100 μM.
7. Loss of an allele of LmNTR causes (~2 to 3-fold) resistance to a number of these nitroaromatics, suggesting that cytotoxicity is mediated *via* LmNTR activation.

7. Discussion

To facilitate the identification of novel leishmanicidal compounds, here we report the construction of an integrative DNA vector containing the gene encoding for luciferase and the characterisation of recombinant *L. major* lines expressing this reporter. This system has allowed us to:

1. Establish a high-throughput, 96-well plate based drug screening assay.
2. Identify several nitroaromatic compounds that exhibit significant growth inhibitory activities against the parasite with little cytotoxicity towards mammalian cells.
3. Evaluate the phenotype of intracellular *L. major* with a reduced type I nitroreductase gene copy number

For several decades, the "gold-standard" method used to screen for leishmanicidal compounds involved directly counting Giemsa stained *Leishmania* cells within infected macrophages. Although giving reproducible results, this has proven to be extremely laborious and incompatible with a high throughput screening process. This type of intact, whole cell analysis has been improved upon using a computer-based cell counting algorithm pioneered for use in *T. cruzi* (Engel *et al.* 2010) and recently applied to *L. donovani* (De Muylder *et al.* 2011). This kind of approach involves fixing parasite-infected mammalian cells after treatment with a given compound, staining the pathogen/host cell's DNA with an appropriate dye (such as DAPI) and then capturing the resultant images. The algorithm then distinguishes between mammalian and pathogen cells simply on the genome size making use of the large cell nucleus in the former as compared to the relatively small kinetoplast (mitochondrial genome) in the parasites. One of the key advantages of this method, as with the Giemsa staining method, is that wild type parasites can be used, allowing the analysis of clinical relevant strains. However, the drawbacks of this method is that it requires proprietary image

capturing equipment and analysis software coupled with the fact that it cannot be applied to *in vivo* animal models. Consequently, most other alternatives to the classical DNA stain approaches involve the creation of genetically modified parasite lines. Cell lines expressing ectopic copies of β-galactosidase, first produced to validate transfection protocols (LeBowitz, Coburn *et al.* 1991), were applied to compound screening regimens in 2003 (Okuno, Goto *et al.* 2003). This method, although not particularly sensitive and suffering from background issues, did establish that such procedures could be employed in drug development. Attempts to improve this system using other colorimetric reporters, *e.g.* the β-lactamase gene, also suffered with sensitivity problems (Buckner and Wilson 2005) and have generally been superseded by other genetically modified parasite lines. One such approach taken has been to label recombinant *Leishmania* with a fluorescent protein such as RFP, GFP or eGFP (Kamau, Grimm *et al.* 2001, Singh and Dube 2004, Singh, Gupta *et al.* 2009, Bolhassani, Taheri *et al.* 2011, Pulido, Muñoz *et al.* 2012; Okuno, Goto *et al.* 2003). Although these systems are relatively easy to implement and allow for easy kinetic monitoring, they often experience sensitivity problems. For example, the signal emitted by the "standard" GFP is too low for use in a 96-well microtitre format although implementation of a multimeric form of this fluorescent protein has been shown to overcome this problem (Chan, Bulinski *et al.* 2003). Additionally, many lines expressing fluorescent proteins do so *via* episomal vectors. Such expression systems are flawed, given that the copy number of such plasmids varies between cells within the same population, resulting in highly variable fluorescence signals. Moreover, without appropriate drug selection such genetic elements can be readily lost. However, the presence of a drug required to maintain plasmid selection could lead to interactions with the compound(s) of interest. As a consequence, cell lines containing a stably-integrated GFP are now available (Singh, Gupta *et al.* 2009, Bolhassani, Taheri *et al.* 2011).

Perhaps the most reliable and versatile *Leishmania* reporter system developed to date involves the use of luciferase. Both episomal and integrative vectors have been constructed and used to indirectly monitor cell numbers as a function of luminescence (Roy *et al.* 2000; Sereno *et al.* 2001; Gupta *et al.* 2005; Lang *et al.* 2005; Thalhofer *et al.* 2010; Michel *et al.* 2011). Although this system requires relatively expensive luciferin-containing buffers, it is sensitive, rapid, and reproducible and can be applied to multiple parasite life cycle stages. Additionally, using luciferase-expressing cell lines is compatible with high throughput screening and *in vivo* imaging in a mammalian model.

After evaluating all the different reporter systems available at the start of the project, we decided to construct our own luciferase vector system and after transfection, generate our own recombinant parasite cells. To this end, we modified an existing *T. cruzi* integration expression vector and made it compatible for use in *L. major* (Figure 4.1.5). The resultant recombinant lines were shown to behave similarly to wild type *L. major* Friedlin with regards promastigote growth, ability to undergo metacyclogenesis and proliferation in the intracellular amastigote form (Sections 4.2 and 4.3). This extended to an *in vivo* animal model situation where the luciferase expressing cells were able to infect and cause cutaneous pathology in BALB/c mice (Figure 4.3.3). Interestingly, standard firefly luciferase systems have recently been applied to combine *in vivo* and *ex vivo* methods for drug screening and monitoring of *Leishmania* in a real time infection (de La Llave *et al.* 2011, Michel, Ferrua *et al.* 2011), with the LmRIX-Luc cell lines now available for similar applications. However, it may be advantageous to use red-shifted variants of the reporter as the luminescence signal derived from these modified proteins show better tissue penetration in whole animals models than standard firefly luciferase (Lewis and Kelly, unpublished). Additionally, studies using luciferase-expressing *T. brucei* showed that *in vivo* imaging is not without its problems.

Assumptions are made that the luciferase substrate luciferin is distributed evenly throughout the animal after administration, and that any luminescence signals are visualised equally irrespective of the infected organ. However, it is apparent that this is not the case with luminescence readings from extracted organs not necessarily agreeing with the signals detected in the live animal (Claes, Vodnala *et al.* 2009).

Once it had been established that luciferase expression by *L. major* did not affect the growth of the replicative stages, we next determined whether these recombinant cells could be used in drug screening. Initially, we conducted a series of assays using nifurtimox as selective agent against promastigote and amastigote parasites. For the promastigotes, we adapted a 96-well plate format growth inhibition protocol that used resazurin (in the form of alamarBlue™) as reporter of cell density (Mikus *et al.* 2000 – modified by Chu & Wilkinson, unpublished). When these conditions were applied to the luciferase-based assay, an IC_{50} value of 7.5 ± 0.42 μM was determined, comparable with the value obtained by other methods (*e.g.* using resazurin). For the amastigote drug assay, the optimal conditions for mammalian cell infection and time course of an infection in a 96-well plate assay were determined (Section 4.3). Using a ratio of 20 infectious-form metacyclic *L. major* (purified from promastigote cultures in the stationary phase of growth) to each mammalian cell, an overnight infection and a 3 day post infection incubation period in the presence of nifurtimox, the IC_{50} was determined to be 0.58 ± 0.06 μM, similar to the value recorded for the related, intracellular parasite *T. cruzi* (Bot, Hall *et al.* 2010). This indicates that amastigote cells are (13-fold) more susceptible to this particular 5-nitrofuran than promastigotes, with nifurtimox displaying little/no cytotoxicity to the mammalian cell line used in the infection (IC_{50} value >100 μM). Why there is a difference in the IC_{50} values is unclear but may reflect variations

between the two parasite forms in relation to prodrug uptake, prodrug activation and/or the availability of molecules targeted by any toxic metabolites generated following activation.

After demonstrating that the luciferase-expressing amastigotes could be used in a 96-well plate drug screening assay we extended these tests to encompass a range of other nitroaromatic compounds, specifically the nitrobenzyl phosphoramide mustards (NBPMs), aziridinyl nitrobenzamides (ANBs), non-aziridinyl nitrobenzamides and nitrofurans. This identified a series of lead structures whose growth inhibition data was then compared to the IC_{50} values obtained against promastigotes and differentiated mammalian THP-1 cells – the promastigote and mammalian IC_{50} values were collected using the vital dye resazurin. For the NBPM series, 8 compounds were shown to affect amastigote parasite growth at a concentration >10 μM, with 7 of these displaying activity against the promastigote form at concentration >30 μM (Table 6.1.1). In parallel, we also evaluated whether the NBPMs functioned as substrates for LmNTR. This demonstrated that all of the leishmanicidal compounds were metabolised by the parasite enzyme with 6 of the most potent anti-parasitic agents eliciting the highest enzymatic activities out of the entire chemical series (Figure 6.1.1). Comparison of the NBPM structures revealed that compounds in this small library could be broadly divided into two sub-classes with the potent leishmanicidal/biochemical substrate data being associated with one of these groups. In general, one class of NBPMs where the phosphoramide linker is part of a cyclical arrangement (Appendix B), did not function as substrates for the parasite enzyme, with 3 showing low to moderate enzyme activity. None of these cyclical compounds affected parasite (promastigote or amastigote) growth. For the other compounds where the phosphoramide linker is part of a linear arrangement connecting the nitrobenzyl moiety to the mustard component, 11 out of 14 were metabolised by LmNTR. The compounds that elicited the highest enzymatic activities were

all related in that they contained an electron-withdrawing halogen substituent located on the nitro-containing aromatic ring. Intriguingly, those structures that were preferentially metabolised by ΔLmNTR displayed the highest potency towards the promastigote and amastigote parasites and had little/no associated mammalian cell cytotoxicity (Table 6.1.1). Previous biochemical and anti-parasitic studies using *T. brucei*/TbNTR or *T. cruzi*/TcNTR generated a similar structure activity relationship (Hall, Wu *et al.* 2010, Hu, Wu *et al.* 2011). Interestingly, comparison of the enzymatic data indicates that TbNTR metabolises the most active compounds at a level 10-100 times greater than that of TcNTR and LmNTR. This may reflect different metabolic requirements of the intracellular parasites *T. cruzi* and *L. major* as compared to *T. brucei* which lives extracellularly in the bloodstream. The involvement of LmNTR in prodrug activation within the parasite itself was demonstrated using LH33 and LH34 as *L. major LmNTR*$^{+/-}$ heterozygote cells (Figures 6.1.3 and 6.1.4) are more resistant (1.6-fold and 3.3-fold respectively) to the NBPMs than wild type controls. Again this is in keeping with observations made using *T. brucei* (Hall, Wu *et al.* 2010).

The mechanism of NPBM activation by NTR as posited by Hall *et al.* (2010) may account for their anti-parasitic behaviour. By analogy with other type I NTRs, the LmNTR-mediated reduction of the electron-withdrawing nitro-group present on the benzyl ring is believed to generate an electron-donating hydroxylamine. This causes an electronic rearrangement along the NBPM backbone, ultimately promoting cleavage of a C-O bond found in the acyclic phosphoramide linker. Fragmentation of the compound then occurs resulting in release of a toxic mustard moiety (Hall, Wu *et al.* 2010, Wilkinson *et al.* 2011). The presence of a second electron-withdrawing group (*e.g.* a halogen) on the benzyl ring adjacent to the phosphoramide leaving group exacerbates this electronic "switch" by making the nitro group more prone to reduction. As a consequence, such NBPMs are more likely to become

"activated" and thus release the cytotoxic metabolites more readily into the cell. As this type of nitroreductase is absent from mammalian cells, it is the expression of type I NTR by the parasite itself that underlies the selectivity of such nitroaromatic prodrugs. When tested against differentiated THP-1 cells, none of the potent leishmanicidal NBPMs identified here displayed cytotoxicity, allowing us to calculate a selective toxicity (ST) value (the ratio between differentiated THP-1 IC_{50} values versus amastigote *L. major*). From this crude measurement, ST values of >143 and >476 were determined for LH34 and LH33 respectively, the 2 most effective anti-*L. major* compounds from this chemical series. Similarly, such compounds displayed significant potency against bloodstream-form *T. brucei*, with LH34 having an IC_{50} value of 8 nM (Hall, Wu *et al.* 2010). However, this study also noted that LH34 did display significant cytotoxicity towards undifferentiated THP-1 cells (LH34 yielded an IC_{50} value of 10 μM) although other reports indicate little effect on other cell lines such as V79 (Chinese hamster fibroblasts) and SKOV3 (human ovarian carcinoma) cells (Hall, Wu *et al.* 2010, Hu, Wu *et al.* 2011). Why these halogenated NBPMs are more effective against *T. brucei* as compared with *L. major* has yet to be fully determined but may reflect that these compounds are more readily metabolised by TbNTR as compared to its leishmanial (and *T. cruzi*) counterpart. However, it must be noted that other factors may also account for this difference. For example, the halogenated NBPMs may be able to access the cell or site where Lm/TbNTR is located more readily in *T. brucei* than in *L. major* (mitochondria in the case of *T. brucei*), or could reflect how readily toxic metabolites are released from this site. Why different mammalian lines display varying susceptibilities to the halogenated NBPMs is again unclear. One possibility may involve the expression profiles of potential nitroaromatic activators in the mammalian cell itself. Although not investigated here, certain FAD-containing mammalian enzymes such as NAD(P)H:quinone oxidoreductase 1 (also known as NQO1 or DT-diaphorase) and NAD(P)H:quinone

oxidoreductase 2 (NQO2), can catalyse the two electron reduction of quinone and nitroaromatic-based agents (having a preference for the former), analogous to the bacterial/protozoal type I NTRs (Ernster *et al.* 1958; Knox *et al.* 1988, Hajos *et al.* 1991; Jaiswal 1994; Miseviciene *et al.* 2006). Expression of such proteins is generally up-regulated under oxidative stress conditions and in cancer lines (Schor *et al.* 1977, Sharp *et al.* 2000). Therefore, the different susceptibilities displayed by the various mammalian lines (THP-1, V79 and SKOV3) where cytotoxicity has been determined may reflect differing expression levels of these potential activators.

The next set of compounds to be analysed using biochemical screening (purified recombinant ΔLmNTR) and anti-proliferative (against promastigote and amastigote *L. major* and differentiated THP-1 cells) assays were the ANBs, based on the CB1954. These compounds have shown promise as anticancer agents using a procedure known as GDEPT (Denny 2003). In this therapy, mammalian cells expressing the *E. coli* NfsB are more susceptible to CB1954 without any significant cytotoxic effects against the NTR-lacking controls (Helsby *et al.* 2004). Initially, we determined whether the ANBs could function as substrates for purified recombinant LmNTR (Figure 6.2.1). These biochemical screens established that out of the 13 compounds tested, only 3 (NH3-5) were not metabolised by the parasite enzyme. When these studies were extended to look at their anti-parasitic activities, 4 compounds including NH3-5, had no affect on *L. major* amastigote growth with screens against promastigotes demonstrating that a total of 6 compounds, including the 4 agents lacking anti-amastigote activity, having no affect on this insect stage (Table 6.2.1). For those compounds that did affect amastigote growth, some generated very low IC_{50} values in the nanomolar range: CB1954 and NH11 yielding IC_{50} values of 50 and 60 nM respectively. None of these leishmanicidal ANBs displayed cytotoxicity towards differentiated THP-1 cells yielding

encouraging ST values: >200 for CB1954 and >1667 for NH11 (Table 6.2.1). When a structure-activity analysis was performed, some interesting trends were observed. Based on the number and positioning of nitro-groups on the benzyl ring and presence/position of other substituent groups on this ring, the ANBs studied here can be broadly divided into three groups. The so-called group Ia compounds, as typified by CB1954, all contain two nitro groups located at the 2- and 4- positions on the benzyl ring relative to an aziridinyl ring plus a side chain at the 5- position (CB1954, NH1-2 and NH9-12). All of these functioned as substrates for LmNTR and had the highest potency towards the parasite. The second group, designated as group Ib, contain an alteration to the group Ia backbone, where the 4-nitro group relative to the aziridinyl ring had been replaced with either a hydrogen or SO_2Me substituent (NH3-5). These are the compounds that were inactive in enzyme and anti-parasitic assays. The final group, called group II, all resemble group Ia compounds but have the side chain at the 6-position (NH6-8). These did function as LmNTR substrates (Figure 6.2.1) but only one (NH6) displayed leishmanicidal properties. One possible reason for the lack of group Ib activity in both enzyme and parasite screens could be due to the structure of LmNTR's active site. Our data suggests that only the 4-nitro group can be reduced (group Ib compounds lack this) with reduction of the 2-nitro group possibly being hindered by the adjacent aziridinyl moiety. All other compounds tested (group Ia and II) contain the second reducible nitro group at the exposed 4- position. However, while TbNTR is also unable to use Ib ANBs as a substrate, it has been demonstrated that, like *E. coli* type I NTRs, either nitro-groups can be readily reduced, though not both on the same molecule (Knox *et al.* 1992, Bot, Hall *et al.* 2010). Taken together this implies that the configuration of electrons around the aromatic ring when featuring one or two nitro groups in relation to the 2- or 4-nitro moieties is the important factor.

Further screens using other nitroaromatic compound classes such as the non-aziridinyl nitrobenzamides and 5-nitrofurans were also performed. While a number of the nitrofuran compounds exhibited potential cytotoxicity problems against differentiated THP-1 cells, MNG10a and MNG5a were still able to give selective toxicity values of 234 and 153 respectively due to their potency against amastigote *L. major* (Table 6.3.2). To put these in context, nifurtimox currently represents one of the partner drugs in the NECT formulation used against African sleeping sickness, and exhibits a low ST of 36 when comparing the IC_{50} values against *T. brucei* and THP-1 cells (Hall, Wu *et al.* 2010). It is worth noting, however, that this previous study uses undifferentiated THP-1 cells, which could be misleadingly low for reasons detailed earlier in this section. A possible source for this toxic effect on mammalian cells could be activation by the aldehyde dehydrogenase 2 (ALDH2), which has been shown to mediate 5-nitrofuran toxicity in several species, including yeast, zebrafish and human cells (Zhou *et al.* 2012). When we evaluated the IC_{50} of nifurtimox towards differentiated THP-1 cells, no toxicity issues were observed at concentrations up to 100 μM. *In vitro*, the metabolites generated following reduction of nifurtimox by trypanosomal NTRs have been purified (Hall, Bot *et al.* 2011). These products, in particular an unsaturated open-chain nitrile derivative, are cytotoxic and are equally lethal to both trypanosomal and mammalian cells. This suggests that the downstream target(s) of this nitrile derivative is common to both host and parasite cells with proposals indicating that non-specific adduct formation with a range of biological molecules may occur (Hall et al 2011; Wilkinson et al 2011). Whether the leishmanicidal nitrofurans identified here function *via* an open-chain nitrile intermediate was not determined.

In the case of the non-aziridinyl nitrobenzamide compounds, all exhibited activity against *L. major* amastigotes with no toxicity displayed against mammalian cells. Many of these anti-

parasitic agents yielded IC_{50} values in the nano molar range – 7 out of the 9 compounds analysed (Table 6.3.1). As a result several members of this class of nitroaromatic have respectable ST values of >500. In contrast, only 2 of the compounds (IPK1 and 8) were active against the promastigote form. Why there is such a difference in the potency of the non-aziridinyl nitrobenzamide toward the amastigote and promastigote-forms is again unclear but reflects the distinct biological and biochemical properties exhibited between these two life cycle stages as exemplified by proteomic and genomic studies (Cohen-Freue *et al.* 2007; Pescher *et al.* 2011). Out of those compounds biochemically screened, only one (IPK2) was not metabolised by the parasite enzyme (Figure 6.3.1). Intriguingly this compound does have leishmanicidal properties, though presumably not by a type I NTR activation mechanism (not investigated further). For IPK1, LmNTR activity was manifested within the promastigote cell as *LmNTR*$^{+/-}$ heterozygote parasites were approximately 2-fold more resistant to this compound than wild type controls (Figure 6.3.3).

This project also set out to characterise and investigate the functional role played by a type I nitroreductase expressed by *L. major*. Following searches of the *L. major* genome for orthologues of *Tb* and *TcNTR*, the DNA sequence of *LmNTR* was elucidated. By aligning the predicted protein sequence with other NTRs of bacterial and kinetoplastid origins several conserved residues theorised to be important in substrate and flavin cofactor binding were identified (Figure 5.1.2) (Mejia, Hall *et al.* 2012; Hall *et al*., unpublished). Additionally, as previously noted with the trypanosomal sequences, LmNTR contains an (approximately) 80 residue amino-terminal extension as compared to its bacterial counterparts (Wilkinson, Taylor *et al.* 2008). When analysed further using protein prediction algorithms, this region has the potential to function as a mitochondrial targeting sequence. This was not investigated here (see Section 8) but has been studied in *T. brucei* where epitope tagging of the *TbNTR*

leader sequence fused to GFP demonstrated that this protein is located in the mitochondrion (Wilkinson, Taylor *et al.* 2008). As a general rule trypanosomatid mitochondrial leader sequences are small and correspond to the first (approximately) 10 amino acids of the protein. If this is the case for LmNTR (and its trypanosomal counterparts) then there are approximately 70 residues of the protein from the end of the putative targeting signal to the start of the catalytic domain whose function still remains unknown.

To confirm that LmNTR does actually function as a type I NTR, the catalytic region was expressed in *E. coli* as an amino terminal His_6-tagged fusion protein. This recombinant enzyme could be readily purified by one round of affinity chromatography on a Ni-NTA column, with LmNTR-containing elutions appearing yellow in colour. This is suggestive that LmNTR has a flavin co-factor. Using a fluorescence-based assay (Faeder and Siegel 1973), it was subsequently shown that recombinant LmNTR non-covalently bound FMN, a characteristic feature of all type I NTRs (Figure 5.3.1) (Zenno *et al.* 1996, Watanabe *et al.* 1998; Hall *et al.*, unpublished). As bacterial type I NTRs can use NAD(P)H, the electron donor preference of LmNTR was studied. This revealed that both NADH and NADPH could supply reducing equivalents to the parasite enzyme with NADH being the preferred option (Figure 5.3.2 C). This is in agreement with observations made using the trypanosomal enzymes (Wilkinson, Taylor *et al.* 2008; Hall *et al*., unpublished).

Once the optimal source for reducing equivalents had been established, the range of electron acceptor structures was analysed. Using spectrophotometric-based assays, it was shown that recombinant ΔLmNTR could metabolise a wide range of compounds including several classes of nitroaromatics (*e.g.* nitrofurans, nitroimidazoles, nitrobenzyls) and 1,4-benzoquinones (Table 5.3.1). By calculating the apparent V_{MAX} and k_{CAT}/K_M values, the

preferred substrate of LmNTR appear to be quinone-based, similar to observations made using trypanosomal NTRs (Hall *et al.*, unpublished). This finding could be indicative of the as yet unknown endogenous function of LmNTR. Trypanosomal NTRs are similar to NADH dehydrogenases, that metabolise NADH and in doing so transfer electrons over to ubiquinone to generate ubiquinol (Brandt 2006). It is interesting to note that the highest k_{CAT}/K_M value recorded here for LmNTR was for coenzyme Q1, a synthetic member of the ubiquinone family. In trypanosomes, NADH dehydrogenase activities have been recorded from several distinct proteins (Fang *et al.* 2001, Fang *et al.* 2002, Fang *et al.* 2003). It is indeed tempting to speculate that the kinetoplastid NTR is in fact the 33 kDa FMN-containing, mitochondrial NADH dehydrogenase isolated from *T. brucei* in 2002 (Fang and Beattie 2002). In the case of benznidazole, a detailed kinetic analysis was carried out to investigate how this electron acceptor and NADH interact with LmNTR (Figure 5.3.3). As with other oxidoreductase systems, this was shown to occur *via* a ping-pong mechanism. This interaction was shown to be subject to noncompetitive substrate inhibition indicating that the relative ratios of electron donor to acceptor are critical for the function of this enzyme. Again, this pattern is typical for many oxidoreductase and has been observed in studies using TbNTR and TcNTR (Hall and Wilkinson 2012).

To address the role and importance of LmNTR to *L. major*, attempts to alter expression levels of this enzyme were made by genetically manipulating the copy number of the corresponding gene within the parasite itself. In *T. brucei* and *T. cruzi*, such studies have categorically implicated the type I NTR in the activation of nitroaromatic prodrugs, with loss of *TbNTR* or *TcNTR* leading to resistance while cells expressing elevated levels of the oxidoreductase were more susceptible to these compounds (Wilkinson, Taylor *et al.* 2008). Additionally, this work also showed that the type I NTR activity was essential to the parasite forms present in the

mammalian host, indicating that inhibition of this enzyme can also be targeted for drug development.

When attempts were made to express LmNTR within *L. major* promastigotes using several different vector systems with either wild type or epitope-tagged versions of the gene, no stable recombinant parasites were selected. Consequently, it appears that introducing ectopic copies of *LmNTR* (and thus increasing LmNTR expression) has an adverse effect on the growth of *L. major* promastigotes. This is reminiscent of the situation in *T. cruzi* epimastigotes where TcNTR could not be readily over expressed (Wilkinson, unpublished). The only case where an ectopic copy of *TcNTR* has been expressed within *T. cruzi* employed a parasite line selected for benznidazole resistance, cells shown to be *TcNTR*$^{+/-}$ heterozygotes (Mejia, Hall *et al.* 2012). Furthermore, following electroporation of pTEX-TcNTR, Southern hybridisation demonstrated that these recombinant trypanosomes contained only a single copy of the episome. Interestingly, when investigating the effects of the antiparasitic compound fexinidazole, Wyllie *et al.* (2012) was able to over express LmNTR in *L. donovani* using a vector containing an amastigote-specific expression site. When this plasmid was electroporated into promastigote cells, LmNTR expression is repressed and then following differentiation into amastigotes forms up-regulated. These recombinant cells were then shown to be more susceptible to fexinidazole than controls, indicating successful over expression of the oxidoreductase. However, it is important to note that the *L. major* protein was being expressed in *L. donovani*, which may also account for the apparent contrast to our data.

When the converse approach was taken, aimed at reducing the copy number of *LmNTR* by targeted gene deletion, we could readily generate two heterozygote lines (Figure 5.4.11).

However, repeated attempts to a construct *LmNTR*$^{-/-}$ null mutant cells failed. Based on our previous findings relating to failed over expression of the nitroreductase within the insect stage, we did not introduce an ectopic copy of *LmNTR* into the heterozygote parasite line. Together this data strongly suggests that LmNTR is essential to *L. major* promastigote viability. Interestingly, repeated attempts to establish *LmNTR*$^{+/-}$ heterozygote parasites within cultured macrophages (differentiated THP-1 cells) and in a mouse model failed despite the appropriate controls working (Figures 5.4.15 and 5.4.16). This indicates that LmNTR activity is important, if not essential, to the intracellular amastigote form, even in an animal. Certain aspects of these observations bear some similarity and some differences to the situation noted with other trypanosomastids. For *T. cruzi*, both allelic copies of *TcNTR* could readily be deleted from epimastigote (insect-form) parasites to construct null mutant lines (Wilkinson, Taylor *et al.* 2008). However, these cells could not be cultured in mammalian cells and in a mouse model. This suggests that NTR activity is important, if not essential, to intracellular-form trypanosomes, as we observed with *L. major*. In the case of the bloodstream-form of *T. brucei*, *TbNTR* could not be deleted unless an ectopic copy was expressed, again implying that NTR activity is important to the viability of extracellular parasites also (Wilkinson, Taylor *et al.* 2008). This finding is backed up by a series of studies on *T. brucei* using RNAi (Wilkinson, Taylor *et al.* 2008, Hall, Wu *et al.* 2010, Sokolova, Wyllie *et al.* 2010, Baker, Alsford *et al.* 2011, Alsford, Eckert *et al.* 2012). In a number of these experiments, whole genome loss-of-function assays performed at different resolutions, using nifurtimox as selective agent, repeatedly identify TbNTR as the key factor that interacts with this 5-nitrofuran. These studies also implicated several enzymes involved in ubiquinone synthesis and FMN formation as minor factors whose reduction in function also leads to nifurtimox resistance, all of which appears to again demonstrate the importance of TbNTR in mediating nifurtimox activation.

The fact that this oxidoreductase preferentially metabolises quinone-based substrates and is located in the mitochondrion adds further weight to the argument that the biological function of NTRs in trypanosomatids involves the regeneration of NAD^+ in this particular organelle (Wilkinson *et al.* 2008; Wilkinson, Taylor *et al.* 2008, Hall, Wu *et al.* 2010, Sokolova, Wyllie *et al.* 2010, Baker, Alsford *et al.* 2011, Alsford, Eckert *et al.* 2012). The reducing equivalents are subsequently transferred to ubiquinone Q9 (Martin *et al.* 1979, Martin *et al.* 1979, Ranganathan *et al.* 1995) molecules to form the corresponding ubiquinol that then drives different types of redox cascades dependent upon the trypanosomatid parasite. For bloodstream-form *T. brucei*, ubiquinone Q9 is regenerated *via* a trypanosomal alternative oxidase and TbNTR may represent the "enigmatic" NADH:ubiquinone oxidoreductase activity previously noted (Clarkson *et al.* 1989, Bienen *et al.* 1993, Chaudhuri *et al.* 2006, Surve *et al.* 2012). The situation in intracellular trypanosomes or *Leishmania* is unclear as the gene encoding for the trypanosomal alternative oxidase is not present in the *T. cruzi* and *L. major* genomes, although they do possess a gene that has potential to encode for a mitochondrially targeted alternative oxidase-like protein (GenBank accession number EAN97989). However, this enzyme lacks certain key features that typify this class of oxidase and its activity has yet to be confirmed.

Taken together all of our data and the published material relating to the function of NTR in *L. major*, *T. cruzi* and *T. brucei* strongly indicate that NTR is essential to parasite forms that replicate in the mammalian host and therefore represents a genetically validated target, prime for exploitation for drug development. These data also make the potential for using nitroaromatic compounds as future antileishmanial prodrugs particularly encouraging. There is mounting data showing that by mutating/silencing/deleting a single allele of *Tb* or *TcNTR* in laboratory trypanosomal cell lines, cross resistance to nitroaromatic compounds occurs as

the prodrugs can no longer be activated (Wilkinson, Taylor *et al.* 2008, Hall, Wu *et al.* 2010, Sokolova, Wyllie *et al.* 2010, Baker, Alsford *et al.* 2011, Alsford, Eckert *et al.* 2012). This has also been reported in clinical *T. cruzi* cell lines (Mejia, Hall *et al.* 2012). In this case, it would then be feasible to then treat the patient using a different compound to inhibit the remaining levels of NTR, resulting in parasites unable to survive/infect. However, this approach would also require an extra, accompanying development cycle for an NTR inhibitor-based drug. However if, as is the case in *L. major*, by decreasing the quantity of the parasite NTR the cell is then already prevented from establishing a mammalian infection, the concern of resistance to nitroaromatic treatments (and the cost in developing NTR inhibitors in this case) is then defunct. This, together with the highly selective antileishmanial properties exhibited by some of the compounds reported here makes the nitroaromatics a highly promising class of compounds that warrant increased attention and research in the field of leishmaniasis treatment.

8. Future work

This project has described the production of a luciferase-expressing *L. major* reporter cell line, which was then used in a nitroaromatic compound screening program. Additionally, we have investigated the function of a type I NTR expressed by *L. major* (LmNTR), a potential activator of these prodrugs, *in vitro*, *in vivo* and within a BALB/c mouse infection model.

The LmRIX-Luc cell line developed here was used to screen 4 distinct classes of nitroaromatics. This identified several structures with significant potency against amastigote parasites and little/no cytotoxicity to cultured mammalian cells, as judged by their IC_{50} values. This screening program, initially validated on a small number of compounds, can be readily extended to include a greater selection of other chemical classes, nitroaromatic or otherwise. In fact, due to the effects of reducing *LmNTR* copy number on *L. major* infectivity reported here, a new direction would be to begin screening potential inhibitors of LmNTR as possible therapeutic agents. Theoretically, by inhibiting this enzyme *L. major* would be no longer able to proliferate in the mammalian life cycle stage. The system reported here has been optimised for use in a 96-well plate but could be further refined to other multi-well plate formats. Additionally, the *L. major* reporter cell line in conjunction with appropriate imaging facilities could be applied to follow mouse infections, aimed at monitoring variables such as infection rates and tissue tropisms, and observing how nitroaromatic treatments *in vivo* may affect these.

The nitroaromatic compounds that show promise in anti-parasitic screens can be further investigated for their mechanism of parasitic cell killing. It has been shown that nifurtimox and benznidazole, once reduced by TbNTR, produce cytotoxic metabolites (Hall, Bot *et al.* 2011; Hall and Wilkinson 2012). It would be interesting to see if LmNTR-mediated

metabolism of these compounds (including other members of the same compound class) resulted in the same cytotoxic products. Equally, whatever metabolites are produced, the next step would be to discern their downstream targets within the cell, be it protein, lipid or nucleic acid. For example, the effect on DNA could be readily monitored using the bacterial Ames test, TUNEL assay or immunofluorescence labelling, for example using histone γH2A antibodies. Such studies could incorporate the new leishmanicidal compounds identified here.

To further investigate the function of LmNTR within the parasite itself, similar approaches to that reported by Wilkinson, Taylor *et al.* 2008) could be used to elucidate the localisation of LmNTR within the *L. major* cell. This would involve expression of recombinant proteins consisting of the putative LmNTR leader sequence fused to an appropriate epitope tag (*e.g.* a fluorescent protein) in the parasite. Additionally, LmNTR mutants could be produced (for example, in arginine 96 or one of the other catalytic residues conserved across kinetoplastids) and the activity *in vitro* and *in vivo* monitored. It would be interesting to see if, after the difficulty in transfecting ectopic copies of wild type *LmNTR* into *L. major* promastigotes, it would be possible to produce cell lines capable of expressing an inactive version of the enzyme. Equally, is it possible to reintroduce (through episomal or integrative vectors described in Section 5.4.1) an ectopic copy of wild type (or 9E10-epitope tagged) of the oxidoreductase into $LmNTR^{+/-}$ heterozygote cell lines? If this is possible, does this reverse the resistance phenotype against nitroaromatic compounds shown in Figures 5.4.13, 6.1.3, 6.1.4 and 6.3.3? The above analysis would help in establishing what the biological role of LmNTR actually is within the parasite itself. Additionally, the findings in regard to the $LmNTR^{+/-}$ heterozygote cell line could also take another direction – that of vaccine development. The mouse in Figure 5.4.16 that was challenged with $LmNTR^{+/-}$ heterozygote parasites did not exhibit any external symptoms, however now has an immune system that has been exposed to

L. major. Consequently it could be possible that the mouse would now be resistant to subsequent *L. major* infection with wild type parasites.

Finally, with further optimisation of the expression and purification process that produces high levels of pure recombinant LmNTR, it would hopefully be possible to produce suitable crystals to elucidate the structure of LmNTR through X-ray diffraction. This would allow for even greater insight into the biochemistry of nitroaromatic prodrug activation. Together with the structure-activity relationships already determined in this project, the LmNTR crystal structure could allow rational drug design methods to maximise the leishmanicidal properties of nitroaromatic compounds while maintaining selectivity against mammalian host cells, as well as providing a valuable resource in developing inhibitors to target this essential activity itself.

9. Thesis summary

1. A novel luciferase-expression system, LmRIX-Luc, has been produced in *L. major*, which has no effect on the parasite's ability to grow as either promastigotes or amastigotes; or to differentiate into infective metacyclic cells.

2. Using the LmRIX-Luc cell line, a compound screening protocol has been developed and validated in the medically-relevant amastigote life cycle stage of *L. major*.

3. LmNTR is a type I NTR that contains noncovalently-bound FMN as cofactor and uses NADH as a preferred electron donor to reduce a wide variety of nitroaromatic and quinone-based compounds via a ping-pong kinetic mechanism.

4. It appears that introducing ectopic copies LmNTR into *L. major* promastigotes is deleterious, as is removing both LmNTR alleles. However, $LmNTR^{+/-}$ heterozygote promastigote cells can be readily produced with no apparent effects on promastigote growth or metacyclogenesis.

5. $LmNTR^{+/-}$ heterozygote *L. major* are cross resistant to several nitroaromatics, though are not able to proliferate as amastigotes *in vitro* or in a mouse infection model.

6. A series of nitroaromatics across 4 compound classes have been screened against recombinant ΔLmNTR protein, promastigote and amastigote *L. major*, as well as differentiated mammalian THP-1 macrohages.

7. A number of nitroaromatic compounds, particularly those shown in Figure 6.3.5 show great potential as very effective antileishmanials with high selective toxicities.

10. Appendix A: Primers

primer name	primer sequence (5' – 3')
LmrRNA-1	GAG ***GAGCTC CCTGCAGG*** TGATGAGGTGCCGCGTGTGTG
LmrRNA-2	AAA ***GGATCC*** TCCGTCGTTGCCCAGACACTT
LmrRNA-3	GGG ***GGTACC*** AAGGCAACAACGCAAGCGCAT
LmrRNA-4	AAA ***GGTACC GGCGCGCC*** CCACGTGCGTCCTCTAAAAGG
LmrRNA-5	CCC ***AGATCT*** TTTAATTATTTTTATCCCTTT
LmrRNA-6	GGG ***GGATCC*** GACAAAGCTTTTCTTGTGTGT
LmNTR-1	AAA ***GGATCC*** CTCGACGCCGTCGAGGCCGTCG
LmNTR-2	GGG ***AAGCTT*** CTAGAACTTGTTCCACCGCAC
LmNTR-4	AAA ***GGGTCC*** ATGCTTCGCCGCAGCCCCCG
LmNTR-18	GGG ***GTCGAC*** CTAGAACTTGTTCCACCGCAC
LmNTR-9	AAA ***GAGCTC CCGCGG*** CCGTCTCTGCCCTCTTTTCCT
LmNTR-10	GGG ***TCTAGA*** TGTAGTTTCTCTTGCTGCTCT
LmNTR-11	GGG ***GGGCCC*** TGTTGACTCAACACTAGAGAT
LmNTR-13	GAA ***GGTACC*** AGGGAAGGCAAGCACCAGGTG

Table 10.1: Oligonucleotides used in this study
Restriction enzyme recognition sites included for cloning purposes are highlighted in bold italics.

11. Appendix B: Compound structures

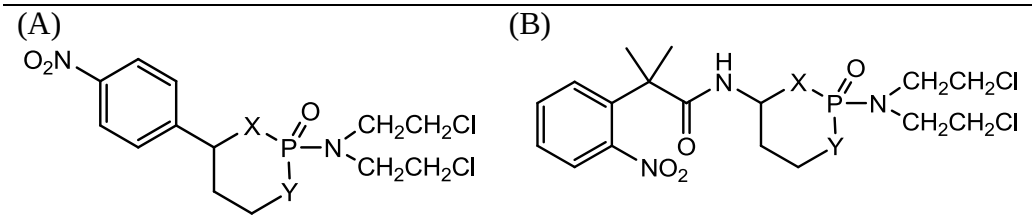

compound	structure	diastereomer
compounds based on (A)		
LH3	X=O; Y=NH	*cis*
LH4	X=O; Y=NH	*trans*
LH5	X=NH; Y=O	*cis*
LH6	X=NH; Y=O	*trans*
LH12	X=NH; Y=NH	*cis*
LH13	X=NH;Y=NH	*trans*
compounds based on (B)		
LH8	X=O; Y=NH	*cis*
LH9	X=O; Y=NH	*trans*

Table 11.1: Structures of cyclic nitrobenzylphophoramide mustards

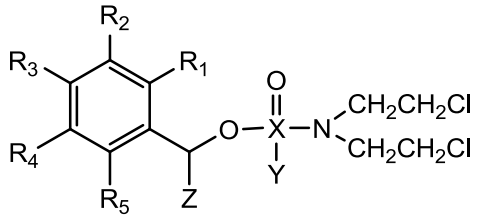

compound	structure
LH7	R_3=NO_2; X=P; Y=NH_2; R_1=R_2=R_4=R_5=Z=H
LH14	R_3=NO_2; X=P; Y=NH_2; Z=CH_3; R_1=R_2=R_4=R_5=H
LH15	R_5=NO_2; X=P; Y=NH_2; R_1=R_2=R_3=R_4=Z=H
LH16	R_4=NO_2; X=P; Y=NH_2; R_1=R_2=R_3=R_5=Z=H
LH17	R_3=NO_2; R_5=OCH_3; X=P; Y=NH_2; R_1=R_2=R_4=Z=H
LH18	R_3=NO_2; R_4=OCH_3; X=P; Y=NH_2; R_1=R_2=R_5=Z=H
LH19	R_3=NO_2; R_4=CH_3; X=P; Y=NH_2; R_1=R_2=R_5=Z=H
LH24	R_3=NO_2; X=P; Y=NH_2; Z=CH_3; R_1=R_2= R_4=R_5=H
LH27	R_3=NO_2; X–Y=C; R_1=R_2= R_4=R_5=Z=H
LH31	R_2=F; R_3=NO_2; X=P; Y=NH_2; R_1=R_4=R_5=Z=H
LH32	R_1=F; R_3=NO_2; X=P; Y=NH_2; R_2= R_4=R_5=Z=H
LH33	R_1=CF_3; R_3=NO_2; X=P; Y=NH_2; R_2= R_4=R_5=Z=H
LH34	R_1=Cl; R_3=NO_2; X=P; Y=NH_2; R_2= R_4=R_5=Z=H
LH37	R_1=R_5=F; X=P; R_3=NO_2; Y=NH_2; R_2= R_4=Z=H

Table 11.2: Structures of acyclic nitrobenzylphophoramide mustards

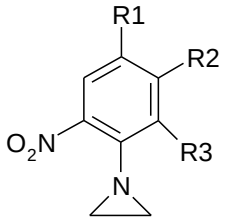

compound	group	structure
CB1954	Ia	R_1=NO_2; R_2=$CONH_2$; R_3=H
NH1	Ia	R_1=NO_2; R_2=$CONH(CH_2)_2$Nmorpholide; R_3=H
NH2	Ia	R_1=NO_2; R_2=$CONH(CH_2)_2CO_2Me$; R_3=H
NH3	Ib	R_1=H; R_2=$CONH_2$; R_3=H
NH4	Ib	R_1= SO_2Me; R_2= $CONH_2$; R_3=H
NH5	Ib	R_1=SO_2Me; R_2= $NHCH_2CH(OH)CH_2OH$; R_3=H
NH6	II	R_1= NO_2; R_2=H; R_3=$CONH_2$
NH7	II	R_1= NO_2; R_2=H; R_3=$NHCH_2CH(OH)CH_2OH$
NH8	II	R_1= NO_2; R_2=H; R_3=$CONH(CH_2)_2$Nmorpholide
NH9	Ia	R_1= NO_2; R_2=oxazole; R_3=H
NH10	Ia	R_1=NO_2; R_2=$CONHCH_2CHCH_2$; R_3=H
NH11	Ia	R_1=NO_2; R_2=$CON(CH_3)CH_3$; R_3=H
NH12	Ia	R_1=NO_2; R_2=R_3=H

Table 11.3: Structures of aziridinyl nitrobenzamides

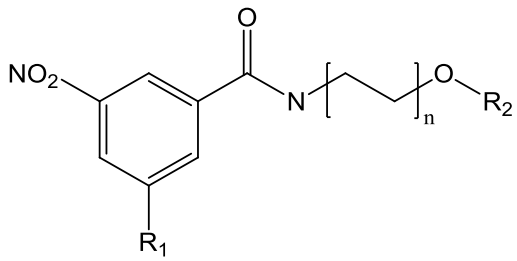

compound	structure
IPK1	R_1=NO_2; R_2= CH_2(3-chloro)benzyl; n=0
IPK2	R_1=NH_2 ; R_2=CH_2(3-chloro)benzyl; n=0
IPK3	R_1=NO_2; R_2= CH_2(2-fluoro)benzyl; n=0
IPK4	R_1=NO_2; R_2= (4-methoxy)benzyl; n=0
IPK5	R_1=NO_2; R_2= CH_2 benzyl; n=0
IPK6	R_1=NO_2; R_2= (4-methoxy)benzyl; n=3
IPK7	R_1=NO_2; R_2=methylbenzoate; n=2
IPK8	R_1=NO_2; R_2= CH_2(3-trifluoromethyl)benzyl; n=0
IPK9	R_1=NO; R_2= (4-methoxy)benzyl; n=2

Table 11.4: Structure of the non-azirinidyl nitrobenzamide compounds

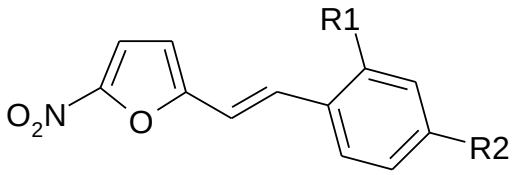

compound	structure
AD1	R_1=R_2=H
AD2	R_1=H; R_2=NO_2
AD3	R_1=H; R_2=OMe
MNG5a	R_1=H; R_2=CF_3
MNG7a	R_1=H; R_2=F
MNG10a	R_1=NO_2; R_2=H
MNG11a	R_1=F; R_2=H

Table 11.5: Structure of the 5-nitrofuran compounds

12. References

Abboud, P., V. Lemée, G. Gargala, P. Brasseur, J. J. Ballet, F. Borsa-Lebas, F. Caron and L. Favennec (2001). "Successful treatment of metronidazole- and albendazole-resistant *Giardiasis* with nitazoxanide in a patient with Acquired Immunodeficiency Syndrome." Clinical Infectious Diseases **32**(12): 1792-1794.

Aga, E., D. M. Katschinski, G. van Zandbergen, H. Laufs, B. Hansen, K. Muller, W. Solbach and T. Laskay (2002). "Inhibition of the spontaneous apoptosis of neutrophil granulocytes by the intracellular parasite *Leishmania major*." Journal of Immunology **169**(2): 898-905.

Aguirre, G., M. Boiani, E. Cabrera, H. Cerecetto, R. Di Maio, M. Gonzalez, A. Denicola, C. M. Sant'anna and E. J. Barreiro (2006). "New potent 5-nitrofuryl derivatives as inhibitors of *Trypanosoma cruzi* growth. 3D-QSAR (CoMFA) studies." Eur J Med Chem **41**(4): 457-466.

Aguirre, G., E. Cabrera, H. Cerecetto, R. Di Maio, M. Gonzalez, G. Seoane, A. Duffaut, A. Denicola, M. J. Gil and V. Martinez-Merino (2004). "Design, synthesis and biological evaluation of new potent 5-nitrofuryl derivatives as anti-*Trypanosoma cruzi* agents. Studies of trypanothione binding site of trypanothione reductase as target for rational design." Eur J Med Chem **39**(5): 421-431.

Alexander, J. and K. Vickerman (1975). "Fusion of host cell secondary lysosomes with the parasitophorous vacuoles of *Leishmania mexicana*-infected macrophages." J Protozool **22**(4): 502-508.

Alfonzo, J. D. and J. Lukes (2011). "Assembling Fe/S-clusters and modifying tRNAs: ancient co-factors meet ancient adaptors." Trends Parasitol **27**(6): 235-238.

Alfonzo, J. D., O. Thiemann and L. Simpson (1997). "The mechanism of U insertion/deletion RNA editing in kinetoplastid mitochondria." Nucleic Acids Res **25**(19): 3751-3759.

Alipour, E., S. Emami, A. Yahya-Meymandi, M. Nakhjiri, F. Johari, S. K. Ardestani, F. Poorrajab, M. Hosseini, A. Shafiee and A. Foroumadi (2011). "Synthesis and antileishmanial activity of 5-(5-nitroaryl)-2-substituted-thio-1,3,4-thiadiazoles." J Enzyme Inhib Med Chem **26**(1): 123-128.

Alsford, S., S. Eckert, N. Baker, L. Glover, A. Sanchez-Flores, K. F. Leung, D. J. Turner, M. C. Field, M. Berriman and D. Horn (2012). "High-throughput decoding of antitrypanosomal drug efficacy and resistance." Nature **482**: 232-236.

Alsford, S. and D. Horn (2008). "Single-locus targeting constructs for reliable regulated RNAi and transgene expression in *Trypanosoma brucei*." Mol Biochem Parasitol **161**(1): 76-79.

Alsford, S., T. Kawahara, L. Glover and D. Horn (2005). "Tagging a *T. brucei RRNA* locus improves stable transfection efficiency and circumvents inducible expression position effects." Mol Biochem Parasitol **144**(2): 142-148.

Alsford, S., D. J. Turner, S. O. Obado, A. Sanchez-Flores, L. Glover, M. Berriman, C. Hertz-Fowler and D. Horn (2011). "High-throughput phenotyping using parallel sequencing of RNA interference targets in the African trypanosome." Genome Res **21**(6): 915-924.

Alvar, J., C. Canavate, B. GutierrezSolar, M. Jimenez, F. Laguna, R. LopezVelez, R. Molina and J. Moreno (1997). "Leishmania and human immunodeficiency virus coinfection: The first 10 years." Clinical Microbiology Reviews **10**(2): 298-319.

Alvar, J., S. Yactayo and C. Bern (2006). "Leishmaniasis and poverty." Trends in Parasitology **22**(12): 552-557.

Anderson, V. R. and M. P. Curran (2007). "Nitazoxanide: A review of its use in the treatment of gastrointestinal infections." Drugs **67**(13): 1947-1967.

Andrade, H. M., S. M. Murta, A. Chapeaurouge, J. Perales, P. Nirde and A. J. Romanha (2008). "Proteomic analysis of *Trypanosoma cruzi* resistance to benznidazole." J Proteome Res **7**(6): 2357-2367.

Angermaier, L. and H. Simon (1983). "On nitroaryl reductase activities in several *Clostridia*." Hoppe Seylers Z Physiol Chem **364**(12): 1653-1663.

Arevalo, I., B. Ward, R. Miller, T.-C. Meng, E. Najar, E. Alvarez, G. Matlashewski and L.-C. Alejandro (2001). "Successful treatment of drug-resistant cutaneous leishmaniasis in humans by use of imiquimod, an immunomodulator." Clinical Infectious Diseases **33**(11): 1847-1851.

Arnold, H., F. Bourseaux and N. Brock (1958). "Chemotherapeutic action of a cyclic nitrogen mustard phosphamide ester (B 518-ASTA) in experimental tumours of the rat." Nature **181**(4613): 931.

Arya, S. C. and N. Agarwal (2009). "Nitrofurantoin: the return of an old friend in the wake of growing resistance." BJU Int **103**(7): 994-995.

Aytekin, S., M. Ertem, O. Yagdiran and N. Aytekin (2006). "Clinico-epidemiologic study of cutaneous leishmaniasis in Diyarbakir, Turkey." Dermatol Online J **12**(3): 14.

Badaro, R., T. C. Jones, E. M. Carvalho, D. Sampaio, S. G. Reed, A. Barral, R. Teixeira and W. D. Johnson, Jr. (1986). "New perspectives on a subclinical form of visceral leishmaniasis." J Infect Dis **154**(6): 1003-1011.

Badaro, R., T. C. Jones, R. Lorenco, B. J. Cerf, D. Sampaio, E. M. Carvalho, H. Rocha, R. Teixeira and W. D. Johnson (1986). "A prospective study of Visceral Leishmaniasis in an endemic area of Brazil." Journal of Infectious Diseases **154**(4): 639-649.

Baker, N., S. Alsford and D. Horn (2011). "Genome-wide RNAi screens in African trypanosomes identify the nifurtimox activator NTR and the eflornithine transporter AAT6." Mol Biochem Parasitol **176**(1): 55-57.

Balasegaram, M., S. Balasegaram, D. Malvy and P. Millet (2008). "Neglected diseases in the news: A content analysis of recent international media coverage focussing on leishmaniasis and trypanosomiasis." PLoS Negl Trop Dis **2**(5): e234.

Baliani, A., G. J. Bueno, M. L. Stewart, V. Yardley, R. Brun, M. P. Barrett and I. H. Gilbert (2005). "Design and synthesis of a series of melamine-based nitroheterocycles with activity against Trypanosomatid parasites." J Med Chem **48**(17): 5570-5579.

Baliani, A., V. Peal, L. Gros, R. Brun, M. Kaiser, M. P. Barrett and I. H. Gilbert (2009). "Novel functionalized melamine-based nitroheterocycles: synthesis and activity against trypanosomatid parasites." Org Biomol Chem **7**(6): 1154-1166.

Bang, S. Y., J. H. Kim, P. Y. Lee, K. H. Bae, J. S. Lee, P. S. Kim, H. Lee do, P. K. Myung, B. C. Park and S. G. Park (2012). "Confirmation of Frm2 as a novel nitroreductase in *Saccharomyces cerevisiae*." Biochem Biophys Res Commun **423**(4): 638-641.

Barrett, M. P., A. H. Fairlamb, B. Rousseau, G. Chauviere and J. Perie (2000). "Uptake of the nitroimidazole drug megazol by African trypanosomes." Biochem Pharmacol **59**(6): 615-620.

Basselin, M., M. A. Badet-Denisot and M. Robert-Gero (1998). "Modification of kinetoplast DNA minicircle composition in pentamidine-resistant *Leishmania*." Acta Trop **70**(1): 43-61.

Basselin, M., H. Denise, G. H. Coombs and M. P. Barrett (2002). "Resistance to pentamidine in *Leishmania mexicana* involves exclusion of the drug from the mitochondrion." Antimicrob Agents Chemother **46**(12): 3731-3738.

Bastien, P., C. Blaineau and M. Pages (1992). "Molecular karyotype analysis in *Leishmania*." Subcell Biochem **18**: 131-187.

Bates, D. W., L. Su, D. T. Yu, G. M. Chertow, D. L. Seger, D. R. Gomes, E. J. Dasbach and R. Platt (2001). "Mortality and costs of acute renal failure associated with amphotericin B therapy." Clin Infect Dis **32**(5): 686-693.

Bates, P. A. (2007). "Transmission of *Leishmania* metacyclic promastigotes by phlebotomine sand flies." Int J Parasitol **37**(10): 1097-1106.

Bates, P. A. (2008). "*Leishmania* sand fly interaction: progress and challenges." Curr Opin Microbiol **11**(4): 340-344.

Benne, R. (1993). "RNA editing in mitochondria of *Leishmania tarentolae* and *Crithidia fasciculata*." Semin Cell Biol **4**(4): 241-249.

Berman, J. (2005). "Miltefosine to treat leishmaniasis." Expert Opin Pharmacother **6**(8): 1381-1388.

Berman, J. D. (1997). "Human leishmaniasis: clinical, diagnostic, and chemotherapeutic developments in the last 10 years." Clin Infect Dis **24**(4): 684-703.

Berman, J. D. and L. S. Lee (1983). "Activity of oral drugs against *Leishmania tropica* in human macrophages *in vitro*." Am J Trop Med Hyg **32**(5): 947-951.

Berman, J. D. and D. J. Wyler (1980). "An *in vitro* model for investigation of chemotherapeutic agents in leishmaniasis." J Infect Dis **142**(1): 83-86.

Bern, C., J. Adler-Moore, J. Berenguer, M. Boelaert, M. den Boer, R. N. Davidson, C. Figueras, L. Gradoni, D. A. Kafetzis, K. Ritmeijer, E. Rosenthal, C. Royce, R. Russo, S. Sundar and J. Alvar (2006). "Liposomal amphotericin B for the treatment of visceral leishmaniasis." Clin Infect Dis **43**(7): 917-924.

Berriman, M., E. Ghedin, C. Hertz-Fowler, G. Blandin, H. Renauld, D. C. Bartholomeu, N. J. Lennard, E. Caler, N. E. Hamlin, B. Haas, U. Bohme, L. Hannick, M. A. Aslett, J. Shallom, L. Marcello, L. Hou, B. Wickstead, U. C. M. Alsmark, C. Arrowsmith, R. J. Atkin, A. J. Barron, F. Bringaud, K. Brooks, M. Carrington, I. Cherevach, T.-J. Chillingworth, C. Churcher, L. N. Clark, C. H. Corton, A. Cronin, R. M. Davies, J. Doggett, A. Djikeng, T. Feldblyum, M. C. Field, A. Fraser, I. Goodhead, Z. Hance, D. Harper, B. R. Harris, H. Hauser, J. Hostetler, A. Ivens, K. Jagels, D. Johnson, J. Johnson, K. Jones, A. X. Kerhornou, H. Koo, N. Larke, S. Landfear, C. Larkin, V. Leech, A. Line, A. Lord, A. MacLeod, P. J. Mooney, S. Moule, D. M. A. Martin, G. W. Morgan, K. Mungall, H. Norbertczak, D. Ormond, G. Pai, C. S. Peacock, J. Peterson, M. A. Quail, E. Rabbinowitsch, M.-A. Rajandream, C. Reitter, S. L. Salzberg, M. Sanders, S. Schobel, S. Sharp, M. Simmonds, A. J. Simpson, L. Tallon, C. M. R. Turner, A. Tait, A. R. Tivey, S. Van Aken, D. Walker, D. Wanless, S. Wang, B. White, O. White, S. Whitehead, J. Woodward, J. Wortman, M. D. Adams, T. M. Embley, K. Gull, E. Ullu, J. D. Barry, A. H. Fairlamb, F. Opperdoes, B. G. Barrell, J. E. Donelson, N. Hall, C. M. Fraser, S. E. Melville and N. M. El-Sayed (2005). "The Genome of the African Trypanosome *Trypanosoma brucei*." Science **309**(5733): 416-422.

Bhattacharya, S. K., P. K. Sinha, S. Sundar, C. P. Thakur, T. K. Jha, K. Pandey, V. R. Das, N. Kumar, C. Lal, N. Verma, V. P. Singh, A. Ranjan, R. B. Verma, G. Anders, H. Sindermann and N. K. Ganguly (2007). "Phase 4 trial of miltefosine for the treatment of Indian visceral leishmaniasis." J Infect Dis **196**(4): 591-598.

Bienen, E. J., R. K. Maturi, G. Pollakis and A. B. Clarkson, Jr. (1993). "Non-cytochrome mediated mitochondrial ATP production in bloodstream form *Trypanosoma brucei brucei*." Eur J Biochem **216**(1): 75-80.

Blum, B., N. Bakalara and L. Simpson (1990). "A model for RNA editing in kinetoplastid mitochondria: RNA molecules transcribed from maxicircle DNA provide the edited information." Cell **60**(2): 189-198.

Blum, J., P. Desjeux, E. Schwartz, B. Beck and C. Hatz (2004). "Treatment of cutaneous leishmaniasis among travellers." J Antimicrob Chemother **53**(2): 158-166.

Blumenstiel, K., R. Schöneck, V. Yardley, S. L. Croft and R. L. Krauth-Siegel (1999). "Nitrofuran drugs as common subversive substrates of *Trypanosoma cruzi* lipoamide dehydrogenase and trypanothione reductase." Biochem Pharmacol **58**(11): 1791-1799.

Bock, M., R. Gonnert and A. Haberkorn (1969). "Studies with Bay 2502 on animals." Bol Chil Parasitol **24**(1): 13-19.

Bolhassani, A., T. Taheri, Y. Taslimi, S. Zamanilui, F. Zahedifard, N. Seyed, F. Torkashvand, B. Vaziri and S. Rafati (2011). "Fluorescent *Leishmania* species: development of stable GFP expression and its application for *in vitro* and *in vivo* studies." Exp Parasitol **127**(3): 637-645.

Borst, P. (1989). "Peroxisome biogenesis revisited." Biochim Biophys Acta **1008**(1): 1-13.

Bot, C., B. S. Hall, N. Bashir, M. C. Taylor, N. A. Helsby and S. R. Wilkinson (2010). "Trypanocidal Activity of Aziridinyl Nitrobenzamide Prodrugs." Antimicrob. Agents Chemother. **54**(10): 4246-4252.

Bouteille, B., A. Marie-Daragon, G. Chauviere, C. de Albuquerque, B. Enanga, M. L. Darde, J. M. Vallat, J. Perie and M. Dumas (1995). "Effect of megazol on *Trypanosoma brucei brucei* acute and subacute infections in Swiss mice." Acta Trop **60**(2): 73-80.

Boveris, A., H. Sies, E. E. Martino, R. Docampo, J. F. Turrens and A. O. Stoppani (1980). "Deficient metabolic utilization of hydrogen peroxide in *Trypanosoma cruzi*." Biochem J **188**(3): 643-648.

Brandt, U. (2006). "Energy converting NADH:quinone oxidoreductase (complex I)." Annu Rev Biochem **75**: 69-92.

Buates, S. and G. Matlashewski (1999). "Treatment of experimental leishmaniasis with the immunomodulators imiquimod and S-28463: Efficacy and mode of action." Journal of Infectious Diseases **179**(6): 1485-1494.

Buckner, F. S. and A. J. Wilson (2005). "Colorimetric assay for screening compounds against *Leishmania* amastigotes grown in macrophages." Am J Trop Med Hyg **72**(5): 600-605.

Burchmore, R. J., D. Rodriguez-Contreras, K. McBride, P. Merkel, M. P. Barrett, G. Modi, D. Sacks and S. M. Landfear (2003). "Genetic characterization of glucose transporter function in *Leishmania mexicana*." Proc Natl Acad Sci U S A **100**(7): 3901-3906.

Campos, F. M., D. B. Liarte, R. A. Mortara, A. J. Romanha and S. M. Murta (2009). "Characterization of a gene encoding alcohol dehydrogenase in benznidazole-susceptible and -resistant populations of *Trypanosoma cruzi*." Acta Trop **111**(1): 56-63.

Cancado, J. R., U. D. Marra and Z. Brener (1964). "Clinical therapeutic trial of 5-nitro-2-furaldehyde-semicarbazone (nitrofurazone) in the chronic form of chagas' disease." Rev Inst Med Trop Sao Paulo **6**: 12-16.

Carli, M., E. Passone, G. Perilongo and G. Bisogno (2003). "Ifosfamide in pediatric solid tumors." Oncology **65 Suppl 2**: 99-104.

Carvalho, A. S., R. F. Menna-Barreto, N. C. Romeiro, S. L. de Castro and N. Boechat (2007). "Design, synthesis and activity against *Trypanosoma cruzi* of azaheterocyclic analogs of megazol." Med Chem **3**(5): 460-465.

Carvalho, S. A., E. F. da Silva, R. M. Santa-Rita, S. L. de Castro and C. A. Fraga (2004). "Synthesis and antitrypanosomal profile of new functionalized 1,3,4-thiadiazole-2-arylhydrazone derivatives, designed as non-mutagenic megazol analogues." Bioorg Med Chem Lett **14**(24): 5967-5970.

Carvalho, S. A., F. A. Lopes, K. Salomao, N. C. Romeiro, S. M. Wardell, S. L. de Castro, E. F. da Silva and C. A. Fraga (2008). "Studies toward the structural optimization of new brazilizone-related trypanocidal 1,3,4-thiadiazole-2-arylhydrazone derivatives." Bioorg Med Chem **16**(1): 413-421.

Castro, J. A. and E. G. Diaz de Toranzo (1988). "Toxic effects of nifurtimox and benznidazole, two drugs used against American trypanosomiasis (Chagas' disease)." Biomed Environ Sci **1**(1): 19-33.

Cenas, N., S. Prast, H. Nivinskas, J. Sarlauskas and E. S. Arner (2006). "Interactions of nitroaromatic compounds with the mammalian selenoprotein thioredoxin reductase and the relation to induction of apoptosis in human cancer cells." J Biol Chem **281**(9): 5593-5603.

Cerecetto, H., R. Di Maio, M. Gonzalez, M. Risso, G. Sagrera, G. Seoane, A. Denicola, G. Peluffo, C. Quijano, A. O. Stoppani, M. Paulino, C. Olea-Azar and M. A. Basombrio (2000). "Synthesis and antitrypanosomal evaluation of E-isomers of 5-nitro-2-furaldehyde and 5-nitrothiophene-2-carboxaldehyde semicarbazone derivatives. structure-activity relationships." Eur J Med Chem **35**(3): 343-350.

Cerecetto, H., R. Di Maio, G. Ibarruri, G. Seoane, A. Denicola, G. Peluffo, C. Quijano and M. Paulino (1998). "Synthesis and anti-trypanosomal activity of novel 5-nitro-2-furaldehyde and 5-nitrothiophene-2-carboxaldehyde semicarbazone derivatives." Farmaco **53**(2): 89-94.

Chan, M. M., J. C. Bulinski, K. P. Chang and D. Fong (2003). "A microplate assay for *Leishmania amazonensis* promastigotes expressing multimeric green fluorescent protein." Parasitol Res **89**(4): 266-271.

Charest, H. and G. Matlashewski (1994). "Developmental gene expression in *Leishmania donovani*: differential cloning and analysis of an amastigote-stage-specific gene." Mol Cell Biol **14**(5): 2975-2984.

Chaudhuri, G. and K.-P. Chang (1988). "Acid protease activity of a major surface membrane glycoprotein (gp63) from *Leishmania mexicana* promastigotes." Mol Biochem Parasitol **27**(1): 43-52.

Chaudhuri, M., R. D. Ott and G. C. Hill (2006). "Trypanosome alternative oxidase: from molecule to function." Trends Parasitol **22**(10): 484-491.

Chauviere, G., B. Bouteille, B. Enanga, C. de Albuquerque, S. L. Croft, M. Dumas and J. Perie (2003). "Synthesis and biological activity of nitro heterocycles analogous to megazol, a trypanocidal lead." J Med Chem **46**(3): 427-440.

Checchi, F., P. Piola, H. Ayikoru, F. Thomas, D. Legros and G. Priotto (2007). "Nifurtimox plus Eflornithine for Late-Stage Sleeping Sickness in Uganda: A Case Series." PLoS Negl Trop Dis **1**(2): e64.

Chen, I. and A. Y. Ting (2005). "Site-specific labeling of proteins with small molecules in live cells." Curr Opin Biotechnol **16**(1): 35-40.

Chen, Y. and L. Hu (2009). "Design of anticancer prodrugs for reductive activation." Med Res Rev **29**(1): 29-64.

Christophe, T., M. Jackson, H. K. Jeon, D. Fenistein, M. Contreras-Dominguez, J. Kim, A. Genovesio, J. P. Carralot, F. Ewann, E. H. Kim, S. Y. Lee, S. Kang, M. J. Seo, E. J. Park, H. Skovierova, H. Pham, G. Riccardi, J. Y. Nam, L. Marsollier, M. Kempf, M. L. Joly-Guillou, T. Oh, W. K. Shin, Z. No, U. Nehrbass, R. Brosch, S. T. Cole and P. Brodin (2009). "High content screening identifies decaprenyl-phosphoribose 2' epimerase as a target for intracellular antimycobacterial inhibitors." PLoS Pathog **5**(10): e1000645.

Chung-Faye, G., D. Palmer, D. Anderson, J. Clark, M. Downes, J. Baddeley, S. Hussain, P. I. Murray, P. Searle, L. Seymour, P. A. Harris, D. Ferry and D. J. Kerr (2001). "Virus-directed, Enzyme Prodrug Therapy with Nitroimidazole Reductase." Clinical Cancer Research **7**(9): 2662-2668.

Claes, F., S. K. Vodnala, N. van Reet, N. Boucher, H. Lunden-Miguel, T. Baltz, B. M. Goddeeris, P. Buscher and M. E. Rottenberg (2009). "Bioluminescent imaging of Trypanosoma brucei shows preferential testis dissemination which may hamper drug efficacy in sleeping sickness." PLoS Negl Trop Dis **3**(7): e486.

Clarkson, A. B., Jr., E. J. Bienen, G. Pollakis and R. W. Grady (1989). "Respiration of bloodstream forms of the parasite *Trypanosoma brucei brucei* is dependent on a plant-like alternative oxidase." J Biol Chem **264**(30): 17770-17776.

Clayton, C. and M. Shapira (2007). "Post-transcriptional regulation of gene expression in trypanosomes and leishmanias." Molecular and Biochemical Parasitology **156**(2): 93-101.

Clayton, C. E. (1999). "Genetic manipulation of Kinetoplastida." Parasitol Today **15**(9): 372-378.

Clayton, C. E. (2002). "Life without transcriptional control? From fly to man and back again." EMBO J **21**(8): 1881-1888.

Coelho, A. C., N. Messier, M. Ouellette and P. C. Cotrim (2007). "Role of the ABC transporter PRP1 (ABCC7) in pentamidine resistance in *Leishmania* amastigotes." Antimicrob Agents Chemother **51**(8): 3030-3032.

Cohen-Freue, G., T. R. Holzer, J. D. Forney and W. R. McMaster (2007). "Global gene expression in *Leishmania*." Int J Parasitol **37**(10): 1077-1086.

Cohen, B. E. (2010). "Amphotericin B membrane action: role for two types of ion channels in eliciting cell survival and lethal effects." J Membr Biol **238**(1-3): 1-20.

Colvin, O. M. (1999). "An overview of cyclophosphamide development and clinical applications." Curr Pharm Des **5**(8): 555-560.

Coombs, G. H., L. Tetley, V. A. Moss and K. Vickerman (1986). "Three dimensional structure of the *Leishmania* amastigote as revealed by computer-aided reconstruction from serial sections." Parasitology **92 (Pt 1)**: 13-23.

Corbett, M. D. and B. R. Corbett (1995). Bioorganic chemistry of the arylhydroxylamine and nitrosoarene functional groups. Biodegradation of Nitroaromatic Compounds. J. C. Spain. New York, Plenum Press**:** 151-182.

Correia, D., V. O. Macedo, E. M. Carvalho, A. Barral, A. V. Magalhaes, M. V. de Abreu, M. L. Orge and P. Marsden (1996). "Comparative study of meglumine antimoniate, pentamidine isethionate and aminosidine

sulfate in the treatment of primary skin lesions caused by *Leishmania* (*Viannia*) *braziliensis*." Rev Soc Bras Med Trop **29**(5): 447-453.

Cory, M., R. R. Tidwell and T. A. Fairley (1992). "Structure and DNA binding activity of analogues of 1,5-bis(4-amidinophenoxy)pentane (pentamidine)." J Med Chem **35**(3): 431-438.

Coustou, V., F. Guegan, N. Plazolles and T. Baltz (2012). "Complete *in vitro* life cycle of *Trypanosoma congolense*: development of genetic tools." PLoS Negl Trop Dis **4**(3): e618.

Cox, F. E. G. (2002). "History of Human Parasitology." Clinical Microbiology Reviews **15**(4): 595-612.

Croft, S. L. and G. H. Coombs (2003). "Leishmaniasis--current chemotherapy and recent advances in the search for novel drugs." Trends Parasitol **19**(11): 502-508.

Croft, S. L., R. A. Neal, W. Pendergast and J. H. Chan (1987). "The activity of alkyl phosphorylcholines and related derivatives against *Leishmania donovani*." Biochem Pharmacol **36**(16): 2633-2636.

Croft, S. L. and P. Olliaro (2012). "Leishmaniasis chemotherapy—challenges and opportunities." Clinical Microbiology and Infection **17**(10): 1478-1483.

Croft, S. L., S. Sundar and A. H. Fairlamb (2006). "Drug resistance in leishmaniasis." Clin Microbiol Rev **19**(1): 111-126.

Cruz, A. and S. M. Beverley (1990). "Gene replacement in parasitic protozoa." Nature **348**(6297): 171-173.

Cruz, A., C. M. Coburn and S. M. Beverley (1991). "Double targeted gene replacement for creating null mutants." Proc Natl Acad Sci U S A **88**(16): 7170-7174.

Cruz, A. K., R. Titus and S. M. Beverley (1993). "Plasticity in chromosome number and testing of essential genes in *Leishmania* by targeting." Proc Natl Acad Sci U S A **90**(4): 1599-1603.

Cruz, I., M. A. Morales, I. Noguer, A. Rodriguez and J. Alvar (2002). "*Leishmania* in discarded syringes from intravenous drug users." The Lancet **359**(9312): 1124-1125.

da Silva, R. and D. L. Sacks (1987). "Metacyclogenesis is a major determinant of *Leishmania* promastigote virulence and attenuation." Infect. Immun. **55**(11): 2802-2806.

Davidson, R. N. (1998). "Practical guide for the treatment of leishmaniasis." Drugs **56**(6): 1009-1018.

Davidson, R. N., M. den Boer and K. Ritmeijer (2009). "Paromomycin." Trans R Soc Trop Med Hyg **103**(7): 653-660.

Davies, C. R., P. Kaye, S. L. Croft and S. Sundar (2003). "Leishmaniasis: new approaches to disease control." BMJ **326**(7385): 377-382.

De Alencar, J. E. (1958). "Visceral Leishmaniasis in Brazil." Rev Assoc Med Bras **4**(3): 222-236.

De Carneri, I. (1969). "Antiprotozoan activity of nitroimidazoles." Arzneimittelforschung **19**(3): 382-386.

de La Llave, E., H. Lecoeur, A. Besse, G. Milon, E. Prina and T. Lang (2011). "A combined luciferase imaging and reverse transcription polymerase chain reaction assay for the study of *Leishmania* amastigote burden and correlated mouse tissue transcript fluctuations." Cell Microbiol **13**(1): 81-91.

De Muylder, G., K. K. Ang, S. Chen, M. R. Arkin, J. C. Engel and J. H. McKerrow (2011). "A screen against *Leishmania* intracellular amastigotes: comparison to a promastigote screen and identification of a host cell-specific hit." PLoS Negl Trop Dis **5**(7): e1253.

de Souza, W., M. Attias and J. C. Rodrigues (2009). "Particularities of mitochondrial structure in parasitic protists (Apicomplexa and Kinetoplastida)." Int J Biochem Cell Biol **41**(10): 2069-2080.

Denny, W. A. (2003). "Prodrugs for Gene-Directed Enzyme-Prodrug Therapy (Suicide Gene Therapy)." J Biomed Biotechnol **2003**(1): 48-70.

Denton, H., J. C. McGregor and G. H. Coombs (2004). "Reduction of anti-leishmanial pentavalent antimonial drugs by a parasite-specific thiol-dependent reductase, TDR1." Biochem J **381**(Pt 2): 405-412.

Desjeux, P. (2004). "Leishmaniasis: current situation and new perspectives." Comparative Immunology Microbiology and Infectious Diseases **27**(5): 305-318.

Desjeux, P. and J. Alvar (2003). "*Leishmania*/HIV co-infections: epidemiology in Europe." Ann Trop Med Parasitol **97 Suppl 1**: 3-15.

Dey, S., M. Ouellette, J. Lightbody, B. Papadopoulou and B. P. Rosen (1996). "An ATP-dependent As(III)-glutathione transport system in membrane vesicles of *Leishmania tarentolae*." Proc Natl Acad Sci U S A **93**(5): 2192-2197.

Diacon, A. H., R. Dawson, J. du Bois, K. Narunsky, A. Venter, P. R. Donald, C. van Niekerk, N. Erondu, A. M. Ginsberg, P. Becker and M. K. Spigelman (2012). "Phase II dose-ranging trial of the early bactericidal activity of PA-824." Antimicrob Agents Chemother **56**(6): 3027-3031.

Diacon, A. H., R. Dawson, F. von Groote-Bidlingmaier, G. Symons, A. Venter, P. R. Donald, C. van Niekerk, D. Everitt, H. Winter, P. Becker, C. M. Mendel and M. K. Spigelman (2012). "14-day bactericidal activity of PA-824, bedaquiline, pyrazinamide, and moxifloxacin combinations: a randomised trial." Lancet **380**(9846): 986-993.

Docampo, R., R. P. Mason, C. Mottley and R. P. Muniz (1981). "Generation of free radicals induced by nifurtimox in mammalian tissues." J Biol Chem **256**(21): 10930-10933.

Docampo, R. and A. O. Stoppani (1979). "Generation of superoxide anion and hydrogen peroxide induced by nifurtimox in *Trypanosoma cruzi*." Arch Biochem Biophys **197**(1): 317-321.

Dodd, M. and W. Stillman (1944). "The *in vitro* bacteriostatic action of some simple furan derivatives." J Pharm Exp Ther **82**(11).

Donovan, C. (1903). "Memoranda: On the possibility of the occurrence of trypanosomiasis in India." British Medical Journal: 79.

Dufernez, F., C. Yernaux, D. Gerbod, C. Noel, M. Chauvenet, R. Wintjens, V. P. Edgcomb, M. Capron, F. R. Opperdoes and E. Viscogliosi (2006). "The presence of four iron-containing superoxide dismutase isozymes in trypanosomatidae: characterization, subcellular localization, and phylogenetic origin in *Trypanosoma brucei*." Free Radic Biol Med **40**(2): 210-225.

El-Sayed, N. M., P. J. Myler, D. C. Bartholomeu, D. Nilsson, G. Aggarwal, A.-N. Tran, E. Ghedin, E. A. Worthey, A. L. Delcher, G. Blandin, S. J. Westenberger, E. Caler, G. C. Cerqueira, C. Branche, B. Haas, A. Anupama, E. Arner, L. Aslund, P. Attipoe, E. Bontempi, F. Bringaud, P. Burton, E. Cadag, D. A. Campbell, M. Carrington, J. Crabtree, H. Darban, J. F. da Silveira, P. de Jong, K. Edwards, P. T. Englund, G. Fazelina, T.

Feldblyum, M. Ferella, A. C. Frasch, K. Gull, D. Horn, L. Hou, Y. Huang, E. Kindlund, M. Klingbeil, S. Kluge, H. Koo, D. Lacerda, M. J. Levin, H. Lorenzi, T. Louie, C. R. Machado, R. McCulloch, A. McKenna, Y. Mizuno, J. C. Mottram, S. Nelson, S. Ochaya, K. Osoegawa, G. Pai, M. Parsons, M. Pentony, U. Pettersson, M. Pop, J. L. Ramirez, J. Rinta, L. Robertson, S. L. Salzberg, D. O. Sanchez, A. Seyler, R. Sharma, J. Shetty, A. J. Simpson, E. Sisk, M. T. Tammi, R. Tarleton, S. Teixeira, S. Van Aken, C. Vogt, P. N. Ward, B. Wickstead, J. Wortman, O. White, C. M. Fraser, K. D. Stuart and B. Andersson (2005). "The Genome Sequence of *Trypanosoma cruzi*, Etiologic Agent of Chagas Disease." Science **309**(5733): 409-415.

El-Sayed, N. M., P. J. Myler, G. Blandin, M. Berriman, J. Crabtree, G. Aggarwal, E. Caler, H. Renauld, E. A. Worthey, C. Hertz-Fowler, E. Ghedin, C. Peacock, D. C. Bartholomeu, B. J. Haas, A.-N. Tran, J. R. Wortman, U. C. M. Alsmark, S. Angiuoli, A. Anupama, J. Badger, F. Bringaud, E. Cadag, J. M. Carlton, G. C. Cerqueira, T. Creasy, A. L. Delcher, A. Djikeng, T. M. Embley, C. Hauser, A. C. Ivens, S. K. Kummerfeld, J. B. Pereira-Leal, D. Nilsson, J. Peterson, S. L. Salzberg, J. Shallom, J. C. Silva, J. Sundaram, S. Westenberger, O. White, S. E. Melville, J. E. Donelson, B. Andersson, K. D. Stuart and N. Hall (2005). "Comparative Genomics of Trypanosomatid Parasitic Protozoa." Science **309**(5733): 404-409.

Enanga, B., M. R. Ariyanayagam, M. L. Stewart and M. P. Barrett (2003). "Activity of megazol, a trypanocidal nitroimidazole, is associated with DNA damage." Antimicrob Agents Chemother **47**(10): 3368-3370.

Engel, J. C., K. K. Ang, S. Chen, M. R. Arkin, J. H. McKerrow and P. S. Doyle (2010). "Image-based high-throughput drug screening targeting the intracellular stage of *Trypanosoma cruzi*, the agent of Chagas' disease." Antimicrob Agents Chemother **54**(8): 3326-3334.

Eriksson, U., B. Seifert and A. Schaffner (2001). "Comparison of effects of amphotericin B deoxycholate infused over 4 or 24 hours: randomised controlled trial." BMJ **322**(7286): 579-582.

Ernster, L. and F. Navazio (1958). "Soluble diaphorase in animal tissues." Acta Chem Scand **12**: 595-602.

Evens, F., K. Niemegeers and A. Packchanian (1957). "Nitrofurazone therapy of *Trypanosoma gambiense* sleeping sickness in man." Am J Trop Med Hyg **6**(4): 665-678.

Fadok, V. A., D. L. Bratton, A. Konowal, P. W. Freed, J. Y. Westcott and P. M. Henson (1998). "Macrophages that have ingested apoptotic cells *in vitro* inhibit proinflammatory cytokine production through

autocrine/paracrine mechanisms involving TGF-beta, PGE2, and PAF." Journal of Clinical Investigation **101**(4): 890-898.

Faeder, E. J. and L. M. Siegel (1973). "A rapid micromethod for determination of FMN and FAD in mixtures." Analytical Biochemistry **53**(1): 332-336.

Fairlamb, A. H., P. Blackburn, P. Ulrich, B. T. Chait and A. Cerami (1985). "Trypanothione: a novel bis(glutathionyl)spermidine cofactor for glutathione reductase in trypanosomatids." Science **227**(4693): 1485-1487.

Fairlamb, A. H. and I. B. Bowman (1980). "Uptake of the trypanocidal drug suramin by bloodstream forms of *Trypanosoma brucei* and its effect on respiration and growth rate *in vivo*." Mol Biochem Parasitol **1**(6): 315-333.

Fairlamb, A. H. and A. Cerami (1992). "Metabolism and functions of trypanothione in the Kinetoplastida." Annu Rev Microbiol **46**: 695-729.

Fang, J. and D. S. Beattie (2002). "Novel FMN-Containing Rotenone-Insensitive NADH Dehydrogenase from *Trypanosoma brucei* Mitochondria: Isolation and Characterizationâ€ " Biochemistry **41**(9): 3065-3072.

Fang, J. and D. S. Beattie (2003). "Identification of a gene encoding a 54 kDa alternative NADH dehydrogenase in *Trypanosoma brucei*." Molecular and Biochemical Parasitology **127**(1): 73-77.

Fang, J., Y. Wang and D. S. Beattie (2001). "Isolation and characterization of complex I, rotenone-sensitive NADH:ubiquinone oxidoreductase, from the procyclic forms of *Trypanosoma brucei*." European Journal of Biochemistry **268**(10): 3075-3082.

Fernandez, M. M., E. L. Malchiodi and I. D. Algranati (2011). "Differential effects of paromomycin on ribosomes of *Leishmania mexicana* and mammalian cells." Antimicrob Agents Chemother **55**(1): 86-93.

Figarella, K., N. L. Uzcategui, Y. Zhou, A. LeFurgey, M. Ouellette, H. Bhattacharjee and R. Mukhopadhyay (2007). "Biochemical characterization of *Leishmania major* aquaglyceroporin LmAQP1: possible role in volume regulation and osmotaxis." Mol Microbiol **65**(4): 1006-1017.

Filardi, L. S. and Z. Brener (1982). "A nitroimidazole-thiadiazole derivative with curative action in experimental *Trypanosoma cruzi* infections." Ann Trop Med Parasitol **76**(3): 293-297.

Firooz, A., A. Khamesipour, M. H. Ghoorchi, M. Nassiri-Kashani, S. E. Eskandari, A. Khatami, B. Hooshmand, F. Gorouhi, M. Rashighi-Firoozabadi and Y. Dowlati (2006). "Imiquimod in combination with meglumine antimoniate for cutaneous leishmaniasis: A randomized assessor-blind controlled trial." Archives of Dermatology **142**(12): 1575-1579.

Fleit, H. B. and C. D. Kobasiuk (1991). "The human monocyte-like cell line THP-1 expresses Fc gamma RI and Fc gamma RII." J Leukoc Biol **49**(6): 556-565.

Flohe, L., H. J. Hecht and P. Steinert (1999). "Glutathione and trypanothione in parasitic hydroperoxide metabolism." Free Radic Biol Med **27**(9-10): 966-984.

Freedman, D. J. and S. M. Beverley (1993). "Two more independent selectable markers for stable transfection of *Leishmania*." Mol Biochem Parasitol **62**(1): 37-44.

Fritze, C. E. and T. R. Anderson (2000). "Epitope tagging: general method for tracking recombinant proteins." Methods Enzymol **327**: 3-16.

Gavin, J. J., F. F. Ebetino, R. Freedman and W. E. Waterbury (1966). "The aerobic degradation of 1-(5-nitrofurfurylideneamino)-2-imidazolidinone (NF-246) by *Escherichia coli*." Arch Biochem Biophys **113**(2): 399-404.

Gerpe, A., G. Alvarez, D. Benitez, L. Boiani, M. Quiroga, P. Hernandez, M. Sortino, S. Zacchino, M. Gonzalez and H. Cerecetto (2009). "5-Nitrofuranes and 5-nitrothiophenes with anti-*Trypanosoma cruzi* activity and ability to accumulate squalene." Bioorg Med Chem **17**(21): 7500-7509.

Gerpe, A., I. Odreman-Nunez, P. Draper, L. Boiani, J. A. Urbina, M. Gonzalez and H. Cerecetto (2008). "Heteroallyl-containing 5-nitrofuranes as new anti-*Trypanosoma cruzi* agents with a dual mechanism of action." Bioorg Med Chem **16**(1): 569-577.

Ginger, M. L., N. Portman and P. G. McKean (2008). "Swimming with protists: perception, motility and flagellum assembly." Nat Rev Microbiol **6**(11): 838-850.

Gluenz, E., M. L. Ginger and P. G. McKean (2010). "Flagellum assembly and function during the *Leishmania* life cycle." Curr Opin Microbiol **13**(4): 473-479.

González, C., O. Wang, S. E. Strutz, C. González-Salazar, V. Sánchez-Cordero and S. Sarkar (2010). "Climate Change and Risk of Leishmaniasis in North America: Predictions from Ecological Niche Models of Vector and Reservoir Species." PLoS Negl Trop Dis **4**(1): e585.

Gorski, S., S. M. Collin, K. Ritmeijer, K. Keus, F. Gatluak, M. Mueller and R. N. Davidson (2010). "Visceral leishmaniasis relapse in Southern Sudan (1999 - 2007): A retrospective study of risk factors and trends." PLoS Negl Trop Dis **4**(6): e705.

Gourbal, B., N. Sonuc, H. Bhattacharjee, D. Legare, S. Sundar, M. Ouellette, B. P. Rosen and R. Mukhopadhyay (2004). "Drug uptake and modulation of drug resistance in *Leishmania* by an aquaglyceroporin." J Biol Chem **279**(30): 31010-31017.

Goyard, S. and S. M. Beverley (2000). "Blasticidin resistance: a new independent marker for stable transfection of Leishmania." Mol Biochem Parasitol **108**(2): 249-252.

Grondin, K., A. Haimeur, R. Mukhopadhyay, B. P. Rosen and M. Ouellette (1997). "Co-amplification of the gamma-glutamylcysteine synthetase gene gsh1 and of the ABC transporter gene pgpA in arsenite-resistant *Leishmania tarentolae*." EMBO J **16**(11): 3057-3065.

Grunberg, E., G. Beskid, R. Cleeland, W. F. DeLorenzo, E. Titsworth, H. J. Scholer, R. Richle and Z. Brener (1967). "Antiprotozoan and antibacterial activity of 2-nitroimidazole derivatives." Antimicrob Agents Chemother (Bethesda) **7**: 513-519.

Grunberg, E. and E. H. Titsworth (1973). "Chemotherapeutic properties of heterocyclic compounds: monocyclic compounds with five-membered rings." Annu Rev Microbiol **27**: 317-346.

Guerin, P. J., P. Olliaro, S. Sundar, M. Boelaert, S. L. Croft, P. Desjeux, M. K. Wasunna and A. D. M. Bryceson (2002). "Visceral leishmaniasis: current status of control, diagnosis, and treatment, and a proposed research and development agenda." Lancet Infectious Diseases **2**(8): 494-501.

Gupta, S., Ramesh, S. Sundar and N. Goyal (2005). "Use of *Leishmania donovani* field isolates expressing the luciferase reporter gene in *in vitro* drug screening." Antimicrob Agents Chemother **49**(9): 3776-3783.

Haberkorn, A. (1979). "The effect of nifurtimox on experimental infections with trypanosomatidae other than *Trypanosoma cruzi*." Zentralbl Bakteriol Orig A **244**(2-3): 331-338.

Haimeur, A., C. Brochu, P. Genest, B. Papadopoulou and M. Ouellette (2000). "Amplification of the ABC transporter gene PGPA and increased trypanothione levels in potassium antimonyl tartrate (SbIII) resistant *Leishmania tarentolae*." Mol Biochem Parasitol **108**(1): 131-135.

Haimeur, A., C. Guimond, S. Pilote, R. Mukhopadhyay, B. P. Rosen, R. Poulin and M. Ouellette (1999). "Elevated levels of polyamines and trypanothione resulting from overexpression of the ornithine decarboxylase gene in arsenite-resistant *Leishmania*." Mol Microbiol **34**(4): 726-735.

Hajos, A. K. and G. W. Winston (1991). "Dinitropyrene nitroreductase activity of purified NAD(P)H-quinone oxidoreductase: role in rat liver cytosol and induction by Aroclor-1254 pretreatment." Carcinogenesis **12**(4): 697-702.

Hall, B. S., C. Bot and S. R. Wilkinson (2011). "Nifurtimox Activation by Trypanosomal Type I Nitroreductases Generates Cytotoxic Nitrile Metabolites." Journal of Biological Chemistry **286**(15): 13088-13095.

Hall, B. S. and S. R. Wilkinson (2012). "Activation of Benznidazole by Trypanosomal Type I Nitroreductases Results in Glyoxal Formation." Antimicrobial Agents and Chemotherapy **56**(1): 115-123.

Hall, B. S., X. Wu, L. Hu and S. R. Wilkinson (2010). "Exploiting the drug-activating properties of a novel trypanosomal nitroreductase." Antimicrob Agents Chemother **54**(3): 1193-1199.

Harbarth, S., J. P. Burke, J. F. Lloyd, R. S. Evans, S. L. Pestotnik and M. H. Samore (2002). "Clinical and economic outcomes of conventional amphotericin B-associated nephrotoxicity." Clin Infect Dis **35**(12): e120-127.

Heise, N. and F. R. Opperdoes (1997). "The dihydroxyacetonephosphate pathway for biosynthesis of ether lipids in *Leishmania mexicana* promastigotes." Mol Biochem Parasitol **89**(1): 61-72.

Helmick, C. G. and J. K. Green (1985). "Pentamidine-associated hypotension and route of administration." Ann Intern Med **103**(3): 480.

Helsby, N. A., G. J. Atwell, S. Yang, B. D. Palmer, R. F. Anderson, S. M. Pullen, D. M. Ferry, A. Hogg, W. R. Wilson and W. A. Denny (2004). "Aziridinyldinitrobenzamides: Synthesis and structure-activity relationships for activation by *E. coli* nitroreductase." J Med Chem **47**(12): 3295-3307.

Herwaldt, B. L. (1999). "Leishmaniasis." Lancet **354**(9185): 1191-1199.

Hidron, A. and C. Franco-Paredes (2012). Trypanosomiasis, American (Chagas Disease). CDC Health Information for International Travel 2012. G. Brunette. Oxford, NY, Oxford University Press.

Hiraku, Y., A. Sekine, H. Nabeshi, K. Midorikawa, M. Murata, Y. Kumagai and S. Kawanishi (2004). "Mechanism of carcinogenesis induced by a veterinary antimicrobial drug, nitrofurazone, via oxidative DNA damage and cell proliferation." Cancer Letters **215**(2): 141-150.

Hu, L., X. Wu, J. Han, L. Chen, S. O. Vass, P. Browne, B. S. Hall, C. Bot, V. Gobalakrishnapillai, P. F. Searle, R. J. Knox and S. R. Wilkinson (2011). "Synthesis and structure-activity relationships of nitrobenzyl phosphoramide mustards as nitroreductase-activated prodrugs." Bioorg Med Chem Lett **21**(13): 3986-3991.

Hu, L., C. Yu, Y. Jiang, J. Han, Z. Li, P. Browne, P. R. Race, R. J. Knox, P. F. Searle and E. I. Hyde (2003). "Nitroaryl Phosphoramides as Novel Prodrugs for *E. coli* Nitroreductase Activation in Enzyme Prodrug Therapy." Journal of Medicinal Chemistry **46**(23): 4818-4821.

Irigoin, F., L. Cibils, M. A. Comini, S. R. Wilkinson, L. Flohe and R. Radi (2008). "Insights into the redox biology of *Trypanosoma cruzi*: Trypanothione metabolism and oxidant detoxification." Free Radic Biol Med **45**(6): 733-742.

Ivens, A. C., C. S. Peacock, E. A. Worthey, L. Murphy, G. Aggarwal, M. Berriman, E. Sisk, M.-A. Rajandream, E. Adlem, R. Aert, A. Anupama, Z. Apostolou, P. Attipoe, N. Bason, C. Bauser, A. Beck, S. M. Beverley, G. Bianchettin, K. Borzym, G. Bothe, C. V. Bruschi, M. Collins, E. Cadag, L. Ciarloni, C. Clayton, R. M. R. Coulson, A. Cronin, A. K. Cruz, R. M. Davies, J. De Gaudenzi, D. E. Dobson, A. Duesterhoeft, G. Fazelina, N. Fosker, A. C. Frasch, A. Fraser, M. Fuchs, C. Gabel, A. Goble, A. Goffeau, D. Harris, C. Hertz-Fowler, H. Hilbert, D. Horn, Y. Huang, S. Klages, A. Knights, M. Kube, N. Larke, L. Litvin, A. Lord, T. Louie, M. Marra, D. Masuy, K. Matthews, S. Michaeli, J. C. Mottram, S. Muller-Auer, H. Munden, S. Nelson, H. Norbertczak, K. Oliver, S. O'Neil, M. Pentony, T. M. Pohl, C. Price, B. Purnelle, M. A. Quail, E. Rabbinowitsch, R. Reinhardt, M. Rieger, J. Rinta, J. Robben, L. Robertson, J. C. Ruiz, S. Rutter, D. Saunders, M. Schafer, J. Schein, D. C.

Schwartz, K. Seeger, A. Seyler, S. Sharp, H. Shin, D. Sivam, R. Squares, S. Squares, V. Tosato, C. Vogt, G. Volckaert, R. Wambutt, T. Warren, H. Wedler, J. Woodward, S. Zhou, W. Zimmermann, D. F. Smith, J. M. Blackwell, K. D. Stuart, B. Barrell and P. J. Myler (2005). "The Genome of the Kinetoplastid Parasite, *Leishmania major*." Science **309**(5733): 436-442.

Jaiswal, A. K. (1994). "Human NAD(P)H:quinone oxidoreductase2. Gene structure, activity, and tissue-specific expression." J Biol Chem **269**(20): 14502-14508.

Jha, S. N., N. K. Singh and T. K. Jha (1991). "Changing response to diamidine compounds in cases of kala-azar unresponsive to antimonial." J Assoc Physicians India **39**(4): 314-316.

Kaiser, M., M. A. Bray, M. Cal, B. Bourdin Trunz, E. Torreele and R. Brun (2011). "Antitrypanosomal activity of fexinidazole, a new oral nitroimidazole drug candidate for treatment of sleeping sickness." Antimicrob Agents Chemother **55**(12): 5602-5608.

Kakkar, P. and B. K. Singh (2007). "Mitochondria: a hub of redox activities and cellular distress control." Mol Cell Biochem **305**(1-2): 235-253.

Kamau, S. W., F. Grimm and A. B. Hehl (2001). "Expression of green fluorescent protein as a marker for effects of antileishmanial compounds *in vitro*." Antimicrob Agents Chemother **45**(12): 3654-3656.

Kamhawi, S., M. Ramalho-Ortigao, V. M. Pham, S. Kumar, P. G. Lawyer, S. J. Turco, C. Barillas-Mury, D. L. Sacks and J. G. Valenzuela (2004). "A role for insect galectins in parasite survival." Cell **119**(3): 329-341.

Kashanian, J., P. Hakimian, M. Blute, Jr., J. Wong, H. Khanna, G. Wise and R. Shabsigh (2008). "Nitrofurantoin: the return of an old friend in the wake of growing resistance." BJU Int **102**(11): 1634-1637.

Kedderis, G. L., L. S. Argenbright and G. T. Miwa (1989). "Covalent interaction of 5-nitroimidazoles with DNA and protein *in vitro*: mechanism of reductive activation." Chem Res Toxicol **2**(3): 146-149.

Kelly, J. M., M. C. Taylor, K. Smith, K. J. Hunter and A. H. Fairlamb (1993). "Phenotype of recombinant *Leishmania donovani* and *Trypanosoma cruzi* which over-express trypanothione reductase. Sensitivity towards agents that are thought to induce oxidative stress." Eur J Biochem **218**(1): 29-37.

Kelly, J. M., H. M. Ward, M. A. Miles and G. Kendall (1992). "A shuttle vector which facilitates the expression of transfected genes in *Trypanosoma cruzi* and *Leishmania*." Nucleic Acids Res **20**(15): 3963-3969.

Kim, D. H., H. J. Chung, J. Bleys and R. F. Ghohestani (2009). "Is paromomycin an effective and safe treatment against cutaneous leishmaniasis? A meta-analysis of 14 randomized controlled trials." PLoS Negl Trop Dis **3**(2): e381.

Kima, P. E. (2007). "The amastigote forms of *Leishmania* are experts at exploiting host cell processes to establish infection and persist." Int J Parasitol **37**(10): 1087-1096.

Knox, R. J., M. P. Boland, F. Friedlos, B. Coles, C. Southan and J. J. Roberts (1988). "The nitroreductase enzyme in Walker cells that activates 5-(aziridin-1-yl)-2,4-dinitrobenzamide (CB 1954) to 5-(aziridin-1-yl)-4-hydroxylamino-2-nitrobenzamide is a form of NAD(P)H dehydrogenase (quinone) (EC 1.6.99.2)." Biochem Pharmacol **37**(24): 4671-4677.

Knox, R. J., F. Friedlos and M. P. Boland (1993). "The bioactivation of CB 1954 and its use as a prodrug in antibody-directed enzyme prodrug therapy (ADEPT)." Cancer Metastasis Rev **12**(2): 195-212.

Knox, R. J., F. Friedlos, R. F. Sherwood, R. G. Melton and G. M. Anlezark (1992). "The bioactivation of 5-(aziridin-1-yl)-2,4-dinitrobenzamide (CB1954)-II: A comparison of an *Escherichia coli* nitroreductase and Walker DT diaphorase." Biochem Pharmacol **44**(12): 2297-2301.

Kolev, N. G., C. Tschudi and E. Ullu (2011). "RNA interference in protozoan parasites: achievements and challenges." Eukaryot Cell **10**(9): 1156-1163.

Koto, K. S., P. Lescault, L. Brard, K. Kim, R. K. Singh, J. Bond, S. Illenye, M. A. Slavik, T. Ashikaga and G. L. Saulnier Sholler (2011). "Antitumor activity of nifurtimox is enhanced with tetrathiomolybdate in medulloblastoma." Int J Oncol **38**(5): 1329-1341.

Kramer, S. (2012). "Developmental regulation of gene expression in the absence of transcriptional control: the case of kinetoplastids." Mol Biochem Parasitol **181**(2): 61-72.

Lacomble, S., S. Vaughan, C. Gadelha, M. K. Morphew, M. K. Shaw, J. R. McIntosh and K. Gull (2009). "Three-dimensional cellular architecture of the flagellar pocket and associated cytoskeleton in trypanosomes revealed by electron microscope tomography." J Cell Sci **122**(Pt 8): 1081-1090.

Lang, T., S. Goyard, M. Lebastard and G. Milon (2005). "Bioluminescent *Leishmania* expressing luciferase for rapid and high throughput screening of drugs acting on amastigote-harbouring macrophages and for quantitative real-time monitoring of parasitism features in living mice." Cell Microbiol **7**(3): 383-392.

Laskay, T., G. van Zandbergen and W. Solbach (2003). "Neutrophil granulocytes - Trojan horses for *Leishmania major* and other intracellular microbes?" Trends in Microbiology **11**(5): 210-214.

LeBowitz, J. H., C. M. Coburn and S. M. Beverley (1991). "Simultaneous transient expression assays of the trypanosomatid parasite *Leishmania* using beta-galactosidase and beta-glucuronidase as reporter enzymes." Gene **103**(1): 119-123.

Leishman, W. B. (1903). "On the possibility of the occurrence of trypanosomiasis in India." British Medical Journal: 1252-1254.

Leitsch, D., D. Kolarich, I. B. Wilson, F. Altmann and M. Duchene (2007). "Nitroimidazole action in *Entamoeba histolytica*: a central role for thioredoxin reductase." PLoS Biol **5**(8): e211.

Liu, B., Y. Liu, S. A. Motyka, E. E. Agbo and P. T. Englund (2005). "Fellowship of the rings: the replication of kinetoplast DNA." Trends Parasitol **21**(8): 363-369.

Liu, N., G. Caderas, C. Deillon, S. Hoffmann, S. Klauser, T. Cui and B. Gutte (2001). "Fusion proteins from artificial and natural structural modules." Curr Protein Pept Sci **2**(2): 107-121.

Lux, H., N. Heise, T. Klenner, D. Hart and F. R. Opperdoes (2000). "Ether-lipid (alkyl-phospholipid) metabolism and the mechanism of action of ether-lipid analogues in *Leishmania*." Mol Biochem Parasitol **111**(1): 1-14.

Lye, L.-F., K. Owens, H. Shi, S. M. F. Murta, A. C. Vieira, S. J. Turco, C. Tschudi, E. Ullu and S. M. Beverley (2010). "Retention and loss of RNA interference pathways in trypanosomatid protozoans." PLoS Pathog **6**(10): e1001161.

Maarouf, M., F. Lawrence, S. L. Croft and M. Robert-Gero (1995). "Ribosomes of *Leishmania* are a target for the aminoglycosides." Parasitol Res **81**(5): 421-425.

Manson-Bahr, P. E. and B. A. Southgate (1964). "Recent research on kala azar in East Africa." J Trop Med Hyg **67**: 79-84.

Marin-Neto, J. A., A. Rassi, Jr., A. Avezum, Jr., A. C. Mattos, A. Rassi, C. A. Morillo, S. Sosa-Estani and S. Yusuf (2009). "The BENEFIT trial: testing the hypothesis that trypanocidal therapy is beneficial for patients with chronic Chagas heart disease." Mem Inst Oswaldo Cruz **104 Suppl 1**: 319-324.

Marsden, P. D. (1986). "Mucosal leishmaniasis ("espundia" Escomel, 1911)." Trans R Soc Trop Med Hyg **80**(6): 859-876.

Martin, E. and A. J. Mukkada (1979). "Identification of the terminal respiratory chain in kinetoplast. Mitochondrial complexes of *Leishmania tropica* promastigotes." J Biol Chem **254**(23): 12192-12198.

Martin, E. and A. J. Mukkada (1979). "Respiratory chain components of *Leishmania tropica* promastigotes." J Protozool **26**(1): 138-142.

Mbongo, N., P. M. Loiseau, M. A. Billion and M. Robert-Gero (1998). "Mechanism of amphotericin B resistance in *Leishmania donovani* promastigotes." Antimicrob Agents Chemother **42**(2): 352-357.

McCalla, D. R. (1983). "Mutagenicity of nitrofuran derivatives: review." Environ Mutagen **5**(5): 745-765.

McCalla, D. R., C. Kaiser and M. H. Green (1978). "Genetics of nitrofurazone resistance in *Escherichia coli*." J Bacteriol **133**(1): 10-16.

McCalla, D. R., A. Reuvers and C. Kaiser (1971). "Breakage of bacterial DNA by nitrofuran derivatives." Cancer Res **31**(12): 2184-2188.

McConville, M. J., K. A. Mullin, S. C. Ilgoutz and R. D. Teasdale (2002). "Secretory pathway of trypanosomatid parasites." Microbiol Mol Biol Rev **66**(1): 122-154.

McKinnell, J. A., N. S. Stollenwerk, C. W. Jung and L. G. Miller (2011). "Nitrofurantoin compares favorably to recommended agents as empirical treatment of uncomplicated urinary tract infections in a decision and cost analysis." Mayo Clin Proc **86**(6): 480-488.

Meagher, L. C., J. S. Savill, A. Baker, R. W. Fuller and C. Haslett (1992). "Phagocytosis of apoptotic neutrophils does not induce macrophage release of thromboxane B2." Journal of Leukocyte Biology **52**(3): 269-273.

Meheus, F., M. Balasegaram, P. Olliaro, S. Sundar, S. Rijal, M. A. Faiz and M. Boelaert (2010). "Cost-effectiveness analysis of combination therapies for visceral leishmaniasis in the Indian subcontinent." PLoS Negl Trop Dis **4**(9).

Mehregan, D. R., A. H. Mehregan and D. A. Mehregan (1999). "Histologic diagnosis of cutaneous leishmaniasis." Clinics in Dermatology **17**(3): 297-304.

Mejia, A. M., B. S. Hall, M. C. Taylor, A. Gomez-Palacio, S. R. Wilkinson, O. Triana-Chavez and J. M. Kelly (2012). "Benznidazole-resistance in *Trypanosoma cruzi* Is a readily acquired trait that can arise independently in a single population." J Infect Dis **206**(2): 220-228.

Michel, G., B. Ferrua, T. Lang, M. P. Maddugoda, P. Munro, C. Pomares, E. Lemichez and P. Marty (2011). "Luciferase-expressing *Leishmania infantum* allows the monitoring of amastigote population size, *in vivo*, *ex vivo* and *in vitro*." PLoS Negl Trop Dis **5**(9): e1323.

Michels, P. A., F. Bringaud, M. Herman and V. Hannaert (2006). "Metabolic functions of glycosomes in trypanosomatids." Biochim Biophys Acta **1763**(12): 1463-1477.

Mikus, J. and D. Steverding (2000). "A simple colorimetric method to screen drug cytotoxicity against *Leishmania* using the dye Alamar Blue." Parasitol Int **48**(3): 265-269.

Minodier, P. and P. Parola (2007). "Cutaneous leishmaniasis treatment." Travel Med Infect Dis **5**(3): 150-158.

Miranda-Verástegui, C., A. Llanos-Cuentas, I. Arévalo, B. J. Ward and G. Matlashewski (2005). "Randomized, double-blind clinical trial of topical imiquimod 5% with parenteral meglumine antimoniate in the treatment of cutaneous leishmaniasis in Peru." Clinical Infectious Diseases **40**(10): 1395-1403.

Miseviciene, L., Z. Anusevicius, J. Sarlauskas and N. Cenas (2006). "Reduction of nitroaromatic compounds by NAD(P)H:quinone oxidoreductase (NQO1): the role of electron-accepting potency and structural parameters in the substrate specificity." Acta Biochim Pol **53**(3): 569-576.

Moore, E., D. O'Flaherty, H. Heuvelmans, J. Seaman, H. Veeken, S. de Wit and R. N. Davidson (2001). "Comparison of generic and proprietary sodium stibogluconate for the treatment of visceral leishmaniasis in Kenya." Bull World Health Organ **79**(5): 388-393.

Moosavi, Z., A. Nakhli and S. Rassaii (2005). "Comparing the efficiency of topical paromomycin with intralesional meglumine antimoniate for cutaneous leishmaniasis." Int J Dermatol **44**(12): 1064-1065.

Moreno, S. N., R. Docampo, R. P. Mason, W. Leon and A. O. Stoppani (1982). "Different behaviors of benznidazole as free radical generator with mammalian and *Trypanosoma cruzi* microsomal preparations." Arch Biochem Biophys **218**(2): 585-591.

Mosser, D. M., T. A. Springer and M. S. Diamond (1992). "*Leishmania* promastigotes require opsonic complement to bind to the human leukocyte integrin Mac-1 (CD11b/CD18)." J Cell Biol **116**(2): 511-520.

Mukherjee, A., P. K. Padmanabhan, M. H. Sahani, M. P. Barrett and R. Madhubala (2006). "Roles for mitochondria in pentamidine susceptibility and resistance in *Leishmania donovani*." Mol Biochem Parasitol **145**(1): 1-10.

Muller, J., J. Wastling, S. Sanderson, N. Muller and A. Hemphill (2007). "A novel *Giardia lamblia* nitroreductase, GlNR1, interacts with nitazoxanide and other thiazolides." Antimicrob Agents Chemother **51**(6): 1979-1986.

Murta, S. M., F. B. Nogueira, P. F. Dos Santos, F. M. Campos, C. Volpe, D. B. Liarte, P. Nirde, C. M. Probst, M. A. Krieger, S. Goldenberg and A. J. Romanha (2008). "Differential gene expression in *Trypanosoma cruzi* populations susceptible and resistant to benznidazole." Acta Trop **107**(1): 59-65.

Musa, A. M., B. Younis, A. Fadlalla, C. Royce, M. Balasegaram, M. Wasunna, A. Hailu, T. Edwards, R. Omollo, M. Mudawi, G. Kokwaro, A. El-Hassan and E. Khalil (2010). "Paromomycin for the treatment of visceral leishmaniasis in Sudan: a randomized, open-label, dose-finding study." PLoS Negl Trop Dis **4**(10): e855.

Nacher, M., B. Carme, D. Sainte Marie, P. Couppie, E. Clyti, P. Guibert and R. Pradinaud (2001). "Influence of clinical presentation on the efficacy of a short course of pentamidine in the treatment of cutaneous leishmaniasis in French Guiana." Ann Trop Med Parasitol **95**(4): 331-336.

Neal, R. A., J. van Bueren and G. Hooper (1988). "The activity of nitrofurazone and furazolidone against *Leishmania donovani*, *L. major* and *L. enriettii in vitro* and *in vivo*." Ann Trop Med Parasitol **82**(5): 453-456.

Nesslany, F., S. Brugier, M. A. Mouries, F. Le Curieux and D. Marzin (2004). "*In vitro* and *in vivo* chromosomal aberrations induced by megazol." Mutat Res **560**(2): 147-158.

Nixon, J. E., A. Wang, J. Field, H. G. Morrison, A. G. McArthur, M. L. Sogin, B. J. Loftus and J. Samuelson (2002). "Evidence for lateral transfer of genes encoding ferredoxins, nitroreductases, NADH oxidase, and alcohol dehydrogenase 3 from anaerobic prokaryotes to *Giardia lamblia* and *Entamoeba histolytica*." Eukaryot Cell **1**(2): 181-190.

Nogueira, F. B., M. A. Krieger, P. Nirde, S. Goldenberg, A. J. Romanha and S. M. Murta (2006). "Increased expression of iron-containing superoxide dismutase-A (TcFeSOD-A) enzyme in *Trypanosoma cruzi* population with *in vitro*-induced resistance to benznidazole." Acta Trop **100**(1-2): 119-132.

Nogueira, F. B., J. F. Rodrigues, M. M. Correa, J. C. Ruiz, A. J. Romanha and S. M. Murta (2012). "The level of ascorbate peroxidase is enhanced in benznidazole-resistant populations of *Trypanosoma cruzi* and its expression is modulated by stress generated by hydrogen peroxide." Mem Inst Oswaldo Cruz **107**(4): 494-502.

Nozaki, T., J. C. Engel and J. A. Dvorak (1996). "Cellular and molecular biological analyses of nifurtimox resistance in *Trypanosoma cruzi*." Am J Trop Med Hyg **55**(1): 111-117.

Okuno, T., Y. Goto, Y. Matsumoto and H. Otsuka (2003). "Applications of recombinant *Leishmania amazonensis* expressing *egfp* or the beta-galactosidase gene for drug screening and histopathological analysis." Exp Anim **52**(2): 109-118.

Opperdoes, F. R., P. Baudhuin, I. Coppens, C. De Roe, S. W. Edwards, P. J. Weijers and O. Misset (1984). "Purification, morphometric analysis, and characterization of the glycosomes (microbodies) of the protozoan haemoflagellate *Trypanosoma brucei*." J Cell Biol **98**(4): 1178-1184.

Opperdoes, F. R., P. Borst and K. Fonck (1976). "The potential use of inhibitors of glycerol-3-phosphate oxidase for chemotherapy of African trypanosomiasis." FEBS Lett **62**(2): 169-172.

Orna, M. V. and R. P. Mason (1989). "Correlation of kinetic parameters of nitroreductase enzymes with redox properties of nitroaromatic compounds." J Biol Chem **264**(21): 12379-12384.

Ouellette, M., J. Drummelsmith and B. Papadopoulou (2004). "Leishmaniasis: drugs in the clinic, resistance and new developments." Drug Resist Updat **7**(4-5): 257-266.

Overath, P., Y. D. Stierhof and M. Wiese (1997). "Endocytosis and secretion in trypanosomatid parasites - Tumultuous traffic in a pocket." Trends Cell Biol **7**(1): 27-33.

Packchanian, A. (1955). "Chemotherapy of African sleeping sickness. I. Chemotherapy of experimental *Trypanosoma gambiense* infection in mice (*Mus musculus*) with nitrofurazone." Am J Trop Med Hyg **4**(4): 705-711.

Padda, R. S., C. Wang, J. B. Hughes, R. Kutty and G. N. Bennett (2003). "Mutagenicity of nitroaromatic degradation compounds." Environ Toxicol Chem **22**(10): 2293-2297.

Pal, D., S. Banerjee, J. Cui, A. Schwartz, S. K. Ghosh and J. Samuelson (2009). "Giardia, Entamoeba, and Trichomonas Enzymes Activate Metronidazole (Nitroreductases) and Inactivate Metronidazole (Nitroimidazole Reductases)." Antimicrob. Agents Chemother. **53**(2): 458-464.

Palumbo, E. (2010). "Treatment strategies for mucocutaneous leishmaniasis." J Glob Infect Dis **2**(2): 147-150.

Papadopoulou, M. V., W. D. Bloomer, H. S. Rosenzweig, E. Chatelain, M. Kaiser, S. R. Wilkinson, C. McKenzie and J. R. Ioset (2012). "Novel 3-nitro-1H-1,2,4-triazole-based amides and sulfonamides as potential antitrypanosomal agents." J Med Chem **55**(11): 5554-5565.

Papadopoulou, M. V., B. B. Trunz, W. D. Bloomer, C. McKenzie, S. R. Wilkinson, C. Prasittichai, R. Brun, M. Kaiser and E. Torreele (2011). "Novel 3-nitro-1H-1,2,4-triazole-based aliphatic and aromatic amines as anti-chagasic agents." J Med Chem **54**(23): 8214-8223.

Parkinson, G. N., J. V. Skelly and S. Neidle (2000). "Crystal structure of FMN-dependent nitroreductase from *Escherichia coli* B: a prodrug-activating enzyme." J Med Chem **43**(20): 3624-3631.

Patel, P., J. G. Young, V. Mautner, D. Ashdown, S. Bonney, R. G. Pineda, S. I. Collins, P. F. Searle, D. Hull, E. Peers, J. Chester, D. M. Wallace, A. Doherty, H. Leung, L. S. Young and N. D. James (2009). "A phase I/II clinical trial in localized prostate cancer of an adenovirus expressing nitroreductase with CB1954 [correction of CB1984]." Mol Ther **17**(7): 1292-1299.

Pavli, A. and H. C. Maltezou (2010). "Leishmaniasis, an emerging infection in travelers." Int J Infect Dis **14**(12): e1032-1039.

Peacock, C. S., K. Seeger, D. Harris, L. Murphy, J. C. Ruiz, M. A. Quail, N. Peters, E. Adlem, A. Tivey, M. Aslett, A. Kerhornou, A. Ivens, A. Fraser, M. A. Rajandream, T. Carver, H. Norbertczak, T. Chillingworth, Z. Hance, K. Jagels, S. Moule, D. Ormond, S. Rutter, R. Squares, S. Whitehead, E. Rabbinowitsch, C. Arrowsmith, B. White, S. Thurston, F. Bringaud, S. L. Baldauf, A. Faulconbridge, D. Jeffares, D. P. Depledge, S. O. Oyola, J. D. Hilley, L. O. Brito, L. R. Tosi, B. Barrell, A. K. Cruz, J. C. Mottram, D. F. Smith and M. Berriman (2007). "Comparative genomic analysis of three *Leishmania* species that cause diverse human disease." Nat Genet **39**(7): 839-847.

Peres, C. M. and S. N. Agathos (2000). "Biodegradation of nitroaromatic pollutants: from pathways to remediation." Biotechnol Annu Rev **6**: 197-220.

Perry, K. and N. Agabian (1991). "mRNA processing in the Trypanosomatidae." Experientia **47**(2): 118-128.

Pescher, P., T. Blisnick, P. Bastin and G. F. Spath (2011). "Quantitative proteome profiling informs on phenotypic traits that adapt *Leishmania donovani* for axenic and intracellular proliferation." Cell Microbiol **13**(7): 978-991.

Petersen, T. N., S. Brunak, G. von Heijne and H. Nielsen (2011). "SignalP 4.0: discriminating signal peptides from transmembrane regions." Nat Methods **8**(10): 785-786.

Peterson, F. J., R. P. Mason, J. Hovsepian and J. L. Holtzman (1979). "Oxygen-sensitive and -insensitive nitroreduction by *Escherichia coli* and rat hepatic microsomes." J Biol Chem **254**(10): 4009-4014.

Piper, R. C., X. Xu, D. G. Russell, B. M. Little and S. M. Landfear (1995). "Differential targeting of two glucose transporters from *Leishmania enriettii* is mediated by an NH2-terminal domain." J Cell Biol **128**(4): 499-508.

Piscopo, T. V. and A. C. Mallia (2006). "Leishmaniasis." Postgrad Med J **82**(972): 649-657.

Poli, P., M. Aline de Mello, A. Buschini, R. A. Mortara, C. Northfleet de Albuquerque, S. da Silva, C. Rossi and T. M. Zucchi (2002). "Cytotoxic and genotoxic effects of megazol, an anti-Chagas' disease drug, assessed by different short-term tests." Biochem Pharmacol **64**(11): 1617-1627.

Prathalingham, S. R., S. R. Wilkinson, D. Horn and J. M. Kelly (2007). "Deletion of the *Trypanosoma brucei* superoxide dismutase gene sodb1 increases sensitivity to nifurtimox and benznidazole." Antimicrobial Agents and Chemotherapy **51**(2): 755-758.

Priotto, G., C. Fogg, M. Balasegaram, O. Erphas, A. Louga, F. Checchi, S. Ghabri and P. Piola (2006). "Three Drug Combinations for Late-Stage *Trypanosoma brucei gambiense* Sleeping Sickness: A Randomized Clinical Trial in Uganda." PLoS Clinical Trials **1**(8): e39.

Puechberty, J., C. Blaineau, S. Meghamla, L. Crobu, M. Pages and P. Bastien (2007). "Compared genomics of the strand switch region of *Leishmania* chromosome 1 reveal a novel genus-specific gene and conserved structural features and sequence motifs." BMC Genomics **8**: 57.

Pulido, S. A., D. L. Muñoz, A. M. Restrepo, C. V. Mesa, J. F. Alzate, I. D. Velez and S. M. Robledo (2012). "Improvement of the green fluorescent protein reporter system in *Leishmania* spp. for the *in vitro* and *in vivo* screening of antileishmanial drugs." Acta Tropica **122**(1): 36-45.

Race, P. R., A. L. Lovering, S. A. White, J. I. Grove, P. F. Searle, C. W. Wrighton and E. I. Hyde (2007). "Kinetic and structural characterisation of *Escherichia coli* nitroreductase mutants showing improved efficacy for the prodrug substrate CB1954." J Mol Biol **368**(2): 481-492.

Raether, W. and H. Seidenath (1983). "The activity of fexinidazole (HOE 239) against experimental infections with *Trypanosoma cruzi*, trichomonads and *Entamoeba histolytica*." Ann Trop Med Parasitol **77**(1): 13-26.

Raju, T. N. (2000). "The Nobel chronicles. 1988: James Whyte Black, (b 1924), Gertrude Elion (1918-99), and George H Hitchings (1905-98)." Lancet **355**(9208): 1022.

Ralston, K. S. and K. L. Hill (2008). "The flagellum of *Trypanosoma brucei*: new tricks from an old dog." Int J Parasitol **38**(8-9): 869-884.

Ramesh, V., R. Singh and P. Salotra (2007). "Short communication: post-kala-azar dermal leishmaniasis--an appraisal." Trop Med Int Health **12**(7): 848-851.

Ranganathan, G. and A. J. Mukkada (1995). "Ubiquinone biosynthesis in *Leishmania major* promastigotes." Int J Parasitol **25**(3): 279-284.

Raymond, F., S. Boisvert, G. Roy, J. F. Ritt, D. Legare, A. Isnard, M. Stanke, M. Olivier, M. J. Tremblay, B. Papadopoulou, M. Ouellette and J. Corbeil (2012). "Genome sequencing of the lizard parasite *Leishmania tarentolae* reveals loss of genes associated to the intracellular stage of human pathogenic species." Nucleic Acids Res **40**(3): 1131-1147.

Rego, J. V., S. M. Murta, P. Nirde, F. B. Nogueira, H. M. de Andrade and A. J. Romanha (2008). "*Trypanosoma cruzi*: characterisation of the gene encoding tyrosine aminotransferase in benznidazole-resistant and susceptible populations." Exp Parasitol **118**(1): 111-117.

Reithinger, R., J. C. Dujardin, H. Louzir, C. Pirmez, B. Alexander and S. Brooker (2007). "Cutaneous leishmaniasis." Lancet Infectious Diseases **7**(9): 581-596.

Reyes, P. A. and M. Vallejo (2005). "Trypanocidal drugs for late stage, symptomatic Chagas disease (*Trypanosoma cruzi* infection)." Cochrane Database Syst Rev **19**(4): CD004102.

Rieger, P. G., H. M. Meier, M. Gerle, U. Vogt, T. Groth and H. J. Knackmuss (2002). "Xenobiotics in the environment: present and future strategies to obviate the problem of biological persistence." J Biotechnol **94**(1): 101-123.

Roberts, S. C. (2011). "The genetic toolbox for *Leishmania* parasites." Bioeng Bugs **2**(6): 320-326.

Rochette, A., F. McNicoll, J. Girard, M. Breton, É. Leblanc, M. G. Bergeron and B. Papadopoulou (2005). "Characterization and developmental gene regulation of a large gene family encoding amastin surface proteins in *Leishmania* spp." Molecular and Biochemical Parasitology **140**(2): 205-220.

Rogers, M., P. Kropf, B.-S. Choi, R. Dillon, M. Podinovskaia, P. Bates and I. Müller (2009). "Proteophosophoglycans regurgitated by *Leishmania*-infected sand flies target the L-arginine metabolism of host macrophages to promote parasite survival." PLoS Pathog **5**(8): e1000555.

Rogers, M. B., J. D. Hilley, N. J. Dickens, J. Wilkes, P. A. Bates, D. P. Depledge, D. Harris, Y. Her, P. Herzyk, H. Imamura, T. D. Otto, M. Sanders, K. Seeger, J. C. Dujardin, M. Berriman, D. F. Smith, C. Hertz-Fowler and J. C. Mottram (2011). "Chromosome and gene copy number variation allow major structural change between species and strains of *Leishmania*." Genome Res **21**(12): 2129-2142.

Roldan, M., E. Perez-Reinado, F. Castillo and C. Moreno-Vivian (2008). "Reduction of polynitroaromatic compounds: the bacterial nitroreductases." Fems Microbiology Reviews **32**(3): 474-500.

Ross, R. (1903). "Further Notes on Leishman's Bodies." British Medical Journal: 1401.

Ross, W. J. and W. B. Jamieson (1975). "Antiparasitic nitroimidazoles. 8. Derivatives of 2-(4-formylstyryl)-5-nitro-1-vinylimidazole." J Med Chem **18**(2): 158-161.

Ross, W. J. and W. B. Jamieson (1975). "Antiparasitic nitroimidazoles. 9. Synthesis of some 2-(4-dialkylaminomethylstyryl)-and 2-(4-amidinostyryl)5-nitro-1-vinylimidazoles." J Med Chem **18**(4): 430-432.

Ross, W. J., W. B. Jamieson and M. C. McCowen (1972). "Antiparasitic nitroimidazoles. 1. Some 2-styryl-5-nitroimidazoles." J Med Chem **15**(10): 1035-1040.

Ross, W. J., W. B. Jamieson and M. C. McCowen (1973). "Antiparasitic nitroimidazoles. 3. Synthesis of 2-(4-carboxystyryl)-5-nitro-1-vinylimidazole and related compounds." J Med Chem **16**(4): 347-352.

Ross, W. J. and A. Todd (1973). "Antiparasitic nitroimidazoles. 7. Some 4- and 5-styrylnitroimidazoles." J Med Chem **16**(7): 863-865.

Rossignol, J. F., A. Ayoub and Marc S. Ayers (2001). "Treatment of diarrhea caused by *Giardia intestinalis* and *Entamoeba histolytica* or *E. dispar*: A randomized, double blind, placebo controlled study of nitazoxanide." Journal of Infectious Diseases **184**(3): 381-384.

Roy, G., C. Dumas, D. Sereno, Y. Wu, A. K. Singh, M. J. Tremblay, M. Ouellette, M. Olivier and B. Papadopoulou (2000). "Episomal and stable expression of the luciferase reporter gene for quantifying *Leishmania* spp. infections in macrophages and in animal models." Molecular and Biochemical Parasitology **110**(2): 195-206.

Salomao, K., E. M. de Souza, S. A. Carvalho, E. F. da Silva, C. A. Fraga, H. S. Barbosa and S. L. de Castro (2010). "*In vitro* and *in vivo* activities of 1,3,4-thiadiazole-2-arylhydrazone derivatives of megazol against *Trypanosoma cruzi*." Antimicrob Agents Chemother **54**(5): 2023-2031.

Saulnier Sholler, G. L., G. M. Bergendahl, L. Brard, A. P. Singh, B. W. Heath, P. M. Bingham, T. Ashikaga, B. A. Kamen, A. C. Homans, M. A. Slavik, S. R. Lenox, T. J. Higgins and W. S. Ferguson (2011). "A phase 1 study of nifurtimox in patients with relapsed/refractory neuroblastoma." J Pediatr Hematol Oncol **33**(1): 25-30.

Saulnier Sholler, G. L., L. Brard, J. A. Straub, L. Dorf, S. Illeyne, K. Koto, S. Kalkunte, M. Bosenberg, T. Ashikaga and R. Nishi (2009). "Nifurtimox induces apoptosis of neuroblastoma cells *in vitro* and *in vivo*." J Pediatr Hematol Oncol **31**(3): 187-193.

Saulnier Sholler, G. L., S. Kalkunte, C. Greenlaw, K. McCarten and E. Forman (2006). "Antitumor activity of nifurtimox observed in a patient with neuroblastoma." J Pediatr Hematol Oncol **28**(10): 693-695.

Saunders, E. C., D. E. S. DP, T. Naderer, M. F. Sernee, J. E. Ralton, M. A. Doyle, J. I. Macrae, J. L. Chambers, J. Heng, A. Nahid, V. A. Likic and M. J. McConville (2010). "Central carbon metabolism of Leishmania parasites." Parasitology **137**(9): 1303-1313.

Schor, N. A. and H. P. Morris (1977). "The activity of the D-T diaphorase in experimental hepatomas." Cancer Biochem Biophys **2**(1): 5-9.

Sereno, D., A. Cordeiro da Silva, F. Mathieu-Daude and A. Ouaissi (2007). "Advances and perspectives in *Leishmania* cell based drug-screening procedures." Parasitol Int **56**(1): 3-7.

Sereno, D., G. Roy, J. L. Lemesre, B. Papadopoulou and M. Ouellette (2001). "DNA transformation of *Leishmania infantum* axenic amastigotes and their use in drug screening." Antimicrob Agents Chemother **45**(4): 1168-1173.

Serricchio, M. and P. Butikofer (2011). "*Trypanosoma brucei*: a model micro-organism to study eukaryotic phospholipid biosynthesis." FEBS J **278**(7): 1035-1046.

Shaha, C. (2006). "Apoptosis in *Leishmania* species & its relevance to disease pathogenesis." Indian J Med Res **123**(3): 233-244.

Sharp, S. Y., L. R. Kelland, M. R. Valenti, L. A. Brunton, S. Hobbs and P. Workman (2000). "Establishment of an isogenic human colon tumor model for NQO1 gene expression: application to investigate the role of DT-diaphorase in bioreductive drug activation *in vitro* and *in vivo*." Mol Pharmacol **58**(5): 1146-1155.

Siegel, T. N., D. R. Hekstra, L. E. Kemp, L. M. Figueiredo, J. E. Lowell, D. Fenyo, X. Wang, S. Dewell and G. A. Cross (2009). "Four histone variants mark the boundaries of polycistronic transcription units in *Trypanosoma brucei*." Genes Dev **23**(9): 1063-1076.

Silverman, J. M., J. Clos, C. C. de'Oliveira, O. Shirvani, Y. Fang, C. Wang, L. J. Foster and N. E. Reiner (2010). "An exosome-based secretion pathway is responsible for protein export from *Leishmania* and communication with macrophages." J Cell Sci **123**(Pt 6): 842-852.

Simpson, L. (1973). "Structure and function of kinetoplast DNA." J Protozool **20**(1): 2-8.

Singh, N. and A. Dube (2004). "Short report: fluorescent *Leishmania*: application to anti-leishmanial drug testing." Am J Trop Med Hyg **71**(4): 400-402.

Singh, N., R. Gupta, A. K. Jaiswal, S. Sundar and A. Dube (2009). "Transgenic *Leishmania donovani* clinical isolates expressing green fluorescent protein constitutively for rapid and reliable *ex vivo* drug screening." J. Antimicrob. Chemother. **64**(2): 370-374.

Sokolova, A. Y., S. Wyllie, S. Patterson, S. L. Oza, K. D. Read and A. H. Fairlamb (2010). "Cross-Resistance to Nitro Drugs and Implications for Treatment of Human African Trypanosomiasis." Antimicrob. Agents Chemother. **54**(7): 2893-2900.

Soto, J. and J. Berman (2006). "Treatment of New World cutaneous leishmaniasis with miltefosine." Trans R Soc Trop Med Hyg **100 Suppl 1**: S34-40.

Southern, E. M. (1975). "Detection of specific sequences among DNA fragments separated by gel electrophoresis." J Mol Biol **98**(3): 503-517.

Spain, J. C. (1995). Biodegradation of nitroaromatic compounds. New York ; London, Plenum.

Stanimirovic, A., T. Stipic, M. Skerlev and A. Basta-Juzbasic (1999). "Treatment of cutaneous leishmaniasis with 20% paromomycin ointment." J Eur Acad Dermatol Venereol **13**(3): 214-217.

Stevens, J. R., H. A. Noyes, C. J. Schofield and W. Gibson (2001). "The molecular evolution of Trypanosomatidae." Adv Parasitol **48**: 1-56.

Stewart, M. L., G. J. Bueno, A. Baliani, B. Klenke, R. Brun, J. M. Brock, I. H. Gilbert and M. P. Barrett (2004). "Trypanocidal activity of melamine-based nitroheterocycles." Antimicrob Agents Chemother **48**(5): 1733-1738.

Stone, H. H., C. D. Tool and W. S. Pugsley (1952). "Kala-azar (visceral leishmaniasis): report of a case with 34 month incubation period and positive Doan-Wright test." Ann Intern Med **36**(2:2): 686-693.

Stover, C. K., P. Warrener, D. R. VanDevanter, D. R. Sherman, T. M. Arain, M. H. Langhorne, S. W. Anderson, J. A. Towell, Y. Yuan, D. N. McMurray, B. N. Kreiswirth, C. E. Barry and W. R. Baker (2000). "A small-molecule nitroimidazopyran drug candidate for the treatment of tuberculosis." Nature **405**(6789): 962-966.

Streeter, A. J. and B. A. Hoener (1988). "Evidence for the involvement of a nitrenium ion in the covalent binding of nitrofurazone to DNA." Pharm Res **5**(7): 434-436.

Stuart, K., R. Brun, S. Croft, A. Fairlamb, R. E. Gürtler, J. McKerrow, S. Reed and R. Tarleton (2008). "Kinetoplastids: related protozoan pathogens, different diseases." J Clin Invest **118**(4): 1301-1310.

Stuart, K. D., A. Schnaufer, N. L. Ernst and A. K. Panigrahi (2005). "Complex management: RNA editing in trypanosomes." Trends Biochem Sci **30**(2): 97-105.

Sun, E. W. and Y. F. Shi (2001). "Apoptosis: The quiet death silences the immune system." Pharmacology and Therapeutics **92**(2-3): 135-145.

Sundar, S. (2001). "Drug resistance in Indian visceral leishmaniasis." Tropical Medicine & International Health **6**(11): 849-854.

Sundar, S., H. Mehta, A. V. Suresh, S. P. Singh, M. Rai and H. W. Murray (2004). "Amphotericin B treatment for Indian visceral leishmaniasis: conventional versus lipid formulations." Clin Infect Dis **38**(3): 377-383.

Sundar, S. and M. Rai (2005). "Treatment of visceral leishmaniasis." Expert Opin Pharmacother **6**(16): 2821-2829.

Surve, S., M. Heestand, B. Panicucci, A. Schnaufer and M. Parsons (2012). "Enigmatic presence of mitochondrial complex I in *Trypanosoma brucei* bloodstream forms." Eukaryot Cell **11**(2): 183-193.

Tahghighi, A., F. R. Marznaki, F. Kobarfard, S. Dastmalchi, J. S. Mojarrad, S. Razmi, S. K. Ardestani, S. Emami, A. Shafiee and A. Foroumadi (2011). "Synthesis and antileishmanial activity of novel 5-(5-nitrofuran-2-y1)-1,3,4-thiadiazoles with piperazinyl-linked benzamidine substituents." Eur J Med Chem **46**(6): 2602-2608.

Tahghighi, A., S. Razmi, M. Mahdavi, P. Foroumadi, S. K. Ardestani, S. Emami, F. Kobarfard, S. Dastmalchi, A. Shafiee and A. Foroumadi (2012). "Synthesis and anti-leishmanial activity of 5-(5-nitrofuran-2-yl)-1,3,4-thiadiazol-2-amines containing N-[(1-benzyl-1H-1,2,3-triazol-4-yl)methyl] moieties." Eur J Med Chem **50**: 124-128.

Takahashi, M., S. Iizuka, T. Watanabe, M. Yoshida, J. Ando, K. Wakabayashi and A. Maekawa (2000). "Possible mechanisms underlying mammary carcinogenesis in female Wistar rats by nitrofurazone." Cancer Letters **156**: 177-184.

Temperton, N. J., S. R. Wilkinson, D. J. Meyer and J. M. Kelly (1998). "Overexpression of superoxide dismutase in *Trypanosoma cruzi* results in increased sensitivity to the trypanocidal agents gentian violet and benznidazole." Mol Biochem Parasitol **96**(1-2): 167-176.

ter Kuile, B. H. (1994). "Membrane-related processes and overall energy metabolism in *Trypanosoma brucei* and other kinetoplastid species." J Bioenerg Biomembr **26**(2): 167-172.

Thakur, C. P., M. Kumar and A. K. Pandey (1991). "Comparison of regimes of treatment of antimony-resistant kala-azar patients: a randomized study." Am J Trop Med Hyg **45**(4): 435-441.

Thakur, C. P., G. P. Sinha and A. K. Pandey (1996). "Comparison of regimens of amphotericin B deoxycholate in kala-azar." Indian J Med Res **103**: 259-263.

Thalhofer, C. J., J. W. Graff, L. Love-Homan, S. M. Hickerson, N. Craft, S. M. Beverley and M. E. Wilson (2010). "*In vivo* imaging of transgenic *Leishmania* parasites in a live host." J Vis Exp(41).

Thomas, S., A. Green, N. R. Sturm, D. A. Campbell and P. J. Myler (2009). "Histone acetylations mark origins of polycistronic transcription in *Leishmania major*." BMC Genomics **10**: 152.

Thornalley, P. J. (2008). "Protein and nucleotide damage by glyoxal and methylglyoxal in physiological systems--role in ageing and disease." Drug Metabol Drug Interact **23**(1-2): 125-150.

Torreele, E., B. Bourdin Trunz, D. Tweats, M. Kaiser, R. Brun, G. Mazué, M. A. Bray and B. Pécoul (2010). "Fexinidazole - A New Oral Nitroimidazole Drug Candidate Entering Clinical Development for the Treatment of Sleeping Sickness." PLoS Negl Trop Dis **4**(12): e923.

Tosato, V., L. Ciarloni, A. C. Ivens, M. A. Rajandream, B. G. Barrell and C. V. Bruschi (2001). "Secondary DNA structure analysis of the coding strand switch regions of five *Leishmania major* Friedlin chromosomes." Curr Genet **40**(3): 186-194.

Trunz, B. B., R. Jedrysiak, D. Tweats, R. Brun, M. Kaiser, J. Suwinski and E. Torreele (2011). "1-Aryl-4-nitro-1H-imidazoles, a new promising series for the treatment of human African trypanosomiasis." Eur J Med Chem **46**(5): 1524-1535.

Tsuchiya, S., M. Yamabe, Y. Yamaguchi, Y. Kobayashi, T. Konno and K. Tada (1980). "Establishment and characterization of a human acute monocytic leukemia cell line (THP-1)." Int J Cancer **26**(2): 171-176.

Tweats, D., B. Bourdin Trunz and E. Torreele (2012). "Genotoxicity profile of fexinidazole--a drug candidate in clinical development for human African trypanomiasis (sleeping sickness)." Mutagenesis **27**(5): 523-532.

Unger, C., W. Damenz, E. A. Fleer, D. J. Kim, A. Breiser, P. Hilgard, J. Engel, G. Nagel and H. Eibl (1989). "Hexadecylphosphocholine, a new ether lipid analogue. Studies on the antineoplastic activity *in vitro* and *in vivo*." Acta Oncol **28**(2): 213-217.

van Zandbergen, G., N. Hermann, H. Laufs, W. Solbach and T. Laskay (2002). "Leishmania promastigotes release a granulocyte chemotactic factor and induce interleukin-8 release but inhibit gamma interferon-inducible protein 10 production by neutrophil granulocytes." Infection and Immunity **70**(8): 4177-4184.

Verma, N. K. and C. S. Dey (2004). "Possible mechanism of miltefosine-mediated death of *Leishmania donovani*." Antimicrob Agents Chemother **48**(8): 3010-3015.

Viode, C., N. Bettache, N. Cenas, R. L. Krauth-Siegel, G. Chauviere, N. Bakalara and J. Perie (1999). "Enzymatic reduction studies of nitroheterocycles." Biochem Pharmacol **57**(5): 549-557.

Viotti, R., C. Vigliano, B. Lococo, M. G. Alvarez, M. Petti, G. Bertocchi and A. Armenti (2009). "Side effects of benznidazole as treatment in chronic Chagas disease: fears and realities." Expert Rev Anti Infect Ther **7**(2): 157-163.

Warburg, A., R. B. Tesh and D. McMahon-Pratt (1989). "Studies on the attachment of *Leishmania* flagella to sand fly midgut epithelium." J Protozool **36**(6): 613-617.

Watanabe, M., T. Nishino, K. Takio, T. Sofuni and T. Nohmi (1998). "Purification and characterization of wild-type and mutant "classical" nitroreductases of *Salmonella typhimurium*. L33R mutation greatly diminishes binding of FMN to the nitroreductase of *S. typhimurium*." J Biol Chem **273**(37): 23922-23928.

Weigle, K. A., L. Valderrama, A. L. Arias, C. Santrich and N. G. Saravia (1991). "Leishmanin Skin Test standardization and evaluation of safety, dose, storage, longevity of reaction and sensitization." Am J Trop Med Hyg **44**(3): 260-271.

Whiteway, J., P. Koziarz, J. Veall, N. Sandhu, P. Kumar, B. Hoecher and I. B. Lambert (1998). "Oxygen-insensitive nitroreductases: analysis of the roles of nfsA and nfsB in development of resistance to 5-nitrofuran derivatives in *Escherichia coli*." J Bacteriol **180**(21): 5529-5539.

Whitmore, G. F. and A. J. Varghese (1986). "The biological properties of reduced nitroheterocyclics and possible underlying biochemical mechanisms." Biochem Pharmacol **35**(1): 97-103.

Whitmore, G. F., A. J. Varghese and S. Gulyas (1986). "Reaction of 2-nitroimidazole metabolites with guanine and possible biological consequences." IARC Sci Publ(70): 185-196.

WHO. (1999). "Tropical disease research : progress 1997-98 - 14th programme report : leishmaniasis." Retrieved 14 January, 2009, from http://whqlibdoc.who.int/hq/1999/TDR_PR14_LEISH_99.1.pdf.

Wiemer, E. A., I. J. L, J. van Roy, R. J. Wanders and F. R. Opperdoes (1996). "Identification of 2-enoyl coenzyme A hydratase and NADP(+)-dependent 3-hydroxyacyl-CoA dehydrogenase activity in glycosomes of procyclic *Trypanosoma brucei*." Mol Biochem Parasitol **82**(1): 107-111.

Wilkinson, S. R., C. Bot, J. M. Kelly and B. S. Hall (2011). "Trypanocidal activity of nitroaromatic prodrugs: current treatments and future perspectives." Curr Top Med Chem **11**(16): 2072-2084.

Wilkinson, S. R. and J. M. Kelly (2003). "The role of glutathione peroxidases in trypanosomatids." Biol Chem **384**(4): 517-525.

Wilkinson, S. R. and J. M. Kelly (2009). "Trypanocidal drugs: mechanisms, resistance and new targets." Expert Rev Mol Med **11**: e31.

Wilkinson, S. R., D. J. Meyer, M. C. Taylor, E. V. Bromley, M. A. Miles and J. M. Kelly (2002). "The *Trypanosoma cruzi* enzyme TcGPXI is a glycosomal peroxidase and can be linked to trypanothione reduction by glutathione or tryparedoxin." J Biol Chem **277**(19): 17062-17071.

Wilkinson, S. R., S. O. Obado, I. L. Mauricio and J. M. Kelly (2002). "*Trypanosoma cruzi* expresses a plant-like ascorbate-dependent hemoperoxidase localized to the endoplasmic reticulum." Proc Natl Acad Sci U S A **99**(21): 13453-13458.

Wilkinson, S. R., S. R. Prathalingam, M. C. Taylor, A. Ahmed, D. Horn and J. M. Kelly (2006). "Functional characterisation of the iron superoxide dismutase gene repertoire in *Trypanosoma brucei*." Free Radic Biol Med **40**(2): 198-209.

Wilkinson, S. R., M. C. Taylor, D. Horn, J. M. Kelly and I. Cheeseman (2008). "A mechanism for cross-resistance to nifurtimox and benznidazole in trypanosomes." Proceedings of the National Academy of Sciences of the United States of America **105**(13): 5022-5027.

Wilkinson, S. R., N. J. Temperton, A. Mondragon and J. M. Kelly (2000). "Distinct mitochondrial and cytosolic enzymes mediate trypanothione-dependent peroxide metabolism in *Trypanosoma cruzi*." J Biol Chem **275**(11): 8220-8225.

Wincker, P., C. Ravel, C. Blaineau, M. Pages, Y. Jauffret, J. P. Dedet and P. Bastien (1996). "The *Leishmania* genome comprises 36 chromosomes conserved across widely divergent human pathogenic species." Nucleic Acids Res **24**(9): 1688-1694.

Winkelmann, E. and W. Raether (1978). "Chemotherapeutically acitve nitro compounds. 4. 5-Nitroimidazoles (Part III)." Arzneimittelforschung **28**(5): 739-749.

Winkelmann, E., W. Raether and U. Gebert (1978). "Chemotherapeutically active nitro-derivatives. 4. 5-Nitroimidazoles (Part IV)." Arzneimittelforschung **28**(10): 1682-1684.

Winkelmann, E., W. Raether, U. Gebert and A. Sinharay (1977). "Chemotherapeutically active nitro compounds. 4. 5-Nitroimidazoles (Part I)." Arzneimittelforschung **27**(12): 2251-2263.

Winkelmann, E., W. Raether and A. Sinharay (1978). "Chemotherapeutically active nitro compounds. 4.5-Nitroimidazoles (Part II)." Arzneimittelforschung **28**(3): 351-366.

Wiser, M. (2010). Protozoa and human disease, Garland Science.

Worthey, E. A., A. Schnaufer, I. S. Mian, K. Stuart and R. Salavati (2003). "Comparative analysis of editosome proteins in trypanosomatids." Nucleic Acids Res **31**(22): 6392-6408.

Wright, J. H. (1903). "Protozoa in a case of tropical ulcer ("Delhi Sore")." J Med Res **10**(3): 472-482 477.

Wright, N. A., L. E. Davis, K. S. Aftergut, C. A. Parrish and C. J. Cockerell (2008). "Cutaneous leishmaniasis in Texas: A northern spread of endemic areas." Journal of the American Academy of Dermatology **58**(4): 650-652.

Wyllie, S., S. Patterson, L. Stojanovski, F. R. C. Simeons, S. Norval, R. Kime, K. D. Read and A. H. Fairlamb (2012). "The Anti-Trypanosome Drug Fexinidazole Shows Potential for Treating Visceral Leishmaniasis." Science Translational Medicine **4**(119): 119re111.

Zenno, S., H. Koike, A. N. Kumar, R. Jayaraman, M. Tanokura and K. Saigo (1996). "Biochemical characterization of NfsA, the *Escherichia coli* major nitroreductase exhibiting a high amino acid sequence homology to Frp, a *Vibrio harveyi* flavin oxidoreductase." J Bacteriol **178**(15): 4508-4514.

Zhang, J. H., T. D. Chung and K. R. Oldenburg (1999). "A simple statistical parameter for use in evaluation and validation of high throughput screening assays." J Biomol Screen **4**(2): 67-73.

Zhou, L., H. Ishizaki, M. Spitzer, K. L. Taylor, N. D. Temperley, S. L. Johnson, P. Brear, P. Gautier, Z. Zeng, A. Mitchell, V. Narayan, E. M. McNeil, D. W. Melton, T. K. Smith, M. Tyers, N. J. Westwood and E. E. Patton (2012). "ALDH2 mediates 5-nitrofuran activity in multiple species." Chem Biol **19**(7): 883-892.

Zhou, Y., N. Messier, M. Ouellette, B. P. Rosen and R. Mukhopadhyay (2004). "*Leishmania major* LmACR2 is a pentavalent antimony reductase that confers sensitivity to the drug pentostam." J Biol Chem **279**(36): 37445-37451.